



Government of the People's Republic of
Bangladesh

Bangladesh Water Development Board (BWDB)

Coastal Embankment Improvement Project



**Consultancy Services for Feasibility Studies and
Preparation of Detailed Design for the Following Phase of the
Coastal Embankment Improvement Project (CEIP)**

Final Report on Morphology

December 2022

Table of Contents

| | |
|--|-----------|
| Table of Contents..... | ii |
| List of Tables..... | vi |
| List of Figures | vii |
| 1. Introduction..... | 11 |
| 1.1 Background | 11 |
| 1.2 Objectives..... | 13 |
| 1.3 Study Area..... | 13 |
| 1.4 Structure of the Report | 16 |
| 2. Data Collection and Processing..... | 17 |
| 2.1 Historical Maps, Aerial Photographs, and Processing..... | 17 |
| 2.2 Historical Maps, Satellite Images, Processing, and Geo-referencing | 17 |
| 2.3 Co-registration of Satellite Images | 19 |
| 2.4 Bankline Delineation from Satellite Images..... | 19 |
| 2.5 Opportunity to use Google-earth Images | 19 |
| 3. Approach and Methodology..... | 21 |
| Literature Review | 22 |
| Physiographic and Geological Settings..... | 22 |
| Collection and Processing of Historical Maps, Topographic Maps and Satellite images | |
| 22 | |
| Bankline Delineation..... | 22 |
| Long-term Monitoring Data | 22 |
| Enhancing Knowledge Baseline of Geo-Morphological Processes | 22 |
| Assessment of Physiographical and Geological Settings of the study area..... | 22 |
| Historical Development of the Rivers..... | 23 |
| Assessment of the Change in Width and Sinuosity | 23 |
| Assessment of shifting of the Bank lines..... | 23 |
| Assessment of Migration of the Meandering Bends..... | 23 |
| Assessment of Erosion-accretion Pattern and the Rate of Erosion..... | 24 |
| Calculation of Life Span of the Bend & Assessment of the Impact of the Bank Protection Works | 24 |
| Geo-morphological Evolution of the Rivers | 25 |
| Prevailing Morphological Processes..... | 25 |
| Identification of Vulnerable Bends..... | 25 |
| Projection of Future for the Rivers..... | 25 |
| Comparison of CEGIS with LTM Data..... | 26 |
| 4. Physical Processes..... | 27 |

| | |
|--|-----------|
| 4.1 The setting of the Physical Processes..... | 27 |
| Geological Setting..... | 27 |
| Tectonics and Seismicity..... | 28 |
| Physiographical Setting..... | 30 |
| Topographical Setting | 33 |
| Climate Setting | 37 |
| 4.2 System analysis: Historical Development..... | 38 |
| Millennium Scale..... | 38 |
| Centennial and decade-scale..... | 40 |
| Human Interventions | 46 |
| Major events in the ME regions..... | 47 |
| Identifying the main drivers active during the periods from 1776-1840, 1840-1943, and 1943 to 2020 | 47 |
| identifying major events and relevant drivers in the SW and SC..... | 47 |
| Relation between Shifting of the Delta and courses of the Distributaries | 48 |
| Sedimentation/denudation processes..... | 49 |
| 5. River System Analysis in SW, SC, and ME Regions..... | 50 |
| 5.1 Khulna-Satkhira region (SW Region)..... | 50 |
| 5.2 Barishal region (SE Region)..... | 50 |
| 5.3 Meghna Estuary (ME Region)..... | 50 |
| 6. Morphological Analysis of the Rivers in the Khulna Area..... | 53 |
| 6.1 Kholpetua River | 53 |
| Historical Development of the Kholpetua River..... | 54 |
| Average Width of the Kholpetua River | 56 |
| Sinuosity of the Kholpetua River..... | 56 |
| Erosion-Accretion Analysis of the Kholpetua River | 57 |
| Bend Migration of the Kholpetua River | 60 |
| Prediction of the River of the Kholpetua River..... | 62 |
| 6.2 Ichamati-Kalindi River..... | 73 |
| Historical Development of the Ichamati-Kalindi River..... | 73 |
| Average Width of the Ichamati-Kalindi River | 75 |
| Sinuosity of the Ichamati-Kalindi River..... | 75 |
| Erosion-Accretion Analysis of the Ichamati-Kalindi River | 76 |
| Bend Migration of the Ichamati-Kalindi River..... | 79 |
| Projection of the Ichamati-Kalindi River | 81 |
| 6.3 Kapotakshi River..... | 83 |

| | |
|--|------------|
| Historical Development of the Kapotakshi River..... | 83 |
| Average Width of the Kapotakshi River..... | 85 |
| Sinuosity of the Kapotakshi River..... | 85 |
| Erosion-Accretion Analysis of the Kapotakshi River..... | 86 |
| Bend Migration of the Kapotakshi River..... | 89 |
| Projection of the Kapotakshi River | 91 |
| 6.4 The Shibsa River..... | 97 |
| Historical Development of the Shibsa River..... | 97 |
| Average Width of the Shibsa River..... | 99 |
| The sinuosity of the Shibsa River..... | 99 |
| Erosion-Accretion Analysis of the Shibsa River..... | 100 |
| Bend Migration of the Shibsa River..... | 102 |
| Projection of the Shibsa River | 104 |
| 7. Morphological Analysis of the River in the Barishal Area..... | 106 |
| 7.1 Burishwar-Payra River..... | 107 |
| Historical Development of the Burishwar-Payra River..... | 107 |
| Erosion-Accretion Analysis of the Burishwar-Payra River | 108 |
| Average Width of the Burishwar-Payra River | 110 |
| The sinuosity of the Burishwar-Payra River..... | 111 |
| Bend Migration of the Burishwar-Payra River | 111 |
| Projection of the Burishwar-Payra River | 113 |
| 7.2 Baleshwar River..... | 117 |
| Historical Development of the Baleshwar River..... | 118 |
| Erosion-Accretion Analysis of the Baleshwar River..... | 119 |
| Average Width of the Baleshwar River..... | 122 |
| The sinuosity of the Baleshwar River..... | 123 |
| Bend Migration of the Baleshwar River..... | 123 |
| Projection of the Baleshwar River | 125 |
| 7.3 Tentulia River | 129 |
| Historical Development of the Tentulia River | 129 |
| Erosion-Accretion Analysis of the Tentulia River | 131 |
| Bend Migration of the Tentulia River | 134 |
| Projection of the Tentulia River | 136 |
| 8. Length of the Prediction Lines, Maximum Lateral Distance, and Length of Eroded Existing Embankment | 139 |
| 8.1 Length of the Prediction Lines and Maximum Lateral Distance | 139 |

| | |
|--|------------|
| 8.2 Translation of the Prediction lines to Erosion Risk..... | 142 |
| Prioritization Report..... | 142 |
| CEGIS Study | 144 |
| 9. Long Term Monitoring (LTM) | 150 |
| 9.1 LTM Observations..... | 150 |
| 9.2 Observations by CEGIS | 150 |
| 9.3 Comparison between the results..... | 150 |
| 9.4 CEGIS proposed LTM..... | 152 |
| System based..... | 152 |
| Process-based..... | 152 |
| Polder based..... | 152 |
| 10. Conclusions & Recommendations | 153 |
| Annex-A | 154 |
| Annex-B | 177 |
| References | 204 |

List of Tables

| | |
|--|-----|
| Table 2.1: Satellite images used in the study | 17 |
| Table 5.1: Characteristics of the geo-morphological setting of three study regions..... | 51 |
| Table 6.1: Locations, Extent of Bend migration, and Migration direction for Kholpetua River | 60 |
| Table 5.2: Locations, Extent of Bend migration, and Migration direction for Ichamati-Kalindi River..... | 79 |
| Table 6.2: Locations, Extent of Bend migration, and Migration direction for Kapotakshi River..... | 89 |
| Table 6.3: Locations, Extent of Bend migration, and Migration direction for the Shibsa River | 102 |
| Table 7.1: Locations, Extent of Bend migration, and Migration direction for Burishwar-Payra River..... | 112 |
| Table 7.2: Locations, Extent of Bend migration, and Migration direction for Baleshwar River | 124 |
| Table 7.3: Locations, Extent of Bend migration, and Migration direction for Tentulia River | 134 |
| Table 8.1: Length and lateral distance of the prediction lines for the Khulna area..... | 139 |
| Table 8.2: Length and lateral distance of the prediction lines for the Barishal area..... | 140 |
| Table 8.3: The estimated length of bank protection due to high and medium risk for the Khulna Region..... | 147 |
| Table 8.4: The estimated length of bank protection due to high and medium risk for the Barishal Region | 149 |
| Table 9.1: Comparison of erosion-accretion between LTM & CEGIS (Khulna area)..... | 150 |
| Table 9.2: Comparison of erosion-accretion between LTM & CEGIS (Barishal area)..... | 151 |

List of Figures

| | |
|---|----|
| Figure 1.1: Polders and rivers in the Khulna area..... | 15 |
| Figure 1.2: Polders and rivers in the Barishal area..... | 15 |
| Figure 2.1: Flowchart showing steps for geo-referencing of satellite images..... | 18 |
| Figure 2.2: Sample image showing the collection of GCPs from a reference image..... | 18 |
| Figure 2.3: Shifting between the Google-earth images of the same year (2010) | 20 |
| Figure 3.1 Flow diagram of a methodology of the study | 21 |
| Figure 3.2: Concept of bend development (Hooke, 1977)..... | 24 |
| Figure 4.1: Present river system in the southwest region of Bangladesh..... | 27 |
| Figure 4.2: Geological setting (Akter et al., 2016)..... | 28 |
| Figure 4.3: Structural forces affecting the Bengal Basin (Morgan and McIntire, 1959).... | 30 |
| Figure 4.4: Map showing the physiographic units of SW and SC regions..... | 31 |
| Figure 4.5: Contours of elevation are in mPWD based on the DEM of the 1950s and the river courses in 1943..... | 34 |
| Figure 4.6: Topographical setting of the South-West and South-Central regions of Bangladesh..... | 35 |
| Figure 4.7: East-west surface profile in South-West and South-Central regions of Bangladesh..... | 36 |
| Figure 4.8: North -south surface profiles in South-West and South-Central regions of Bangladesh..... | 36 |
| Figure 4.9: Pattern of temperature and rainfall..... | 38 |
| Figure 4.10: Palaeo-geographic maps of the Ganges and Brahmaputra (GB) delta during the Holocene (source: modified from Goodbred and Allison, 2003)..... | 39 |
| Figure 4.11: Changes in the Meghna estuary in the last 250 years (Lines in the figure indicate the locations of the southern tips of the islands in 1776 and 1840 maps for assessing the migration of the Bhola, Hatiya, and Sandwip Islands) | 41 |
| Figure 4.12: Net accretion in the centennial and decade scale..... | 42 |
| Figure 4.13: Rivers found in Rennel's map (1776) | 43 |
| Figure 4.14: Rivers found in Tassin's map (1840)..... | 44 |
| Figure 4.15: Rivers found in Topo map (1943) | 44 |
| Figure 4.16: Rivers found in the satellite image of 2010..... | 45 |
| Figure 4.17: Courses of rivers in the last 250 years..... | 45 |
| Figure 4.18 The salinity intrusion pattern in the Bengal coastal region..... | 46 |
| Figure 4.19: Decade to century-scale net accretion and identification of drivers | 47 |
| Figure 4.20: Qualitative shifting of the delta and its associated distributaries..... | 49 |
| Figure 6.1: Study polders and peripheral rivers in Khulna area..... | 53 |
| Figure 6.2: Historical Development of Kholpetua River..... | 55 |
| Figure 6.3: Average width of the Kholpetua River from 1989-2021..... | 56 |
| Figure 6.4: Sinuosity of Kholpetua River from 1989-2021 | 57 |

| | |
|--|-----|
| Figure 6.5: Net erosion-accretion of the Kholpetua River during (1989-2021)..... | 58 |
| Figure 6.6: Erosion-accretion of Kholpetua River over the years (Reach-1) | 59 |
| Figure 6.7: Erosion-accretion of Kholpetua River over the years (Reach-2) | 60 |
| Figure 6.8: Bend migration of the Kholpetua River (1989-2021) | 61 |
| Figure 6.9: Bend migration in the next 10, 20, and 30 years in the Kholpetua River..... | 64 |
| Figure 6.10: Bend migration in the next 10, 20, and 30 years in the Kholpetua River.... | 65 |
| Figure 6.11: Bend migration in the next 10, 20, and 30 years in the Kholpetua River..... | 66 |
| Figure 6.12: Bend migration in the next 10, 20, and 30 years in the Kholpetua River..... | 67 |
| Figure 6.13: Bend migration in next 10, 20 and 30 years in Kholpetua River..... | 68 |
| Figure 6.15: Bend migration in the next 10, 20, and 30 years in the Kholpetua River.... | 70 |
| Figure 6.16: Bend migration in the next 10, 20, and 30 years in the Kholpetua River.... | 71 |
| Figure 6.17: Bend migration in the next 10, 20, and 30 years in the Kholpetua River.... | 72 |
| Figure 5.18: Historical Development of Ichamati-Kalindi River..... | 74 |
| Figure 5.19: Average width of Ichamati-Kalindi River from 1989-2021..... | 75 |
| Figure 5.20: Sinuosity of Ichamati-Kalindi River from 1989-2021 | 75 |
| Figure 5.21: Erosion-accretion of the Ichamati-Kalindi River during (1989-2021)..... | 77 |
| Figure 5.22: Erosion-accretion of Ichamati-Kalindi River over the years (Reach-1) | 78 |
| Figure 5.23: Erosion-accretion of Ichamati-Kalindi River over the years (Reach-2) | 78 |
| Figure 5.24: Bend migration of the Ichamati-Kalindi River (1989-2021) | 80 |
| Figure 6.25: Bend migration in the next 10, 20, and 30 years in the Ichamati-Kalindi River | 82 |
| Figure 6.26: Historical Development of Kapotakshi River | 84 |
| Figure 6.27: Average width of Kapotakshi River from 1989-2021..... | 85 |
| Figure 6.28: Sinuosity of Kapotakshi River from 1989-2021..... | 86 |
| Figure 6.29: Erosion-accretion of the Kapotakshi River during (1989-2021)..... | 87 |
| Figure 6.301: Erosion-accretion of Kapotakshi River over the years (Reach-1)..... | 88 |
| Figure 6.31: Erosion-accretion of Kapotakshi River over the years (Reach-2)..... | 88 |
| Figure 6.32: Erosion-accretion of Kapotakshi River over the years (Reach-3)..... | 89 |
| Figure 6.33: Bend migration of the Kapotakshi River (1989-2021)..... | 90 |
| Figure 6.34: Bend migration in the next 10, 20, and 30 years in Kapotakshi River..... | 92 |
| Figure 6.35: Bend migration in the next 10, 20, and 30 years in Kapotakshi River | 93 |
| Figure 6.36: Bend migration in the next 10, 20, and 30 years in Kapotakshi River | 94 |
| Figure 6.37: Bend migration in the next 10, 20, and 30 years in Kapotakshi River | 95 |
| Figure 6.38: Bend migration in the next 10, 20, and 30 years in Kapotakshi River | 96 |
| Figure 6.39: Historical Development of Shibsa River | 98 |
| Figure 6.40: Average width of Shibsa River from 1989-2021..... | 99 |
| Figure 6.41: Sinuosity of Shibsa River from 1989-2021 | 99 |
| Figure 6.42: Erosion-accretion of the Shibsa River during (1989-2021)..... | 101 |

| | |
|---|-----|
| Figure 6.43: Erosion-accretion of Shibs River | 102 |
| Figure 6.44: Bend migration of the Shibs River (1989-2021)..... | 103 |
| Figure 6.45: Bend migration in the next 10, 20, and 30 years in Shibs River..... | 105 |
| Figure 7.1: Map showing rivers considered in Barishal Region | 106 |
| Figure 7.2: Historical Development of Burishwar-Payra River..... | 108 |
| Figure 7.3: Erosion-accretion of the Burishwar-Payra River during (1989-2021)..... | 109 |
| Figure 7.4: Erosion-accretion of Burishwar-Payra River over the years..... | 110 |
| Figure 7.5: Average width of Burishwar-Payra River over the years. | 111 |
| Figure 7.6: Sinuosity of Burishwar-Payra River over the years. | 111 |
| Figure 7.7: Bend migration of the Burishwar-Payra River (1989-2021) | 113 |
| Figure 7.8: Bend migration in the next 10, 20, and 30 years in the Burishwar-Payra River | 115 |
| Figure 7.9: Bend migration in the next 10, 20, and 30 years in the Burishwar-Payra River | 116 |
| Figure 7.10: Bend migration in the next 10, 20, and 30 years in the Burishwar-Payra River | 117 |
| Figure 7.11: Historical Development of the Baleshwar River..... | 118 |
| Figure 7.12: Erosion-accretion of the Baleshwar River during (1989-2021)..... | 120 |
| Figure 7.13: Erosion-accretion of Baleshwar River over the years (Reach-1)..... | 121 |
| Figure 7.14: Erosion-accretion of Baleshwar River over the years (Reach-2)..... | 121 |
| Figure 7.15: Erosion-accretion of Baleshwar River over the years (Reach-2)..... | 122 |
| Figure 7.16: Average width of Baleshwar River over the years..... | 123 |
| Figure 7.17: Sinuosity of Baleshwar River over the years | 123 |
| Figure 7.18: Bend migration of the Baleshwar River (1989-2021)..... | 125 |
| Figure 7.19: Bend migration in the next 10, 20, and 30 years in the Baleshwar River ... | 127 |
| Figure 7.20: Bend migration in the next 10, 20, and 30 years in the Baleshwar River ... | 128 |
| Figure 7.21: Historical development of Tentulia River (1943-2021) | 130 |
| Figure 7.22: Erosion-accretion of Tentulia River (1989-2021)..... | 132 |
| Figure 7.23: Erosion-accretion of Tentulia River along both of the banks (1989-2021).133 | 133 |
| Figure 7.24: Erosion-accretion of chars of Tentulia River (1989-2021) | 133 |
| Figure 7.25: Bend migration of Tentulia River (1989-2021)..... | 135 |
| Figure 7.26: Bend migration in the next 10, 20, and 30 years in Tentulia River..... | 137 |
| Figure 7.27: Bend migration in the next 10, 20, and 30 years in Tentulia River..... | 138 |
| Figure 8.3: Erosion risk to the embankment for the polders in Khulna/Satkhira area (source: CEIP Prioritization Report, 2021) | 142 |
| Figure 8.4: Erosion risk to the embankment for the polders in Barishal/Barguna area (source: CEIP Prioritization Report, 2021) | 143 |
| Figure 8.5: Erosion risk of embankment in polders of Khulna area | 145 |
| Figure 8.6: Erosion risk of embankment in polders of Khulna area | 146 |

Figure 9.1: Reason for the difference in erosion area between LTM and CEGIS (Ichamati-Kalindi River) 152

DRAFT

1. Introduction

1.1 Background

Known as one of the world's largest, youngest, and most active deltas, the Coastal Zone of Bangladesh spans more than 580 km along the Bay of Bengal and covers 32% of the country (47,201 km²) (MoWR, 2003). Within the delta resides the confluence of the Ganges, Brahmaputra, and Meghna (GBM). Together these rivers form the largest delta in Asia, which delivers an enormous volume of sediment to the Bay of Bengal (Kuehl et al., 1989).

The GBM delta, with its abundance of natural resources, defines Bangladesh, both regarding its physical and cultural characteristics and the livelihoods of its people. The delta is characterized by its flatness. Sixty-two percent of the coastal land has an elevation less than 3 m above Mean Sea Level (MSL), and 83 percent is less than 5 m (BWDB, 2012). The strength of the tides, in conjunction with the low elevation of the delta, causes the tides to have an influence far upstream in the southern estuaries. Three main zones are typically used to define the coast of Bangladesh as follows:

- The Ganges Tidal Floodplain West contains the renowned and UNESCO world heritage accredited Sundarbans mangrove forest, covering the first 60 to 80 km inland from the coastline. The area has long drainage routes with a shallow gradient and is characterized as a moribund delta formation. Very little freshwater flows from its parent river, the Ganges;
- The Ganges Tidal Floodplain East contains no substantial forest area. Several rivers intersect the land and receive water from the Lower Meghna river as well as the Padma river via the Arial Khan river;
- The Meghna Estuary floodplain includes several large islands, such as Bhola, Hatia, and Sandwip, and mainland areas on the left bank of the Meghna River. The area is morphologically very active, with excess in land accretion compared to land erosion;

Roughly 46 million Bangladeshi (29% of the total population) call Bangladesh's Coastal Zone their home (Ahmad, 2019). The region is predominantly agricultural, and more than 30% of the country's cultivatable land is in the coastal area (MoA, 2010). Other economic activities in the region typically include shrimp and fish farming, forestry, tourism, salt production, ship-breaking, and ports. There are ample growth opportunities to be found in the coastal region. However, these all come with risks, as the coastal zone is well-known for its vulnerability to coastal hazards (Tessler et al., 2015).

Bangladesh's coastal communities are endangered by the constant threat of cyclones, which can cause inundation of the coastal land from high storm surges. Additionally, slow-moving chronic stressors such as erosion, saline intrusion, and water-logging occur frequently and to a large extent in the coastal zone. These stressors can result in land loss, infrastructure failure, challenges operating the drainage systems in the polders, and overall reduced agricultural productivity.

Due to the constant coastal threats formed by cyclonic events, chronic stressors, and the zone, influenced by the river system's fluctuations, Bangladesh is considered one of the most disaster-prone and climate-vulnerable countries in the world.

To save lives, reduce economic losses and protect the hard-earned development gains, the Bangladeshi Government has been making multiple attempts over the past decades. The development of polders has played a crucial role in these attempts. To protect the people and

agricultural land from tidal inundation and saline water intrusion and recover a large extent of land for permanent agriculture, the Government has been constructing polders since the early 1960s.

A polder is a “low-lying tract of land, enclosed by embankments known as dykes that form an independent hydrological entity which has no physical connection with the outside water other than through manually operated devices (i.e., water control structures)” (Jensen Localization, 2018). Polders protect the coastal zone in several ways. First, they prevent saline water from entering the agricultural fields, improving agricultural productivity and providing food security for the zone’s inhabitants. Second, they protect against frequent tidal flooding, which prevents damage to both people and crops, resulting in the stimulation of economic development of the local communities.

Drainage and flushing sluices control the water inside the embanked polder. Along the coastal zone, an area of 1.2 million ha is covered by a total of 139 polders. These combined cover roughly 25% of the coastal zone and contain an embankment length of about 5,665 km. In addition, a total of 1,697 regulators, 1,202 flushing inlets, and a distance of about 5,707 km of drainage channels are in place to control the water. The current embankment crest levels typically protect a storm surge that would occur typically once every 5 to 10 years (with a 2% wave overtopping level) (BWDB, 1983).

The Government’s development of polders has not been without success. Over the past 45-50 years, their construction has significantly reduced the country’s vulnerability to natural disasters and provided improved economic opportunities for the coastal communities. About 70% of the total agricultural land area in the coastal zone (1.2 million ha) has become less subjected to flood hazards, and about 0.9 million ha has been newly cultivated.

The severity of cyclones in Bangladesh and their associated mortalities has fluctuated significantly over the past 50 years (Haque et al., 2011). In 1970 and 1991, the two deadliest cyclones happened in the country, resulting in >500,000 and 140,000 deaths, respectively. More recently, Sidr (2007), Aila (2009), and Amphan (2020) struck the coast of Bangladesh. All in all, Bangladesh has made outstanding progress. It managed to reduce the number of deaths and injuries from cyclones by approximately 100-fold over the last 5 decades.

It must be noted, though, that the effectiveness of the polders has in many cases been compromised due to damages from cyclones, shifting coastal and river bank lines and frequent storm surges. There is room for improvement when it comes to maintenance as well as management of these essential structures.

In the 1960s and '70s, the first significant project, Coastal Embankment Project (CEP), was implemented. It was followed in 1985 by the Coastal Area Rehabilitation and Cyclone Protection Project (CPP-I). In the late 1980s, 1990s, and 2000s, the Government took the following projects, i.e., Cyclone Protection Project (CPP-II), Coastal Embankment Rehabilitation Project (CERP-1), and second Coastal Rehabilitation Project (CERP-II). When severe cyclones Sidr and Aila struck the coastal zone, causing significant damage, the Government of Bangladesh (GoB) obtained an IDA/credit for the Emergency Cyclone Recovery and Restoration Project (ECRRP). The proceeds from this credit were then used to fund the Coastal Embankment Improvement Project (CEIP). The implementation of its first phase (CEIP-1) commenced in 2015 and is expected to be completed by June 2022. The current follow-on project to CEIP-1, CEIP-2, commenced in 2021.

The overall project development objective of the Coastal Embankment Improvement Project (CEIP) is to increase the resilience of the coastal population to natural disasters and climate

change. More specifically, the project aims at (a) reducing the loss of assets, crops, and livestock during natural disasters; (b) reducing the time of recovery after a natural disaster such as a cyclone; (c) improving agricultural production by reducing saline water intrusion which is expected to worsen due to climate change, and (d) improving the Government of Bangladesh's capacity to respond promptly and effectively to an eligible crisis or emergency. Because of obtaining the above objectives requires systematic rehabilitation of the coastal polders, as furnished below. Per the Terms of Reference (ToR), the main aim of the Consultancy Services is to support the Government of Bangladesh's Water Development Board (BWDB) in preparation of a comprehensive coastal embankment improvement program and implementation of the following phases of CEIP.

1.2 Objectives

Assessing the morpho-dynamics of the rivers surrounding the polders is crucial. This will help properly plan and manage the water resources, increasing resilience to natural disasters. In this regard, prediction of the rivers in Khulna and Barishal areas surrounding polders through planform analysis using time series satellite images is an effective way for effective management of the rivers.

The main objective of this morphological study is to predict the rivers for different timescales (10, 20, and 30 years) through planform analysis of the satellite images. Additional objectives are as follows:

- Assessing the geo-morphological evolutions of the rivers within the study area;
- Understanding prevailing morphological processes of the rivers to identify the main drivers;
- Assessment of the historical monitoring data on erosion-accretion and comparison with the Long Term Monitoring (LTM) data, developed by the CEIP II project;
- Identification of erosion vulnerable locations;
- Projection of the rivers in Khulna and Barishal areas.

This report details the morphological study and is a portion of Deliverable 4: Modelling Reports (Storm Surge Modelling and Polder Morphological Analysis and Polder Drainage Modelling) for max. 13 Polders of the CEIP-II Inception Report. This Deliverable meets Task 2.1 (d) planform analysis and river bank erosion forecast.

1.3 Study Area

Morphological analysis has been done for the rivers in the South-West (SW) (Khulna areas) and South-Central (SC) (Barishal) regions (**Figure 1.1** and **Figure 1.2**). Major rivers in the Khulna areas are Kholpetua, Kapotaksha, Shibsia, and Ichamati-Kalindi Rivers. While Burishwar-Payra, Baleshwar, Biskhali, Lohalia-Rabnabad, Tentulia, Andharmanick, and Haodar-Bharani are the major rivers in the Barishal areas.

Furthermore, four (4) project polders lie Khulna area (Khulna and Satkhira Districts), while nine (9) polders lie in the Barishal area (Pirojpur, Barguna, Patuakhali, and Bhola Districts). Seven (7) polders of CEIP (Phase-1) Package 3 have been included in the study.

Hydrologically, the whole of Bangladesh is divided into eight regions. They are- northwest (NW), northcentral (NC), northeast (NE), southeast (SE), eastern hills (EH), southwest (SW), southcentral (SC) and rivers and estuaries (RE). The polders and surrounding rivers those are

considered for this study lie in the Satkhira and Khulna districts of the Khulna region (SW region) and the Pirojpur and Patuakhali districts of the Barishal region (SC region). The hydro-morphological characteristics (connectivity, fluvial input, and so on) of those two regions are different. Settings of different physical processes differ, although they were found to be interrelated and inter-dependent in different time scales. Presently, delta building processes in the estuaries are dormant in the SW region due to losing fluvial connectivity; thus, it is considered a dying delta. However, the delta building process is active in the Meghna Estuary. This functional estuary's dynamic influences the hydro-morphological process of the SW and SC regions.

Two major distributaries contribute to transporting fluvial inputs into the bay other than the Lower Meghna system, water, and sediment. Fluvial and tidal processes dominate the prevailing hydro-morphological processes of the SC region. The Gorai passes through the SW region, a right bank distributary of the Ganges River, delivering about 30 billion m³ of water and 30 million tons of sediment to the bay annually (EGIS, 2001). Two right bank distributaries, Bhairab and the Kabodak, played a vital role in the delta building processes. However, the perennial connection of these distributaries from their parent river, the Ganges, became disrupted a couple of centuries ago (Williams, 1919). This SW region is now in the moribund delta, with no perennial connectivity. On the other hand, the Arial Khan River passes through the SC region, a right bank distributary of the Padma River, which is the combined flow of the Ganges and Jamuna rivers, supplying about 30 billion m³ flow and 25 million tons of sediment every year (Akter et al., 2016).

Understanding the long-term morphological processes of the SW and SC region is required to know the prevailing behavior of the Meghna estuary, an active delta building estuary (Sarker et al., 2011). We, therefore, included the RE region within the study area.

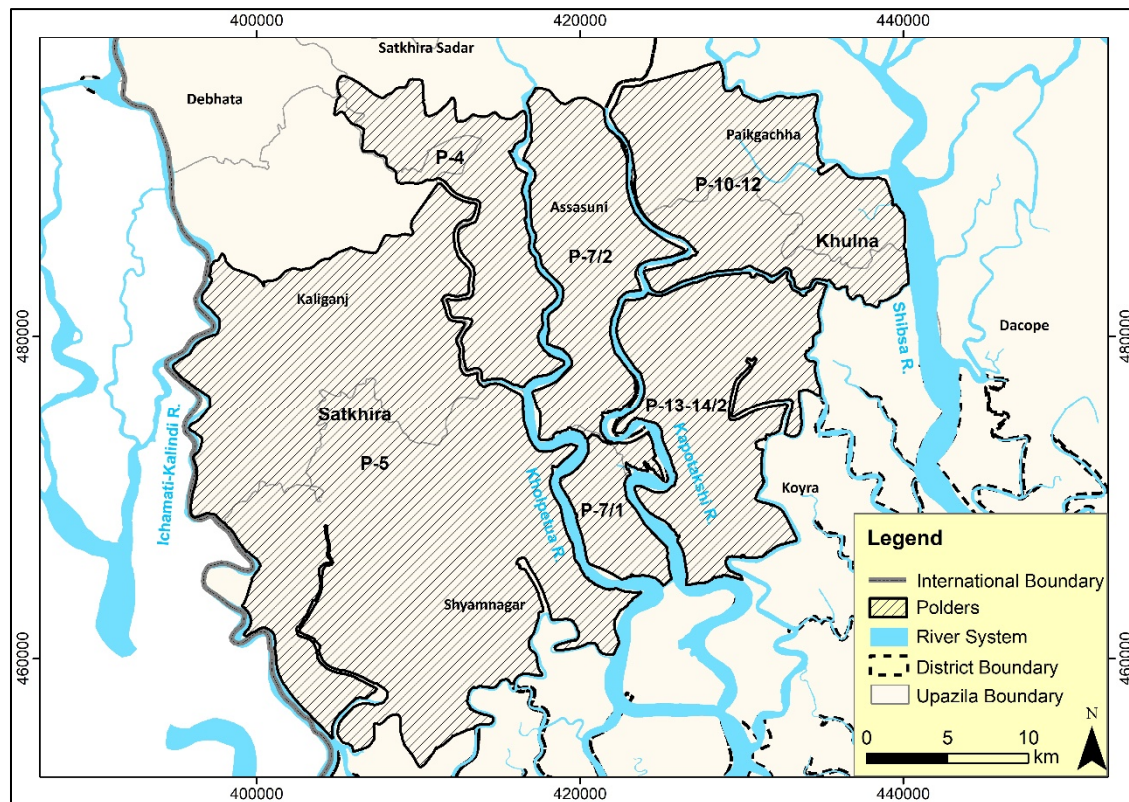


Figure 1.1: Polders and rivers in the Khulna area

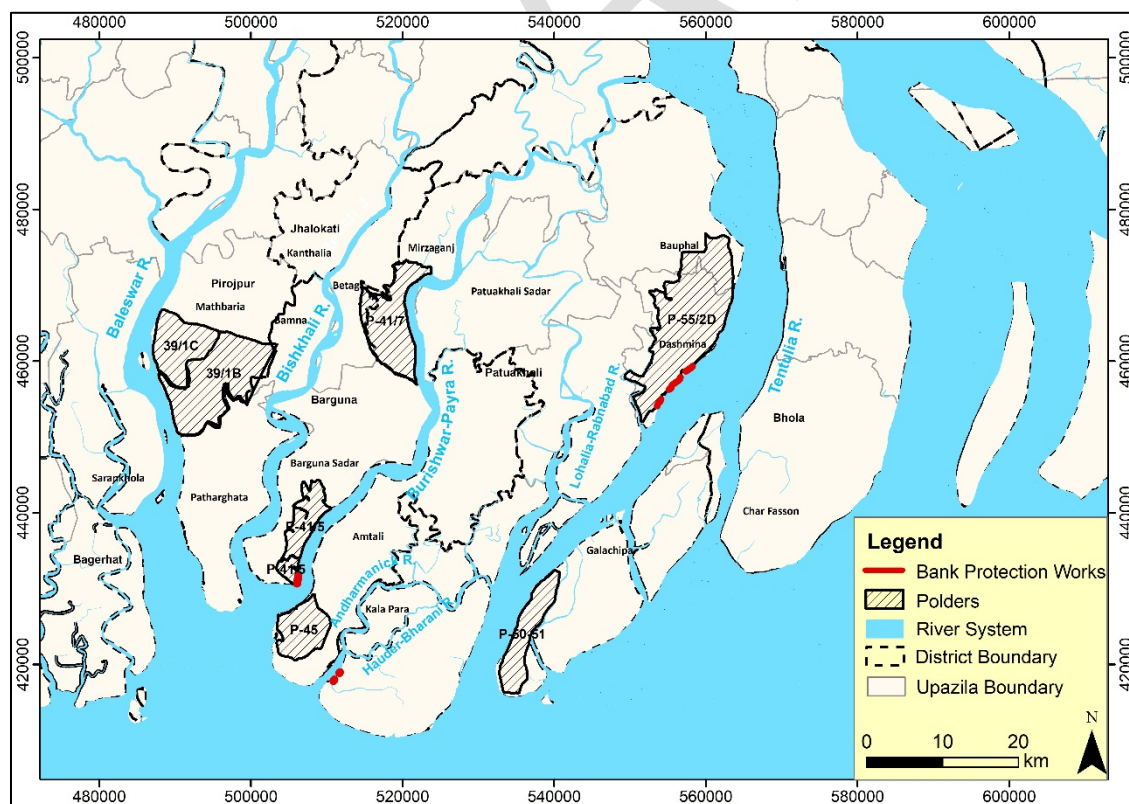


Figure 1.2: Polders and rivers in the Barishal area

1.4 Structure of the Report

The report has the following ten (10) chapters:

Chapter 1: Study with its background, objectives, specific objectives, and study area.

Chapter 2: Information about collecting data of historical maps, satellite images, and processing for conducting this morphological study.

Chapter 3: Approach and methodology of the study.

Chapter 4: Geomorphological evolution and prevailing morphological processes.

Chapter 5: River System Analysis in SW, SC, and ME Regions

Chapter 6: Morphological analysis of the rivers in the Khulna area.

Chapter 7: Morphological analysis of the rivers in the Barishal area.

Chapter 8: Details of Length of the Prediction Lines, Maximum Lateral Distance, and Length of Eroded Existing Embankment

Chapter 9: Highlights, the comparison of the historical erosion-accretion data between LTM and CEGIS, and observed data.

Chapter 10: Conclusions

2. Data Collection and Processing

The study uses aerial photographs and satellite images for the morphological analysis of the rivers in the polders in the southwest and south-central region of Bangladesh. A brief description of the data used for the study and their processing is described below:

2.1 Historical Maps, Aerial Photographs, and Processing

Old maps, including the Rennels map (1776), Tassin map (1840), and topographic maps of 1943, were retrieved from the CEGIS archives. A scanned copy of Rennels map collected in the early 1990s from the British Museum and bank lines of the rivers were digitized. The reference frames and maps produce reasonably accurate for assessing the long-term changes while verified. These maps are the most accurate for comparing the course of the rivers with the present situation considering the same projection system and the bank lines were digitized straight away from these maps. All historical maps were digitized from hard copy under the ARC/INFO's Arc edit module. To accomplish the task, a "stream mode" digitization environment was set up through a coordinated digitizing system with a snap distance of 0.005 and a weed distance of 0.002. The digitized maps were projected into the Bangladesh Transverse Mercator (BTM) projection system.

For checking the accuracy level (compared to the geo-referenced satellite images), the deviation of some fixed points was measured, and the courses of stable reaches of smaller rivers were recognizable in Landsat images. It is confirmed that the accuracy level is acceptable to fulfill the purposes of this study.

2.2 Historical Maps, Satellite Images, Processing, and Geo-referencing

Different satellite images, geo-referenced with GCP (ground control points), were used to examine the shifting of rivers. The customized Bangladesh Transverse Mercator (BTM) system was used for image projection. A description of the satellite images used in this morphological study is presented in Table 2.1.

Table 2.1: Satellite images used in the study

| SL | Image Type | Source | Year | Image Resolution |
|----|------------------|---------------|------|------------------|
| 1 | Rennel's Map | CEGIS Archive | 1776 | - |
| 2 | Tassin's Map | CEGIS Archive | 1840 | - |
| 3 | Topographic Map | CEGIS Archive | 1943 | - |
| 4 | Satellite Images | Landsat | 1989 | 30m X 30m |
| 5 | | | 2003 | 30m X 30m |
| 6 | | | 2010 | 30m X 30m |
| 7 | | | 2015 | 30m X 30m |
| 8 | | | 2020 | 30m X 30m |
| 9 | | | 2021 | 30m X 30m |

Geo-referencing is the process performed on raw (i.e., layer stacked products) images to refer each pixel in the image to the natural world coordinate system. In the present study, the geo-

referencing satellite images were carried out with respect to the available Landsat Images by using a sufficient number of Ground Control Points (GCPs) and rigorous mathematical functions in the image processing software. This enables the satellite image data to be viewed and analyzed along with other GIS data layers.

The steps followed for geo-referencing satellite images are shown in **Figure 2.1**. Moreover, geo-referencing satellite images have been carried out with a maximum Root Mean Square (RMS) error of 1 pixel using referenced Landsat image for maintaining the required positional accuracy (**Figure 2.2**).

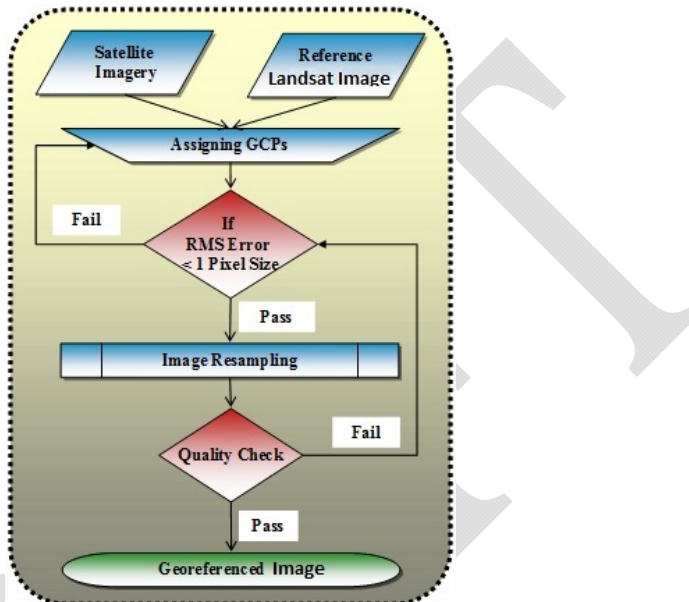


Figure 2.1: Flowchart showing steps for geo-referencing of satellite images

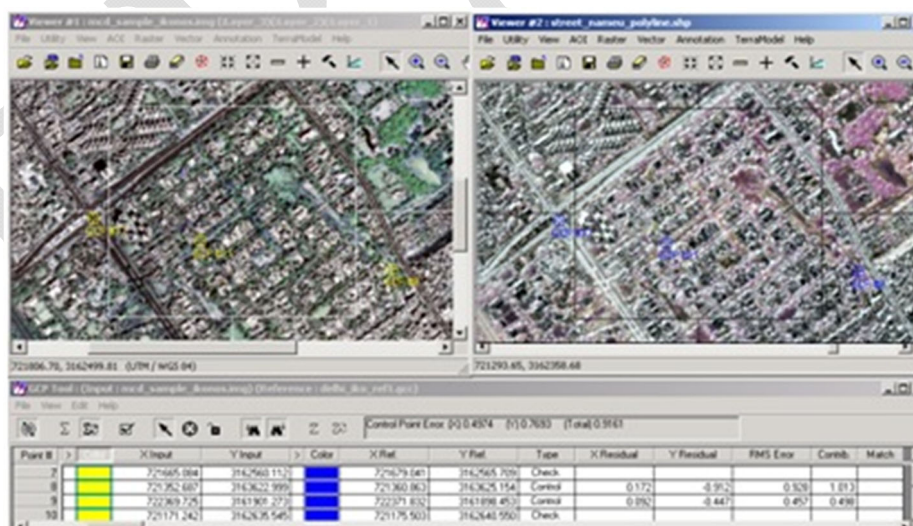


Figure 2.2: Sample image showing the collection of GCPs from a reference image

While geo-referencing the images, the study has emphasized selecting an adequate number of GCPs, especially at bi-junctions, tri-junctions, the corner of an established field, street corners, or the intersection of rail uses and roads. This is to improve the accuracy of the task by

minimizing the RMS error. The following points have been considered while geo-referencing the satellite images:

- ❖ The GCPs cover the entire area of interest;
- ❖ The GCPs are adequately spread to provide better control for the complete area;
- ❖ The GCPs are taken so as to represent the topography.

These control points have been used to build a polynomial transformation that converted the dataset from its existing location to the spatially corrected site. The entire task has been carried out with a proprietary GIS/ RS software package. The computer facilities of CEGIS were used for processing and analyzing the satellite images. The primary software ERDAS Imagine was used for image processing, raster GIS analysis, and Windows NT-based ArcInfo for vector works.

2.3 Co-registration of Satellite Images

After geo-referencing the satellite images, it was found that the images of the same path and row of different years did not match each other. Maximum \pm 60 meters (2 pixels) offset was found within the images. For this reason, co-registration was required to eliminate the offset distance within the images of different years. All the images were co-registered using the 2010 LANDSAT image mosaic of CEGIS, which is a DGPS corrected image. The coordination for the GCPs applied in the geo-referencing process was collected from the image mosaic. Finally, the updated images were used for the morphological analysis of this study.

2.4 Bankline Delineation from Satellite Images

A bank line/coastline is the physical boundary between land and water (Dolan et al., 1980). The position of the coastline varies constantly owing to cross-shore and along-shore sediment transfer, as well as the constant changing of water level with the tide along the coastal border (Boak & Turner, 2006). CEGIS developed a method of defining the shoreline using satellite pictures to mitigate the influence of tidal fluctuation (2009). The image pixel size and the existence of a vast intertidal flat produced errors in the delineation of the shorelines. However, the final result is free of major inaccuracies because the modifications were so enormous compared to the error margins.

After geo-referencing the aerial and satellite images, ArcGIS tools delineated river bank lines through image interpretation. Although the dry season satellite images were used in this study, bank lines were traced considering the wet season extent of the rivers. Furthermore, bank lines were used to observe the maximum shifting of the river to both banks and for further analysis.

2.5 Opportunity to use Google-earth Images

Time-series google-earth images (2005, 2010, 2015 & 2020) were downloaded for better resolution (less than 30 m). The resolution of these images has been found to be 12 m-13.5 m. However, several problems have been found while delineating the bank lines using Google Earth Engine. First, all the images collected from google earth for a specific year may not be on the same date. Thus, bank lines may vary due to temporal differences (i.e., months) for the same year. Moreover, spatial distortion has been found in the images (**Figure 2.3**). As satellite images seem to be more accurate (having satellite images of the same date and distortion-free as well) in identifying the difference between river and floodplain because of existing bands, Google Earth has not been used for the analysis.



Figure 2.3: Shifting between the Google-earth images of the same year (2010)

3. Approach and Methodology

Geomorphological studies presented in this report divided the scales into two: the first is long-term, the millennium to centennial scales, and the second is a decade. The longer-term study comprises the Late Holocene to last two to three centuries. It addressed the river system's delta development processes and evolution during the last 7,000 years. It highlighted the characteristics of the river systems (the Ganges, Jamuna, and Meghna) and different geomorphic constraints such as geology, topography, and physiography in different time scales. This knowledge, however, helped to understand the present-day behavior of the rivers surrounding the tidal plain.

Decade scale behavior includes the processes of riverbank erosion/accretion, widening/narrowing of the rivers, and migration of meandering bends, which were used to predict the future development in 5, 10, 20, and 30-year intervals. While the structures have a design life of 50-years, morphological predictions extending past 30 years have an extremely high degree of uncertainty and are not reliable. Therefore, predictions regarding future bank migration have only been made for a maximum of 30 years past the latest available satellite image. Consequently, monitoring and maintenance is required throughout the embankments' lifetime, and must include bank erosion monitoring.

This section outlines the methodology of the geo-morphological and planform study. The methodology is presented in **Figure 3.1**. The first column shows the inputs, the second column the processes, and finally, the rightmost column, the output. The detail of the approach and methodology has been described in the following sections.

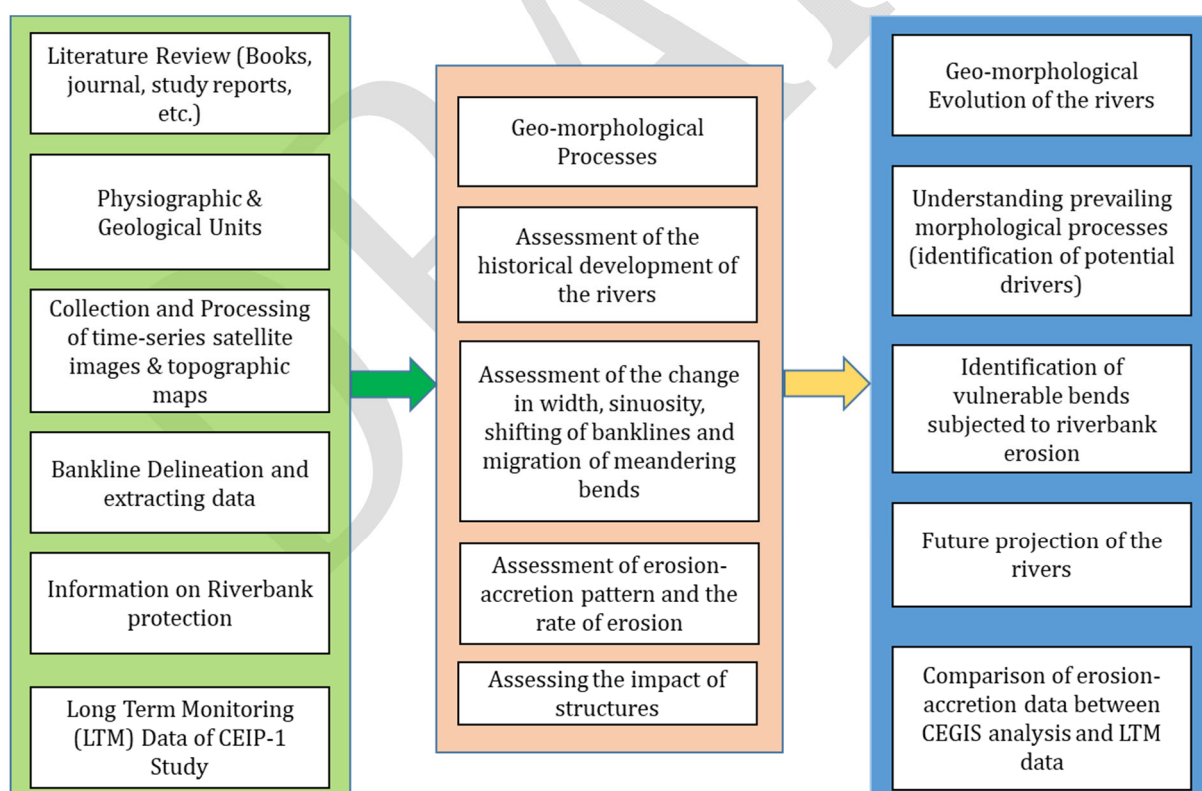


Figure 3.1 Flow diagram of a methodology of the study

Literature Review

By carrying out the morphological study under the CEIP-II project, CEGIS has enhanced the knowledge of river geomorphology and planform. The knowledgeability has been specified and updated for understanding the river system in the polders of Khulna and Barishal areas. The study reviewed concern reports and their inherent development processes to understand the system. River responses to various triggering agents were reviewed in terms of content analysis for a better understanding of the river(s) when so engaged through outside interventions.

Several other studies were carried out during the last decades, particularly on the rivers in the southwest, south-central, and Meghna estuary areas. These documents were thoroughly reviewed to assess the inherent morphological processes of the rivers in the study. The details of this information are explained in Chapter 4.

Physiographic and Geological Settings

Data on physiographic features and geological information in Bangladesh were collected from CEGIS archives and then extracted for the southwest (Khulna) and south-central (Barishal) regions.

Collection and Processing of Historical Maps, Topographic Maps and Satellite images

Along with historical maps from 1776, 1840, and 1943 processed historical maps and topographic maps of 1943 and time series satellite images from 1989 to 2021. These were used as input data for assessing the historical development of the rivers and to understand the change of different morphological parameters (width, sinuosity, change of banklines, erosion-accretion) in the study area over time. Many relevant historic maps, images, and data for the study are available with CEGIS.

Bankline Delineation

Time series satellite images were aligned to delineate the bank lines of the Study Rivers for a different period based on the definition described in Section 2.4. River bank lines separate a river from its floodplains. These bank lines were used to assess the shifting, erosion-accretion calculation, river migration, and finally, the projection of the rivers for the future.

Long-term Monitoring Data

Long-term monitoring data on erosion-accretion for the different rivers in the study area were collected from the CEIP-I report to check the variation of the differences as per the analysis of CEGIS.

Enhancing Knowledge Baseline of Geo-Morphological Processes

A review of literature and studies has established a knowledge baseline of the geo-morphological evolution of the rivers in the Khulna and Barishal areas. This baseline knowledge helped to understand the overall morphological process and future development.

Assessment of Physiographical and Geological Settings of the study area

The physiographical units and geological maps were used in the study area. That helped to assess the physiographical and geological setting of the study rivers.

Historical Development of the Rivers

Historical maps of 1943 and time-series satellite images from 1989 to 2021 were studied to know the historical development of rivers. GIS/RS mapping, overlay techniques, and spatial analyses were carried out to quantify the physical changes over the known period. This exercise, coupled with the exercise, led to defining and describing the baseline of the morphological processes of the river system for comparative analysis and future development. The knowledge baseline, maps, and data helped to determine and quantify the development of the peripheral rivers in the polders of the study area in the historical timescale.

Assessment of the Change in Width and Sinuosity

Channel width is defined as the shortest distance between two banks in any section of a river. The width of the rivers was measured at a different section of the rivers using the Arc-GIS tool. In this study, the average width was calculated for different periods, and the trend of the change in width was observed. This phenomenon has been taken into consideration during the prediction of the rivers for the future.

On the other hand, river sinuosity is defined as the ratio of the curved length to the straight length. Like width, the river's sinuosity was observed for different periods, which helped to assess the change of the river in a particular time period and considered in projecting the rivers.

Assessment of shifting of the Bank lines

For the assessment of the shifting of the rivers, bank lines were overlapped with others. In this study, bank lines of the year 1989, 2003, 2010, 2015, and 2021 were used, and the lateral shifting of the channel was observed from 1989 to 2003, 2003-2010, 2010-2015, and 2015-2021. This shifting of the bank lines helped to understand the shifting process of the channel over time. In addition to that, this information assisted in calculating the life span of the meandering bend of a particular river which is very important for the prediction of the rivers

Assessment of Migration of the Meandering Bends

Time series bank lines of 1989, 2003, 2010, 2015, and 2021 were superimposed to identify the migration of the meandering bends. Meanders result from erosion-deposition processes tending toward the most stable form in which the variability of certain essential properties is minimized. This minimization involves the adjustment of the planimetric geometry and the hydraulic factors of depth, velocity, and local slope (Leopold et al., 1966). The bend development process is different in different types of rivers. The average life span of a bend in the Jamuna River (a braided river) is around 4 to 5 years; meanwhile, bends are much more stable for a meandering river. Bend's development process is very active in the major rivers in Bangladesh. The development process of the meandering bends of this river is well explained by Hooke's description (Hooke 1977), which is presented in both **Figure 3.2**.

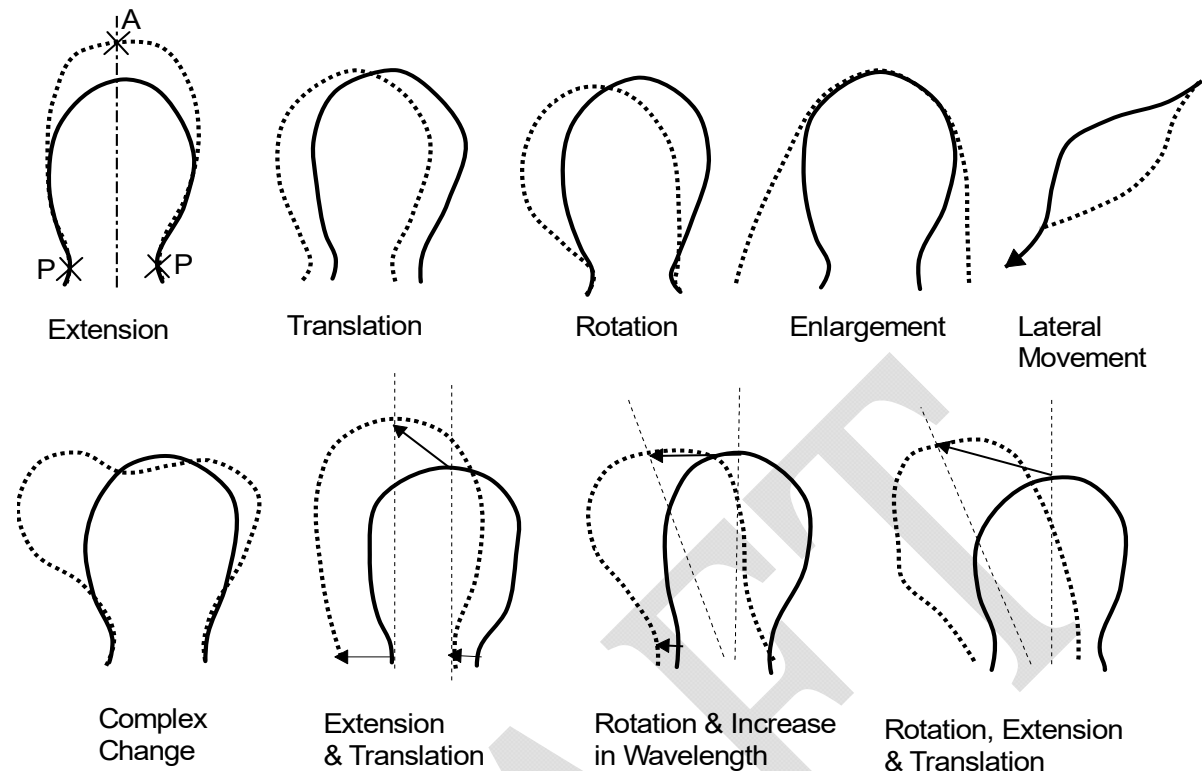


Figure 3.2: Concept of bend development (Hooke, 1977)

In the meandering bend, the type of the bend migration was assessed, whether it is a single type (like extension) or a combination of more than one type (for example, both extension and translation). This process is critical to projecting the rivers in the Khulna and Barishal areas that have taken into account during the delineation of the prediction for different periods.

Assessment of Erosion-accretion Pattern and the Rate of Erosion

For the erosion-accretion calculation of the Study Rivers, bank lines for 1989, 2003, 2010, 2015, and 2021 were superimposed. After that, GIS techniques were applied to calculate the river's erosion-accretion on an annual and decade scale. In addition, an erosion-accretion pattern was observed whether the river is in an increasing or decreasing phase. Additionally, the rate of the maximum lateral extent of erosion and eroded tidal plain, was calculated for each bend.

Calculation of Life Span of the Bend & Assessment of the Impact of the Bank Protection Works

Assessing the life span of eroding the meandering bend of any river has predictive value for water resources planners and engineers. In this study, the average life span of every eroding meandering bend. The lifespan of eroding bends is considered as the period of continuous erosion of a virgin river reach. The temporal resolution of the satellite images varied from 14 to 5 years; therefore, the lifespan of the bends is calculated as the periods of the continuous presence of river bank erosion.

Bank protection structures data were collected from Royal Haskoning. This study collected information on river bank protection for the Barishal polders area. The presence of bank

protection limited the lateral extension of the channel and reduced the life span of the erosion of a particular river bend.

Geo-morphological Evolution of the Rivers

The knowledge baseline on the geo-morphological processes was derived from the literature review helped to understand the geo-morphological evolution of the rivers. The development and gradual progress of the delta towards the sea have brought about changes in the course and planform development of the rivers, which might have long-term influence.

Prevailing Morphological Processes

Analysis of historical maps, satellite images, and physiographical & geological settings of the area and relevant review of the literature made it possible to interpret and quantify the overall morphological processes of channel shifting and off-take dynamics and thus understand the morphological processes of the rivers. Morphological processes of the rivers were reviewed in the millennium, centennial, and decadal times. This has helped to identify the potential drivers for changing the morphological behavior of the rivers.

Identification of Vulnerable Bends

This is the step pre-requisite for the prediction of the rivers. In this regard, the rivers' time series bank lines were overlapped to assess the channel's migration over time. Laterally, locations with the progressive migration of the bank lines were identified as vulnerable locations in different periods.

Projection of Future for the Rivers

A lack of data makes forecasting erosion lines using only statistical methods impossible. For river prediction for different periods, some criteria are considered, such as erosion rate, widening/narrowing of the river, bend characteristics, the trend of the river, and changes in the rivers adjacent to the study river.

Furthermore, projecting the rivers for a specific year depends on the spatial resolution of the bank line shifting and the temporal resolution of the satellite image. The following criteria have been considered for the prediction:

The spatial resolution of bank line shifting > temporal resolution * factor (4 or 5)

The study identified all the erosion-prone areas and assessed the river's extent of bank line shifting. Prediction of the rivers for 10, 20, and 30 years have been delineated with the average line. The annual rate of meandering bend migration was less than the spatial resolution of time-series satellite images. However, because of the coarse resolution of satellite images, uncertainty in predicting for 5 years would be very unrealistic.

Moreover, due to the lack of relevant data for a longer period, prediction for the 50 years yields very high uncertainties, and prediction results will not be representative—of spatial and temporal resolutions of the images. While predicting future migration, the parameters presented below are extracted from the satellite images and analyzed.

- ✓ The starting point of erosion concerning the inflection point bend;
- ✓ The ending point of erosion concerning the inflection point bend;
- ✓ Location of the maximum erosion;

- ✓ The direction of migration and type of migration;
- ✓ The rate of erosion of a particular bend;
- ✓ The life span of the bend.

It is worth noting that erosion-accretion and river shifting have been done for the whole river while the prediction has been made only in those locations surrounding the polders.

Comparison of CEGIS with LTM Data

The study checked erosion-accretion quantity for different periods with the LTM data of CEIP-1. If there is a variation in data, possible reasons were listed to explain the differences.

DRAFT

4. Physical Processes

By carrying out the morphological study under the CEIP-2 project, CEGIS enhanced its knowledge of river geomorphology and planform. This knowledge is further specified and updated for understanding the rivers' system in the polders of Khulna and Barishal areas. Relevant available reports were reviewed for a better understanding of the system and the inherent development processes. River responses to various triggering agents were examined in terms of content analysis for a better experience of the river(s) when engaged through outside interventions.

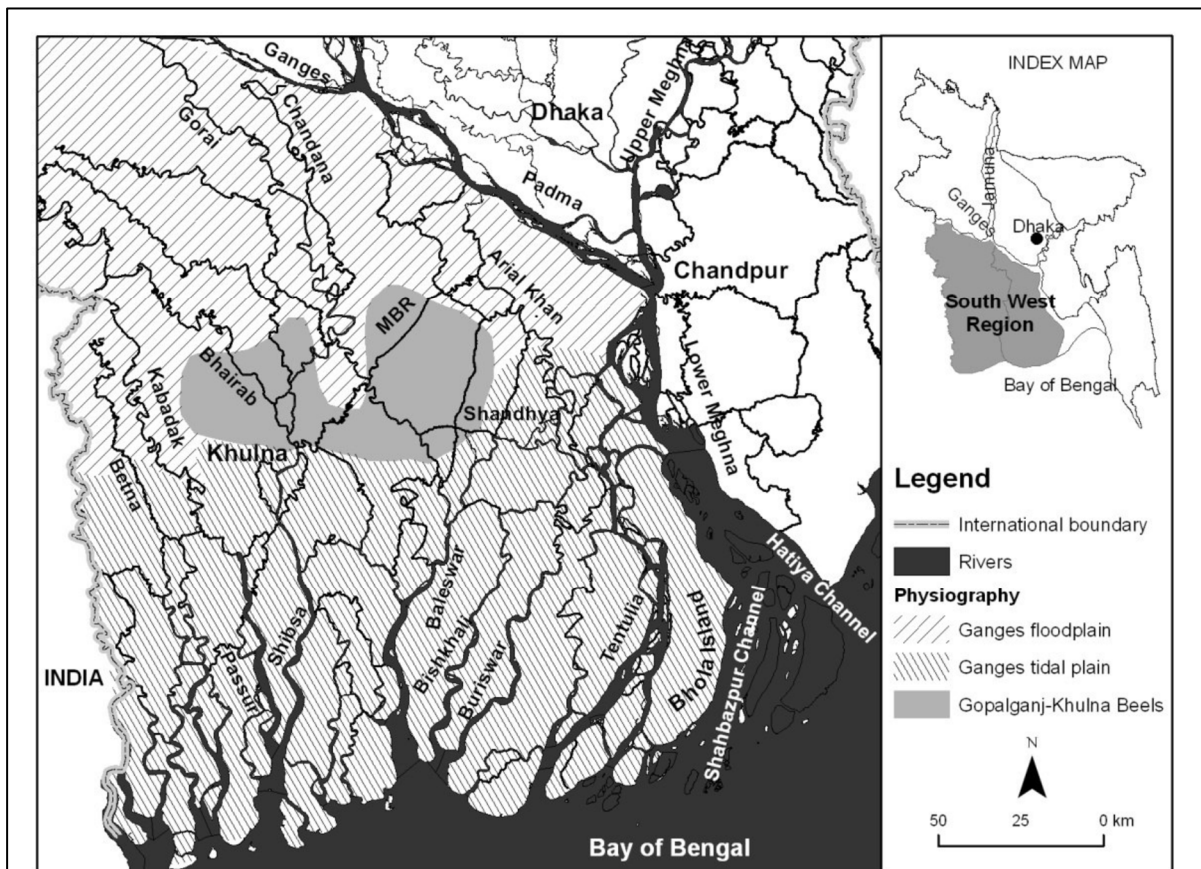


Figure 4.1: Present river system in the southwest region of Bangladesh

4.1 The setting of the Physical Processes

Geological Setting

The Ganges broke through the eastern margin of the Rajmahal Hills to enter the basin during the Pleistocene (Bhuiya, 1993). Since the Pleistocene, the Ganges has, together with the Brahmaputra, delivered enormous quantities of sediment to the Bengal Basin. These sediments have formed the world's largest river delta with an area of about 100,000 km² and a sub-aquatic fan extending 3,000 km south into the Bay of Bengal (Goodbred et al., 2003).

Several million years ago, the NE portion of the Indo-Australian plate fractured and sank below what was then sea level. This depressed basin then attracted all rivers to meet the sea. Over time, this depression filled with sediment to form the present Bengal Basin. The basin is prograding from a NE hinge line (Goodbred and Kuehl, 2000b). 4 km deposition at the hinge

and more than 10 km at the shelf break have made the world's largest fan deposits (Goodbred and Kuehl, 2000b). This has a volume of approximately 1.25 km^3 for approximately 33,106 km^2 of area (Curray, 1994), mainly carried by the Ganges–Brahmaputra (G-B) Rivers from the foreslope and backslope of the Himalayas, respectively (Goodbred and Kuehl, 2000b). **Figure 4.2** shows the geological features of Bangladesh and the presence of 'Hinge Zone', which will be elaborated in the subsequent section.

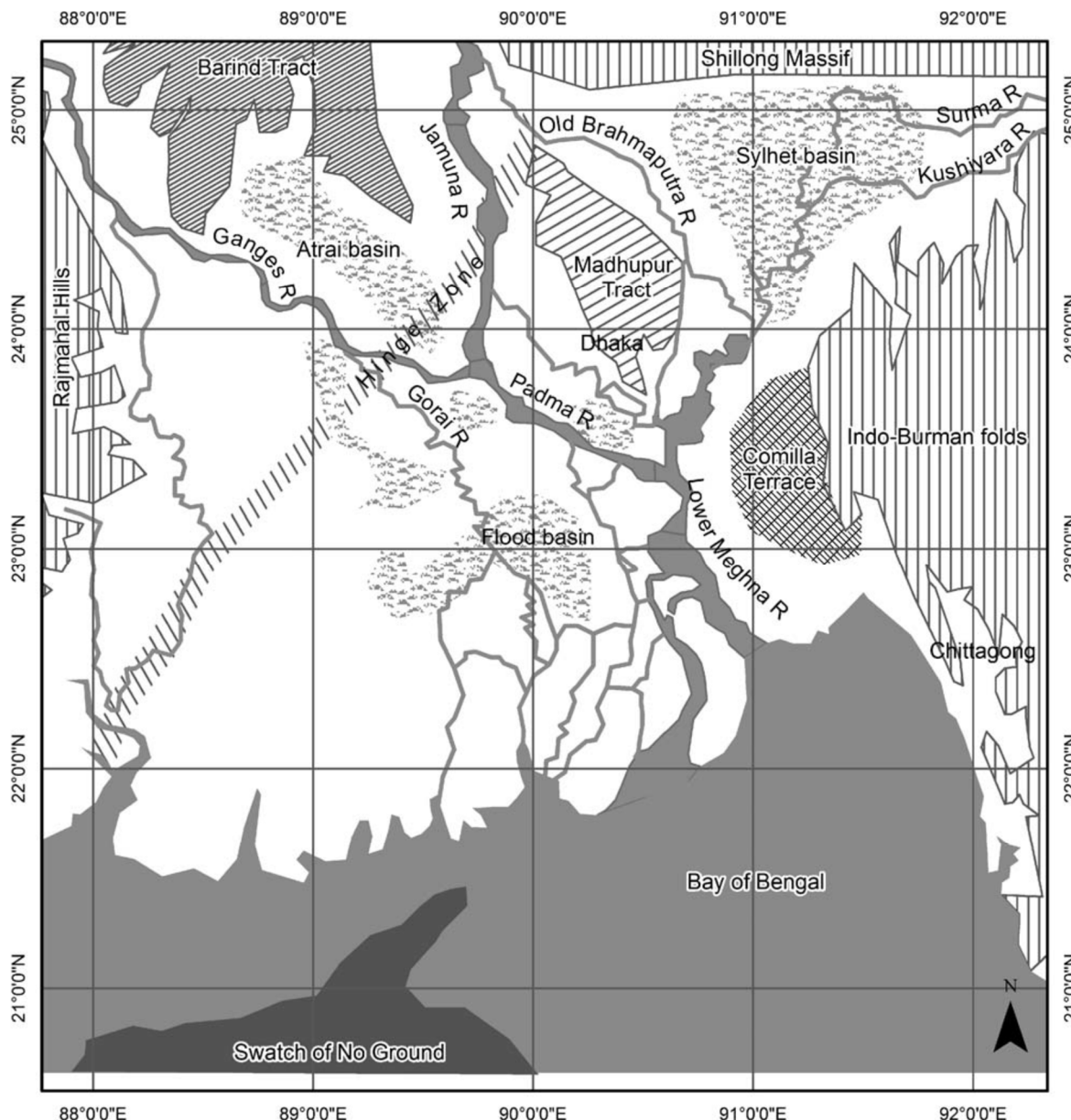


Figure 4.2: Geological setting (Akter et al., 2016)

Tectonics and Seismicity

The Bengal Basin is very active tectonically, being limited to the north by one of the world's main subduction faults along the front range of the Himalayas and to the east by the vast Indo-Burma transform fault (Bhuiya, 1993). Regional and basin tectonics have played and continue

to play significant roles in delta formation processes (Goodbred et al., 2003). The influence of regional scale tectonics involves a consistent and plentiful supply of sediment to the basin due to Himalayan denudation, as well as occasional inputs of extra material due to the destabilizing effects of catastrophic earthquake events. Basin-scale tectonics include a variety of local processes that create local landforms and terrain characteristics, such as over-thrusting, compression, and faulting.

There is substantial evidence that earthquakes and related seismic activity have directly influenced river courses and delta formation processes. The 1762 earthquake, for example, caused a vertical displacement of the Madhupur Jungle, that thought to have contributed to the avulsion of the Brahmaputra River from its former course through the Sylhet Basin (to the east of the Madhupur Jungle) to its present course as the Jamuna, about 60 kilometers to the west, sometime near late 18th century (Fergusson, 1863).

Fergusson, 1863 proposed the presence of a 'zone of weakness' caused by a significant fault at a depth between the Barind and Madhupur Pleistocene terraces, roughly aligned to the current Jamuna River flow. Morgan and McIntire, 1959 relied on this notion to explain historical changes in the courses of the major rivers as mostly the product of concurrent tectonics (**Figure 4.3**).

However, according to Goodbred et al., 2003, when the Brahmaputra River changed course in the late 19th century, it was not the first time it had occupied the 'zone of weakness.' They suggest that its course may shift again in the future, including the possibility of the river reverting to its former course through the Sylhet Basin. According to this explanation of course shifting, reconnection of the Brahmaputra's heavy sediment supply with the Sylhet Basin would more than compensate for land subsidence, resulting in aggradation and, eventually, another shift to the alternative course west of the Madhupur when the gradient became more favorable. This might describe as a form of 'geomorphic threshold' behavior caused by slope changes (Schumm, 1977).

Sarker and Thorne (2006 and 2009) described the effects of the Great 1950 Assam Earthquake, which caused 45 billion m³ landslides in the Himalayas (Vergese (1990). Most of the debris from landslides poured into the Brahmaputra and transported to the Meghna estuary through the wash load and sediment slug. Downstream propagation of wash load took only a few years and did not show any significance in the fluvial system but caused huge net land accretion of 1720 km³ in the Meghna estuary. While bed material traveled through the fluvial system as sediment slug, altering the size, shape, depth, and planform. At the same time, traveling of sediment slug from Assam, India, to the Meghna estuary took nearly five decades to alter the planform and morphological behavior of the rivers.

The study observed major rivers draining through Bangladesh. However, it couldn't specify whether it is primarily controlled by tectonics (as suggested by Morgan and McIntyre, 1959) or by threshold behavior in fluvial processes operating within the context of longer-term, regional tectonics with specific seismic events impact (as explained by Goodbred et al. 2003).

However, the opposing roles of the Ganges and Brahmaputra Rivers in long-term delta construction are beautifully illustrated by Morgan and McIntire, 1959;

"while the Ganges has been building a broad, lateral deltaic mass, the Brahmaputra, because of structural activity, has been building a thicker mass of sediment in structurally subsiding basins."

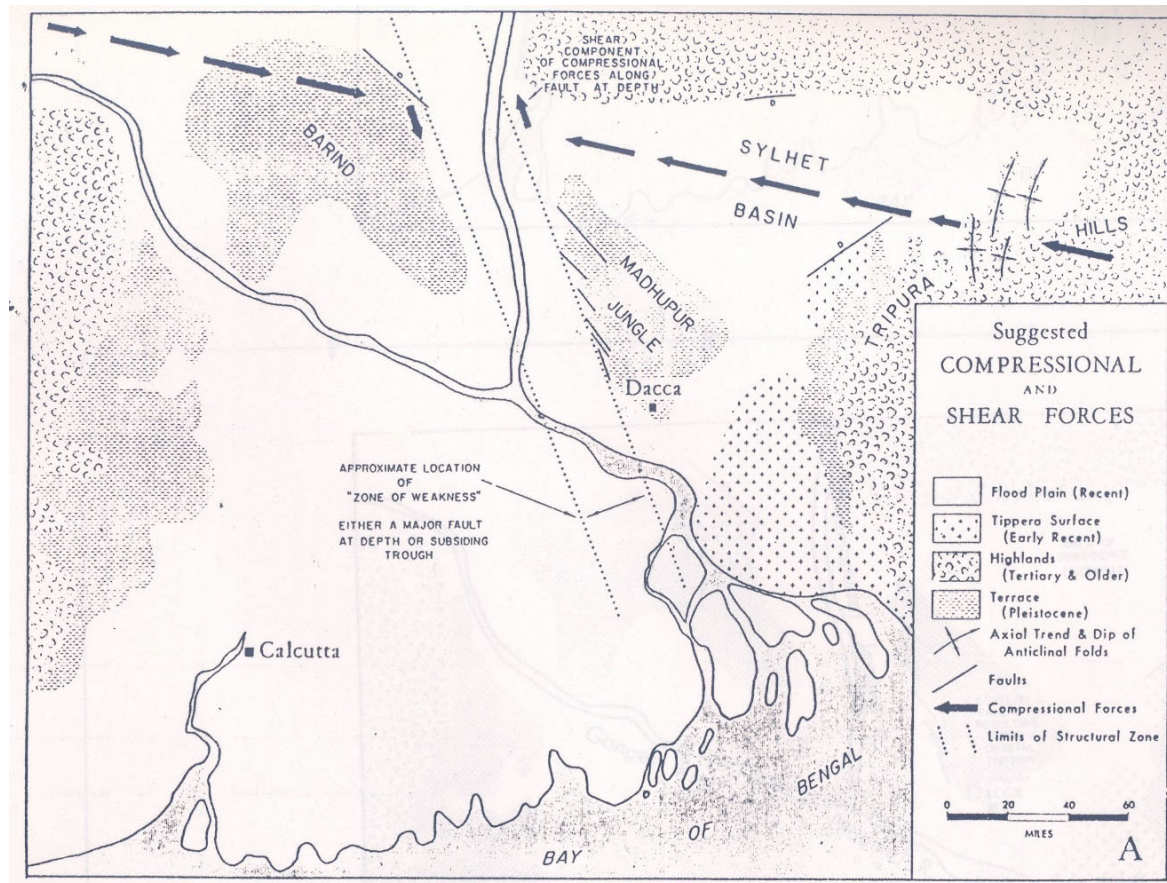


Figure 4.3: Structural forces affecting the Bengal Basin (Morgan and McIntire, 1959)

Southwest Bangladesh is a seismically quiet zone represented by zone III with Bask seismic coefficient of 0.04. The study area lies in the Khulna and Barishal divisions, which are seismically relatively quiet. The eastern and northern parts of the Bengal Basin have more seismic and tectonic activity than the southern and western parts (Morgan and McIntire, 1959).

Physiographical Setting

Based on physiography, soil properties, soil salinity, depth, and duration of flooding, 30 agro-ecological units were demarcated as per the Land Resources Appraisal of Bangladesh for Agricultural Development. Out of 30 units, our study area lies in 8 units, (Figure 4.4) of hydrological zones SW, SC, and ME (Figure 4.4). Brief descriptions of those Units with relevant information areas are presented in the following paras.

The total area of these polders covering this study area lies in the Ganges Tidal Floodplain unit, as shown in **Figure 4.4**.

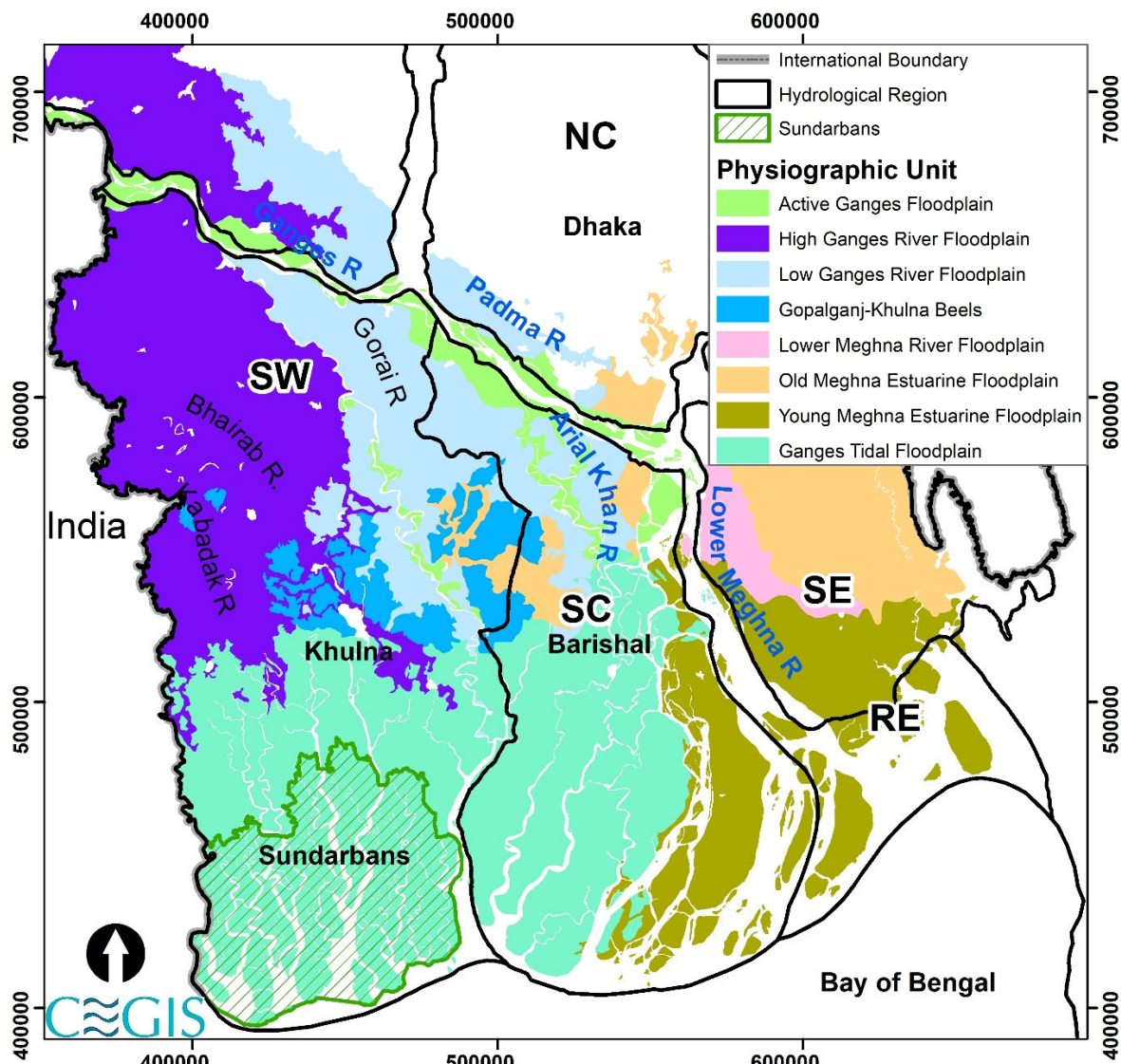


Figure 4.4: Map showing the physiographic units of SW and SC regions

Active Ganges Floodplain

Mainly char areas along with newly accreted floodplain of the Ganges, Padma, Gorai, and Arial Khan rivers have an irregular relief of broad and narrow ridges and depressions, interrupted by cut-off channels. Both the outline and relief of char formations are liable to change in each flood season due to bank erosion by shifting channels and deposition of irregular thicknesses of new alluvium. Local differences in elevation are mainly 2-5 m but become less in the south near the Meghna estuary. This alluvium covers the SW region's northern boundary and the SC's northeast boundary.

The ridges have complex mixtures of calcareous sandy, silty, and clay alluvium, with some shallowly developed loamy soils and depressions, have dark gray clays on older alluvial areas. The proportions of sandy, silty, and clay alluvium vary from place to place and year to year. Downstream from the Ganges- Jamuna confluences, the balance of Ganges and Jamuna sediments also varies yearly. Silty Gange's material is browner and calcareous. Silty Jamuna alluvium is gray or grayish brown and non-calcareous; overall silty sediments are more

extensive than sandy ones, especially in upper and lower sub-regions. In addition to lime, Gange's alluvium is also rich in weighable minerals, and a proportion of its clay fraction is swelling clay.

Ganges Tidal Floodplain

This unit covers the southern part of both the SW and SC regions. The greater part of this region has smooth relief. The region is identified with a close network of interconnected tidal rivers and creeks. River banks generally stand about a meter or less above the level of adjoining basins. In the west, these channels are saline throughout the year, although less saline in the rainy season than in the dry season. In the east, channels carry fresh water in the rainy season, and salinity only affects the dry season, mainly in the second half.

There is a general pattern of gray, slightly calcareous, loamy soils on river banks and gray or dark gray, non-calcareous, heavy silty clays in the extensive basins. Soils become slightly saline to strongly saline at the surface during the dry season, and soils in some portions are subject to tidal flooding with brackish or saline water throughout the year

Young Meghna Estuarine Floodplain

The region is almost level with very low ridges and broad depressions—few or no creeks, except on tidally flooded margins. Shifting channels erode land and deposit new char formations.

The main soils are gray to olive, deep, silt loams, and silty clay loams, stratified either throughout or at a shallow depth. Almost everywhere, the stratification is fine. Young soils are calcareous throughout and mainly saline in the dry season. Older soils are noncalcareous and are only very slightly or not saline. The differences between soils are not significant.

Old Meghna Estuarine Floodplain

Smooth, almost level floodplain ridges and shallow basins characterize this floodplain. Relief is made irregular locally by man-made cultivation platforms east of Chandina and in parts of Munshigonj, Sonagaon and Sariatpur.

Soils are relatively uniform within this region, between adjoining ridges and basins, and between subregions. Silty soils predominate, but there is significant silty clay in clay basin soils in Dhaka, Madaripur-Gopalpur, and Barisal.

Gopalganj-Khulna Beels

The downstream reach of the Madaripur Bill Route is located in the Gopalganj-Khulna Beels area, although the MBR feeds water to the beel area during pre-monsoon and drains out during post-monsoon. This physiographical unit occupies several low-lying areas between the Ganges River Floodplain and the Ganges Tidal Floodplain. Thick peat deposits occupy perennially wet basins, but it covered by clay around the edges and calcareous silty sediments alongside the Ganges distributaries crossing the area. This is the largest peat stock basin of Bangladesh. The basins are flooded by clear rainwater during monsoon.

High Ganges Floodplain

Almost all of these units fall in the SW region. The High Ganges Floodplain covers the upstream of the Ganges from the Gorai off-take that covers a complex relief of broad and narrow ridges and inter-ridge depressions, separated by areas with smooth, wide bridges and basins. The upper parts of high ridges stand above average flood level. The lower parts of ridges and basin margins are seasonally shallowly flooded, but some deep basin centers are moderately or deeply flooded. There is an overall pattern of olive-brown, silt loams, and silty clay loams on

the upper parts of floodplain ridges and dark grey, mottled brown, mainly clay soils on lower ridge sites and basins. Most ridge soils are calcareous throughout. Some higher soils have non-calcareous upper layers of 30-60 cm. Non-calcareous layers are slightly acidic or neutral but strongly acidic in some heavy basin clays.

Low Ganges River Floodplain

The Low Ganges River Floodplain covers the left bank of the Gorai River and extends up to Madaripur and Shariatpur districts. It covers a typical meander floodplain landscape of broad ridges and basins. Generally, there is somewhat irregular relief alongside rivers crossing the region, comprising broad and narrow ridges, inter ridge depressions, and cut-off channels. Differences in elevation between ridge tops and basin centers generally range 3-5 m but are less near the northern and southern boundaries. The general soil pattern is olive-brown silt loams and silty clay loams in the highest parts of floodplain ridges, and dark grey silty clay loams to heavy clays in the lower sites.

Lower Meghna River Floodplain

The deposits of this region are mainly olive silt loams and silty clay loams. They occupy a somewhat irregular ridge and basin relief but with little difference in elevation between the highest and lowest parts. Ridge soils in the extreme south show patches which become slightly saline in the dry season.

All of our study 15 polders are in the Ganges tidal plain. The majority of this area has a flat terrain. The site is distinguished by a dense network of interconnecting tidal rivers and creeks. River banks are typically one meter or less above the level of adjacent basins. These creeks are salty all year at West, but less during the rainy season than the dry season. In the east, tidal creeks convey fresh water throughout the rainy season, while salt only impacts channels during the dry season, primarily in the second half.

There is a common pattern of gray, somewhat calcareous, loamy soils on river banks, and in the wide basins, gray or dark gray, noncalcareous, heavy silty clays. During the dry season, soils become somewhat salty to highly saline at the surface, while soils in particular areas are exposed to tidal inundation with brackish or saline water all year.

Topographical Setting

The study sites are found between 1.5 and 2 mPWD levels. A fairly gradual slope characterizes the delta's terrain, and a considerable portion of the delta is 2 m below the PWD datum, which is around 1.5 m above Mean Sea Level (MSL) (Figure 4.5). The Ganges floodplain dominates the elevated hills near the northern point, which have a steeper gradient (Brammer, 1995). Next to this unit is a low-lying stretch that runs southwest to northeast. Next to this unit is a southwest to northeast aligned stretch of the low-lying area with a minimum elevation below MSL, which is classified as the Gopalganj-Khulna beels. This depression is dissected by recent and old courses of the rivers. River courses from the west margin are the Betna and the Kabodak, the Bhairab in the SW region, and the Madhumati (in the SC region). This depression is clearly marked in Rennel's map (1976). Two remarkable changes occurred here – although the course of the Gorai-Madhumati passed through the depression, it could not raise its level, and the Gopalganj depression was extended up to the south of Barisal. The southernmost areas along the coast consist of the Ganges tidal plain at a higher elevation than the Gopalganj-Khulna beels. The terrain has a reverse slope to the south. Elevated lands are in the east and south.

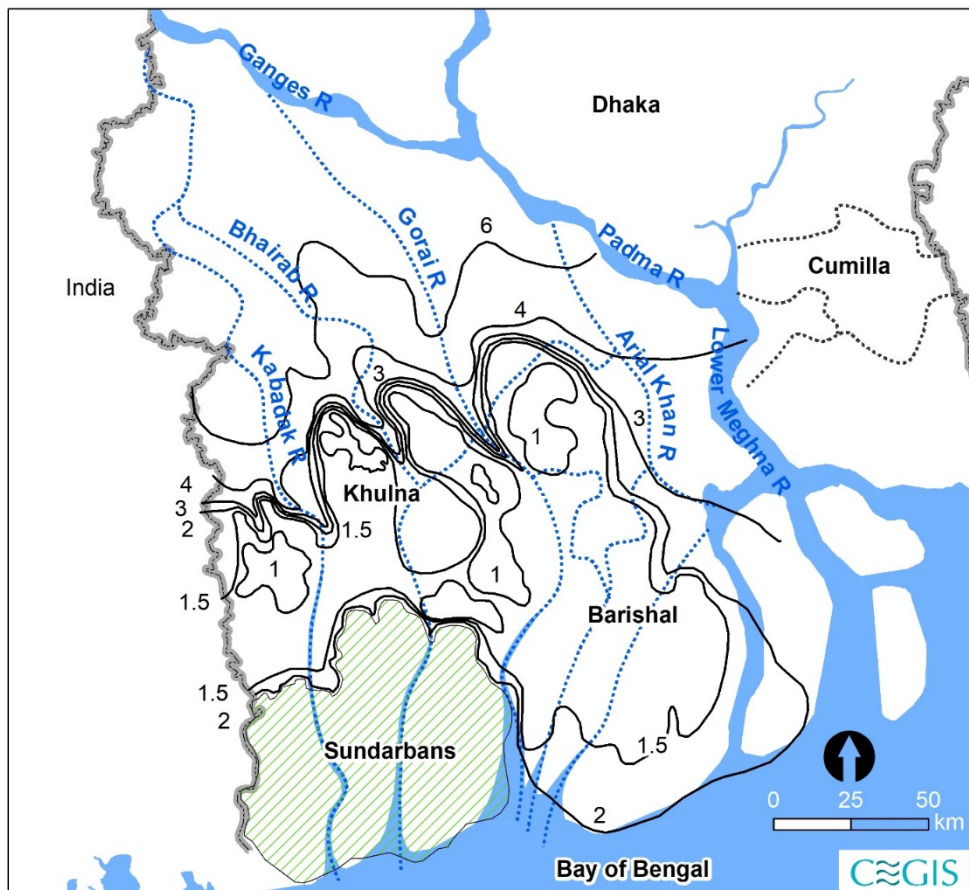


Figure 4.5: Contours of elevation are in mPWD based on the DEM of the 1950s and the river courses in 1943

Based on the elevation model shown in **Figure 4.6**, the southwestern part of the delta is characterized by three distinct features. The elevated area at the northwestern tip has a higher gradient and mainly consists of the Ganges floodplain, as shown in the profile of section SW-1. Next to this unit is a southwest to northeast aligned stretch of the low-lying area with a minimum elevation below MSL, which is classified as the Gopalganj-Khulna Beels, located between Haparkhali and Nunda **Utra** rivers in section SW-2 (**Figure 4.7**). This depression is dissected by recent and old courses of the rivers, like the Bhairab, Atai, Atharobanki, and Gorai-Madhumati rivers. Compared with the depressed area shown in Rennel's Map of 1776, the recent dissection chronologies are Gorai-Madhumati, Bhairab, and Kabadak rivers. Before this, the southernmost section SW-2 shows that the slope found from 390 to 440 km easting is about 9 cm/km, whereas there is a reverse slope with less than 2 cm/km in the rest of the section as a contribution of the delta building process. In the book 'the history of the Rivers in Ganges delta,' William (1919) also indicated the similar topographical formation of two opposite slopes developed in the floodplain and tidal plain.

Two north-south directed profiles of sections SW-3 and SW-4 (**Figure 4.8**) exhibit that a very gentle slope characterizes the topography of the southwest region, and a large part of the delta lies 2m below the PWD datum, which is equivalent to about 1.5 m above Mean Sea Level (MSL). The areas along the coast consist of the Ganges tidal plain at a higher elevation than the Gopalganj-Khulna beels. The terrain has a reverse slope to the south, as in section SW-4. The Sundarbans is the southern part of section SW-3 (not shown in the analysis and results).

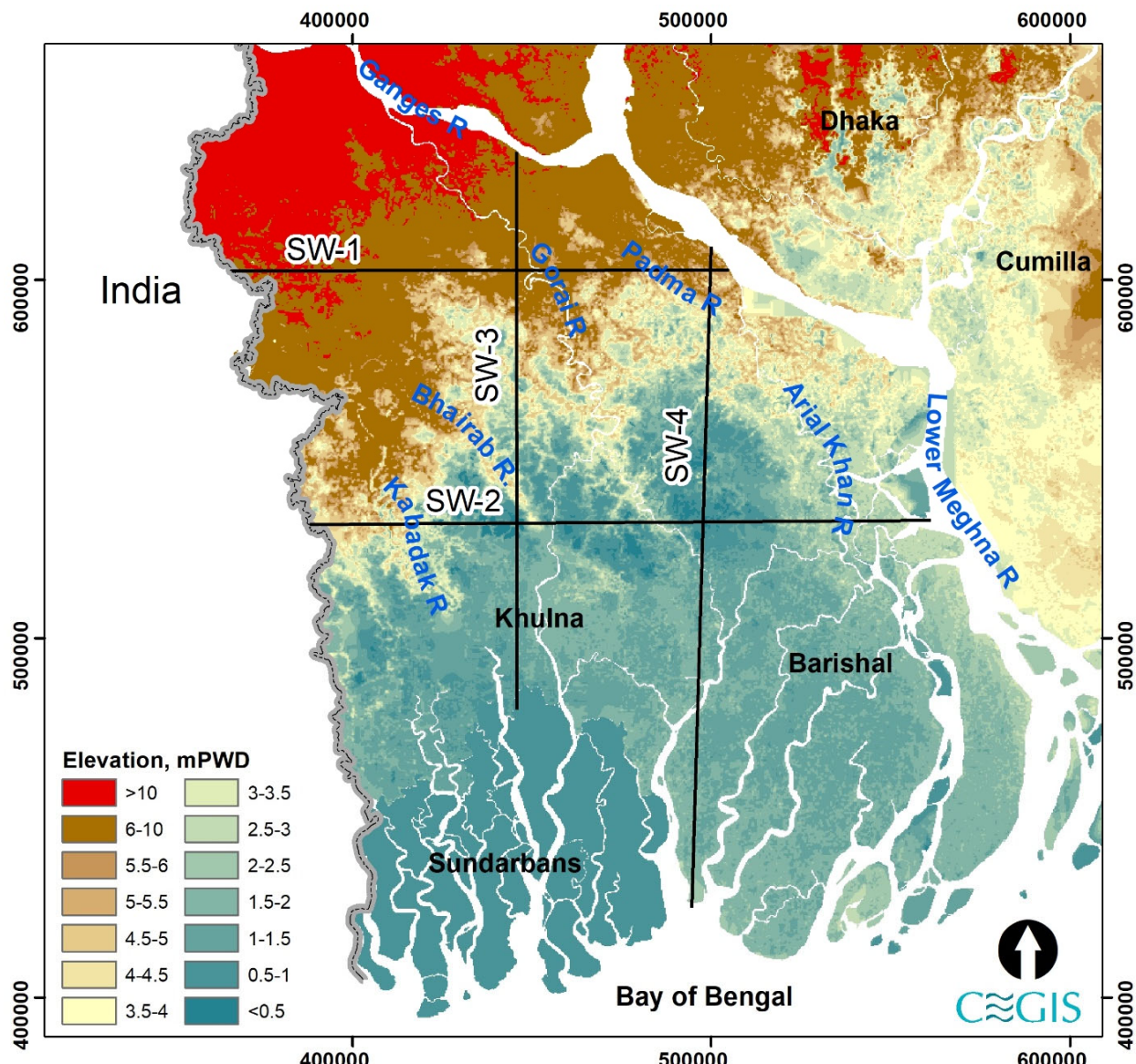


Figure 4.6: Topographical setting of the South-West and South-Central regions of Bangladesh

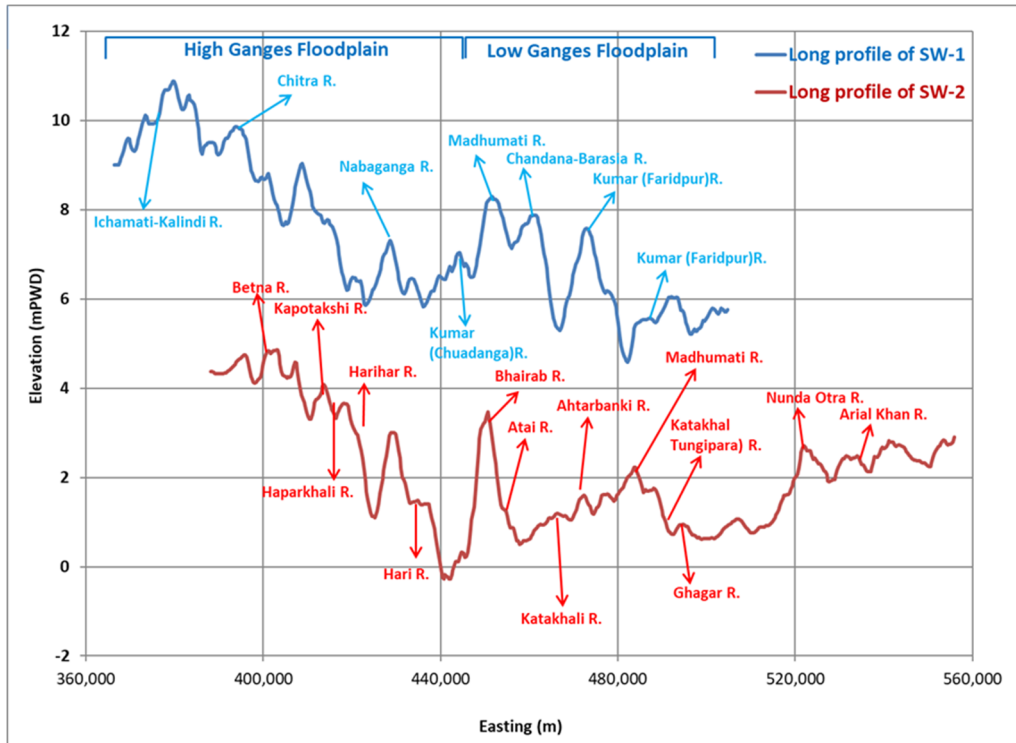


Figure 4.7: East-west surface profile in South-West and South-Central regions of Bangladesh

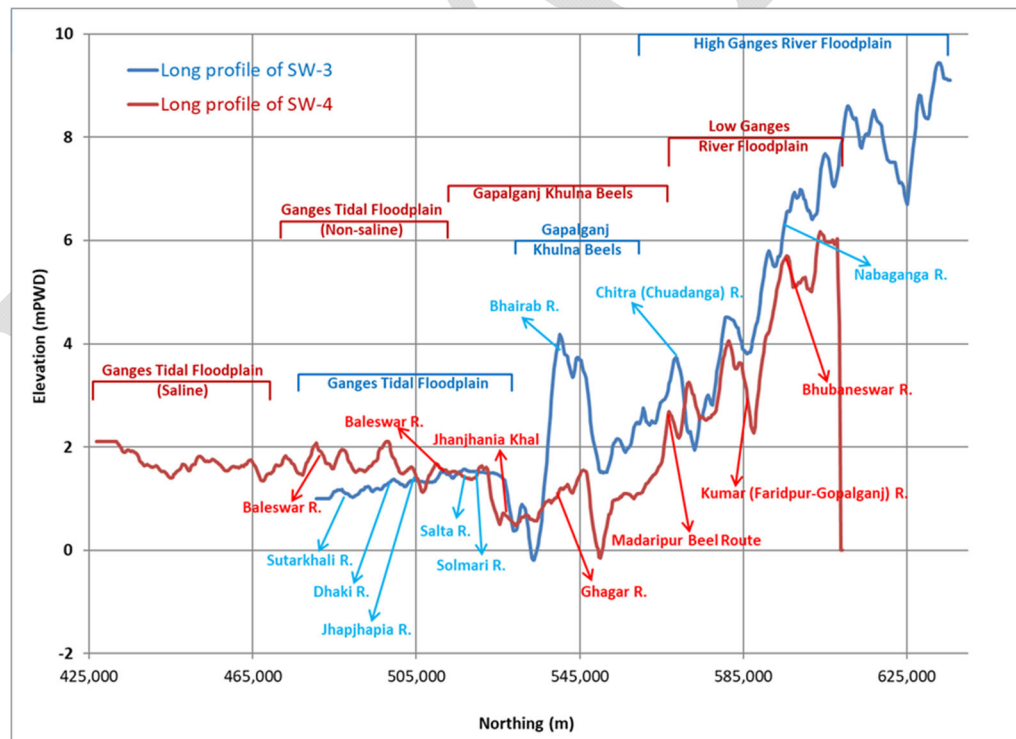


Figure 4.8: North -south surface profiles in South-West and South-Central regions of Bangladesh

Climate Setting

In Bangladesh, cyclical reversals in atmospheric pressure and winds distinguish summer and winter. During the winter, a high-pressure trough exists across the northern section of India. A stream of chilly air moves eastward from this high pressure and enters the country from the northeast corner, turning its trajectory clockwise, practically right-angle. During this time of year, the wind inside the country has a northerly component (flowing from north or northwest). This wind is a component of the South Asian subcontinent's winter monsoon circulation.

In the summer, however, a center of low pressure forms over the west-central section of India due to excessive surface heat. As a result, a stream of warm and moist air from the Bay of Bengal rushes into Bangladesh toward the aforementioned low pressure (similar flow prevails from the Arabian Sea toward India). This wind is a component of the subcontinent's summer monsoon circulation. As a result, the prevalent wind direction in Bangladesh throughout the summer season is often southerly (flowing from the south, southwest, or southeast). Wind directions, on the other hand, vary throughout the transition seasons (spring and fall). Winds are often stronger in the summer (8-16 km/hr) than in the winter (3-6 km/hr).

In January, average temperatures range from 17°C in the northern and northeastern portions of the country to 20°-21°C around the coast. The lowest temperature in the extreme north and northeastern parts of the nation gets within 4 to 7 degrees of freezing point in late December and early January. In April, average temperatures range from around 27°C in the northeast to 30°C in the country's extreme west central region. In some areas of the Rajshahi and Kushtia districts, the maximum temperature during summer might reach 40°C or more. After April, the temperature drops significantly throughout the summer, coinciding with the rainy season. During the latter portion of the pre-monsoon season, widespread cloud cover dampens temperature. In July, average temperatures range from around 27°C in the southeast to 29°C in the nation's northwestern region.

March and April are the least humid months in much of western Bangladesh. From June through September, the relative humidity is consistently above 80%. The Tropic of Cancer is thought to be in the middle of Bangladesh. The Southwestern zone is the extremes of the zones to the north are somewhat tempered. Annual rainfall varies from <1500 mm to >3000 mm in the northwest part to the southern region (SW and SC regions of Bangladesh). **Figure 4.9** shows the pattern of temperature and rainfall in the study area.

The amount of rainfall is exceptionally high due to the country's location in the tropical monsoon area. On the other hand, the yearly precipitation cycle has a unique seasonal pattern that is far more prominent than the annual temperature cycle. The winter season is extremely dry, accounting for just 2% (of the annual total) in the west and south to 4% in the northeast of Bangladesh. Because of the intense surface heat and the entry of moisture from the Bay of Bengal, rainfall during the pre-monsoon season contributes 10% to 25% of total annual rainfall induced by thunderstorms.

The study finds that the Bay of Bengal tropical depressions cause rainfall during the wet season and account for 70% of the yearly total in the east and 80% in the southwest, and 85% in the northwest section. During this season, rainfall ranges from 20 cm in the west central to 80 cm in the northeast. During this season, precipitation ranges from 100 cm in the west central section to more than 200 cm in the south and northeast. Annual rainfall varies geographically, ranging from 150 cm in the west-central region of the nation to more than 400 cm in the northeastern and southeastern parts.

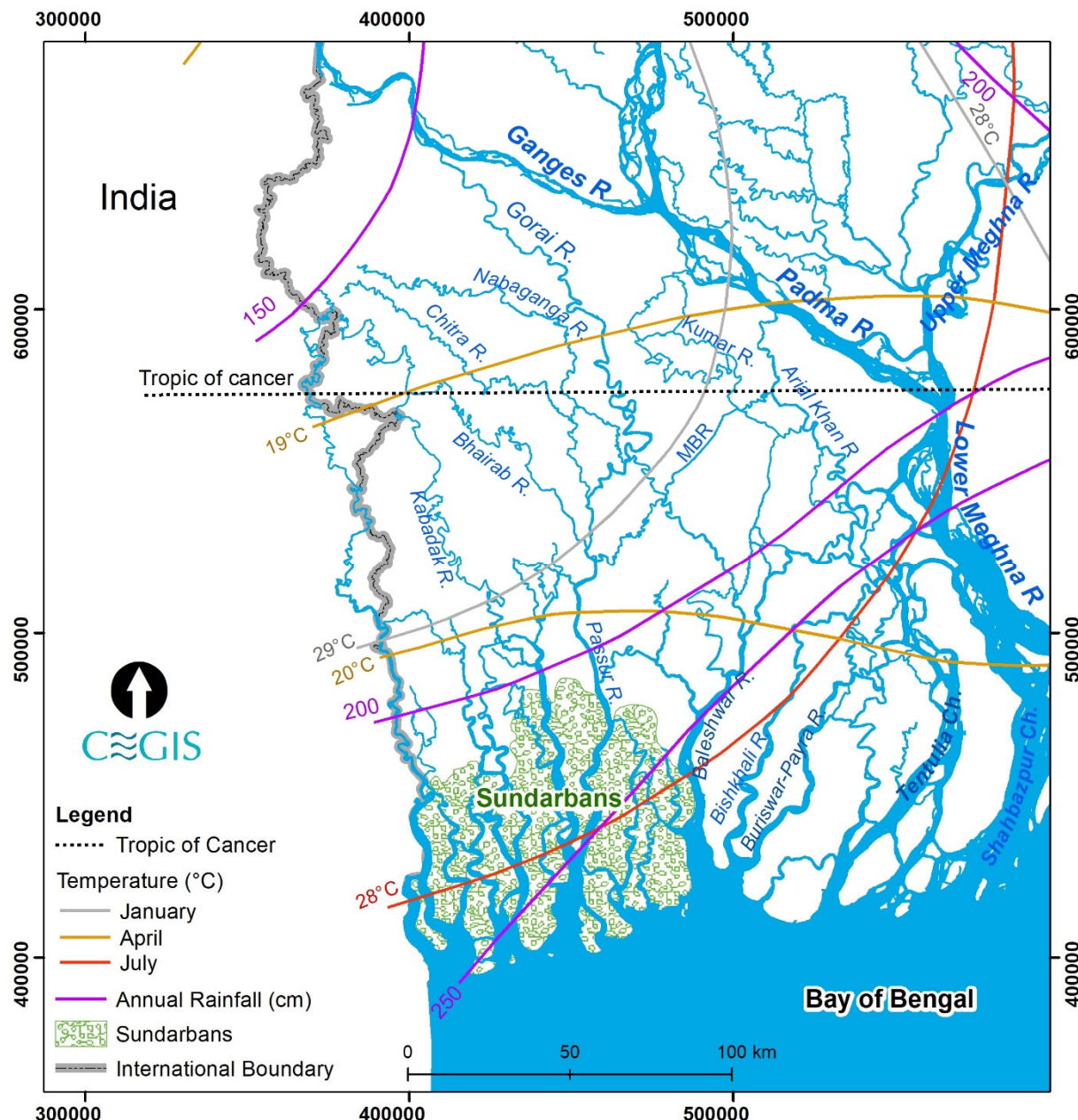


Figure 4.9: Pattern of temperature and rainfall

4.2 System analysis: Historical Development

Millennium Scale

Several studies on river evolution in the Holocene period were carried out by Fergusson (1863), Williams (1919), Umitsu (1993), Goodbred and Kuehl (2000 a & b), and Allison et al. (2003). Among those, the most comprehensive account of the development of the Ganges-Brahmaputra (GB) delta from the late Quaternary and extending through the Holocene, presented by Goodbred and Kuehl (2000 a & b); Allison et al. (2003); Kuehl et al. (2005). Their account was based on borehole data they collected themselves, as well as from Umitsu (1993) and other sources. Based on the compiled data, they developed palaeo-geographic maps (**Figure 4.10**) of the GB delta during the Holocene. They concluded that the delta-building

process resulted in changes to the courses of the Ganges (G) and the Brahmaputra (B). That itself was driven by abundant sediment input from erosion of the Himalayas, conditioned by the sustained sea-level rise that began during the Late Quaternary and modified internally by regional tectonics within the Bengal basin. The paleo-geographic maps show the shifting of the Ganges River from west to east, and the avulsion of the Brahmaputra River occurred a couple of times between the east and west sides of the Madhupur Tract (**Figure 4.10 left panel**).

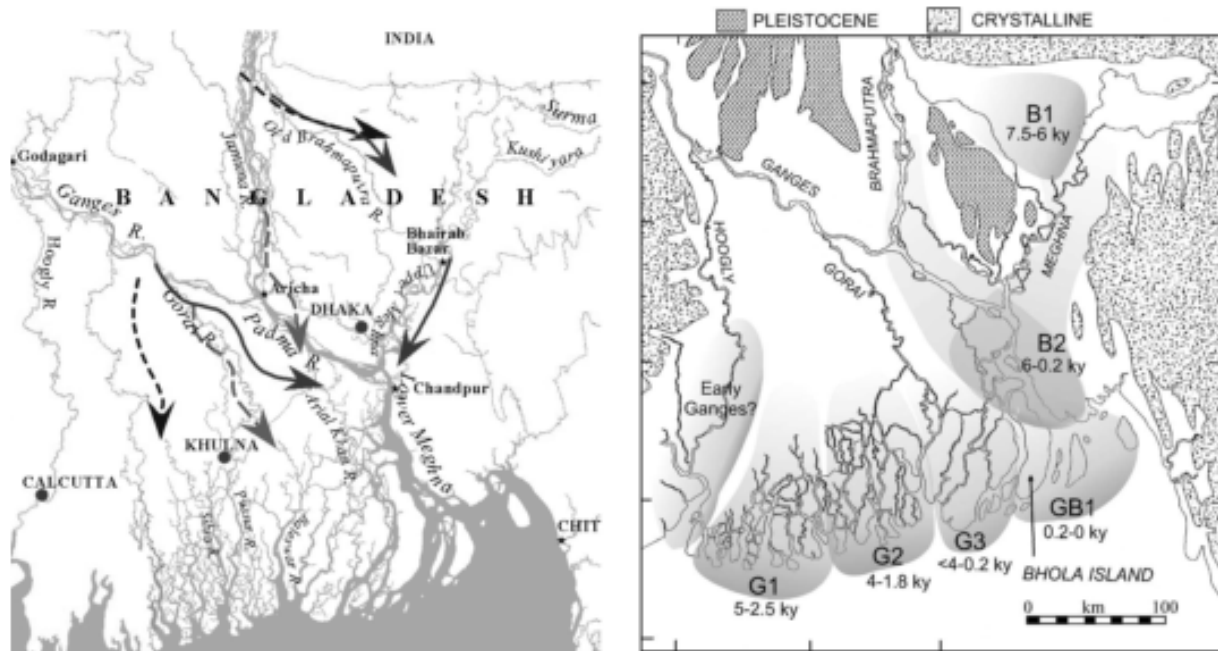


Figure 4.10: Palaeogeographic maps of the Ganges and Brahmaputra (GB) delta during the Holocene (source: modified from Goodbred and Allison, 2003)

Allison et al., examined The mineralogical properties of sediment for assessing sedimentary sequence resulting from the lower delta plain progradation in the late Holocene in 2003. 38 core sites were selected in the Sundarbans, Kuakata, and Hatiya/Noakhali. Clay mineralogical and radio-carbon evidence from that study agrees that the lower delta plain progradation after the maximum transgression may have been in five phases (**Figure 4.10 right panel**). The earliest phase, G1, which the Ganges formed, occurred in the western most delta. Clay mineralogy from this area shows an increasing influence of the Ganges at the upper section, suggesting a progradation of Gange's distributaries into this area. The early (5,000 cal years BP) deltas of the Brahmaputra (B1) and the Ganges were located far inland of the present shoreline as there was an enormous amount of accommodation space available in the tectonically active Bengal basin. They have also found that the shoreline progradation associated with the two rivers was separate after 5000 cal years BP until they merged into the present Meghna estuary about 250 years ago. A series of eastward stepping formed by the Ganges was among three main phases (G1-G3). Delta progradation in each stage took place over a wide front encompassing several active island-shoal complexes. On the other hand, the delta plain formation of the Brahmaputra took place inland along two loci created by channel avulsions east and west of the Pleistocene Madhupur terrace. The Sylhet basin, east of the Bengal delta, faced southward into the Meghna estuary following the Meghna River course. Delta progradation into the Meghna estuary (GB1) becomes limited until they meet the historical times from west to east. This progradation direction matches well with the finding of Goodbred and Kuehl, 2000 a & b.

Major events during the last 7,000 years were: (1) shifting of the Delta lobes of the Ganges along the coast from west to east, (2) Inland Delta lobes developed by the Brahmaputra River in the tectonically active subsiding Sylhet Basin, (3) Joining the Ganges and Brahmaputra together more than 200 years ago.

Drivers: Anthropogenic activity was insignificant; as a result, eastward migration of the Ganges delta lobes can be considered a part of the delta-building process. The third event can be considered as a function of both natural delta building process and influence of neo-tectonics. The Sylhet basin's tectonic activity mainly governs the Brahmaputra's inland delta building (B1).

Centennial and decade-scale

Centennial Scale Delta building processes in SW, SC, and Meghna Estuary have been described in this section mainly based on historical maps such as Rennel's (1776), and Tassin's map (1840), and Topo map (1943), time series satellite images.

Studies of old maps such as Rennel's (1776) and Tassin's (1840), Topo's (1943) map, and Time-series satellite images from 1973 to 2020 illustrated 250 years long history of the SW, SC, and Meghna estuary. Major historical events were identified that played important roles in centennial and decade scale metamorphosis of the rivers, estuary and delta plains and identifying the main relevant drivers. These findings helped to understand interlinking and interrelated processes prevail in different regions and times. It also plays a crucial role in developing scenarios for predicting future development.

A study by Sarker et al., 2021 presented net erosion/accretion in the Meghna estuary both on a centennial and decade scale (**Figure 4.11**). Findings are found to be different than what we know earlier. From 1776 to 1840, net accretion was 950 km^2 , equivalent to $14 \text{ km}^2/\text{y}$. Comparing the maps of 1840 and 1943 showed a net negative accretion (net erosion) of 330 km^2 in 103 years (**Figure 4.12**). In the following 77 years, from 1943 to 2020, changes are more dramatic; net accretion was 1720 km^2 . Splitting this result into the decade-scale rate of net accretion yield a very high magnitude of net accretion as 1200 km^2 , equivalent to $40 \text{ km}^2/\text{y}$ from 1943 to 1973. In the following five decades (1973 to 2020), net accretion was found to vary from $30 \text{ km}^2/\text{y}$ to $7 \text{ km}^2/\text{y}$.

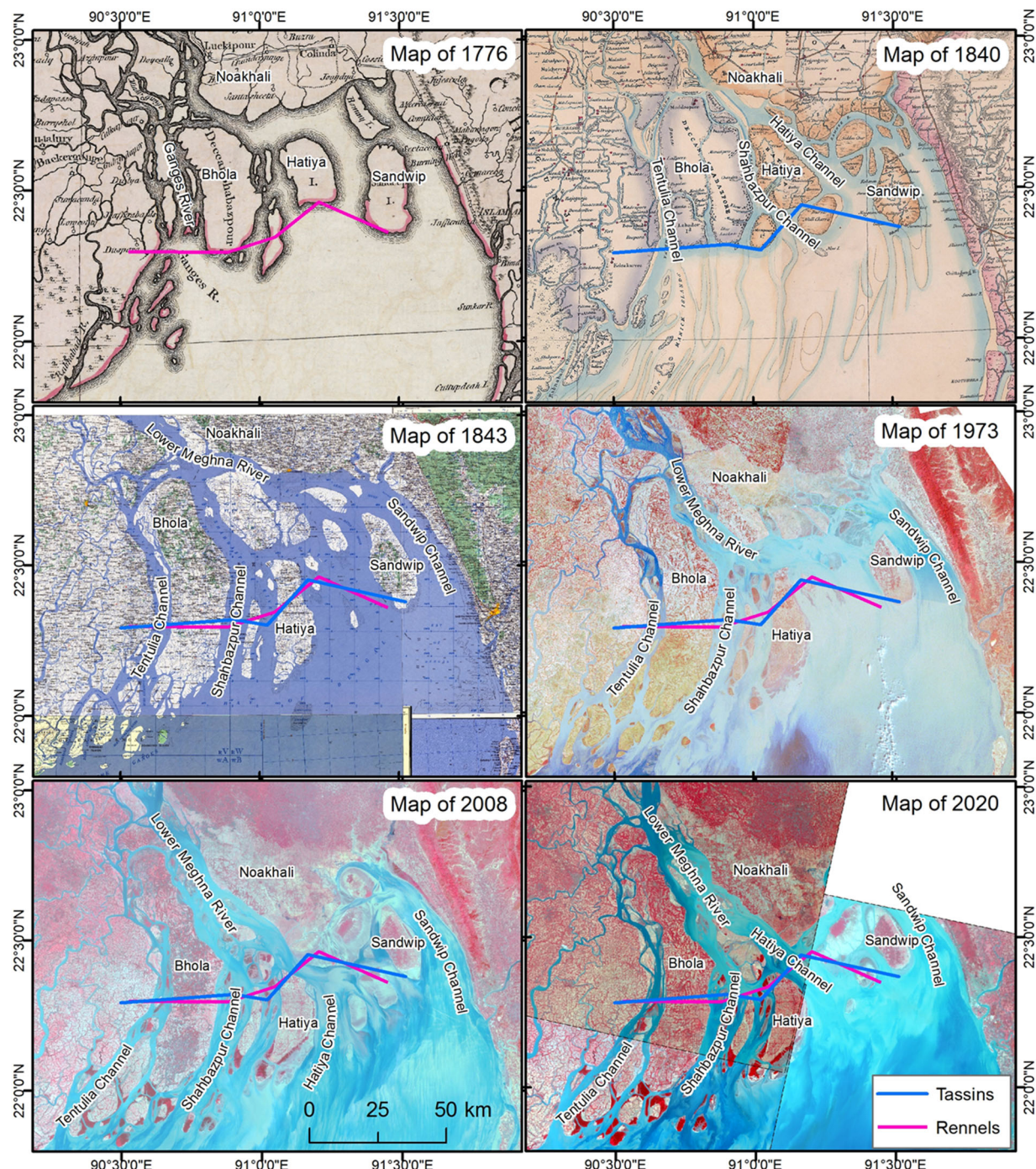


Figure 4.11: Changes in the Meghna estuary in the last 250 years (Lines in the figure indicate the locations of the southern tips of the islands in 1776 and 1840 maps for assessing the migration of the Bhola, Hatiya, and Sandwip Islands)

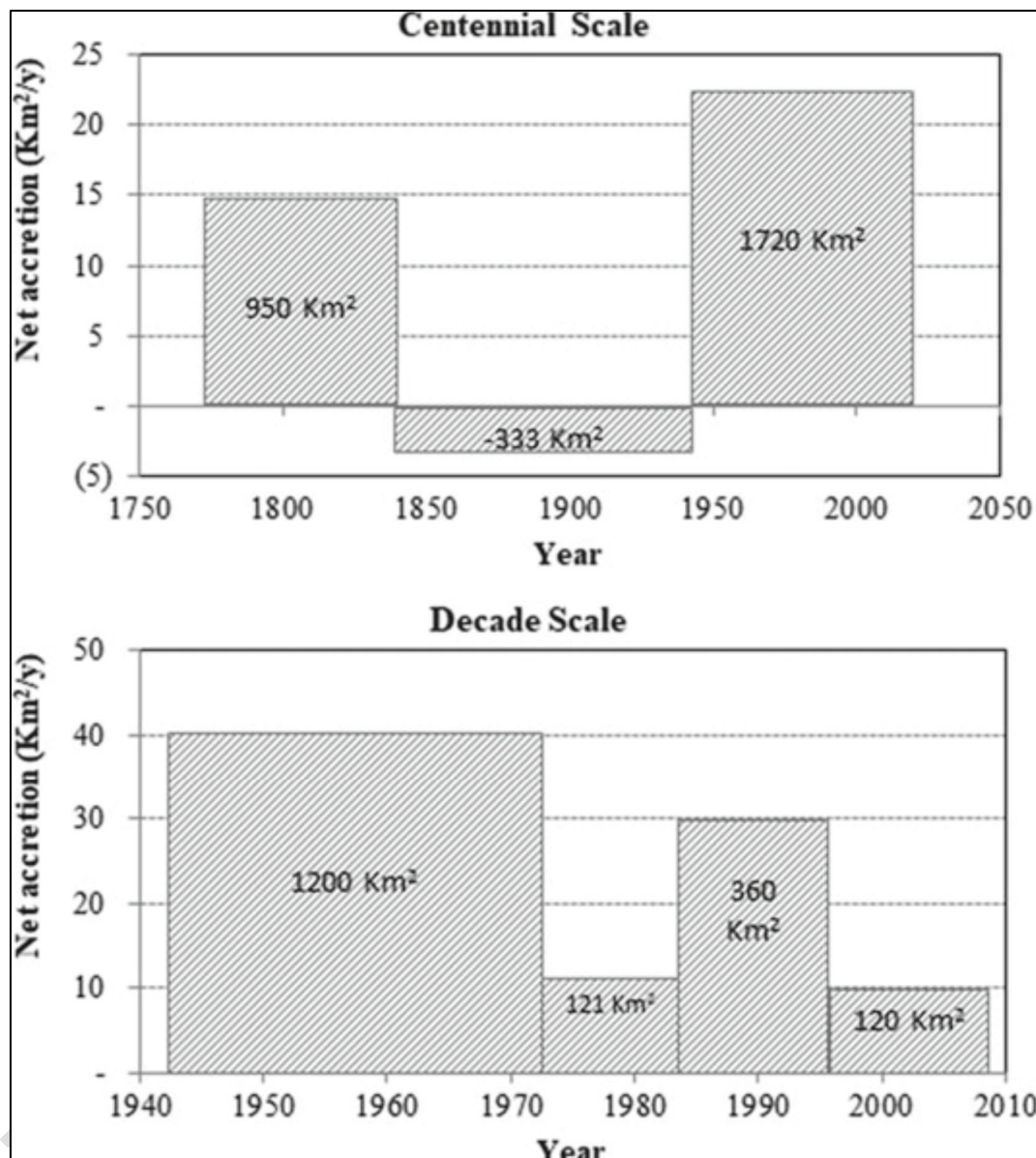


Figure 4.12: Net accretion in the centennial and decade scale

Sarker et al., 2021 studied the dynamics of the Sandwip, Hatia, and Bhola islands in the Meghna estuary, within the framework of the dynamic of the Meghna estuaries. There are no direct relations between net accretion/erosion in the estuary with the islands' increase or decrease in size. On the other hand, a high rate of shoreline erosion generally occurs along the island's flank, which is attached to the distributary channel transporting a major part of fluvial input.

Old maps such as Rennel's (1976) and Tassin's (1840) demonstrate that the old course of the Ganges had become the right bank distributary (namely the Arial Khan) of the Ganges River (**Figure 4.13** and **Figure 4.14**). It is believed that joining the Jamuna to the Ganges raised the water level in the Ganges River, which led to the enlargement of the Gorai (Ferguson, 1863). The southeast flowing Kumar River was dissected by the course of two big south-flowing rivers, the Gorai-Modhumati and the Chandana-Barasia. All the distributaries in this region, along with the Ganges River, were flowing southeast (**Figure 4.17**). The Chandana-Barasia, a south-east flowing river, was the primary source of sweet water for the southwest region with

a small link with the Gorai River. The Kabodak River lost perennial connection but able to maintain a narrow link with the Ganges.

In the last few centuries, considerable changes have been observed in the river systems and their distributaries. Still, degrees of change was intensive in the ME region, which reduced towards the west in SC and SW regions. The Meghna and Arial Khan rivers developed in the southwesterly direction. Several right bank distributaries have taken off, such as the Shyandha River, Bisarkand-Bagda Khal, the Tarki Khal, the Nunda-Otra, the Belua, and so on. A few other small rivers are still developing in the southwest direction. By this time, most of the Gorai flow had diverted to the Nabaganga River.

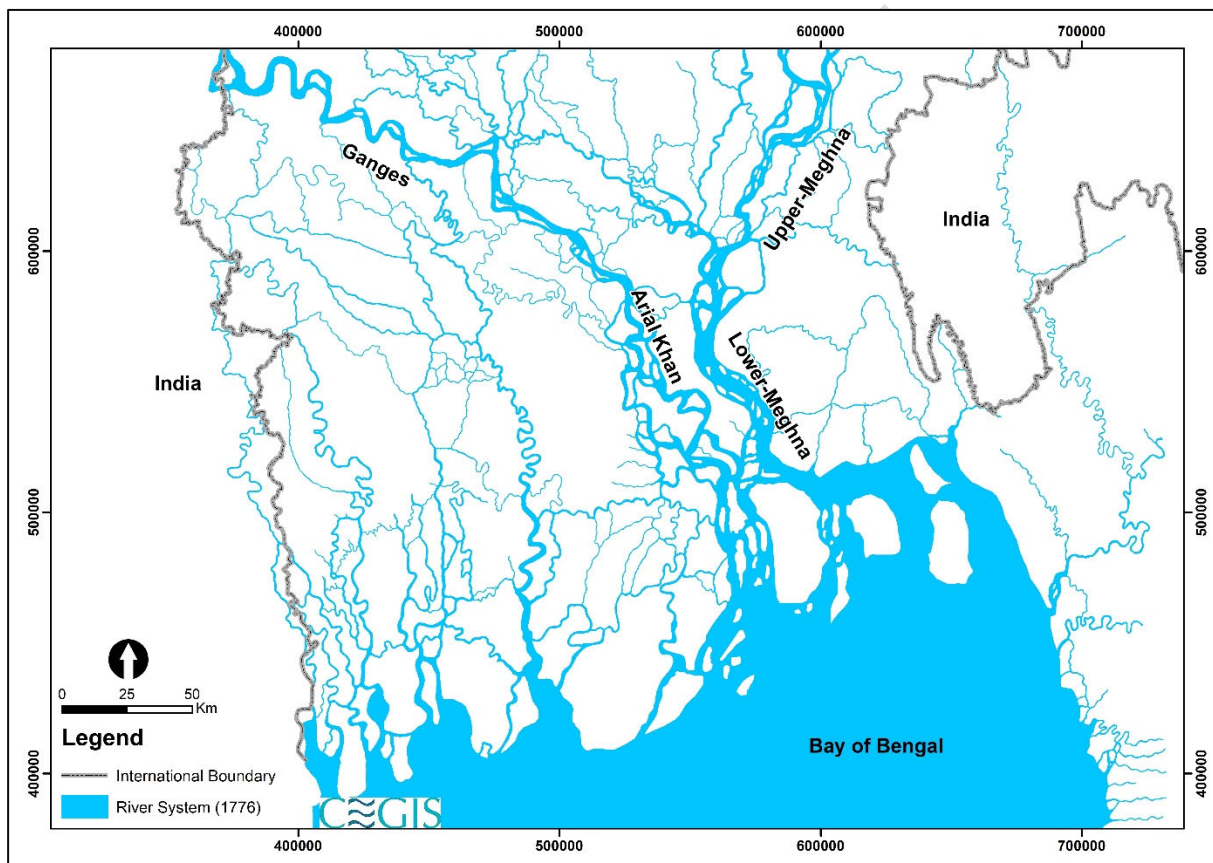


Figure 4.13: Rivers found in Rennel's map (1776)

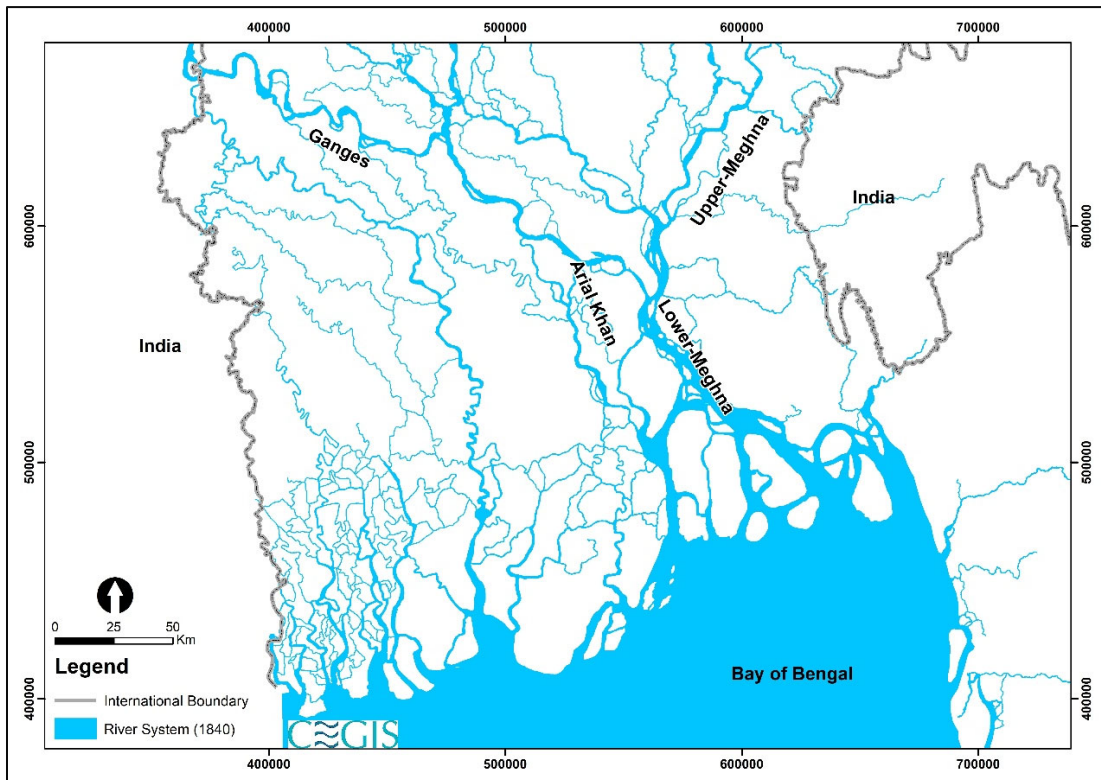


Figure 4.14: Rivers found in Tassin's map (1840)

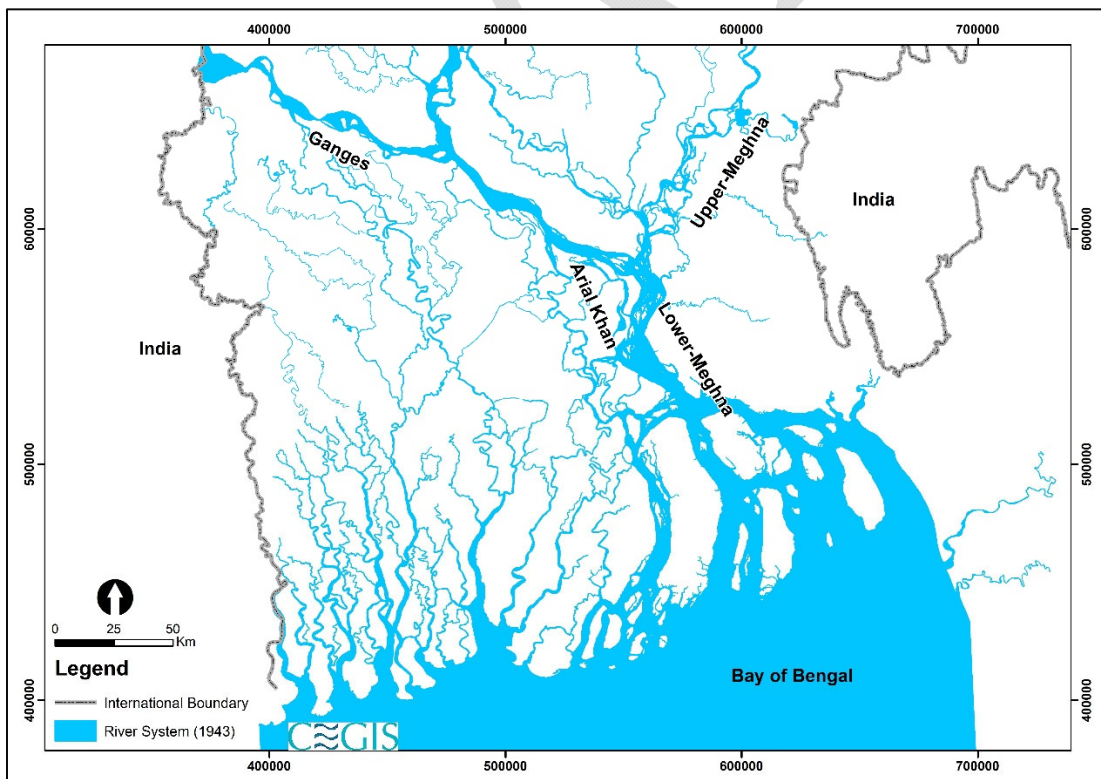


Figure 4.15: Rivers found in Topo map (1943)

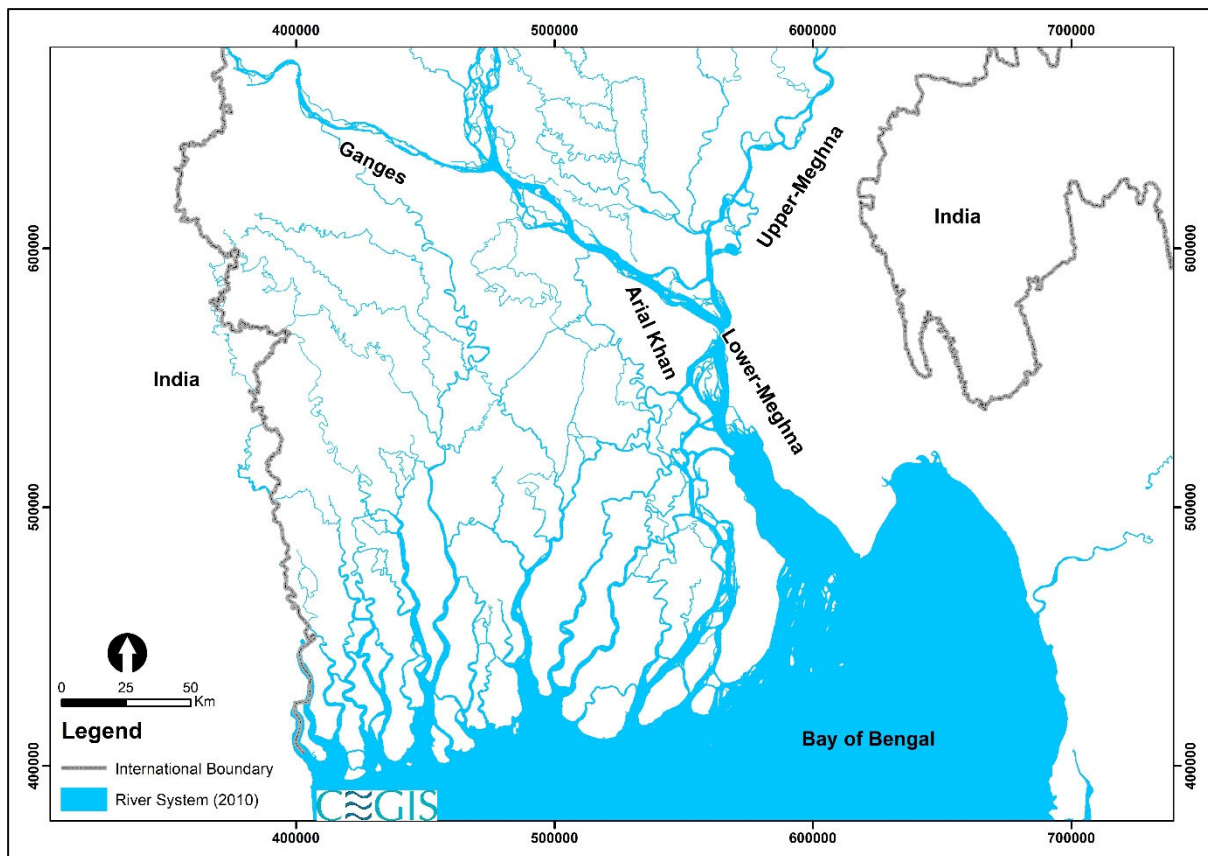


Figure 4.16: Rivers found in the satellite image of 2010

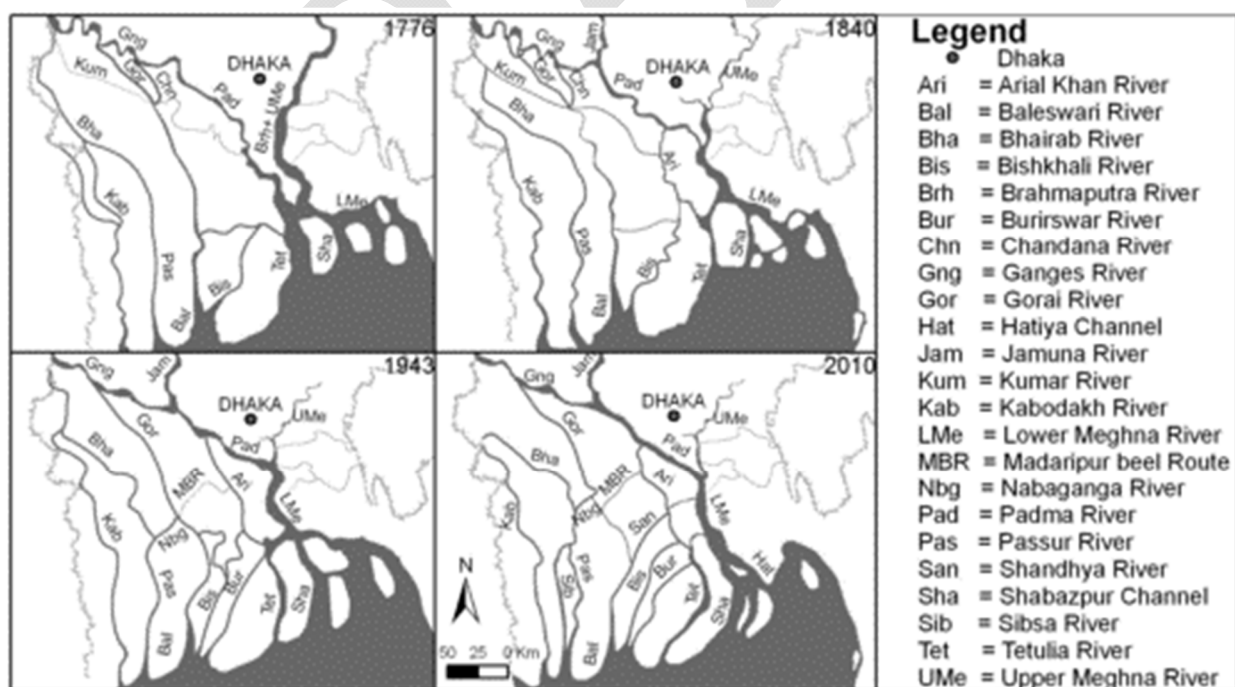


Figure 4.17: Courses of rivers in the last 250 years

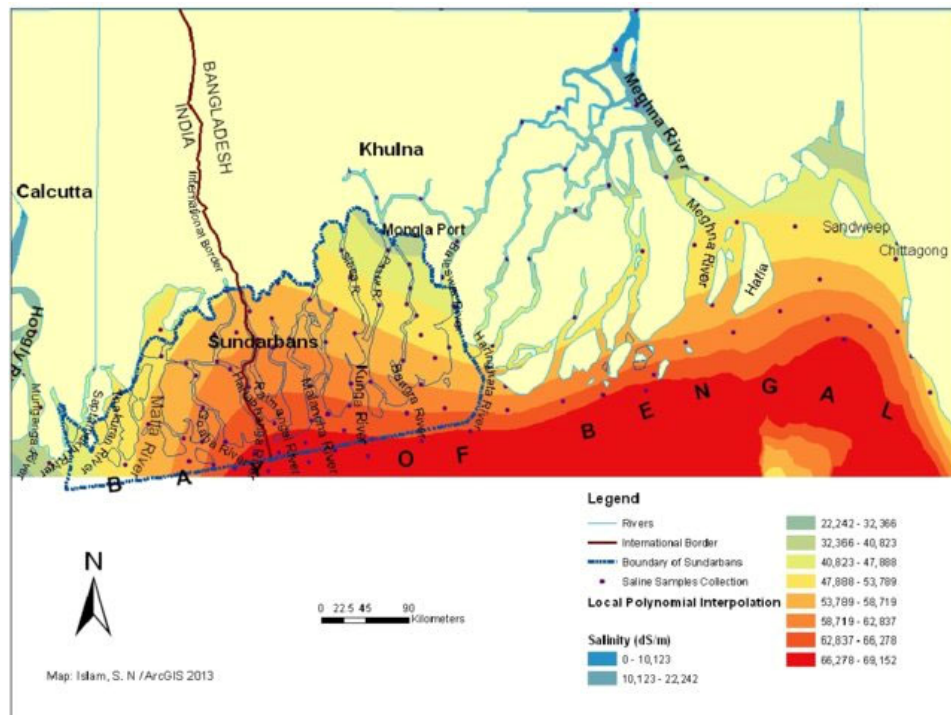


Figure 4.18 The salinity intrusion pattern in the Bengal coastal region

Changes in the flow direction of the right bank distributaries of the Padma and Lower Meghna rivers towards the southwest have long-term consequences on the Delta development process. Increasing the changing direction of the distributaries in SC increases the freshwater towards the south-west, pushing back the salinity south-east (Figure 4.18). It would decrease the surface water salinity along the eastern boundary of the SW region, especially in the Baleshwar system. Rapidity and continuity of the processes depend on the sediment supply in the Meghna estuary, which is very sporadic (long-term monitoring).

Human Interventions

Human interventions in the Meghna were less than those in SW and SC regions. Major interventions were the construction of two cross-dams in Noakhali in 1957 and 1965 to expedite the land accretion processes.

William (1919) presented the accounts of the interventions, the purposes of which were to enhance navigation by excavating canals and construction of embankments and sluices to protect the crop from salinity and drain the water from monsoon rainfall. The density of interventions was high in the G1 in India and the SW region of Bangladesh. William (1919) also described the effects of those interventions, such as amplifying tides and reducing the duration of flood tides (indicating the existence of tidal asymmetry).

During the early twentieth century, canals were excavated to enhance navigability in the SC region, such as Helifex Cut (1910), Madaripur Beel Route (MBR), Gabkhan Canal, Mongla-Ghasiakhali Canal, etc. After excavation of the 23 km MBR during 1910-12, a part of the Arial Khan River into the Madhumati River. The Halifax cut, made in 1910 to shorten the distance from Dhaka to Khulna, connected the Madhumati River with the Nabaganga River. Consequently, a significant amount of flow of the Madhumati River started to divert through the Nabaganga River.

Major interventions were started in the early 1960s in the coastal areas covering SW, SC, and ME regions to avoid drainage congestion and salinity intrusion in the tidal plain and to protect life and lively hoods from tidal floods, cyclones and storm surges. Interventions include coastal embankment, polder embankment, sluice, and regulators. The system's responses vary from region to region, based on the settings of different physical processes in the regions where the concerned river is located. For planning, the predictability of the system is very crucial.

Major events in the ME regions

From 1776 to 1840, (1) abandonment of the lower course of the Padma, which was acting as a main distributary channel of the Ganges river, and (2) combining all three contributory rivers at Chandpur, from 1840-1943 (3) declining of the most easterly distributary channel, (4) elongation, migration, and bending of Bhola and Hatiya islands, 1943 to 2020 (5) net erosion at a rate of 3 km²/y and (5), from 1943 to 2020, (6) substantial net accretion about 1720 km².

Identifying the main drivers active during the periods from 1776-1840, 1840-1943, and 1943 to 2020

Main drivers active in different periods are: (1) (1776-1840) avulsion of the Brahmaputra, which supplied massive sediment to the Meghna estuary, (2) (1840-1943) relaxation process (it usually means the return of a perturbed system into equilibrium), (3) influence of tide coming from Swatch of No Ground, and (4) (1943-2020) input of enormous sediment generated from 1950 Assam earthquake. If there is no additional sediment from upstream, it may continue several decades from now and result in negative accretion.

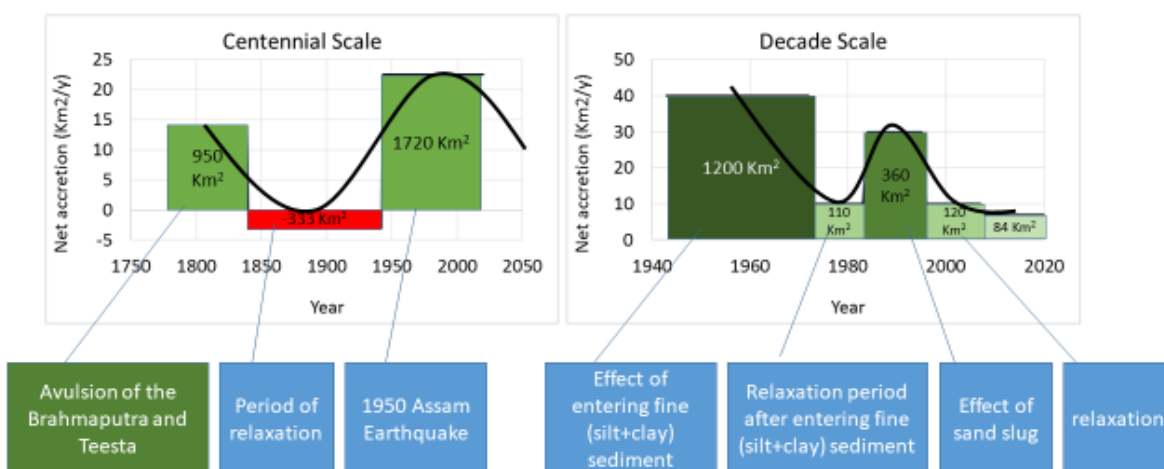


Figure 4.19: Decade to century-scale net accretion and identification of drivers

Identifying major events and relevant drivers in the SW and SC

- (1) Shifting of the distributary courses from SE direction to SW direction mainly in the SC region
- (2) In many cases, SW flowing distributaries get higher fluvial input
- (3) Drainages congestion mainly in the SW region
- (4) Tidal volume reduction primarily in the SW region

The main drivers are:

1. Increased sediment supply due to the avulsion of the Brahmaputra river, (2) Joining of all three contributory rivers at Chandpur, (3) human interventions, and (4) tide are coming through the Swatch of no Ground.

Relation between Shifting of the Delta and courses of the Distributaries

The delta building process continues, causing the active delta to shift at different locations. The assessment of delta shifting is mainly based on indicators such as delta progradation, shifting of the delta building estuary, and also shifting of the direction of the distributaries (**Figure 4.20**), which is, however, a qualitative assessment

After the avulsion of the Brahmaputra joining of all contributory rivers at Chandpur, enormous changes occurred in the following decades. The active delta building estuary shifted towards the east, and the process continued till the middle of the 20th century. The easternmost channel of the Lower Meghna estuary has been abandoned, resulting in the initiation of a reverse shifting of the active delta building estuary towards the west (**Figure 4.20**).

Most of the Ganges' distributaries during the 18th and 19th centuries flowed towards the southeast. By the middle of the 20th century, the flow of the Gorai-Madhumati started to flow southwest along with a few other distributaries from the Lower Meghna and Arial Khan rivers. During the last six decades, more than 90% of the flow of the Gorai River was diverted to the southwest-directed channel. Moreover, several smaller distributaries from the Arial Khan and the major distributary Shandha from the Lower Meghna and Arial Khan rivers were developed. The rate of change appears to have been very high in the later period (**Figure 4.20**).

Time-series salinity data or hydrographic survey charts facilitate a qualitative but confirmatory assessment for freshwater diversion to the southwest-directed distributaries. It may also provide quantitative assessment over time, but unfortunately, there is a lack of reliable data. Analyses of water levels conducted at different locations of these distributaries have also not provided any consistent trend based on any conclusive decision.

The active delta building estuary and associated distributaries frequently shifted their courses. The rate of shifting appears to have been faster during the last seven decades, especially after the 1950 Assam earthquake, which might have had a prominent role in expediting the shifting process. This makes extrapolation for projecting the future very difficult. The centennial and decadal processes inferred that the shifting would continue in the coming decades.

The available information makes it difficult to quantify the shifting rate or project the future rate due to the lack of reliable data on the sediment concentration of the major rivers for the last two decades. Another limitation for future projection is the uncertainty of sediment input, which depends on the land use changes occurring in the upstream riparian countries. Most importantly, the influence of tectonics and seismicity makes it very complicated. Knowing the characteristics of the geo-morphological features in the SW, SC, and Meghna Estuary and their interrelations are very useful for proper planning of the system.

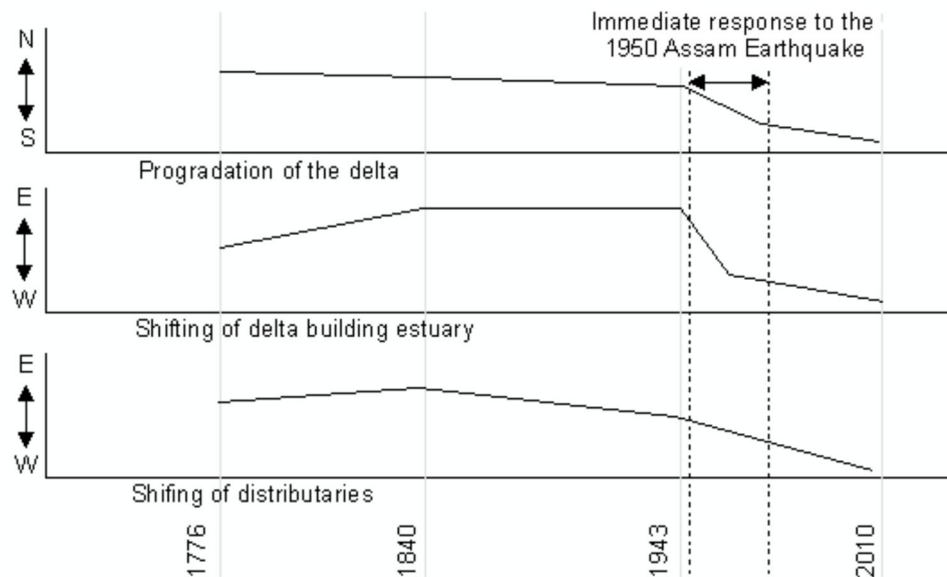


Figure 4.20: Qualitative shifting of the delta and its associated distributaries

Sedimentation/denudation processes

Sedimentation on the riverbed may occur both in the monsoon and dry season, although processes are different. Still, it may differ in magnitude from one system to other. In an active delta, deposition/erosion in tidal and fluvial rivers and on tidal and fluvial floodplains are common phenomena.

During the dry season, sedimentation on a riverbed at any particular location and its rapidity depends on three factors, (1) the existence of the sedimentation environment, (2) the source of sediment, and (3) tidal asymmetry (insignificant fluvial input during dry season) that transports the sediment from its source to the location of sedimentation. For the case of monsoon, the first two factors are the same as the dry season; instead of tidal asymmetry, the third one is flood flow that transports the sediments from upstream.

Like sedimentation, erosion in the riverbed is also a common process in the delta. Several distributary channels in a tide-dominated delta exist that distribute fluvial inputs from upstream. Enlarging/declining of a perennial distributary are frequently occurring phenomena in the deltas. Generally, sedimentation dominates the morphological processes in a declining distributary, while erosion dominates the morphology of the enlarging distributaries.

5. River System Analysis in SW, SC, and ME Regions

In a dynamic system, the behavior of the different hydro-morphological processes also demonstrates its rapidity and complexity; it might vary on different scales. In this study, we tried to illustrate how different processes gradually influence the other; in many cases, proximity may play an important role, but exceptions exist. However, to characterize the regions, the polder surrounding the river's behavior have an active influence, i.e., contributory rivers for delta formation, age of Delta lobe (yrs.), upstream dry season flow, sedimentation process, characteristic of the sediment, erosion/accretion. For a better understanding of the long-term morphological processes of the SW and SC region, it is essential to know the prevailing behavior of the Meghna estuary, an active delta building estuary (Sarker et al., 2011). Therefore, it included the ME region within the study area. A brief description of this study's interest area is given in **Table 5.1**.

5.1 Khulna-Satkhira region (SW Region)

This region was solely developed by the Ganges River (G1 and G2, as shown in **Figure 4.10**) from 1800 to 5000 years ago. The terrain slope is as high as 9 cm/km. It is a dying delta with limited or no fluvial contribution from the upstream rivers. During dry periods, tidal asymmetry increases, rapidly bringing sediment from the downstream or riverbed and sediment upstream. Thus the morphological trend of the river system is deteriorating. Its sedimentary features include high silt and clay content with calcium carbonate, making the material less erosive. Therefore, the erosion-accretion process is not dynamic here compared to other parts of the country. Due to the formation process, higher elevations at upstream and tidal plain make a depression in the middle (**Figure 4.8**). Due to loss of connectivity with upstream, tidal asymmetry in the coastal rivers, and construction of polders, the riverbeds are aggrading. Therefore, long-term drainage congestion in the Khulna region persists, and drainage arteries are declining. In the future, the declining process may prograde downstream.

5.2 Barishal region (SE Region)

The Barishal region is a part of the south-central region of the country. This region is also solely developed by the Ganges. It is a recent development in the geological time scale of 200-4000 years ago. However, this region was active 200 years ago, and presently, the terrain slope of the area is as mild as 1 cm/km. Although the Arial Khan River is declining daily, a significant amount of flow of the Lower Meghna River is coming into the river system. Tidal asymmetry could not be an option to transport the sediment from the estuary due to fluvial flow. The high content of silt and clay causes moderate erosion-accretion in this area. It is believed that the delta has shifted from its easternmost boundary to the west in the last century (Sarker et al., 2013; Akter et al., 2016). As a result, all the distributaries of the Lower Meghna River are in the developing phase. In the future, the sizes of the rivers may increase, supporting the delta-building process.

5.3 Meghna Estuary (ME Region)

The Meghna Estuary is active now. Contributions develop this system from the Ganges and the Brahmaputra rivers within the last 200 years. All the fluvial inputs from the Ganges Jamuna Meghna systems follow this system. Tide dominated sediment dispersion process is active here. Due to high silt and sand and no cohesive sediment in the clay, erosion- the accretion process is

very dynamic here. Delta's building process is also active in the system. Presently, delta progradation (vertically and horizontally) is taking place. But in the future, reducing sediment input from the upstream sediment management may decrease the progression rate. Even, it may create transgression of the delta.

Table 5.1: Characteristics of the geo-morphological setting of three study regions

| Region | Contributory rivers for delta | Age of Delta | Terrain Slope | Upstream flow | Sedimentation process | Characteristic s of the | Erosion/ Accretion | P revailing morphological trend | Future Development |
|--------|-------------------------------|--------------|-----------------|---------------|--|---|--------------------|--|---|
| SW | Ganges (G1, G2) | 18 00- 50 00 | High (9 cm/ km) | Insignificant | Sedimentatio n is rapidly supplied by tidal asymmetry | The high conten t of Silt and clay with calcium carbonate | Low | Long-term drainage congestion causes the decline of main drainage arteries | Downstream propagation of the declining process |
| SC | Ganges (G3) | 20 0- 40 00 | Mild (2 cm/ km) | Significant | Tidal asymmetry could not be developed to transport the sediment from the estuary due to fluvial flow. | The high conten t of Silt and clay | Medi um | Shifting of the distributaries towards south-west direction | The size of the river may increase |

**Bangladesh Water Development Board (BWDB)
Coastal Embankment Improvement Project**

| Region | Contributory rivers for delta | Age of Delta | Terrain Slope | Upstream flow | Sedimentation process | Characteristics of the | Erosion/ Accretion | Prevailing morphological trend | Future Development |
|----------------|-------------------------------|--------------|---------------|---------------|------------------------------------|--|--------------------|--------------------------------|--|
| Meghna Estuary | GB1 | 200 | | High | Tide-dominated sediment dispersion | High Silt and sand, no cohesive sediment in the clay | Very high | Delta progradation | Reduction of the sediment input may decrease the progression rate. Even it may create transgression of the delta |

6. Morphological Analysis of the Rivers in the Khulna Area

This chapter aims to assess the morpho-dynamics of the rivers related to coastal polders to predict future bank erosion. Planform analysis of the rivers in the Khulna area includes the historical development, shifting of the bank lines, bend migration, change in width and sinuosity, quantification of the erosion-accretion, and prediction of the rivers. Thus, Kholpetua, Kapotakshi, Ichamati-Kalindi, and Shibsa River have been selected for this study. In addition, in the prediction of the small rivers, it was not possible to delineate the bank lines using coarse resolution (30 m*30 m) of the satellite image. Expert judgment was applied through knowledge of the system and understanding of the study area for assessing the small rivers. The small rivers were determined to not pose an erosion threat to the Polders. **Figure 6.1** shows the rivers focused in this study.

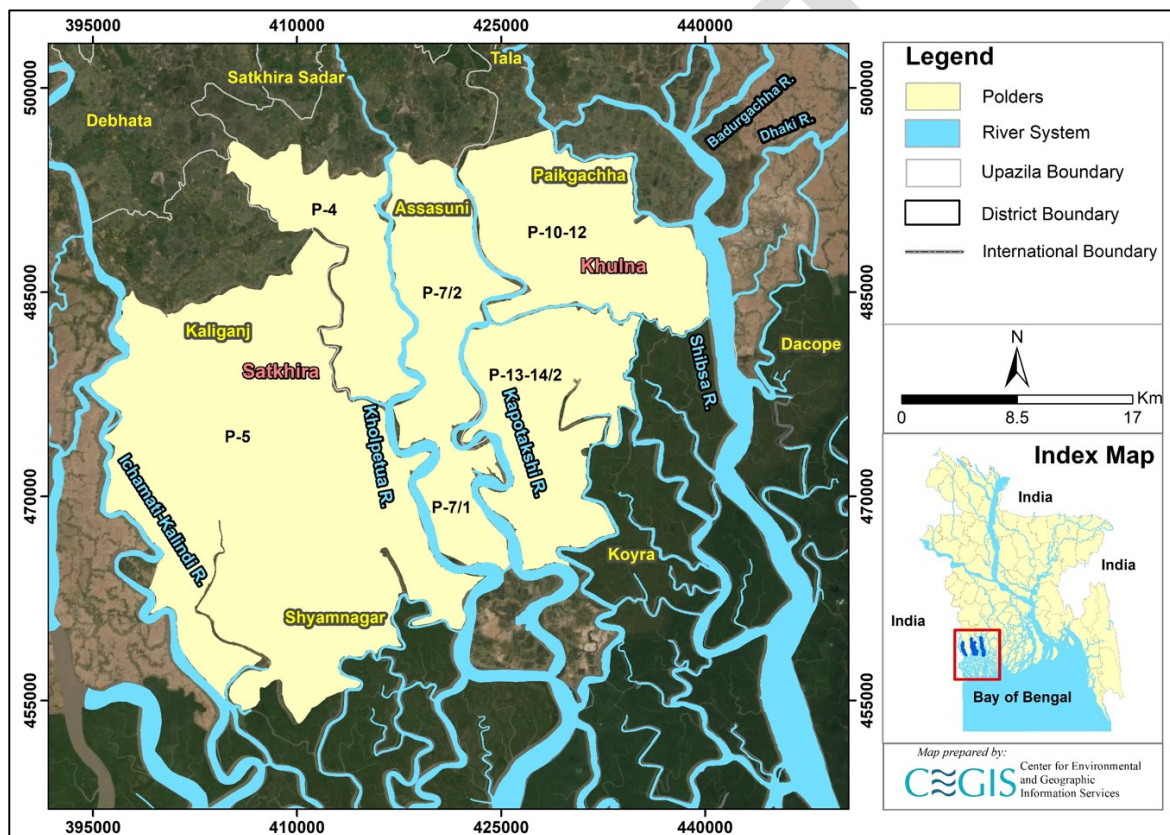


Figure 6.1: Study polders and peripheral rivers in Khulna area

6.1 Kholpetua River

Kholpetua River originates from the Betna River in Assasuni Upazila of Satkhira District and outfalls into the Arphangasia River in Koyra Upazila of Khulna District. This river is perennial. To better understand the morphology, the river has been divided into two reaches as the river is narrower at the upstream but wider near the downstream. Reach-1 is considered from Baradal-Assasuni to Pratap Nagar-Kashimari and Reach-2 from Pratap Nagar-Kashimari to Gabura-Buri Goalini Range (**Figure 6.2**). These reaches have been categorized by observing the variation of the width.

Historical Development of the Kholpetua River

The historical map and satellite images have been compared to assess the historical development of the Kholpetua River. The map of 1943 and the satellite images of 1989, 2003, and 2021 are shown in **Figure 6.2**. Comparing the map and the images, it is evident that the alignment of the river had not changed over the past 78 years. In addition, no cut-off has been observed during this period.

DRAFT

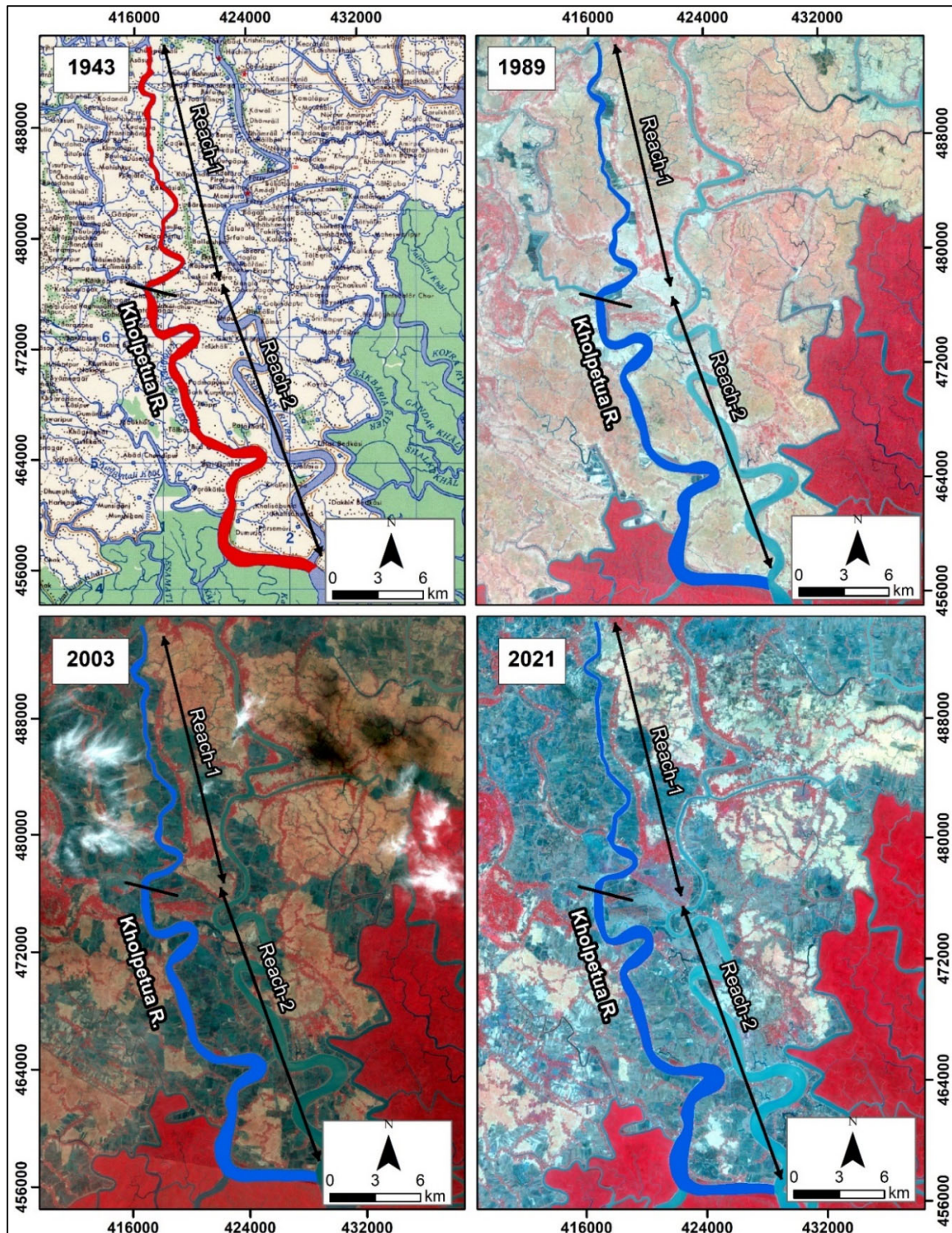


Figure 6.2: Historical Development of Kholpetua River

Average Width of the Kholpetua River

The shortest distance between two banks is defined as the river's width. The average width of the rivers has been calculated to evaluate the changes in the river over time. The average width has been calculated by the total area enclosed and the riverbanks. This has been divided by the length of the centerline of the river. Figure 6.3 shows that the average width of Reach-1 follows decreasing trend due to net accretion. In contrast, there is an increasing trend due to net erosion in Reach-2.

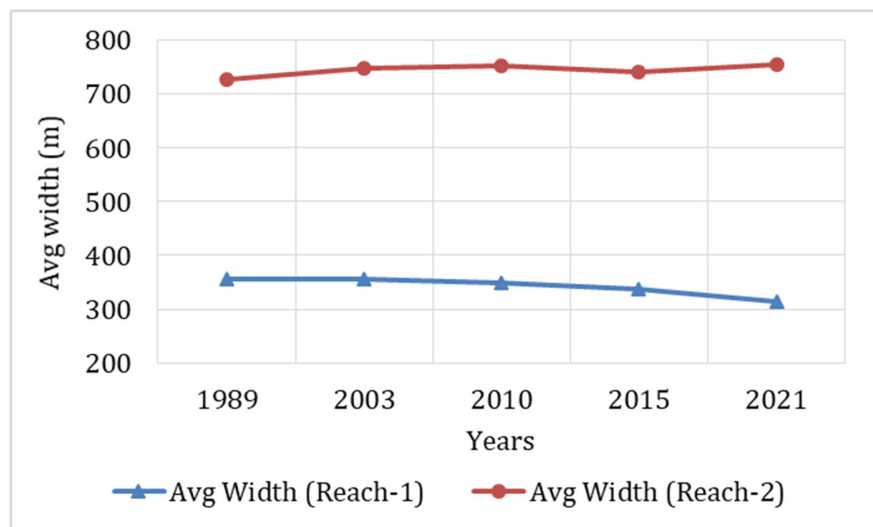


Figure 6.3: Average width of the Kholpetua River from 1989-2021

Sinuosity of the Kholpetua River

Channel sinuosity is simple geometric information that signifies the river's deviation from a straight line. It is the ratio of the curved length to the straight length of a reach of the river. The sinuosity of the Kholpetua River for 1989, 2003, 2010, 2015, and 2021 is represented in **Figure 6.4**.

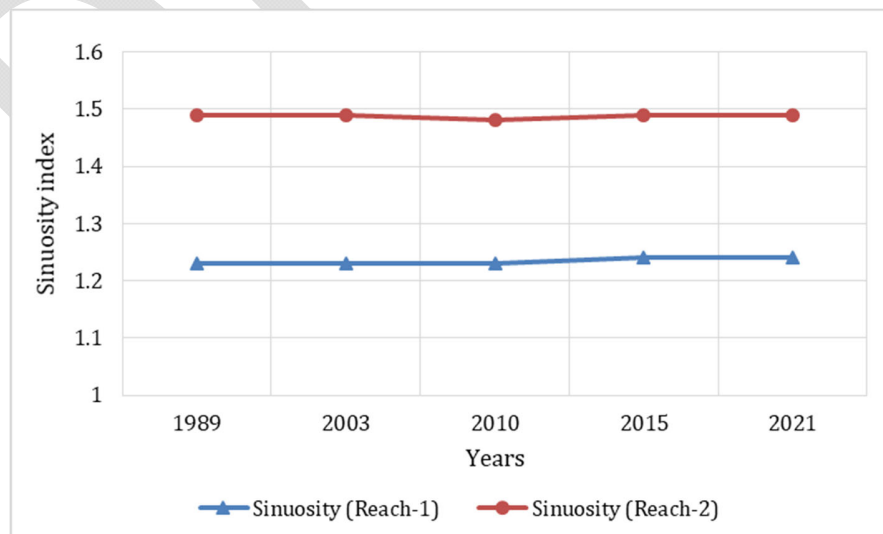


Figure 6.4: Sinuosity of Kholpetua River from 1989-2021

From **Figure 5.4**, it is observed that the sinuosity of these reaches has not changed a significant way over the years. The sinuosity of Reach 1 has a slightly increasing trend, confirming the narrowing of this reach. On the other hand, Reach 2 shows no trend, and the sinuosity magnitude confirms this reach is nearly meandering.

Erosion-Accretion Analysis of the Kholpetua River

For erosion-accretion assessment, bank lines of 1989, 2003, 2010, 2015, and 2021 were superimposed. The erosion and accretion-prone areas along the Kholpetua River are presented in **Figure 6.5** and marked red and green, respectively. The figure shows that Reach-1 of this river is accretion-prone, and Reach-2 is erosion-prone. This may be caused by a lack of fluvial flow, which creates excess sedimentation upstream (Reach-1). However, downstream erosion (Reach 2) was observed; this erosion is because tidal forces play an essential role in changing the shape of the river.

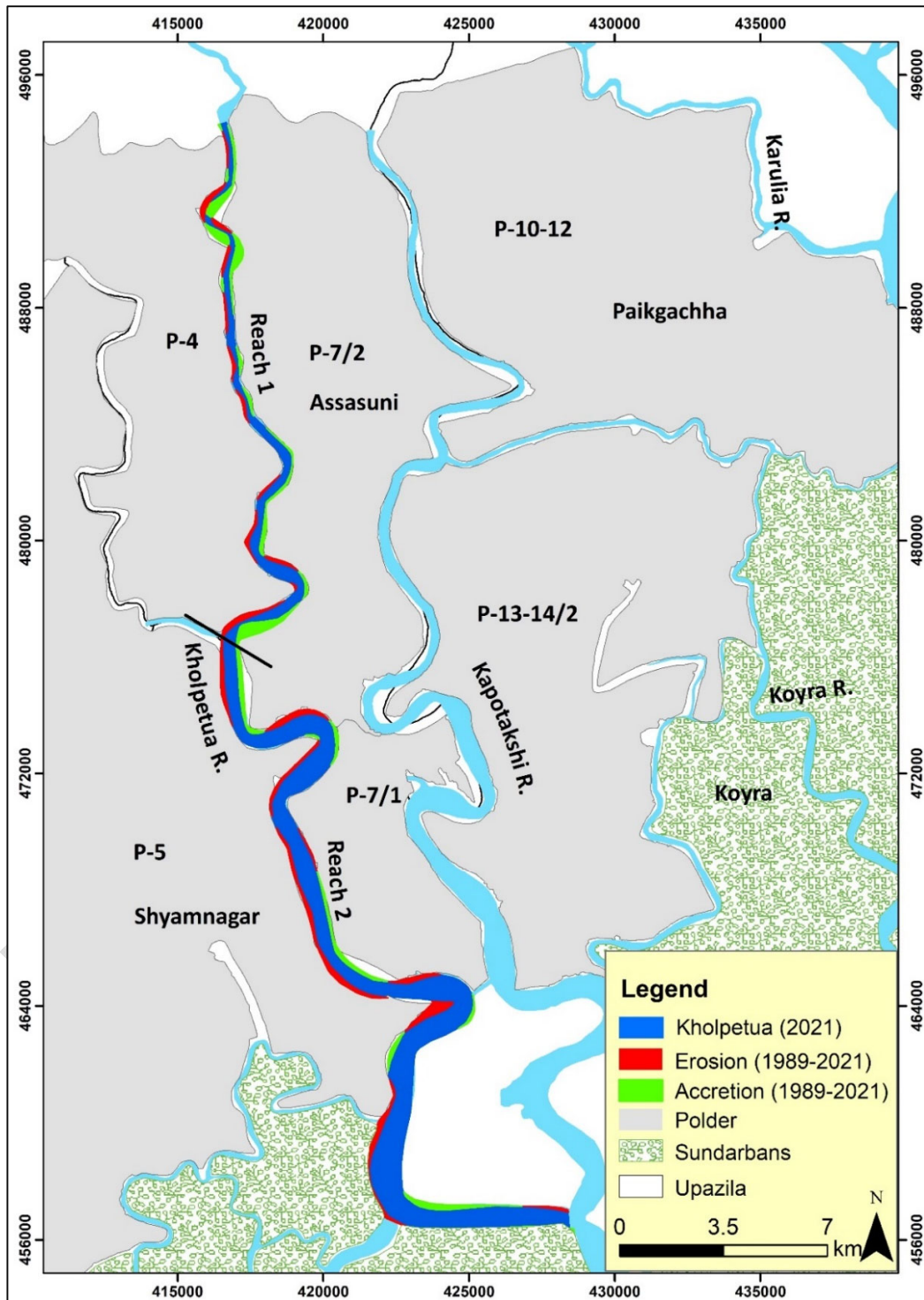


Figure 6.5: Net erosion-accretion of the Kholpetua River during (1989-2021)

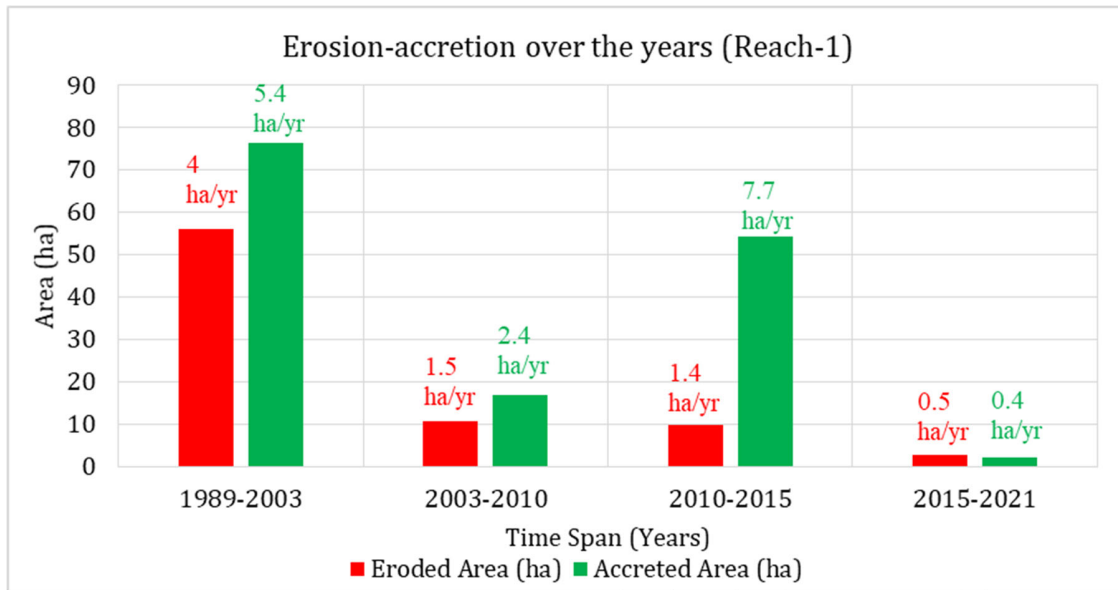


Figure 6.6: Erosion-accretion of Kholpetua River over the years (Reach-1)

Figure 6.6 shows that Reach-1 of the Kholpetua River has experienced more accretion than erosion over the years. From 1989 to 2003, accretion occurred at about 76 ha, whereas erosion was about 56 ha. But from 2003 through 2010, both erosion and accretion rates slowed down. From 2010-2015, accretion rate increased significantly. This might happen because of sedimentation in the river.

Moreover, it is noticeable that the Morirchap-Labangabati River, which is connected upstream of the Kholpetua River, has also faced severe sedimentation. In the 2015-2021 timespan, erosion and accretion rate decreased significantly. Thus, this river is becoming less active over the years.

Figure 6.7 indicates that Reach-2 is more erosion-prone than Reach-1. This is because of tidal dominance in this reach. This reach faced a maximum erosion of 164 ha with an erosion rate of 11.7 ha/yr from 1989 to 2003. After that, both erosion and accretion slowed down in the timespan of 2003-2010. However, both erosion and accretion rates increased in 2015. This might occur because of massive sedimentation. However, about 7 ha of erosion occurred in 2015 to 2021 timespan, and about 2 ha of accretion occurred in 2021.

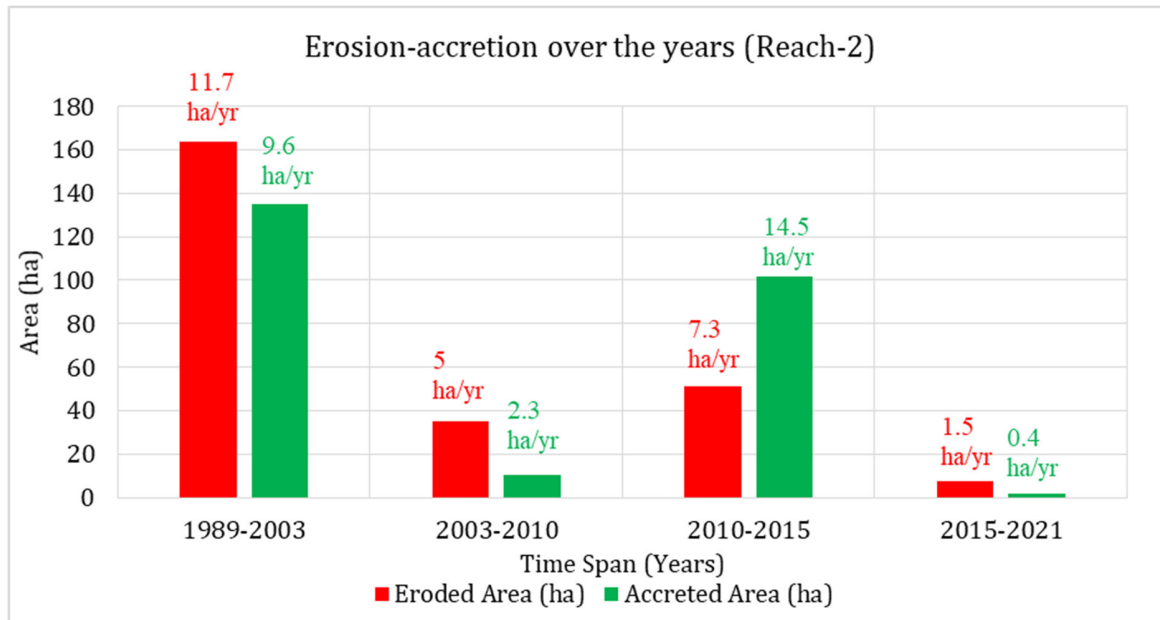


Figure 6.7: Erosion-accretion of Kholpetua River over the years (Reach-2)

Bend Migration of the Kholpetua River

Bend migration has been analyzed from 1989-2021 for the Kholpetua River. The life span of this river has been calculated to be 30 ± 10 years. Locations, the extent of bend migration, migration rate, and direction of bend migration are shown in Table 6.1. Figure 6.8 shows the bend migrations at five major locations where maximum migration occurred.

Table 6.1: Locations, Extent of Bend migration, and Migration direction for Kholpetua River

| Location | The extent of Bend migration (m) | Migration rate (m/yr) | Migration direction |
|----------|----------------------------------|-----------------------|---------------------|
| A | 225 | 8 | North- West |
| B | 200 | 7 | North- West |
| C | 212 | 7 | North- West |
| D | 180, 700 | 6, 23 | North, North- West |

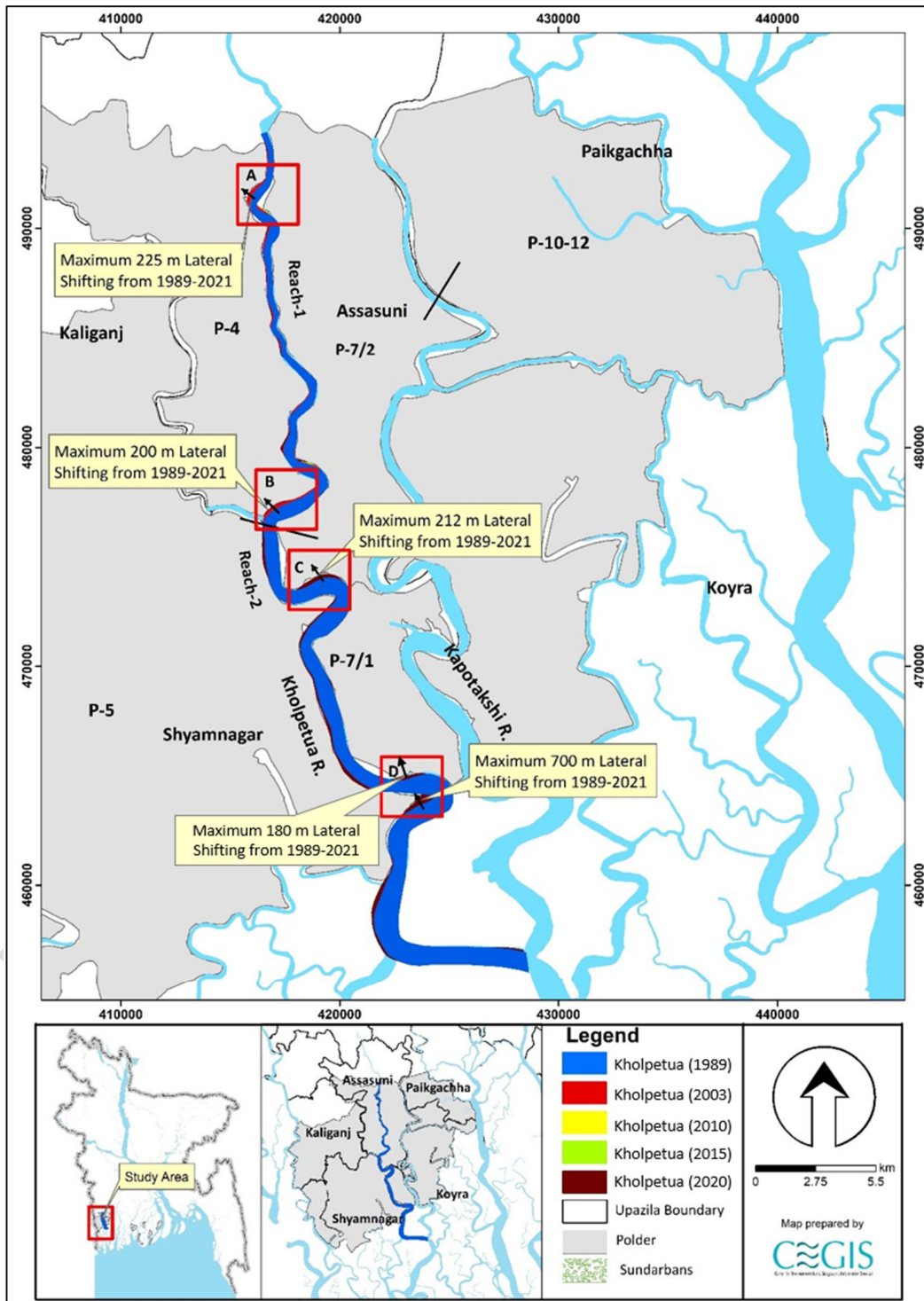


Figure 6.8: Bend migration of the Kholpetua River (1989-2021)

Prediction of the River of the Kholpetua River

Nature is always unpredictable, and it is difficult to predict the morpho-dynamics of a river. Thus, the uncertainty of predicting future migration is very high. However, statistical analysis has been done for nine (9) locations of Kholpetua River to predict future Bend migration for the next 10, 20, and 30 years. These are the locations where historic bank line migration was noted. Sites adjacent to the polders have been selected and named from "Kh-01" to "Kh-09". The existing trend of the Bend migration rate has been considered while predicting this river's future lines. Bend migrations less than 5 times the image resolution have been considered only for 30 years of prediction; prediction lines of 10 and 20 years have been avoided to reduce uncertainty. No cut-off has been seen in this river in the last 78 years. Thus, from morphological analysis and expert observation, it is predicted that no cut-off will occur within the next 30 years. Future migration lines for the next 10, 20 and 30 years at the selected river locations are shown in Figures **6.9** to **Figure 6.17**. The existing embankment alignments are shown with the black lines in the figures. Detailing of prediction lines from Kh-01 to Kh-09 are discussed below.

Kh-01 location is adjacent to Polder 7/2. A maximum of 150m of the bank have been migrated from 1989 to 2021 in this location. It is noticeable that maximum erosion occurred from 1989 to 2003. After that, the erosion rate slowed; after 2015, no erosion occurred in this location. Thus prediction lines for the next 10, 20, and 30 years have been drawn to calculate the rate of delineation of erosion rate (**Figure 6.9**).

In comparison, Kh-02 location is adjacent to Polder 4. This location has migrated a maximum of 100 m of the bank from 1989 to 2021. It is noticeable that erosion occurred from 1989 to 2003 timespan in this location. After that, no erosion occurred till 2015. In 2021, maximum erosion of about 60 m occurred in this location. As maximum migration is less than 4/5 times the image resolution, this location's future prediction for only 30 years has been considered (**Figure 6.10**).

Moreover, Kh-03 location is adjacent to Polder 4. This location has migrated a maximum of 70 m of the bank from 1989 to 2021. Maximum erosion occurred from 1989 to 2003 in this location. As maximum migration is less than 4/5 times the image resolution, future prediction for only 30 years has been considered for this location (**Figure 6.11**). Additionally, the Kh-04 location is adjacent to Polder 7/2. This location has migrated a maximum of 100m of the bank from 1989 to 2021. Figure 6.12 shows that the river bank in this location has been migrating continuously over the last 32 years. Thus, prediction lines for the next 10, 20, and 30 years have been drawn, calculating the migration rate in this location.

Furthermore, the Kh-05 location is adjacent to Polder 4 and Polder 5. This location has migrated a maximum of 160 m of the bank from 1989 to 2021. Figure 6.13 shows that the river bank in this location has been migrating continuously over the last 32 years. Thus, prediction lines for the next 10, 20, and 30 years have been drawn, calculating the migration rate in this location. Kh-06 location is adjacent to Polder 7/2. This location has migrated a maximum of 175 m of the bank from 1989 to 2021. Figure 6.14 shows that the river bank in this location has been migrating continuously over the last 32 years. Thus, prediction lines for the next 10, 20, and 30 years have been drawn, calculating the migration rate in this location.

Besides, the Kh-07 location is adjacent to Polder 5. A maximum of 170 m of the bank have been migrated from 1989 to 2021 in this location. Figure 6.15 shows that river bank in this location has been migrating continuously over last 32 years. Thus, prediction lines for next 10, 20 and 30 years

have been drawn, calculating the migration rate in this location. Kh-08 location is adjacent to Polder 5. This location has migrated a maximum of 700 m of the bank from 1989 to 2021. Figure 6.16 shows that the river bank in this location has been migrating continuously over the last 32 years. Thus, prediction lines for the next 10, 20, and 30 years have been drawn, calculating the migration rate in this location. Kh-09 location is adjacent to Polder 5. This location has migrated a maximum of 200 m of the bank from 1989 to 2021. Figure 6.17 shows that river banks in this location have been migrated mainly till 2010. After that, no significant erosion was observed. In 2021, little Bend migration was observed here, which considered it vulnerable for the future. Thus, prediction lines for the next 30 years have been drawn, calculating this location's migration rate.

To date, we have kept the shapefile as it is as we have received from the client. If any updated shapefiles are provided, the maps will be updated accordingly. This is to mention here that it was observed that the polder boundary lies within the boundary of the Kholpetua River 2021 in a few locations.

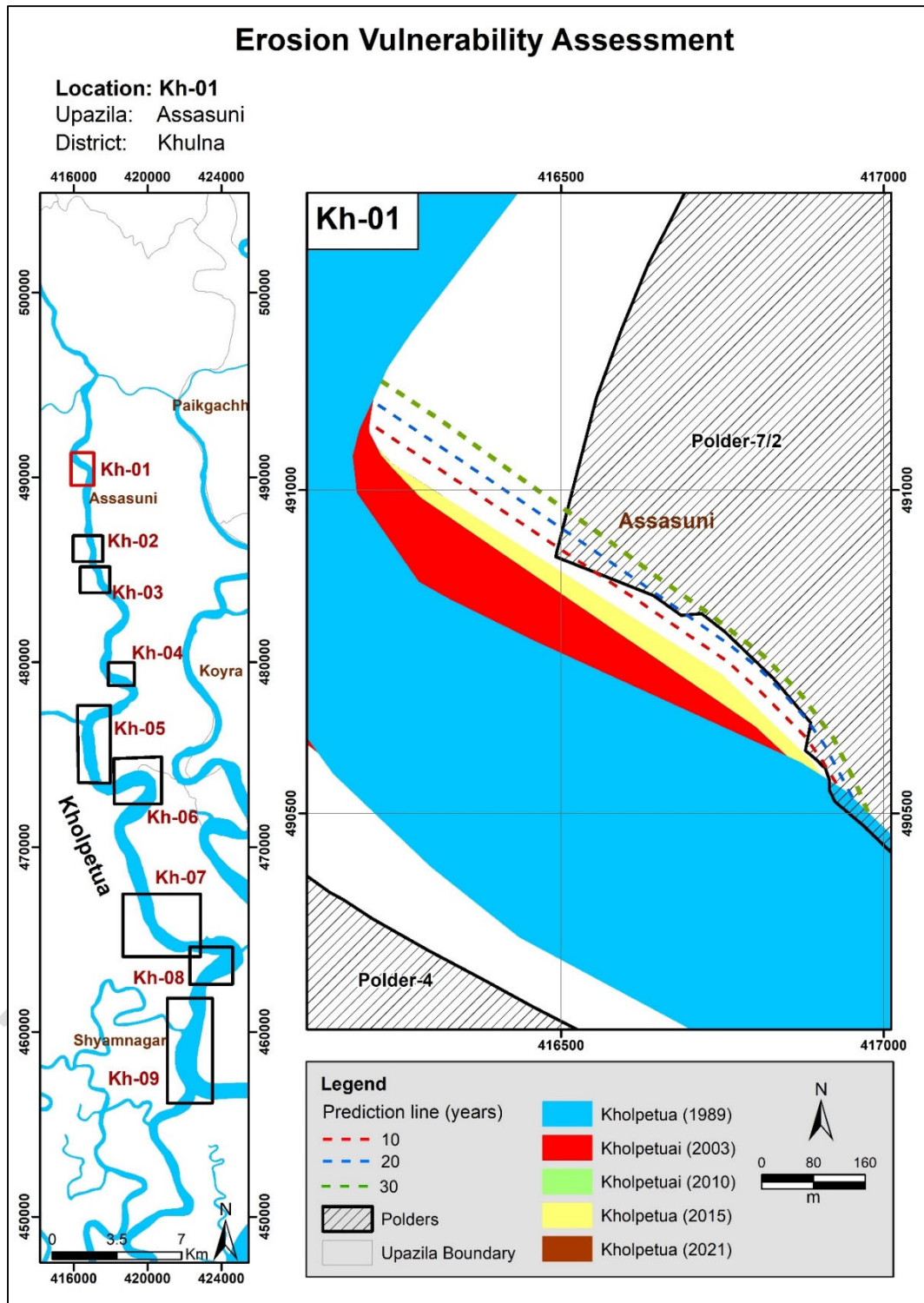


Figure 6.9: Bend migration in the next 10, 20, and 30 years in the Kholpetua River

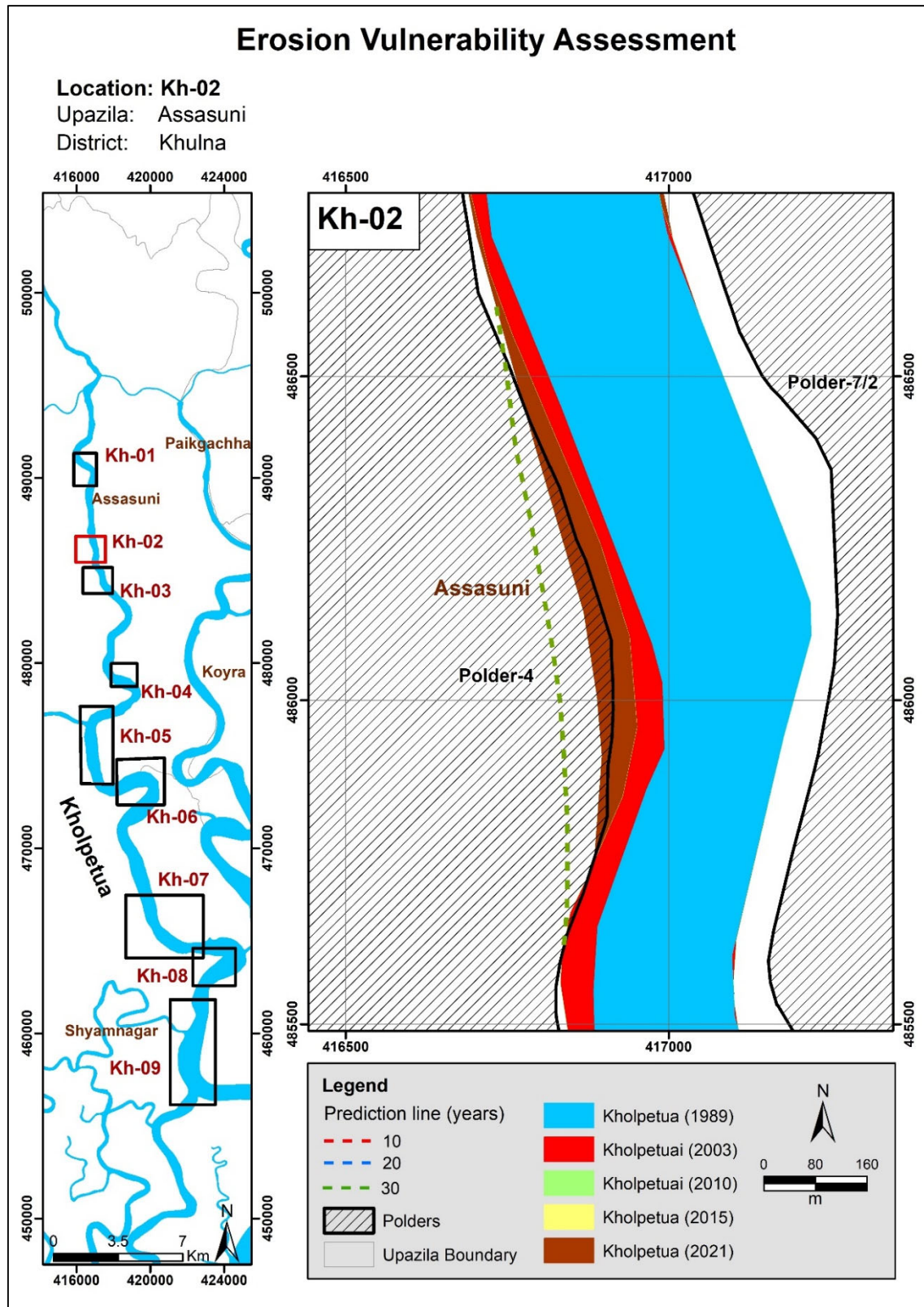


Figure 6.10: Bend migration in the next 10, 20, and 30 years in the Kholpetua River

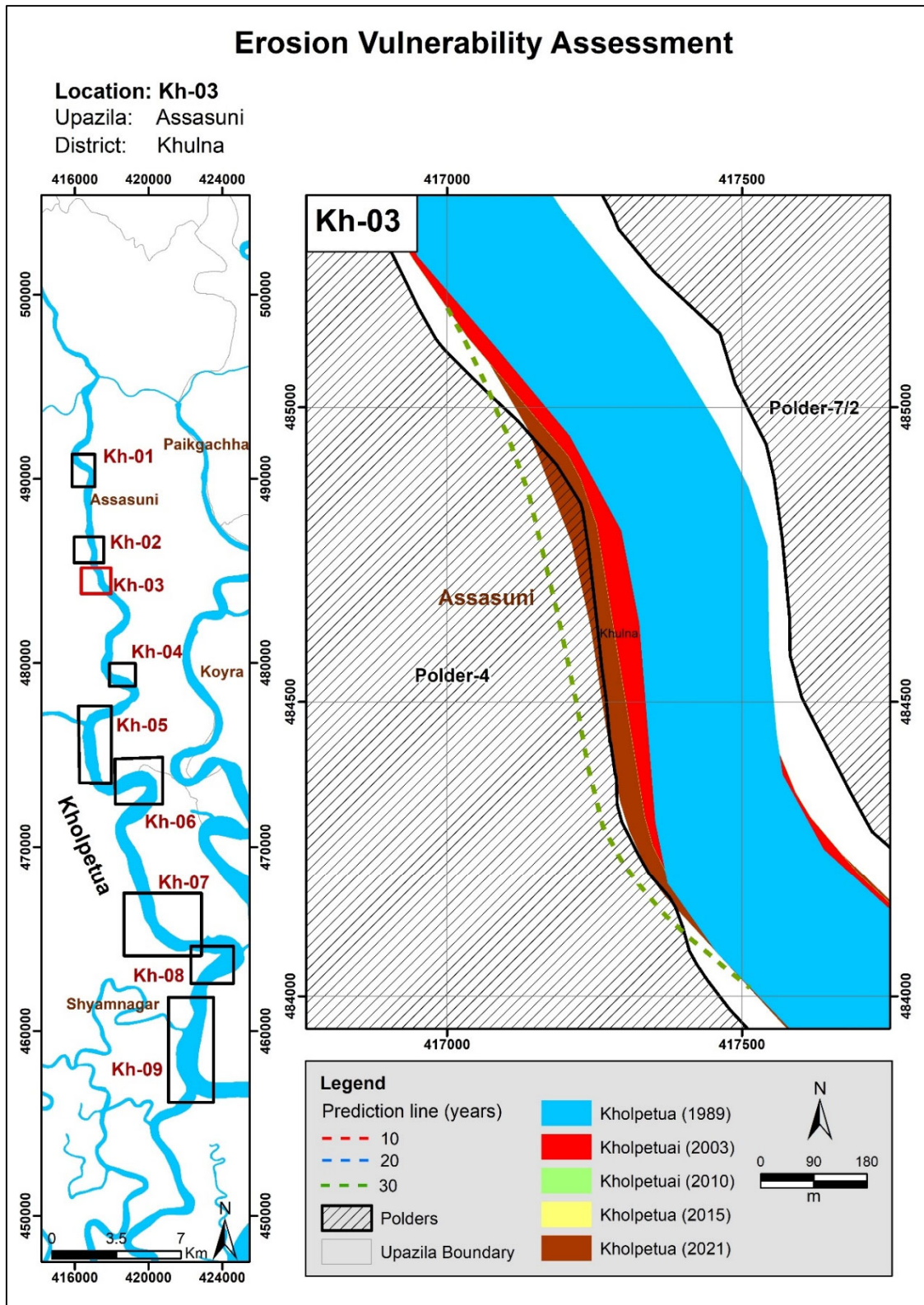


Figure 6.11: Bend migration in the next 10, 20, and 30 years in the Kholpetua River

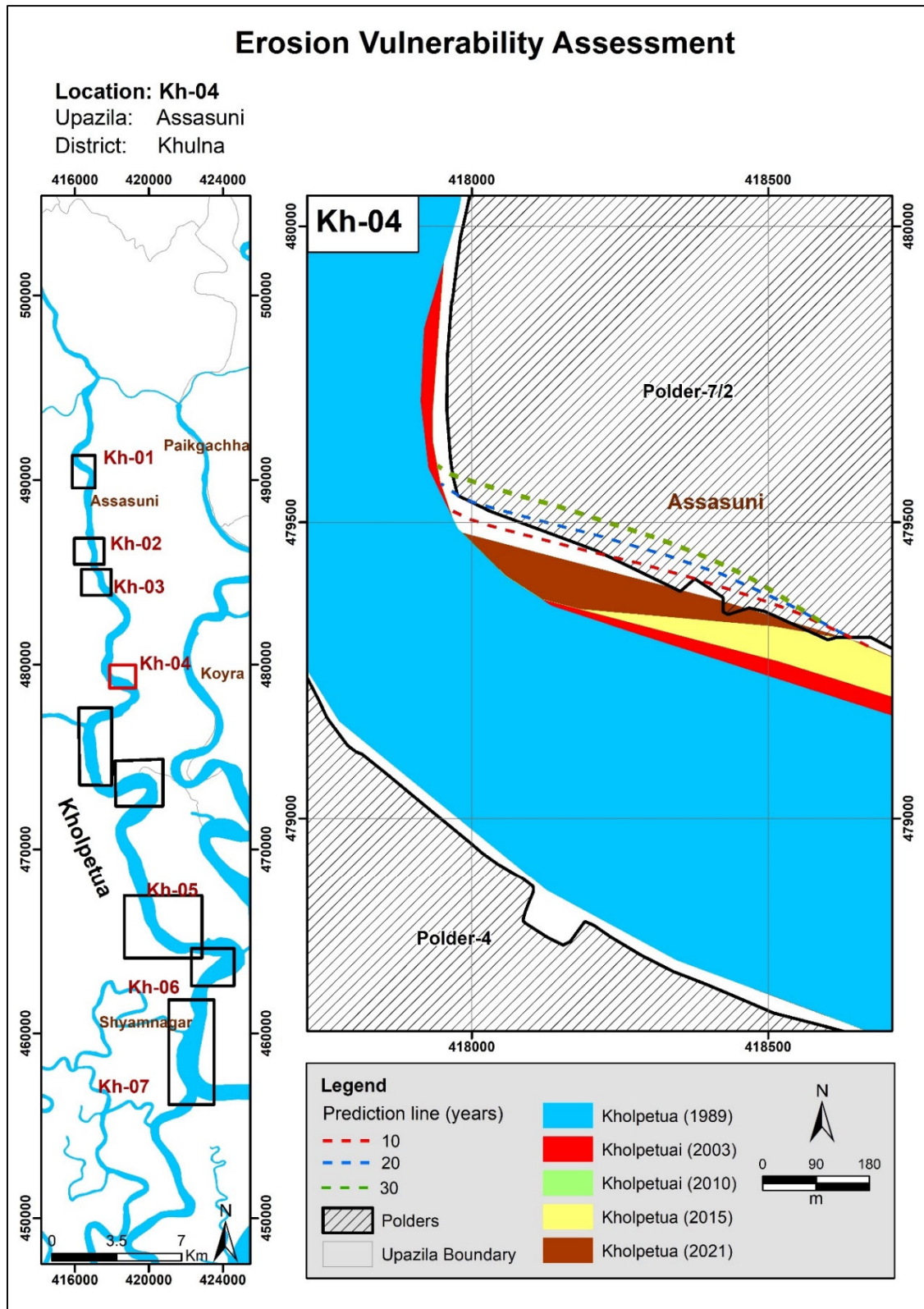


Figure 6.12: Bend migration in the next 10, 20, and 30 years in the Kholpetua River

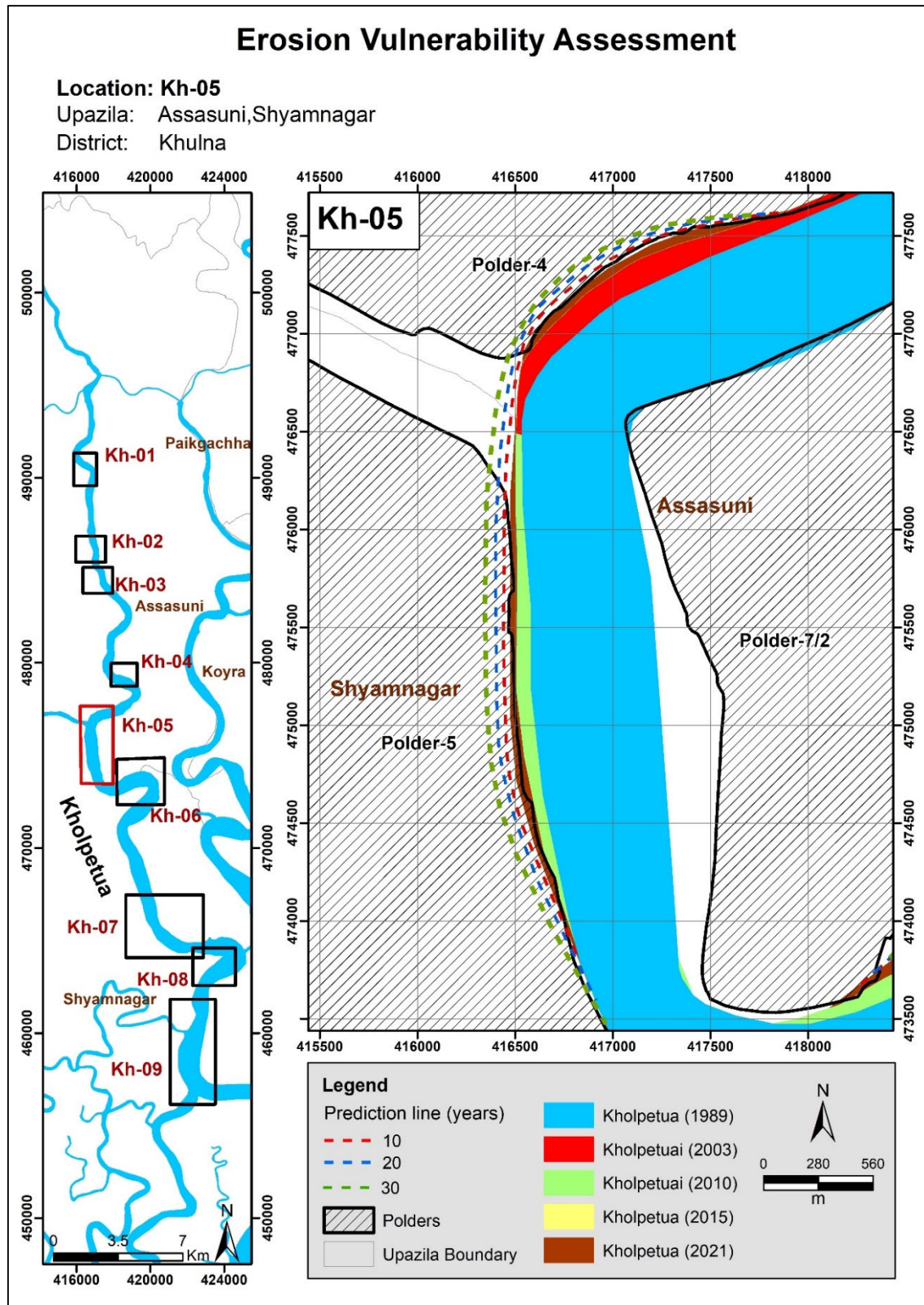


Figure 6.13: Bend migration in next 10, 20 and 30 years in Kholpetua River

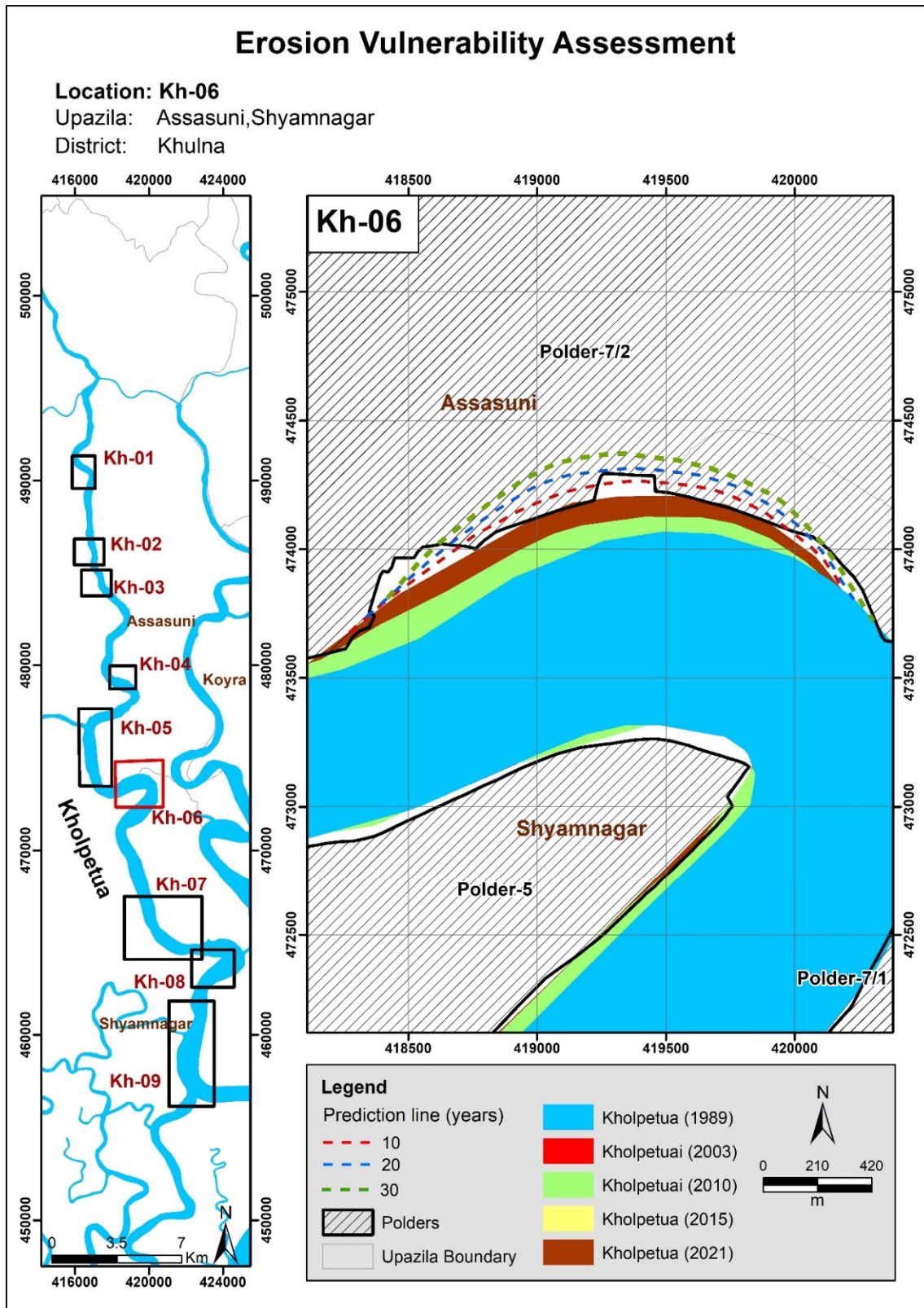


Figure 6.14: Bend migration in the next 10, 20, and 30 years in the Kholpetua River

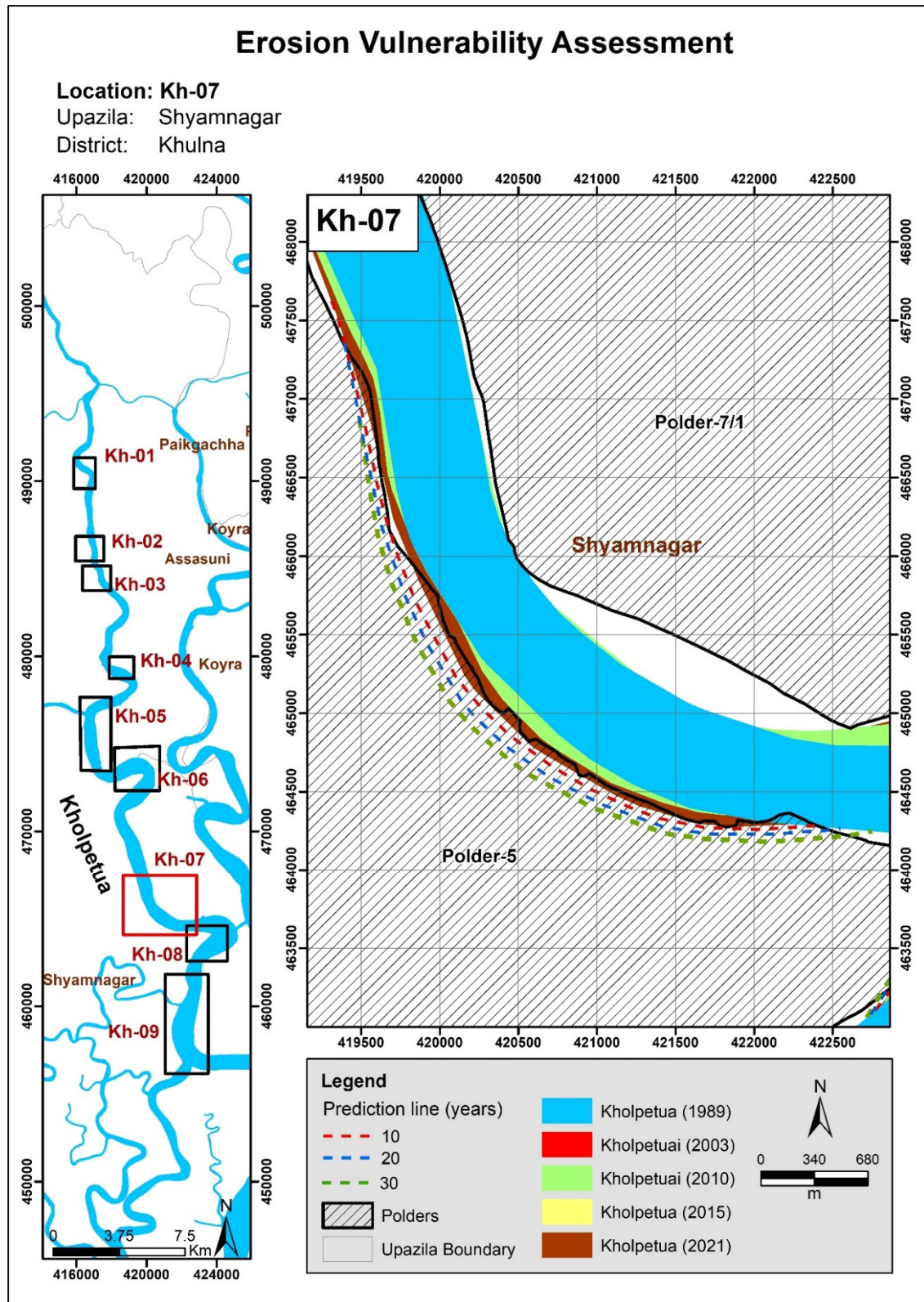


Figure 6.15: Bend migration in the next 10, 20, and 30 years in the Kholpetua River

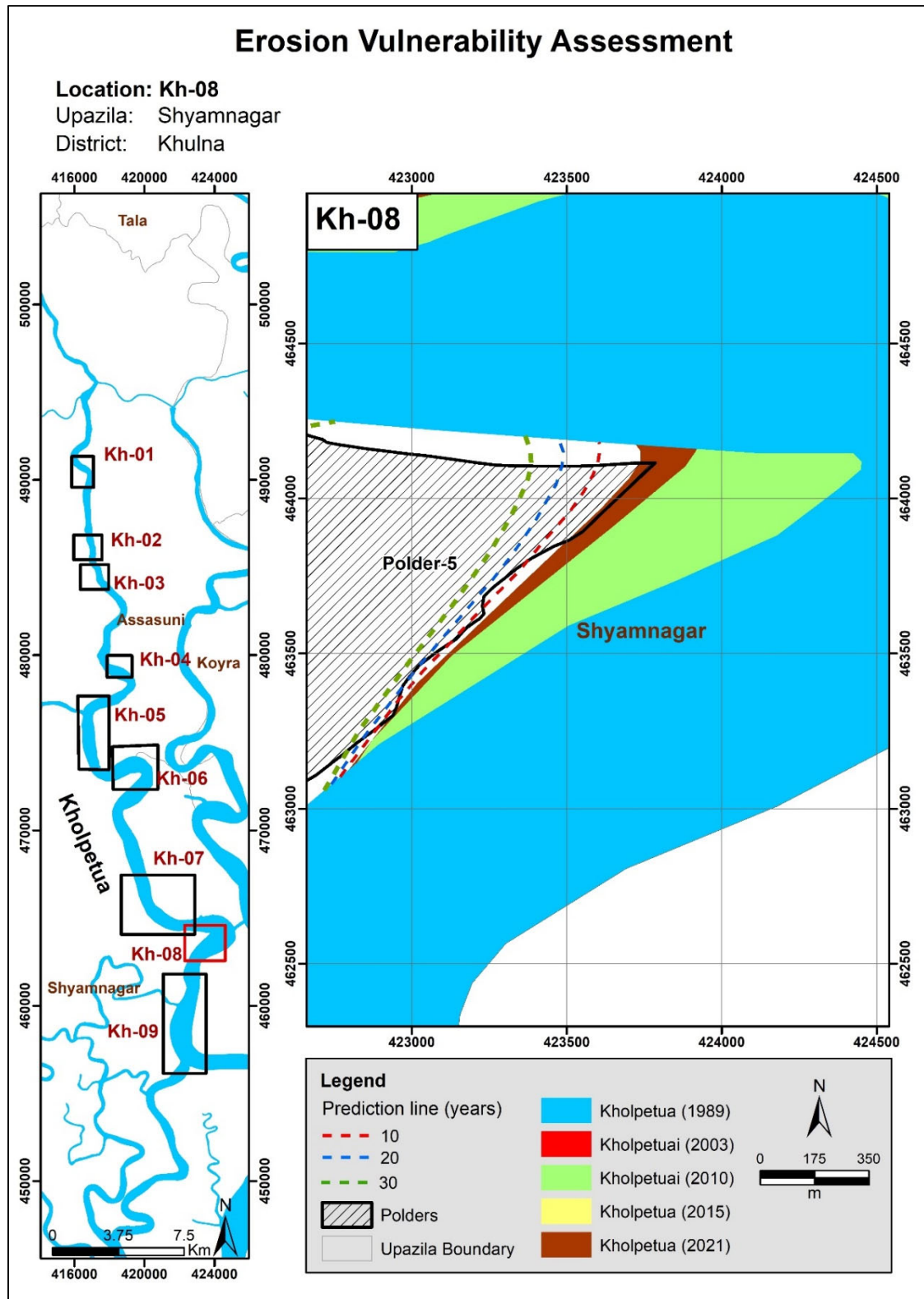


Figure 6.16: Bend migration in the next 10, 20, and 30 years in the Kholpetua River

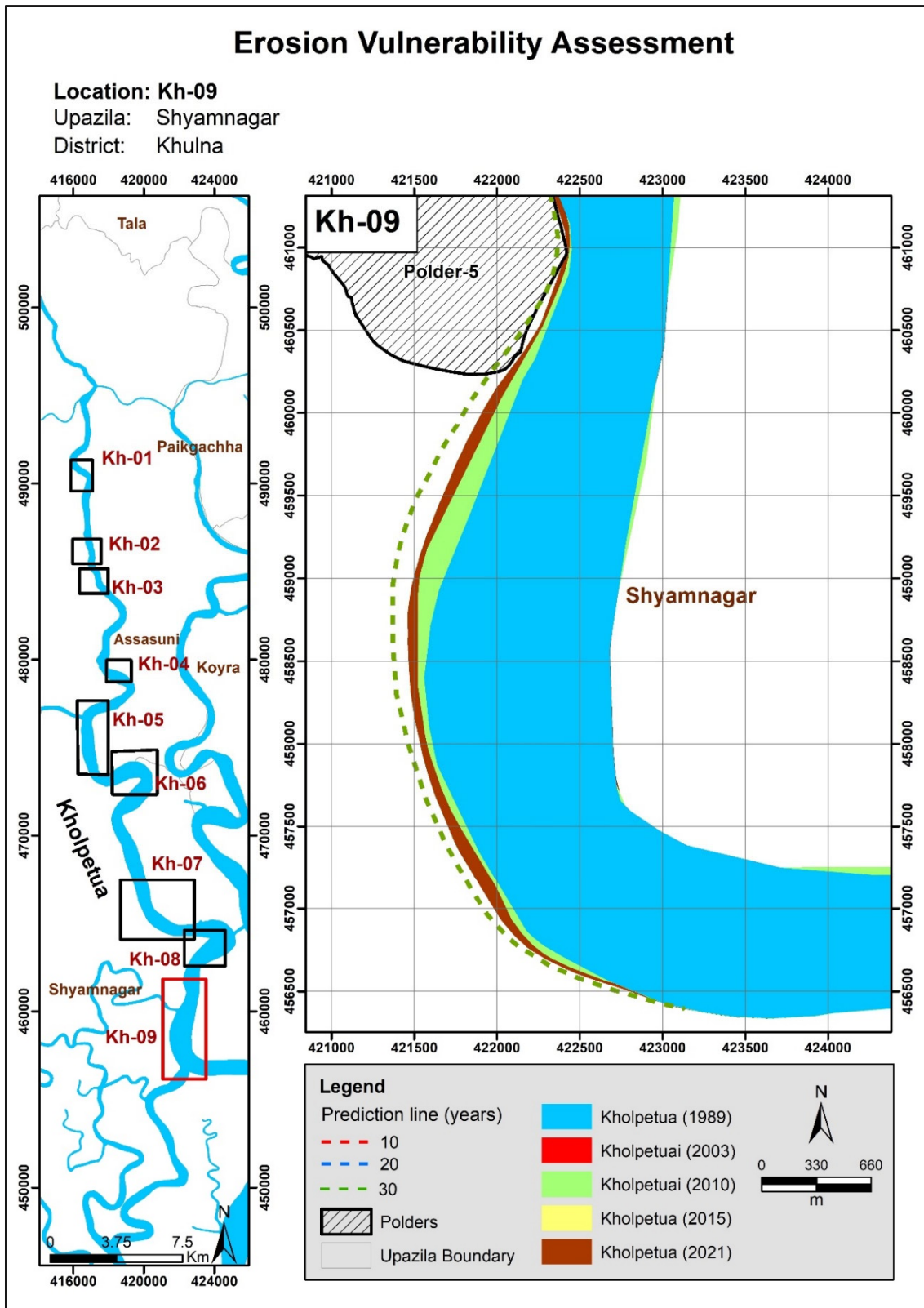


Figure 6.17: Bend migration in the next 10, 20, and 30 years in the Kholpetua River

6.2 Ichamati-Kalindi River

Ichamati-Kalindi is a transboundary River that offtakes from Bhairab-Kapotakshi River in Damurhuda Upazila (Chuadanga) and outfalls in Raimangal River in Shyamnagar Upazila (Satkhira). This river enters India at Damurhuda Upazila (Chuadanga) and re-enters Bangladesh in Jibannagar Upazila; then, the river flows along the international boundary of India and Bangladesh. The river again enters India in Maheshpur Upazila (Jhenaidah) and flows along the international boundary again from Sharsha Upazila (Jessore). In this study, the reach of the Ichamati-Kalindi River has been considered from Kaliganj to Shyamnagar (Satkhira).

To better understand the morphology, the river reach has been divided into two reaches. These reaches have been categorized by observing the variation of the width. Reach-1 is considered from Mathureshpur to Ratanpur, and Reach-2 from Nurnagar to Kaikhali. (Figure 5.18).

Historical Development of the Ichamati-Kalindi River

To assess the historical development, the Ichamati-Kalindi River, the map of 1943, and satellite images of 1989, 2003, and 2021 were used (**Figure 5.18**). Comparing the map and the images, it is evident that the alignment of the river has not changed significantly over the past 78 years.

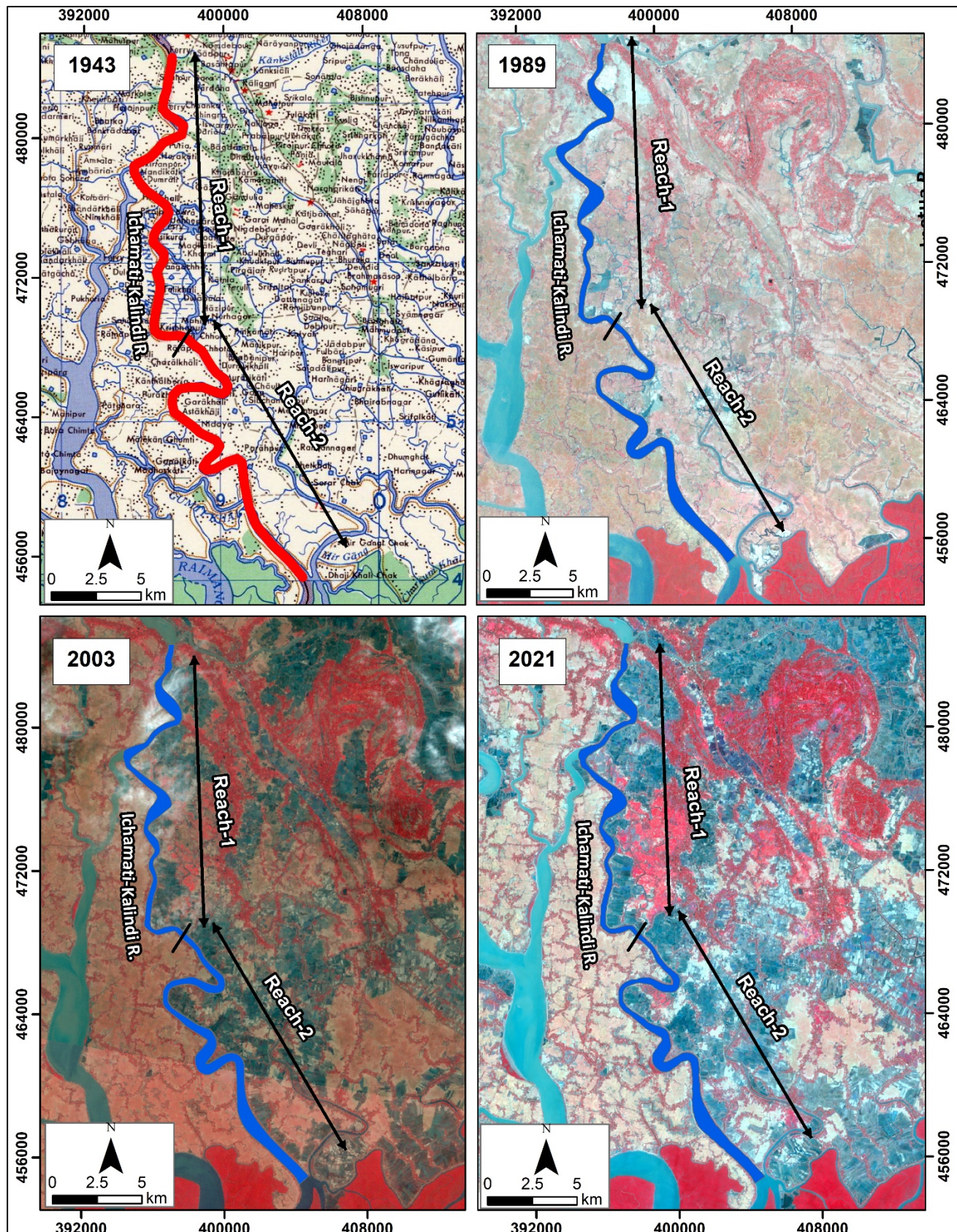


Figure 5.18: Historical Development of Ichamati-Kalindi River

Average Width of the Ichamati-Kalindi River

Changes in the river width from 1989 to 2021 have been assessed and presented in **Figure 5.19**. The average width of reach-1 slightly decreased by about 20 m from 1989 to 2003. After that, no trend has ever been observed in the average width for Reach-1. At Reach-2, the average width increased slightly from 1989 to 2003 by 19m. Then, no significant change occurred in Reach-2 till 2021.

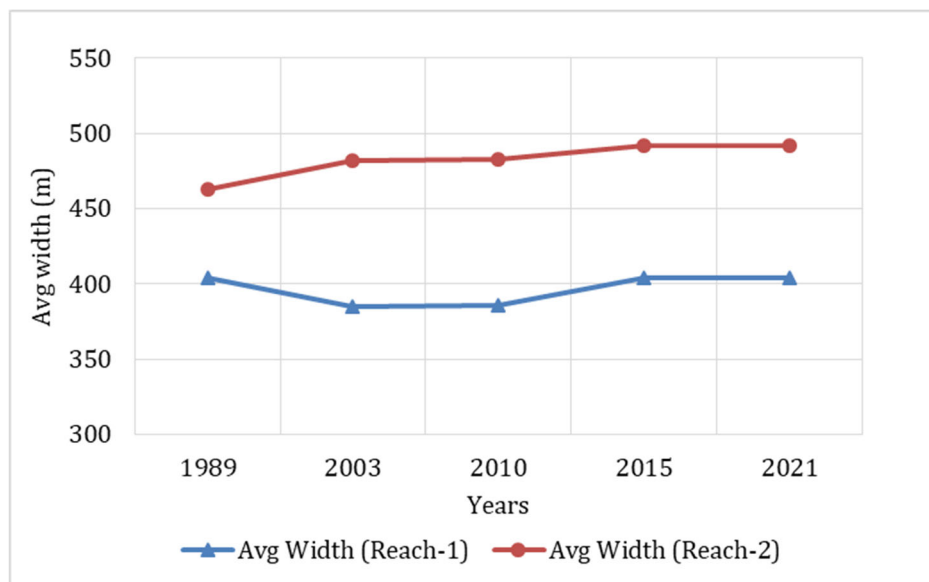


Figure 5.19: Average width of Ichamati-Kalindi River from 1989-2021

Sinuosity of the Ichamati-Kalindi River

The sinuosity of the Ichamati-Kalindi River is represented in **Figure 5.20**. The sinuosity index of Reach-1 has not changed for the last three decades. The sinuosity index shows a slight decreasing trend from 1989 to 2003. After that, no significant change occurred since 2021.

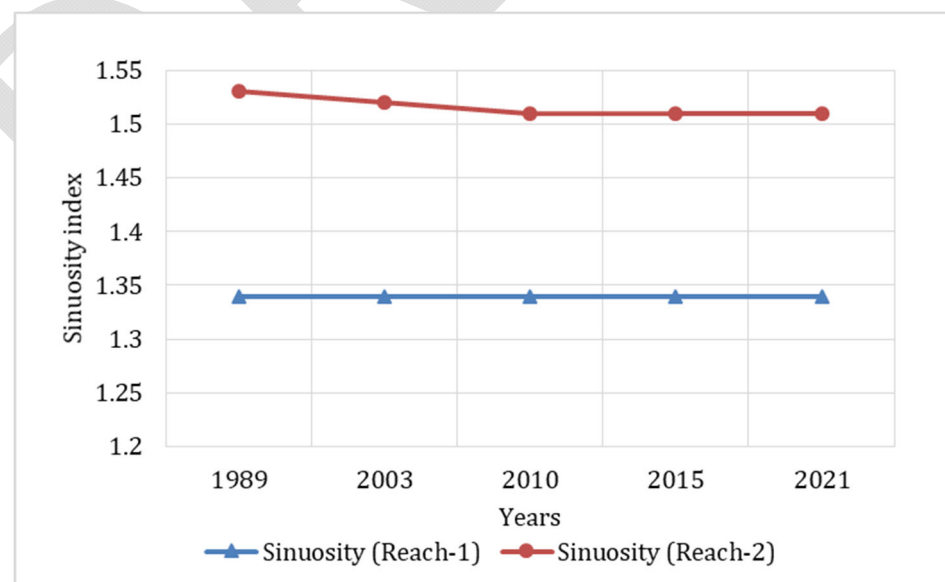


Figure 5.20: Sinuosity of Ichamati-Kalindi River from 1989-2021

Erosion-Accretion Analysis of the Ichamati-Kalindi River

For erosion-accretion assessment, bank lines of 1989, 2003, 2010, 2015, and 2021 were superimposed. The erosion and accretion-prone areas are presented in **Figure 5.21** and marked red and green, respectively. It is observed that the left bank has experienced more accretion, and the right bank has experienced more erosion. Thus, it confirmed that the right bank of Ichamati-Kalindi River is more stable than the left bank.

DRAFT

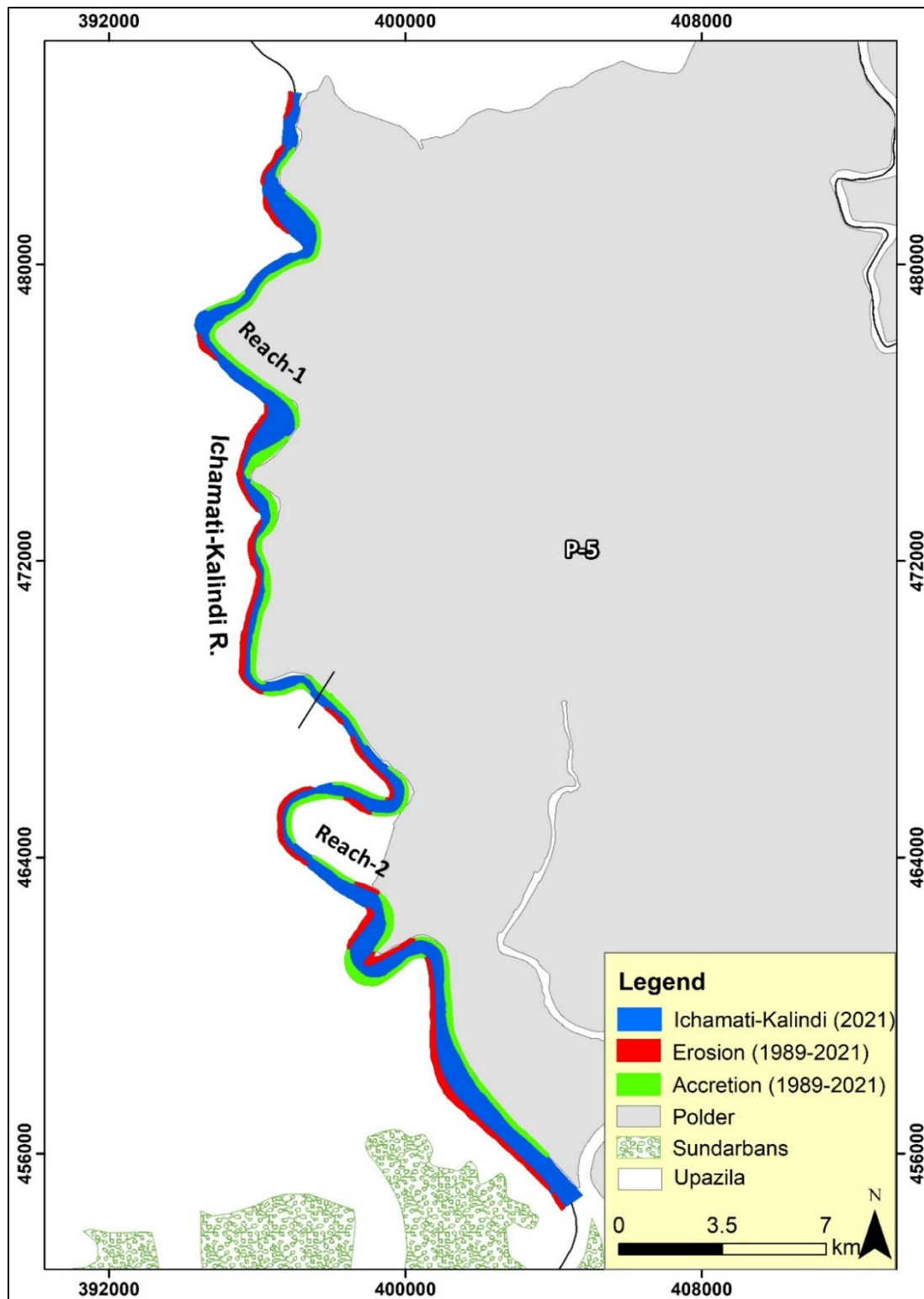


Figure 5.21: Erosion-accretion of the Ichamati-Kalindi River during (1989-2021)

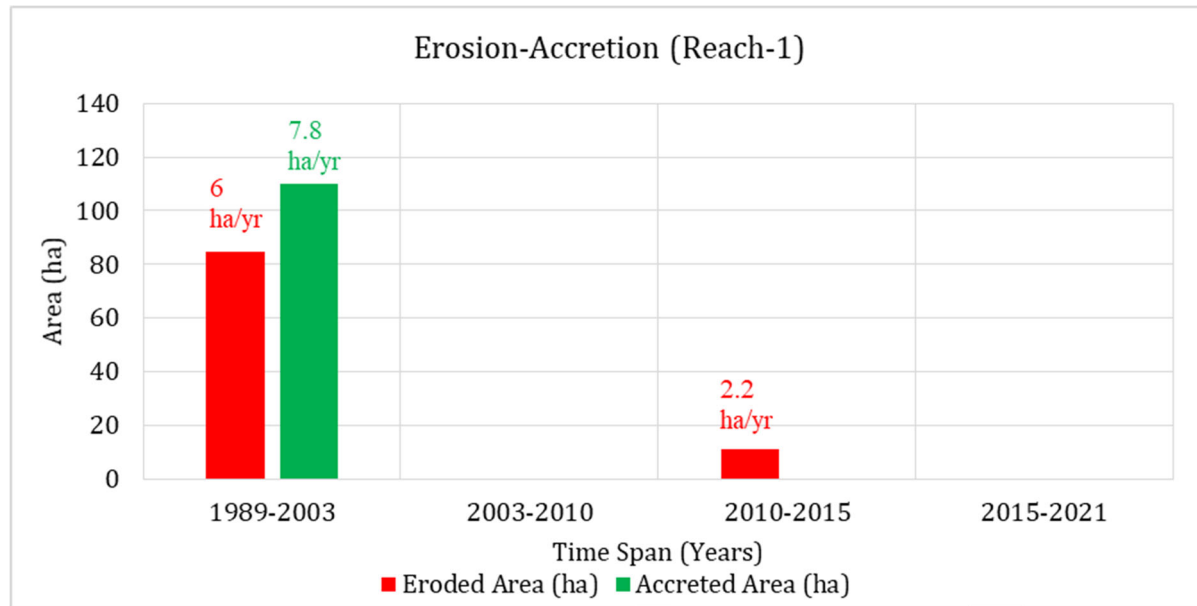


Figure 5.22: Erosion-accretion of Ichamati-Kalindi River over the years (Reach-1)

Figure 5.22 shows that Reach-1 of the Ichamati-Kalindi River has experienced more accretion (109 ha) than erosion (84 ha) from 1989 to 2003. No erosion and accretion occurred in the 2003-2010 timespan. However, in the 2010-2015 timespan, little erosion occurred at about 11 ha. After that, no erosion and accretion occurred in the 2015-2021 timespan. Thus, it confirmed that the river reach has become less dynamic.

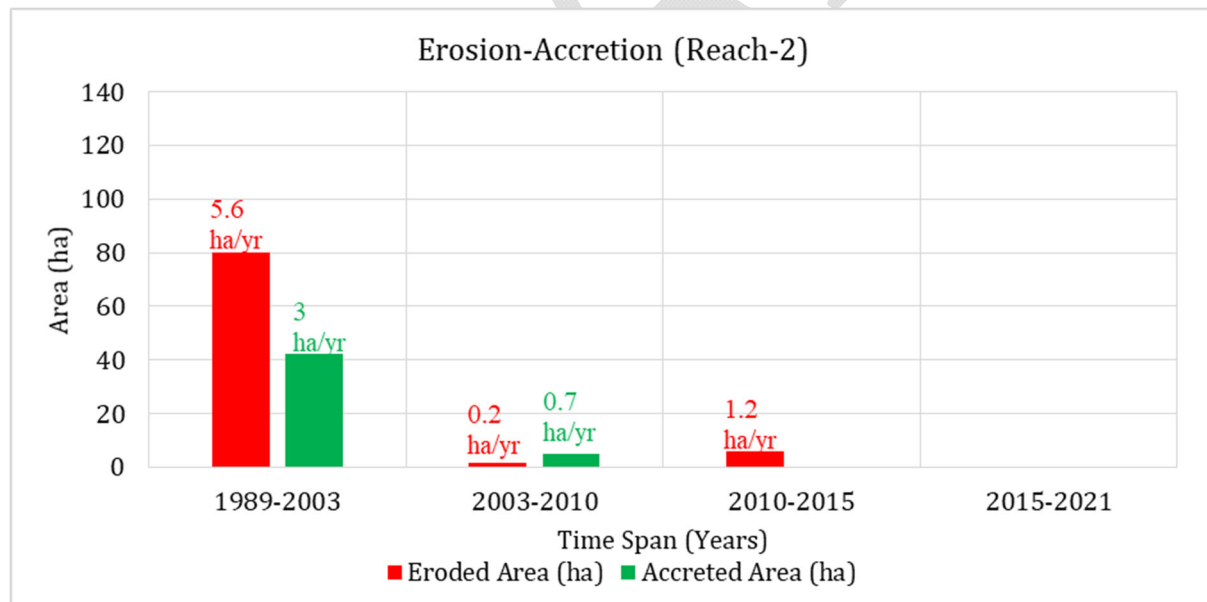


Figure 5.23: Erosion-accretion of Ichamati-Kalindi River over the years (Reach-2)

Figure 5.23 observed that erosion dominated accretion in Reach-2 in the 1989-2003 timespan. This might be because of tidal dominance. Then both erosion and accretion declined significantly in the 2003-2010 timespan. After that, a small amount of erosion occurred in the 2010-2015 timespan. After that, no erosion-accretion occurred in the 2015-2021 timespan.

Bend Migration of the Ichamati-Kalindi River

Bend migration has been analyzed from 1989-2021 for the Ichamati-Kalindi River. The life span of this river has been calculated at 14 ± 10 years. In Figure 5.24, the Bend migrations are shown at four major locations where maximum migration occurred. Locations, Extent of Bend migration, migration rate, and direction of Bend migration are shown in Table 5.2.

Table 5.2: Locations, Extent of Bend migration, and Migration direction for Ichamati-Kalindi River

| Location | The extent of Bend migration (m) | Migration rate (m/yr) | Migration direction |
|----------|----------------------------------|-----------------------|---------------------|
| A | 90 | 6 | North- East |
| B | 125 | 9 | West |
| C | 250 | 11 | North- West |
| D | 150 | 18 | South-West |

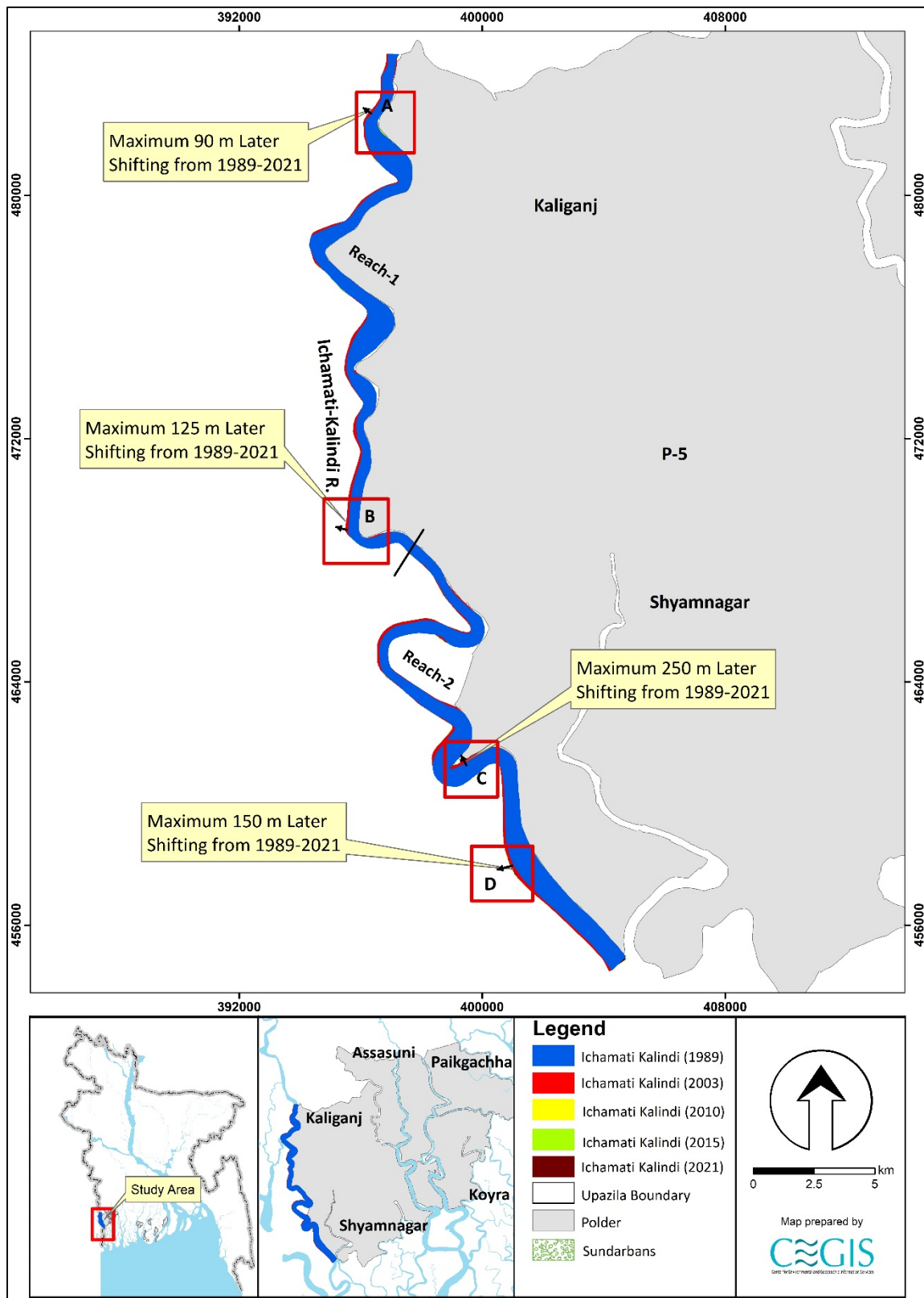


Figure 5.24: Bend migration of the Ichamati-Kalindi River (1989-2021)

Projection of the Ichamati-Kalindi River

Ichamati-Kalindi River is not very dynamic, and banks adjacent to polders are comparatively stable. However, a statistical analysis has been done for one (1) location in this river to predict future Bend migration for the next 30 years. Bend migration extent less than 5 times the image resolution has been considered only for 30 years of prediction. Prediction lines of 10 and 20 years have been avoided to reduce uncertainty. During the last 78 years, no cut-off has been seen in this river; accordingly, no cut-off criteria have been considered. However, the detailing of the prediction line of Ic-01 in this river is described below.

Ic-01 location is adjacent to Polder 5. This location has migrated a maximum of 250 m of the bank from 1989 to 2021. As the migration rate has been significantly less in recent years in this location, future prediction for only 30 years has been considered for this location (**Figure 6.25**).

DRAFT

Erosion Vulnerability Assessment

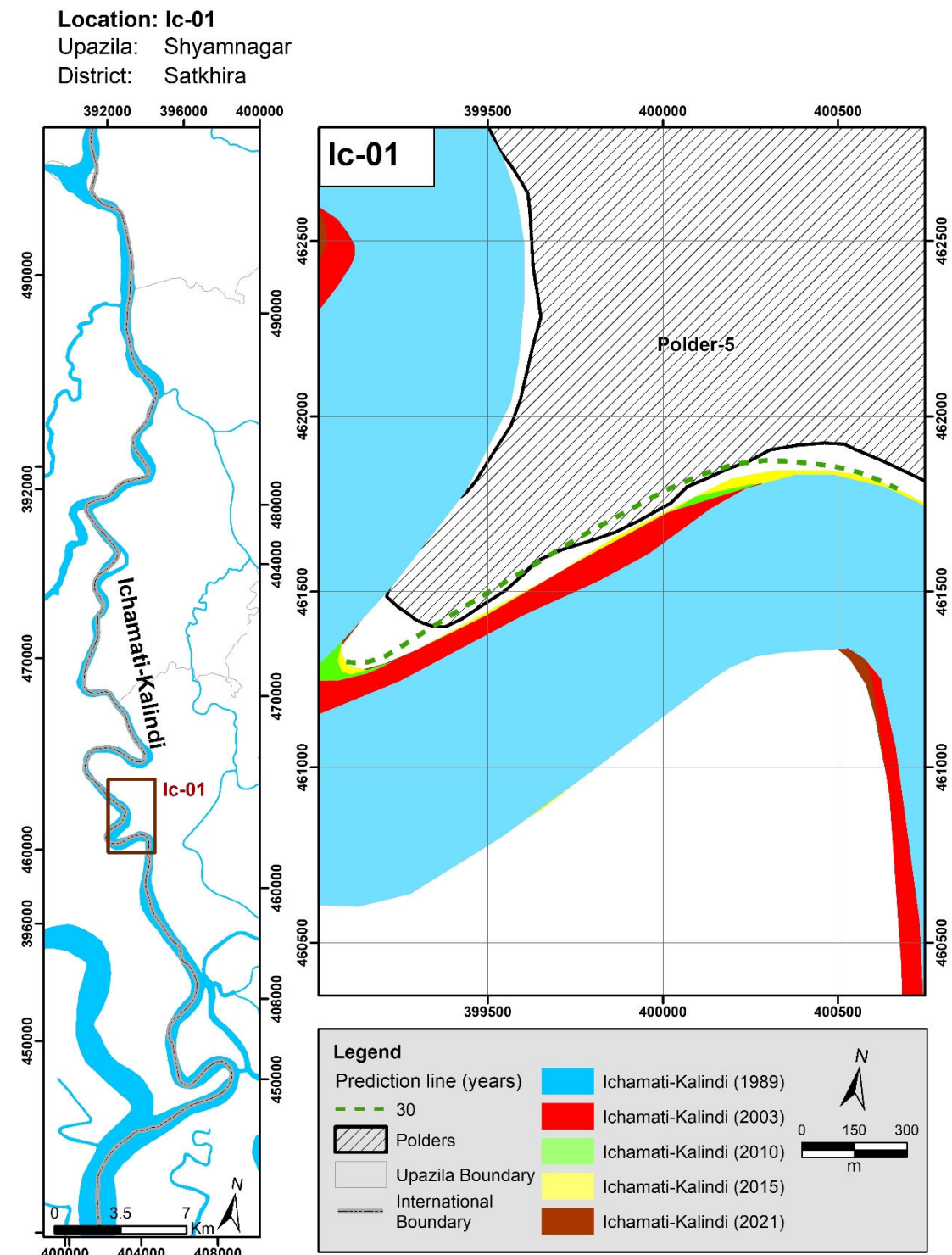


Figure 6.25: Bend migration in the next 10, 20, and 30 years in the Ichamati-Kalindi River

6.3 Kapotakshi River

Kapotakshi River offtakes from Bhairab River in Chaugachha Upazila (Jessore). The river flows through Jhikargachha, Satkhira, Tala (Jessore) and Paikgachha (Khulna) and outfalls in Kholpetua River in Koyra Upazila (Khulna). This study considers the Reach of Kapotakshi River from Paikgachha to its outfall at Kholpetua River at Koyra (Khulna). The river was connected with the Ganges River through the Mathabhanga-Bhairab River system. However, the river has been drying up due to the combined hydro-morphological changes (unfavorable conditions at the off-take of the Mathabhanga River with the Ganges River) and human interventions. Because loss of conveyance also creates water stagnancy in some places. To better understand the morphology, the river reach has been divided into three more reaches. Reach-1 from Laskar-Raruli to Amadi-Khajra, Reach-2 from Amadi-Khajra to Maharajpur-Pratap Nagar and Reach-3 from Maharajpur-Pratap Nagar to South Bedkashi-Gabura. These reaches have been categorized by observing the variation of the width. (Figure 6.18).

Historical Development of the Kapotakshi River

The study referred to the 1943 map and 1989, 2003, and 2021 satellite images to assess the historical development of the Kapotakshi River (**Figure 6.26**). Comparing the map and the images, it is evident that the river's course has not changed over the past 78 years. In addition, no cut-off has been observed during this period.

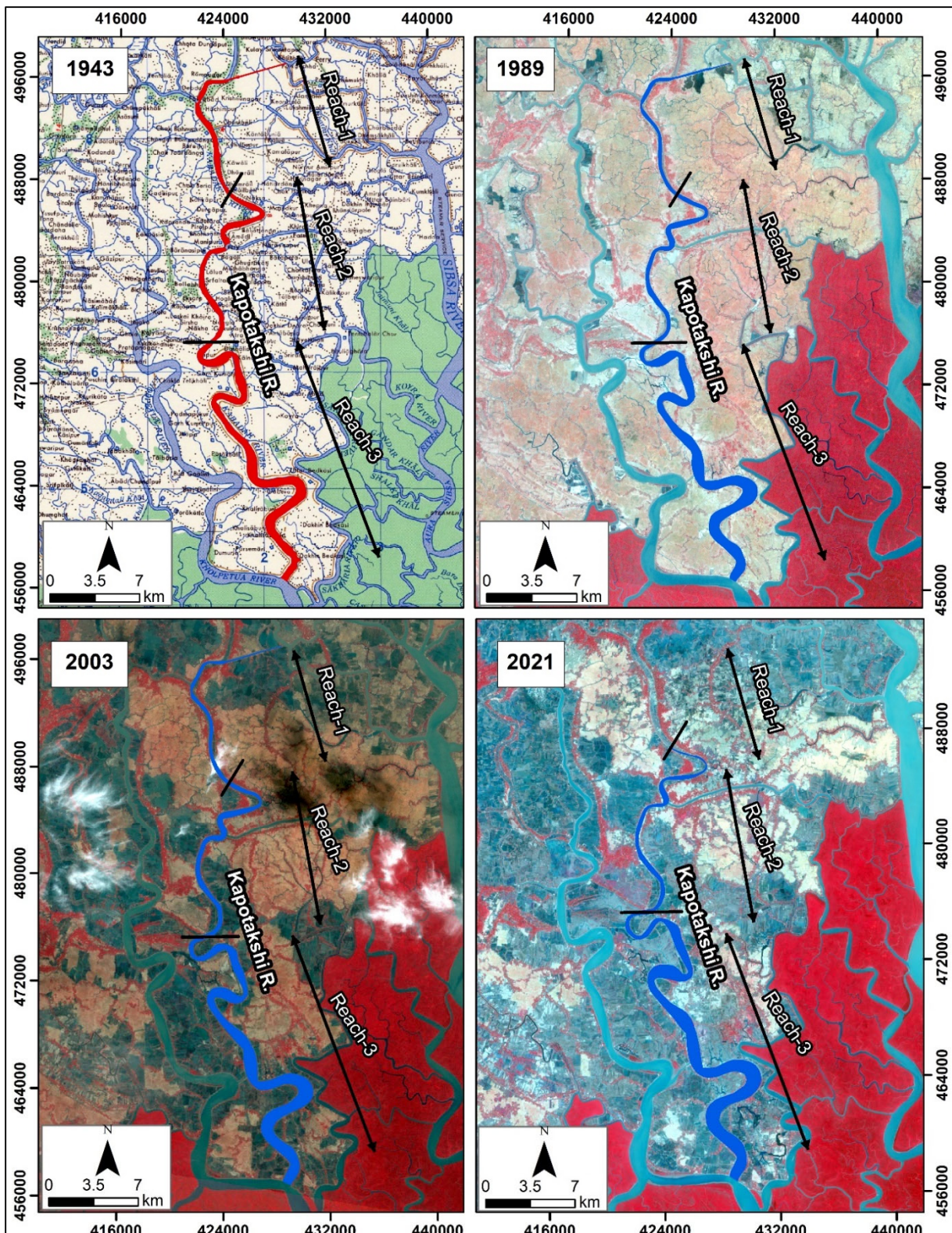


Figure 6.26: Historical Development of Kapotakshi River

Average Width of the Kapotakshi River

Changes in the river width from 1989 to 2021 have been assessed and presented in **Figure 6.27**. Reach 1 narrowed from 1989 (230 m) to 2010 (162 m). After that, the reach dried significantly. So, bank delineation was not possible through satellite images. From Google Earth analysis, the average width of the river was about 10-30 m in 2015. In 2021, most of the portion of this reach has completely dried. In addition, the average width of Reach 2 shows a decreasing trend from 342 m in 1989 to 289 m to 2021. The average width of the Reach 3 shows no significant change over the past 32 years. This reach has not experienced high dynamicity.

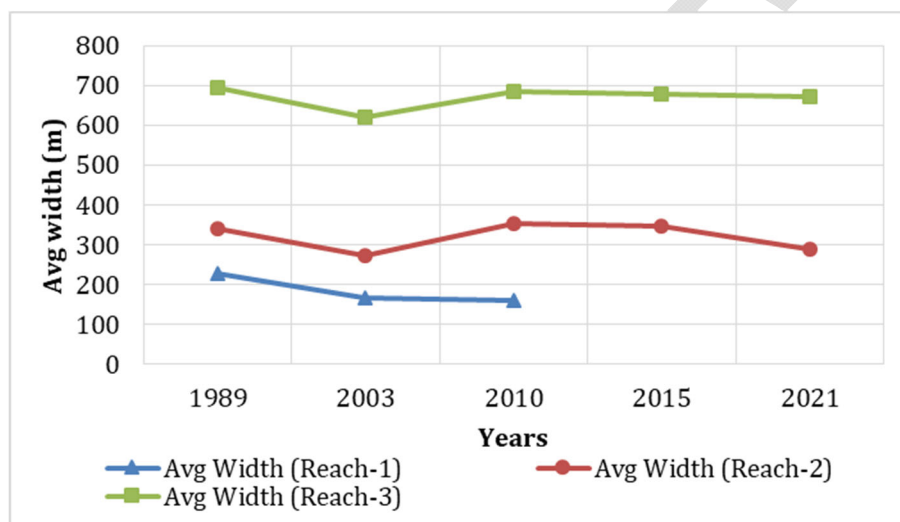


Figure 6.27: Average width of Kapotakshi River from 1989-2021

Sinuosity of the Kapotakshi River

The sinuosity of the Kapotakshi River is represented in **Figure 6.28**. The sinuosity of Reach 1 of Kapotakshi River has not changed from 1989 to 2010. The sinuosity of Reach 2 has increased from about 1.48 to approximately 1.54 from 1989 to 2021. Thus the reach has become more meandering, thus confirming narrowing. However, the sinuosity of Reach 3 of the river has increased on a small scale from 1989 (1.67) to 2021 (1.76). Thus, this reach has become more meandering throughout the years, indicating a drying up of this reach.

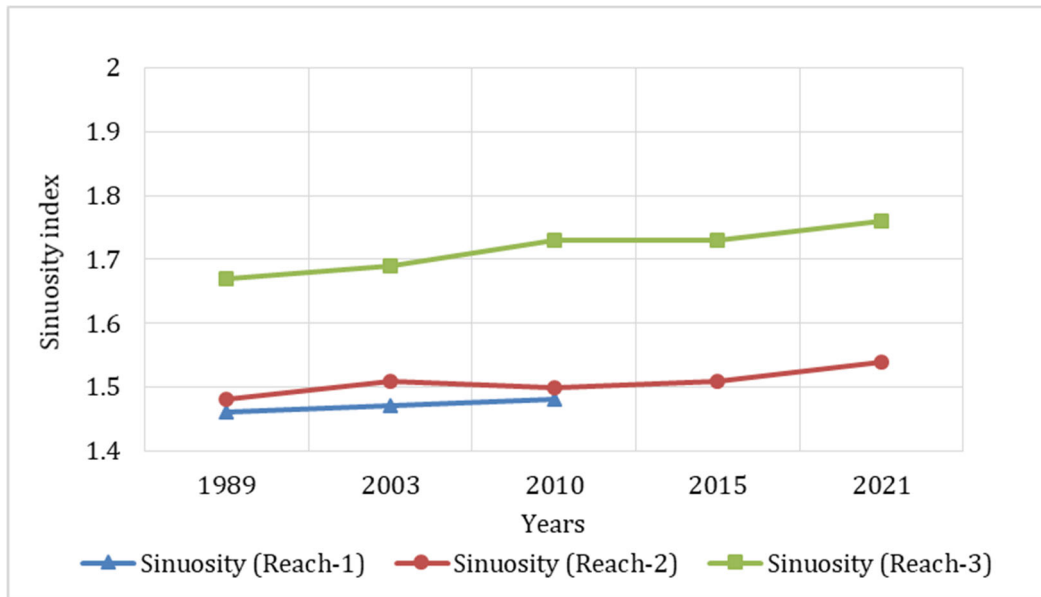


Figure 6.28: Sinuosity of Kapotakshi River from 1989-2021

Erosion-Accretion Analysis of the Kapotakshi River

For the assessment of erosion-accretion, bank lines of 1989, 2003, 2010, 2015, and 2021 were superimposed. The erosion and accretion-prone areas are presented in **Figure 6.29** and marked red and green, respectively. The study observed that upstream of the river has dried up significantly over the last 32 years. This could be the unfavorable condition of the Mathabhanga River upstream from where freshwater flow comes to the system. Additionally, the main channel of the Ganges River shifted towards the opposite bank, which would trigger the situation mentioned above. Subsequently, human activities like encroachment and cultivation of the riverbed contributed to narrowing the river. Moreover, erosion has been observed in this river downstream. This might be because of tidal dominance.

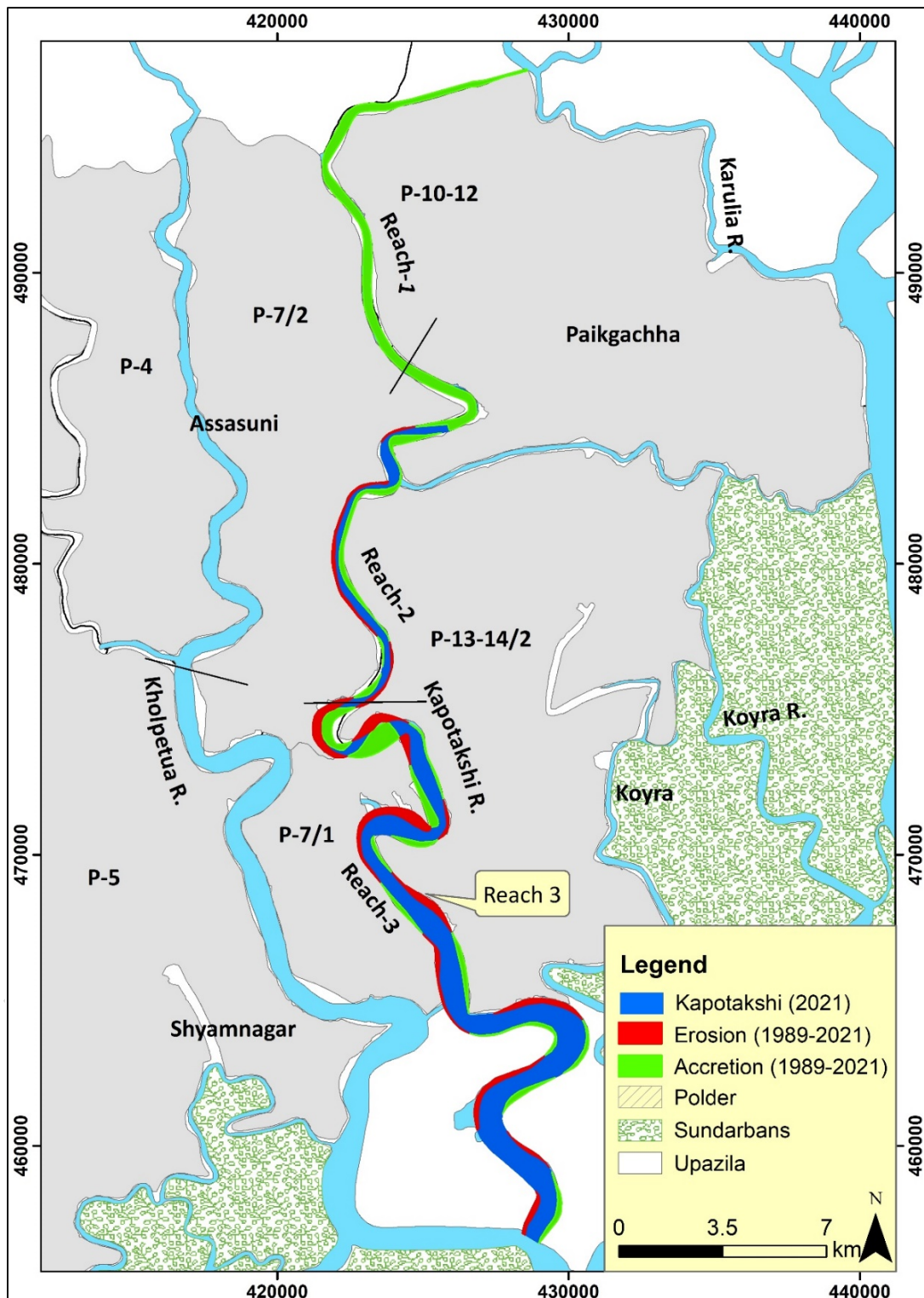


Figure 6.29: Erosion-accretion of the Kapotakshi River during (1989-2021)

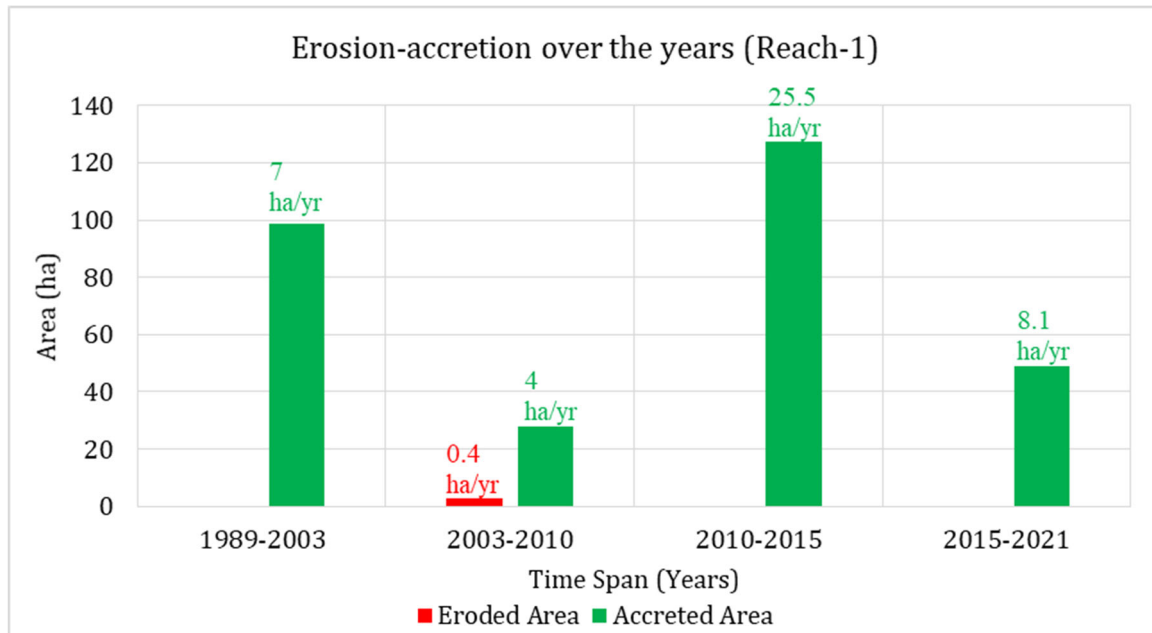


Figure 6.301: Erosion-accretion of Kapotakshi River over the years (Reach-1)

Figure 6.301 shows that reach-1 has been accretion prone over the past 32 years. In the 1989-2003 timespan, about 98 ha of land accretion while no erosion occurred. In the 2003-2010 timespan, the accretion rate declined slightly, and about 2.7 ha of land eroded. Moreover, in the 2010-2015 timespan, huge sedimentation occurred in this reach (about 127 ha of land) which continues till 2021. At present, this reach has completely dried up. Human interventions and lack of upstream flow are mainly the reasons for massive sedimentation in this area.

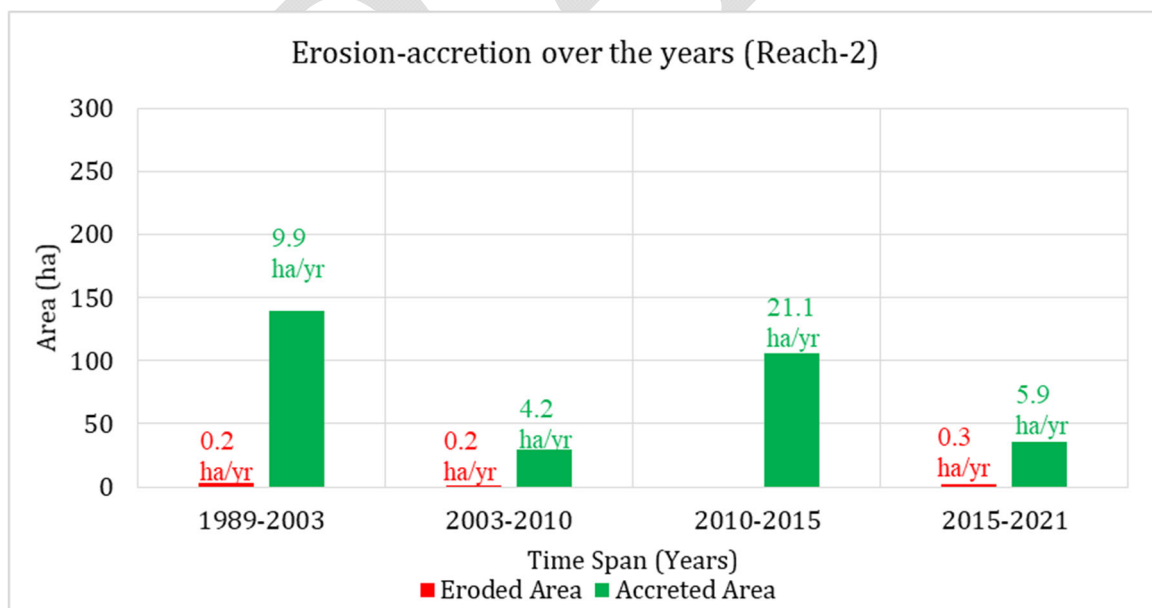


Figure 6.31: Erosion-accretion of Kapotakshi River over the years (Reach-2)

Reach-2 of Kapotakshi River has also been accretion prone because of huge sedimentation over the past 32 years (**Figure 6.31**). About 140 ha and 30 ha of land accreted in this reach in 1989-2003 and 2003-2010 timespan consecutively. Very little erosion occurred in this reach from 1989 to 2010 timespan. Maximum amount of accretion occurred in 2010-2015 timespan

(21.1 ha/yr) similar to Reach-1. After that, about 36 ha of land accreted and only 2 ha of land eroded in this reach in the 2015-2021 timespan. Thus, it concludes that this reach is also drying up because of colossal sedimentation.

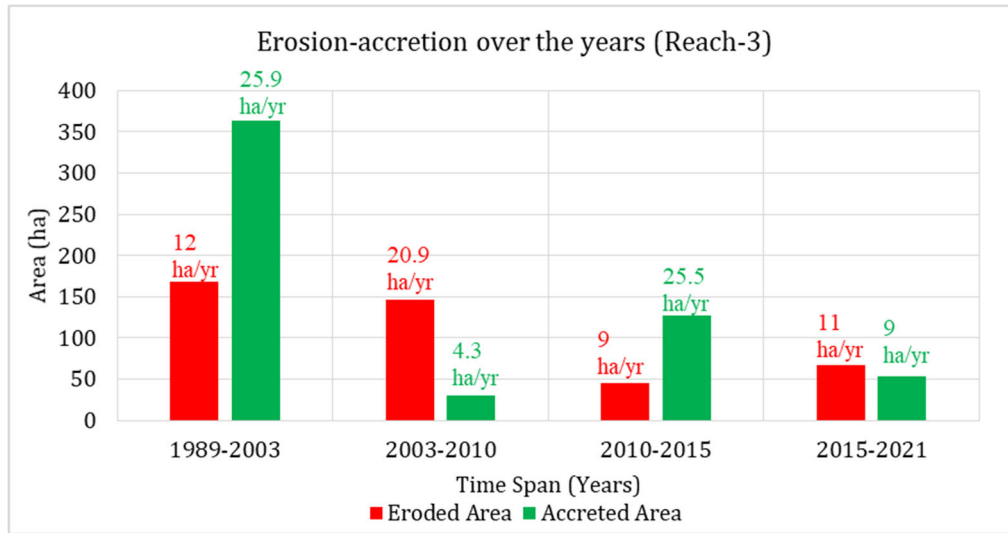


Figure 6.32: Erosion-accretion of Kapotakshi River over the years (Reach-3)

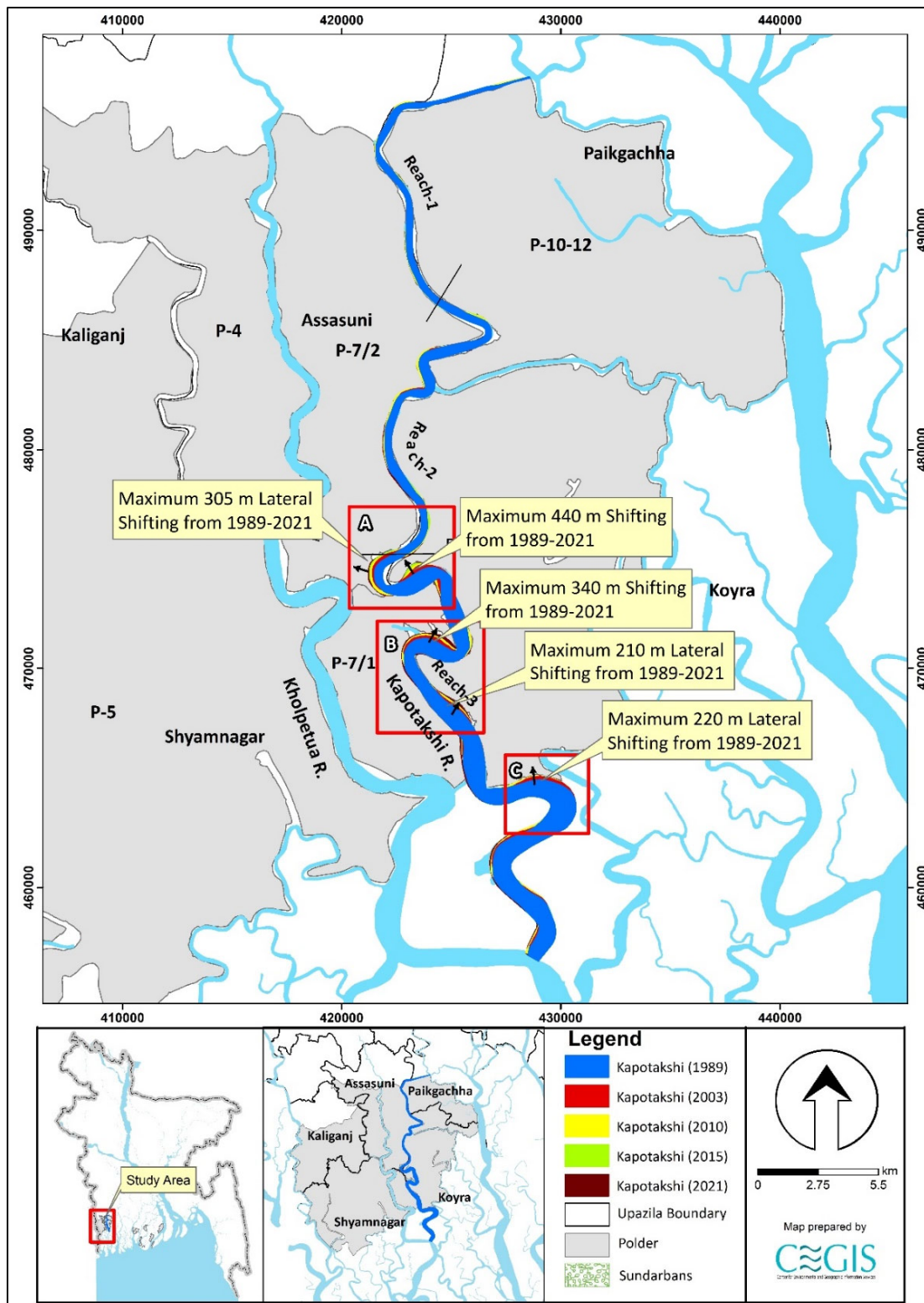
This reach of the Kapotakshi River is erosion-prone because of tidal dominance. Figure 6.32 shows, during the 1989-2003, accretion dominated over erosion in this reach (363 ha of accretion and 168 ha of erosion). But the situation reversed in 2003-2010 timespan where erosion dominant over accretion (30 ha of accretion and 146 ha of erosion). After that, erosion rate declined and accretion rate increased in 2010-2015 timespan. Erosion rate increased (11 ha/yr) and accretion rate decreased (9 ha/yr) a little in 2015-2021 timespan.

Bend Migration of the Kapotakshi River

Bend migration was analyzed from 1989 to 2021 for the Kapotakshi River (**Figure 6.33**). In Figure 2-33, the Bend migrations are shown at five major locations where maximum migration occurred. Locations, Extent of Bend migration, migration rate, and direction of Bend migration are shown in **Table 6.2**. The life span of this river has been calculated at 30 ± 10 years.

Table 6.2: Locations, Extent of Bend migration, and Migration direction for Kapotakshi River

| Location | The extent of Bend migration (m) | Migration rate (m/yr) | Migration direction |
|----------|----------------------------------|-----------------------|--------------------------|
| A | 305, 440 | 10,14 | West, North- West |
| B | 340, 210 | 11,7 | North- East, North- East |
| C | 220 | 7 | North |



Projection of the Kapotakshi River

Uncertainty in predicting future migration is very high in this river. However, a statistical analysis has been done for five (5) locations of Kapotaksi River to predict future Bend migration for the next 10, 20, and 30 years. Locations adjacent to the polders have been selected and named from "Ka-01" to "Ka-05". The existing trend of the Bend migration rate has been considered while predicting the future lines in this river. Bend migrations extent less than 5 times the image resolution have been considered only for 30 years of prediction. Prediction lines of 10 and 20 years have been avoided to reduce uncertainty. No cut-off has been seen in this river in the last 78 years. Thus, from morphological analysis and expert observation, it is predicted that no cut-off will occur within the next 30 years. Future migration lines for the next 10, 20 and 30 years at the river's selected locations are shown in Figures **6.34** to Figure **6.38**. The existing embankment alignments are indicated with the black lines in the figures. Detailing of prediction lines from Ka-01 to Ka-05 in this river are discussed below.

Ka-01 location is adjacent to Polder 7/1 and 7/2. This location has migrated a maximum of 250m of the bank from 1989 to 2021. It is observed that river banks in this location have been migrating continuously over the last 32 years. Thus, prediction lines for the next 10, 20, and 30 years have been drawn to calculate the migration rate in this location (**Figure 6.34**). Ka-02 location is adjacent to Polder 13-14/2. A maximum of 460 m of the bank have been migrated from 1989 to 2021 in this location. It shows that river banks in this location have been migrating continuously over the last 32 years. Thus, prediction lines for the next 10, 20, and 30 years have been drawn to calculate the migration rate in this location (**Figure 6.35**). In Addition to that, the Ka-03 location is adjacent to Polder 7/1. This location has migrated a maximum of 240m of the bank from 1989 to 2021. Figure 6.36 shows that the river bank in this location has been migrating continuously over the last 32 years. Thus, prediction lines for the next 10, 20, and 30 years have been drawn, calculating the migration rate in this location.

Moreover, the Ka-04 location is adjacent to Polder 7/1. A maximum of 350 m of the bank have been migrated from 1989 to 2021 in this location (**Figure 6.37**). It is observed that river banks in this location have been migrating continuously over the last 32 years. Thus, prediction lines for the next 10, 20, and 30 years have been drawn, calculating the migration rate in this location. On the other hand, the Ka-05 location is adjacent to Polder 13-14/2. This location has migrated a maximum of 240 m of the bank from 1989 to 2021. It is observed that river banks in this location have been migrating continuously over the last 32 years. Thus, prediction lines for the next 10, 20, and 30 years have been drawn to calculate the migration rate in this location (**Figure 6.38**).

Actually, we have kept the shapefile as it is as we have received from the client. If any modification requires, map will be updated accordingly. Worthy mention that, in a few locations, the polder boundary lies within the perimeter of the Kapotakshi River as of 2021.

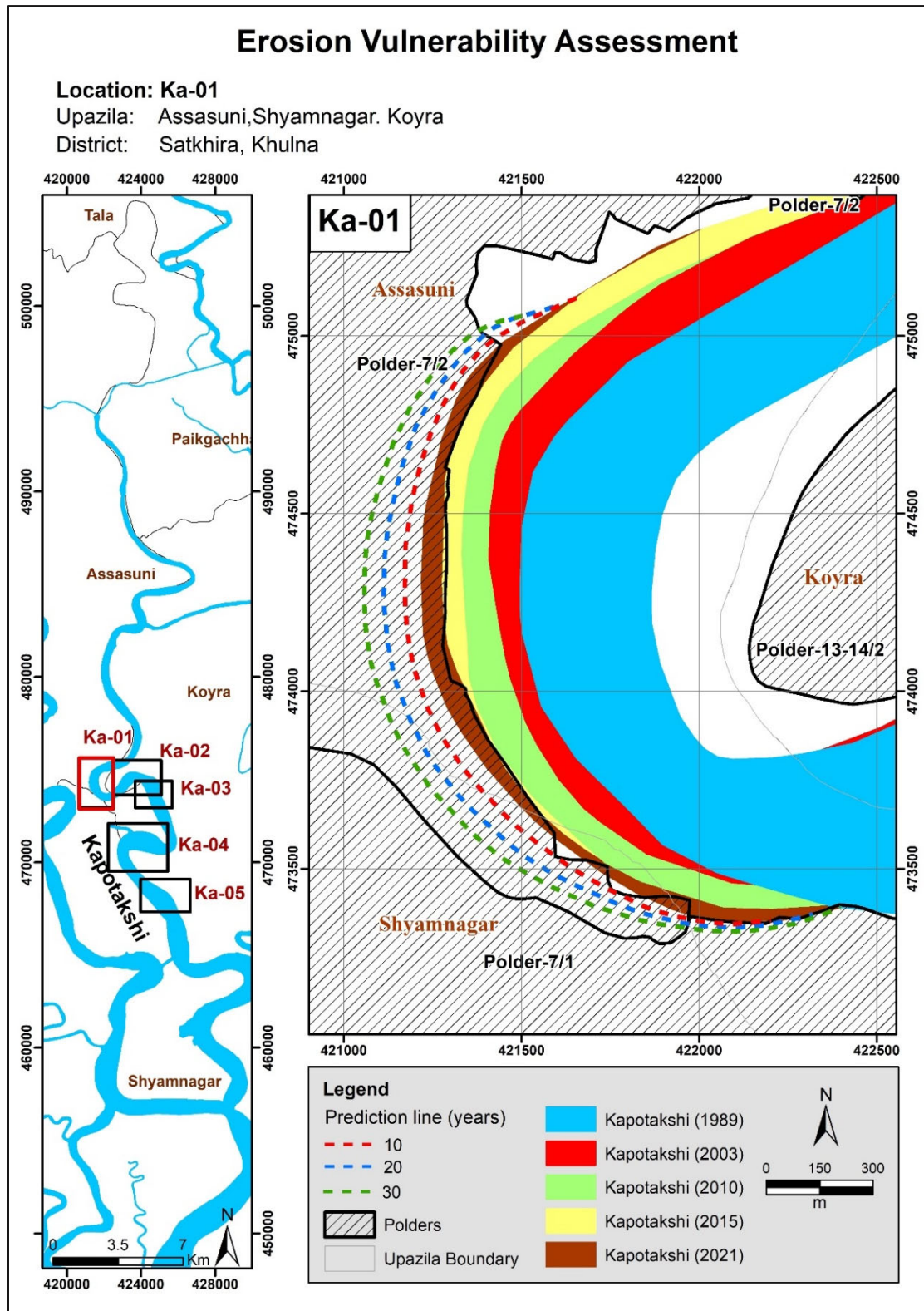


Figure 6.34: Bend migration in the next 10, 20, and 30 years in Kapotakshi River

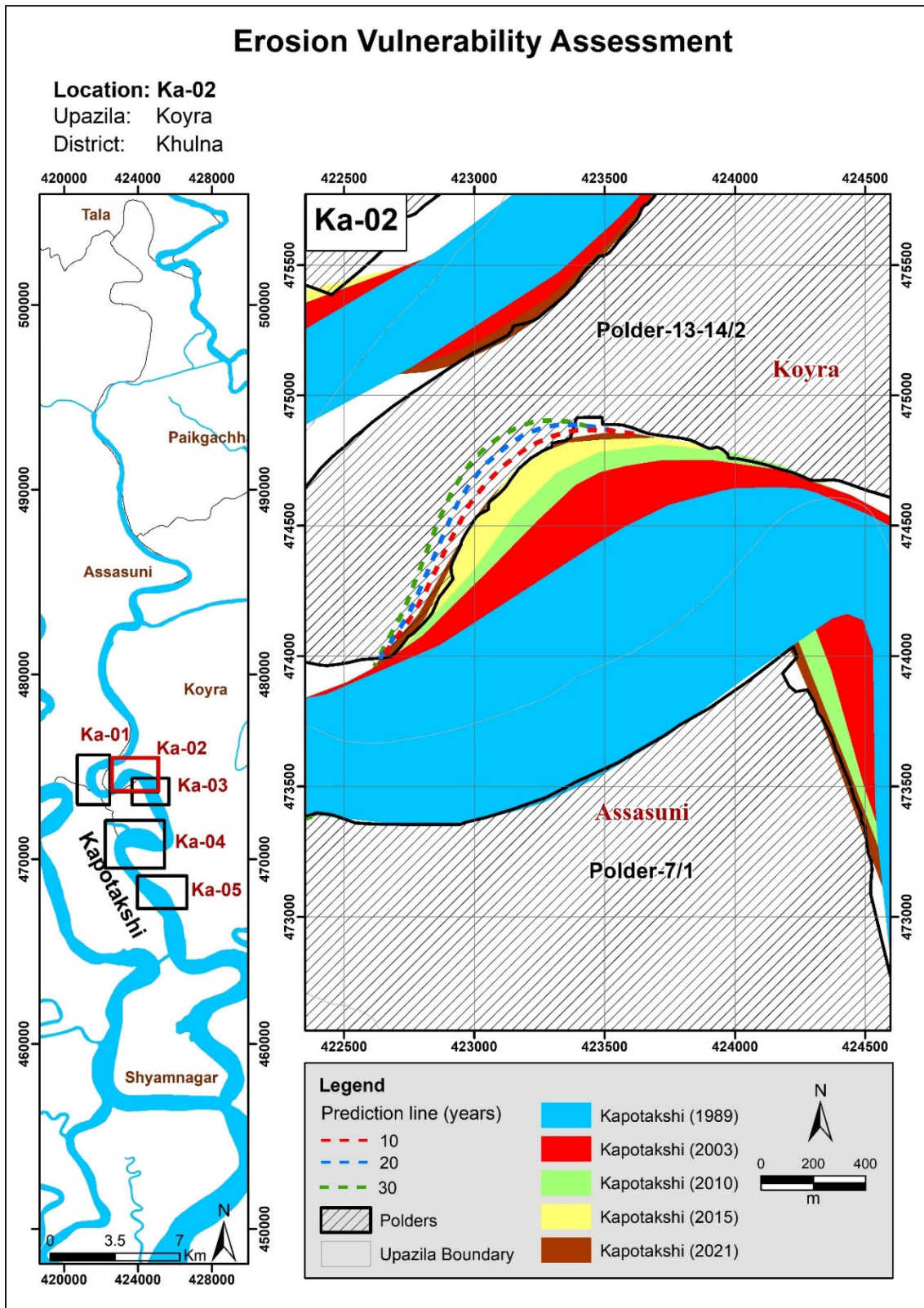


Figure 6.35: Bend migration in the next 10, 20, and 30 years in Kapotakshi River

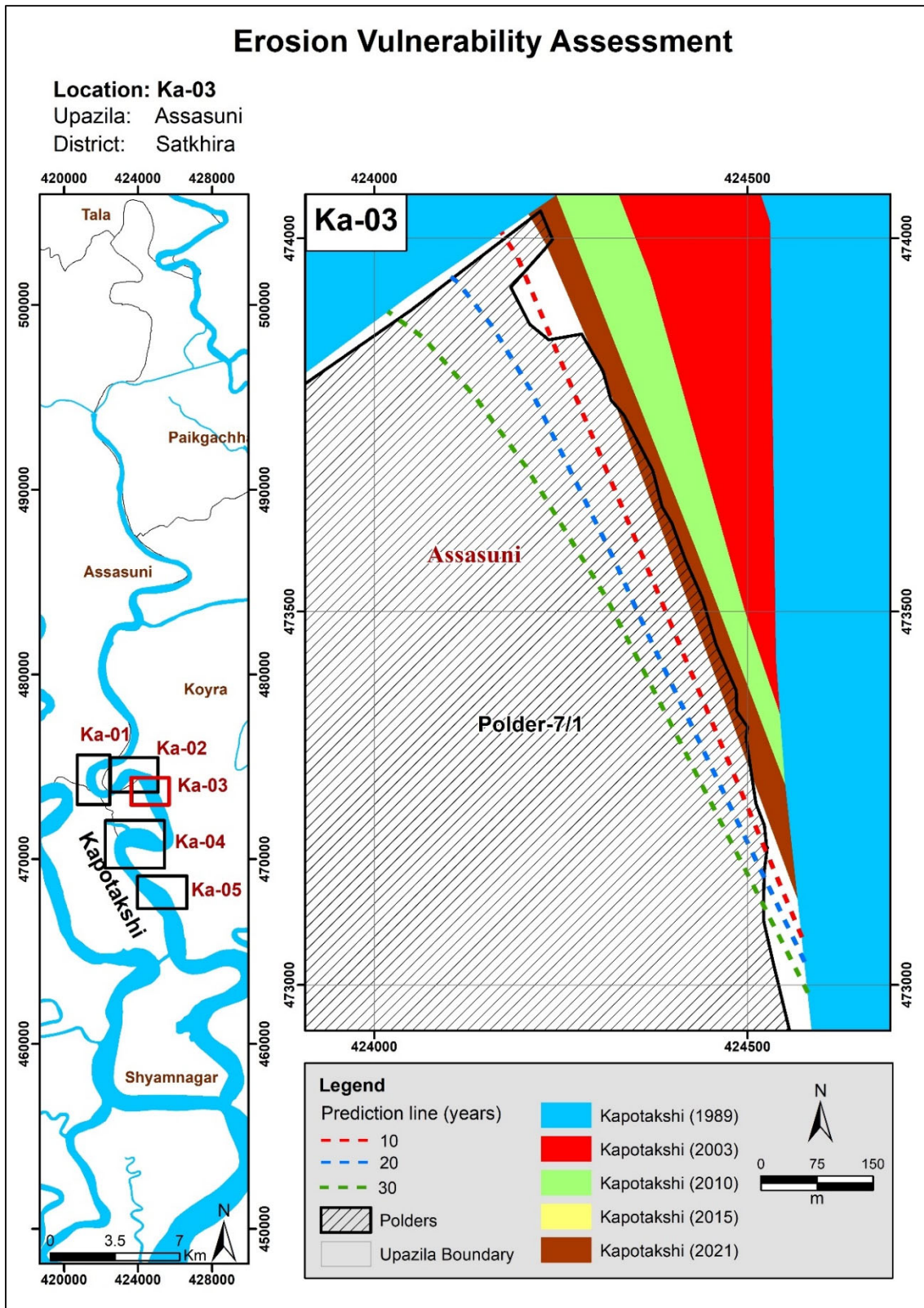


Figure 6.36: Bend migration in the next 10, 20, and 30 years in Kapotakshi River

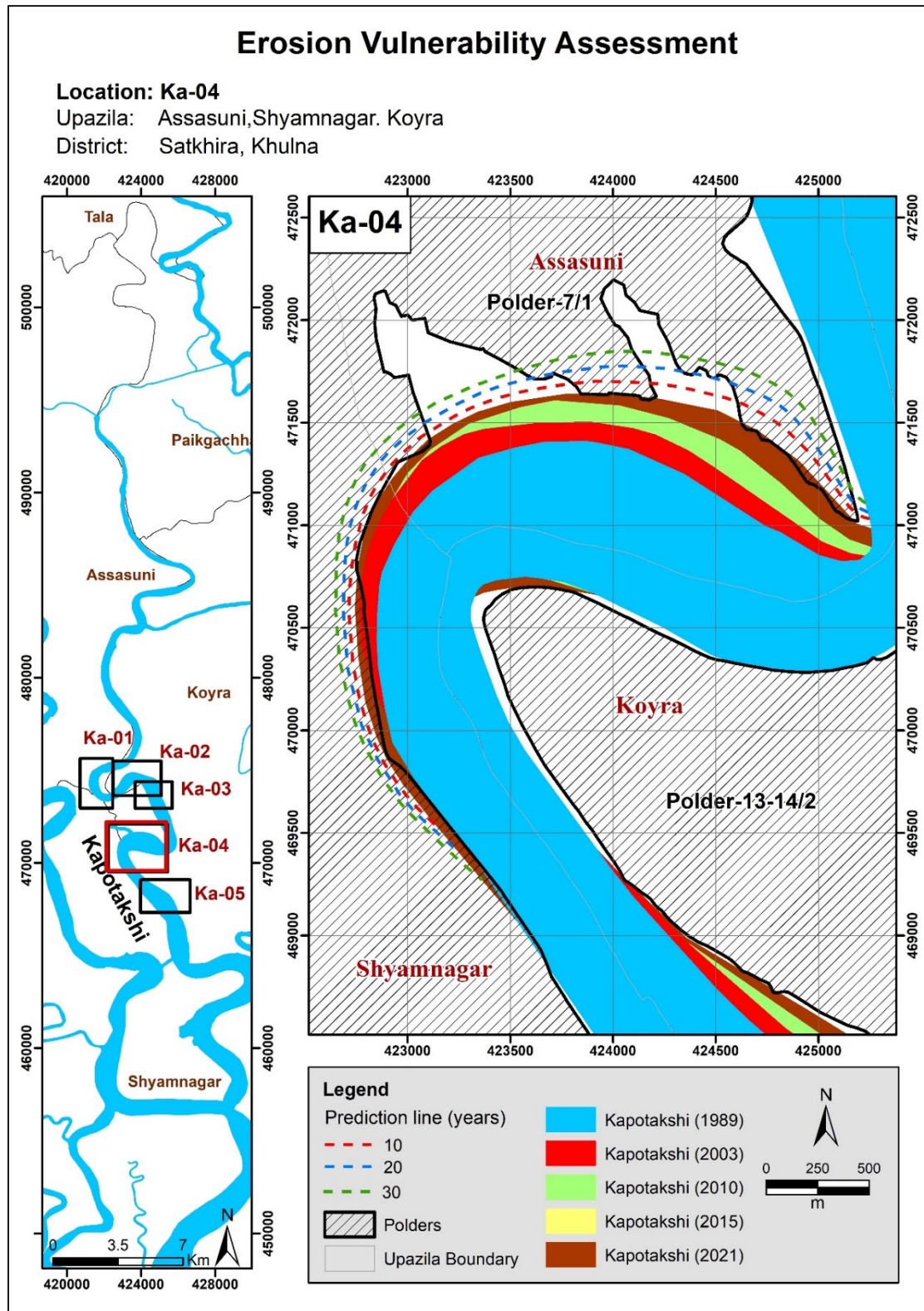


Figure 6.37: Bend migration in the next 10, 20, and 30 years in Kapotakshi River

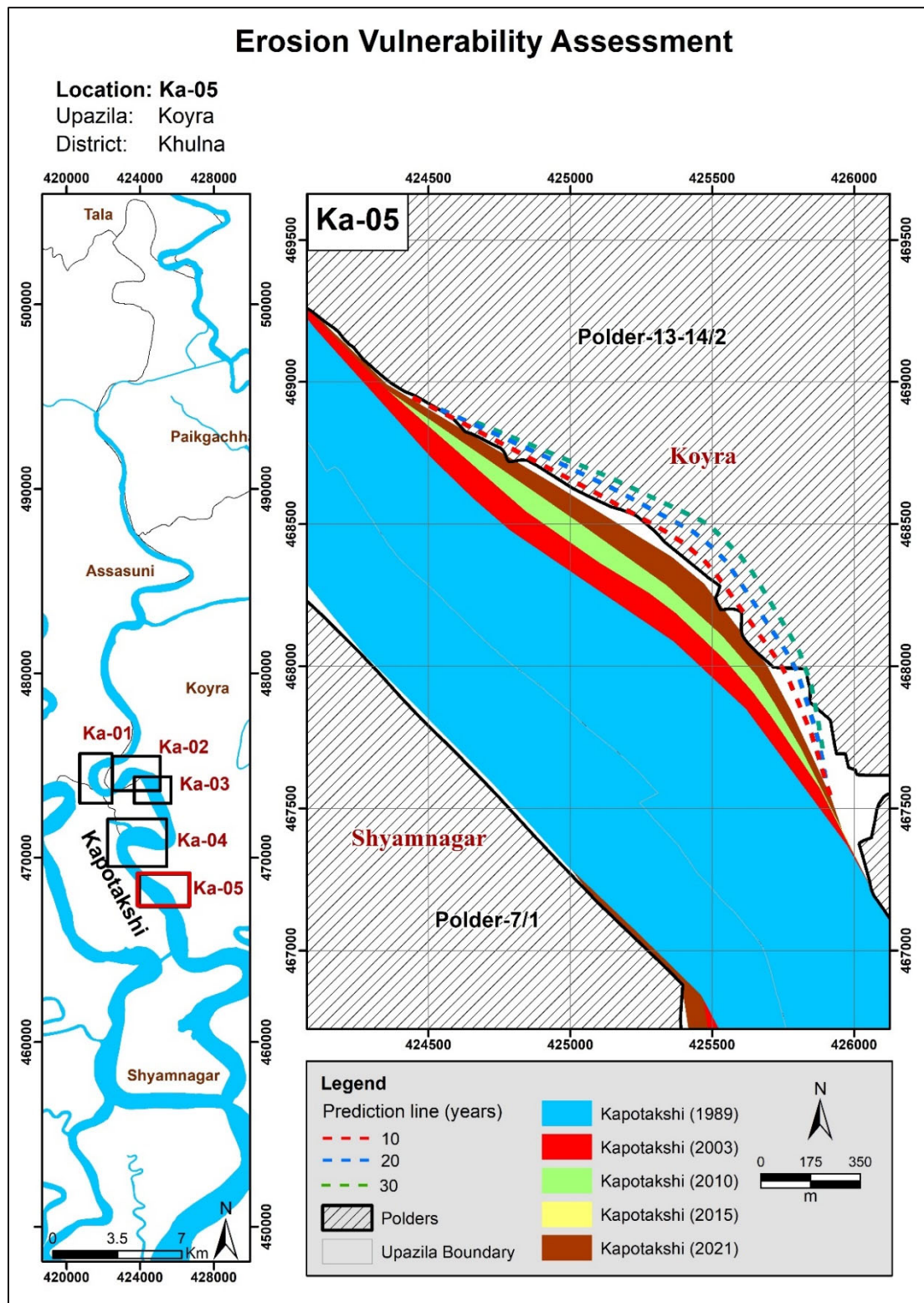


Figure 6.38: Bend migration in the next 10, 20, and 30 years in Kapotakshi River

6.4 The Shibs River

The Shibs River is a offtake from Kapotakshi River in Paikgaccha (Khulna). The river flows through Dakope Upazila and outfalls Passur River. The overall morphological analysis of Shibs River has been performed considering the river as a Single Reach as the river's geometry is almost the same from upstream to downstream (Figure 6.39). This study considers the Shibs River from Sholadana Union (Paikgachha) to Nalian Range Union (Koyray).

Historical Development of the Shibs River

A 1943 map and satellite images of 1989, 2003, and 2021 were referred to assess the river's historical development over time (**Figure 6.39**). It was observed that the alignment of the river route had not changed much over the years.

DRAFT

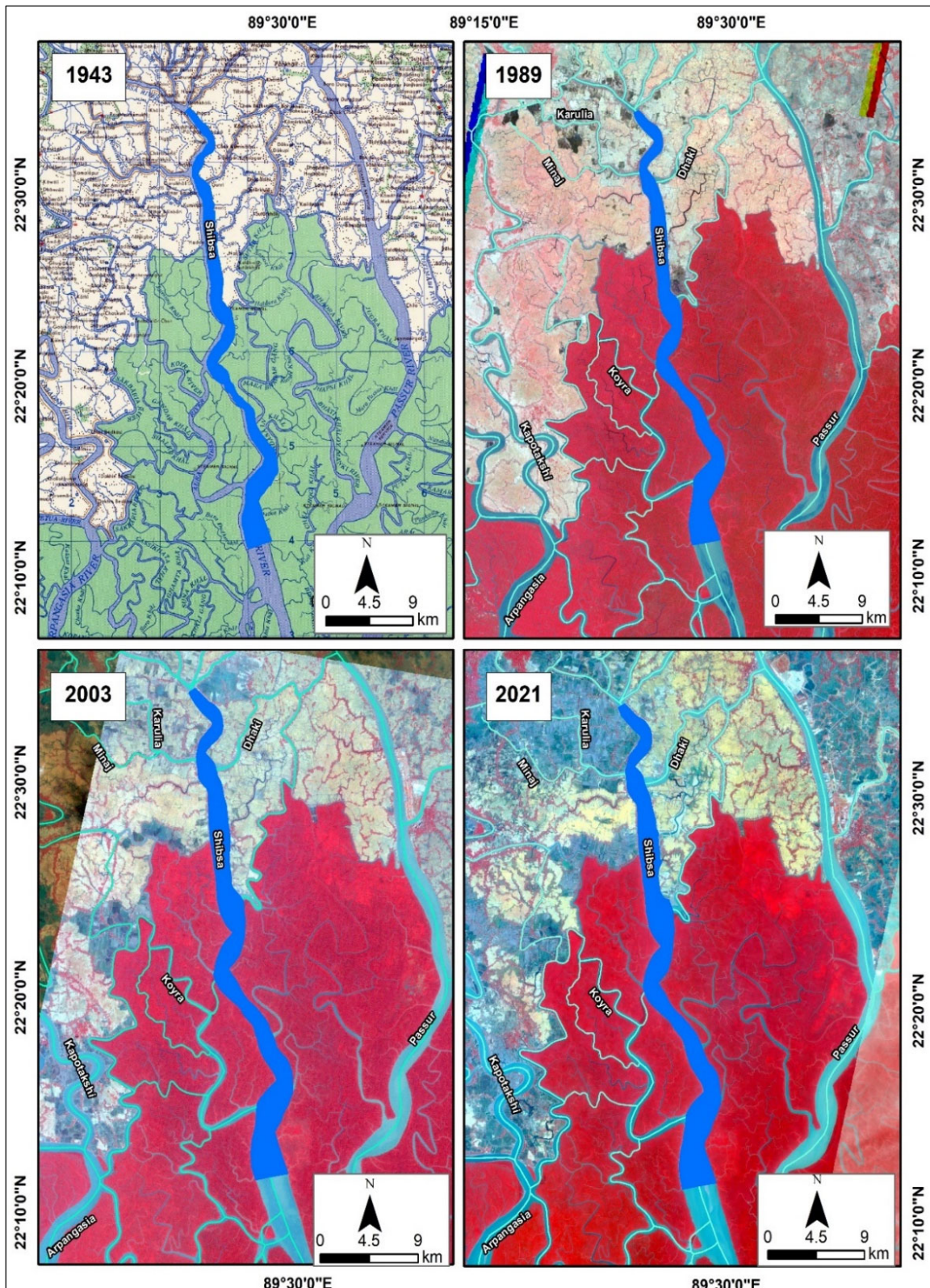


Figure 6.39: Historical Development of Shiba River

Average Width of the Shabsa River

From **Figure 6.40**, the average width of the river shows an increased trend over the past 32 years. The average width of this river increased by 210 m during 1989-2021; it indicates the river has widened due to erosion. This might be because of tidal dominance.

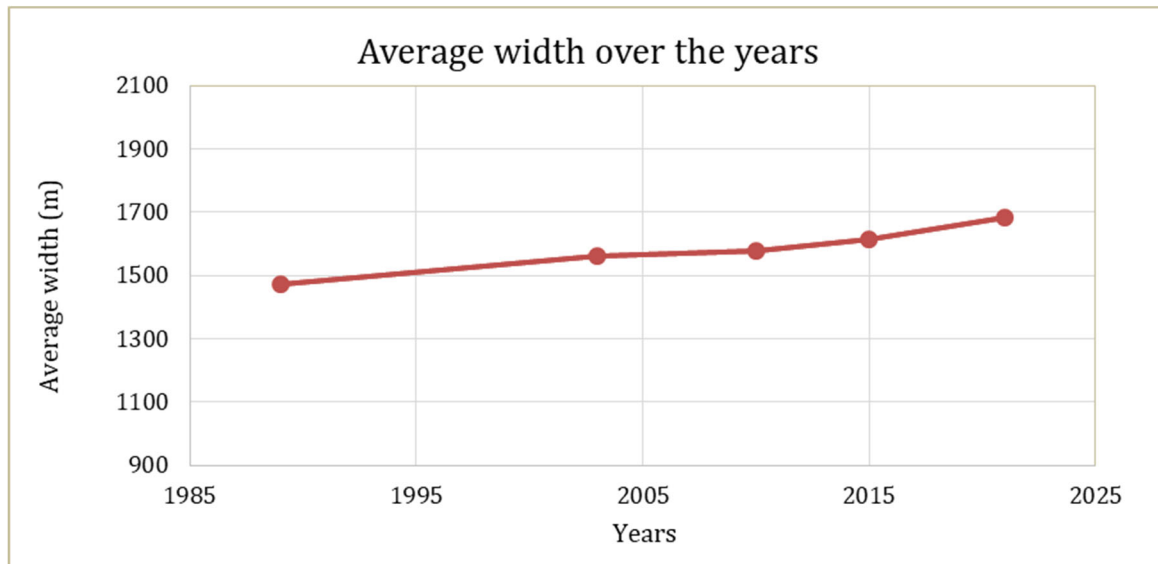


Figure 6.40: Average width of Shabsa River from 1989-2021

The sinuosity of the Shabsa River

The sinuosity of the river remained almost unchanged from 1989 to 2003. In contrast, the sinuosity decreased slightly in the last two decades (from 2003 to 2021). Figure 6.41 shows the Sinuosity of Shabsa River from 1989-2021.

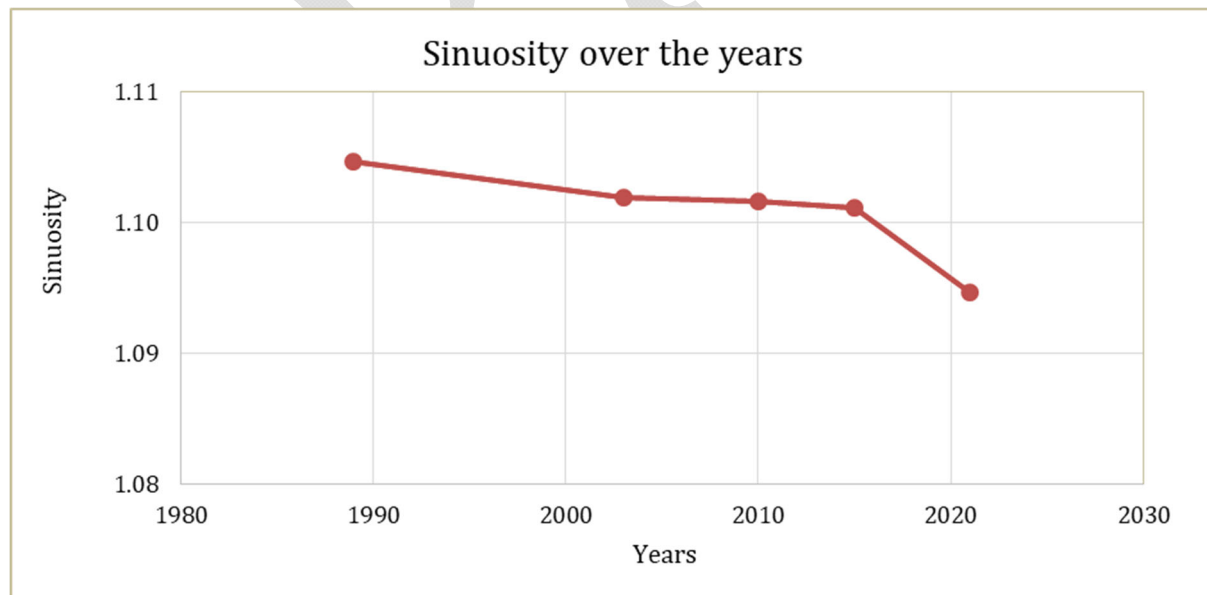


Figure 6.41: Sinuosity of Shabsa River from 1989-2021

Erosion-Accretion Analysis of the Shibsia River

For erosion-accretion assessment, bank lines of 1989, 2003, 2010, 2015, and 2021 were superimposed. The erosion and accretion-prone areas are presented in **Figure 6.42** and marked red and green, respectively. It was observed that the erosion rate is high along the Shibsia River, which resulted in the widening of the river. On the other hand, the rate of accretion is found to be very low compared to the rate of erosion. The rate of erosion and accretion in different periods are provided in **Figure 6.43**.

DRAFT

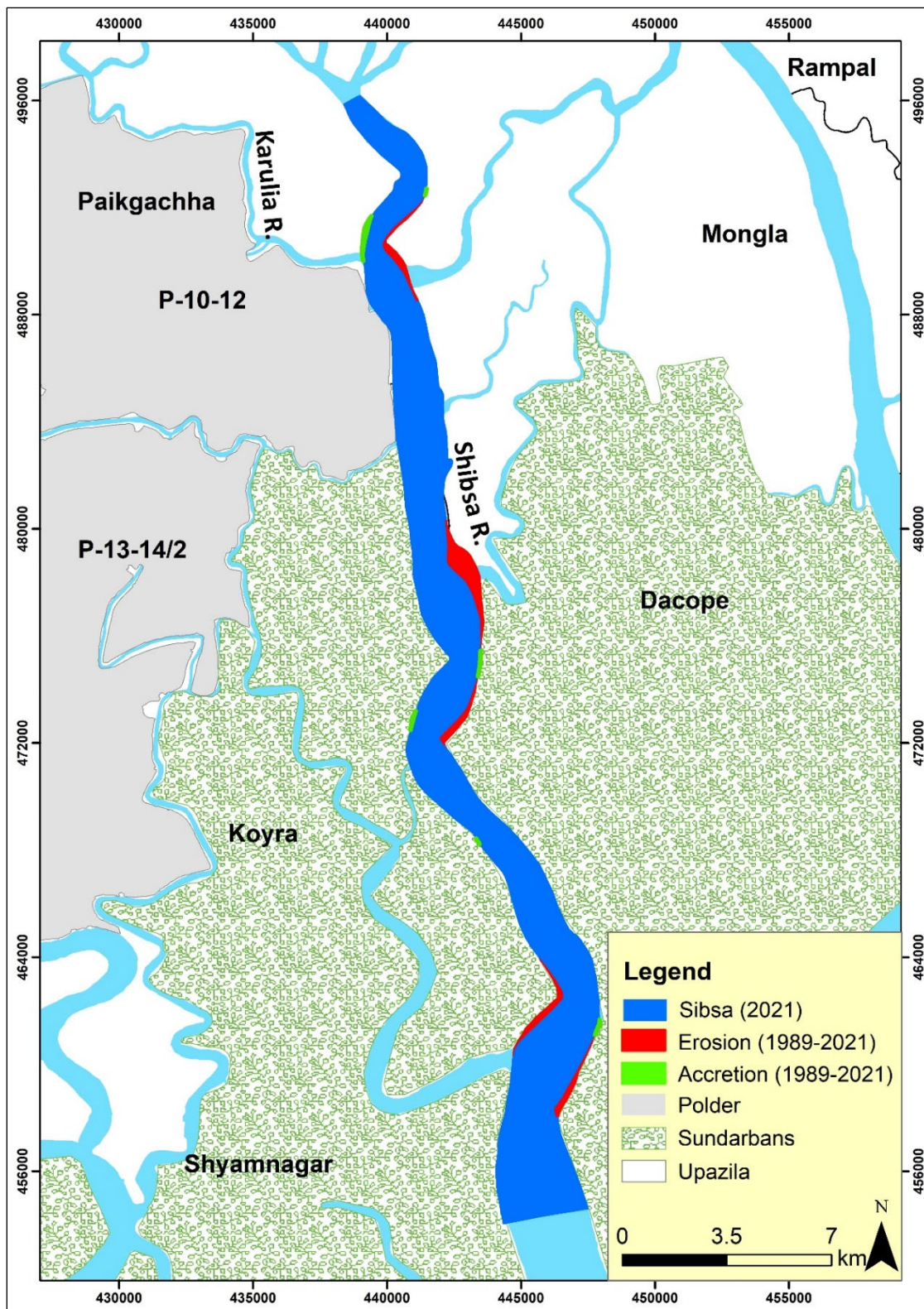


Figure 6.42: Erosion-accretion of the Shibsia River during (1989-2021)

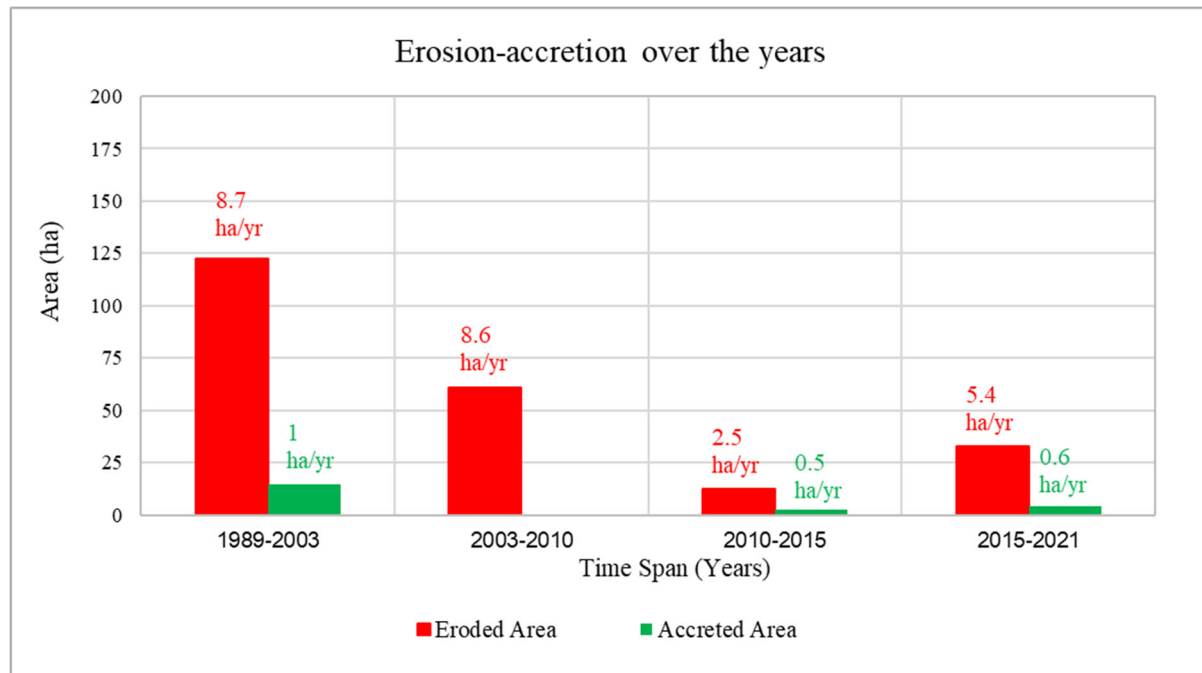


Figure 6.43: Erosion-accretion of Shabsa River

Shabsa River has been erosion prone over the past 32 years. Maximum erosion was observed from 1989 to 2003 (8.7 ha/year) while the accretion rate was minimal. After that, erosion and accretion rates declined in the 2003-2010 and 2010-2015 timespan. However, during 2015-2021, the erosion rate increased slightly (5.4 ha/year), and the accretion rate remained less during this time.

Bend Migration of the Shabsa River

Locations, Extent of Bend migration, migration rate and direction of Bend migration are shown in Table 6.3. The bend migration is shown at two major locations where maximum migration occurred (Figure 6.44). The life span of this river has been calculated at 30 ± 10 years.

Table 6.3: Locations, Extent of Bend migration, and Migration direction for the Shabsa River

| Location | The extent of Bend migration (m) | Migration rate (m/yr) | Migration direction |
|----------|----------------------------------|-----------------------|---------------------|
| A | 285 | 9 | North- East |
| B | 800 | 25 | North- East |

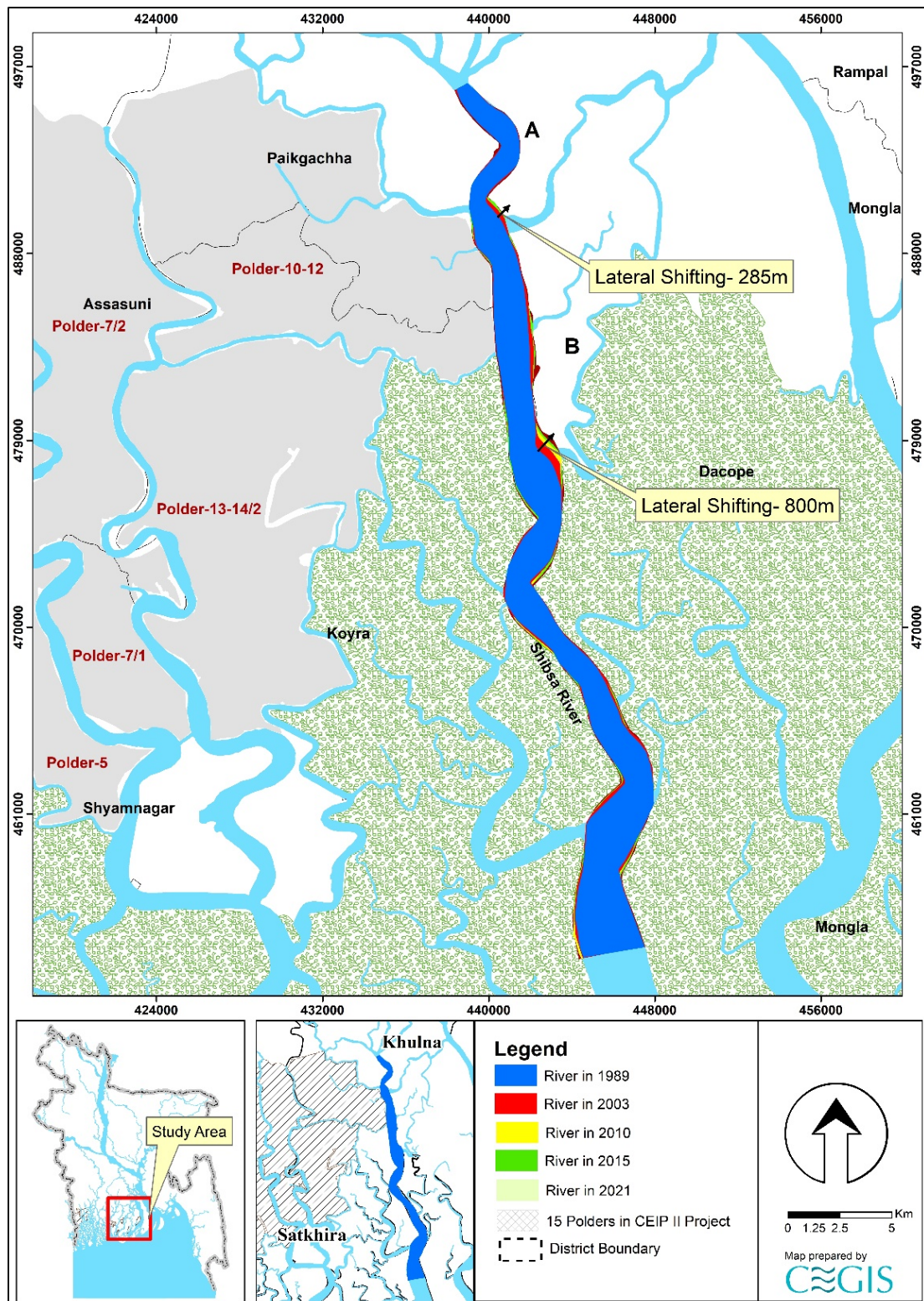


Figure 6.44: Bend migration of the Shibsar River (1989-2021)

Projection of the Shibsia River

Shibsia River is not very dynamic, and banks adjacent to polders are comparatively stable. However, a statistical analysis has been done for one (1) location in this river to predict future Bend migration for the next 30 years. Bend migration extent less than 5 times the image resolution has been considered only for 30 years of prediction. Prediction lines of 10 and 20 years have been avoided to reduce uncertainty. As no cut-off has been seen in this river in the last 78 years, no cut-off criteria has been considered. The detailing of the prediction line of Sh-01 in this river is discussed below.

Sh-01 location is adjacent to Polder 10-12. A maximum of 130 m of the bank have been migrated from 1989 to 2021 in this location. As maximum migration is less than 4/5 times the image resolution and migration rate is very low, future prediction for only 30 years has been considered for this location (**Figure 6.45**).

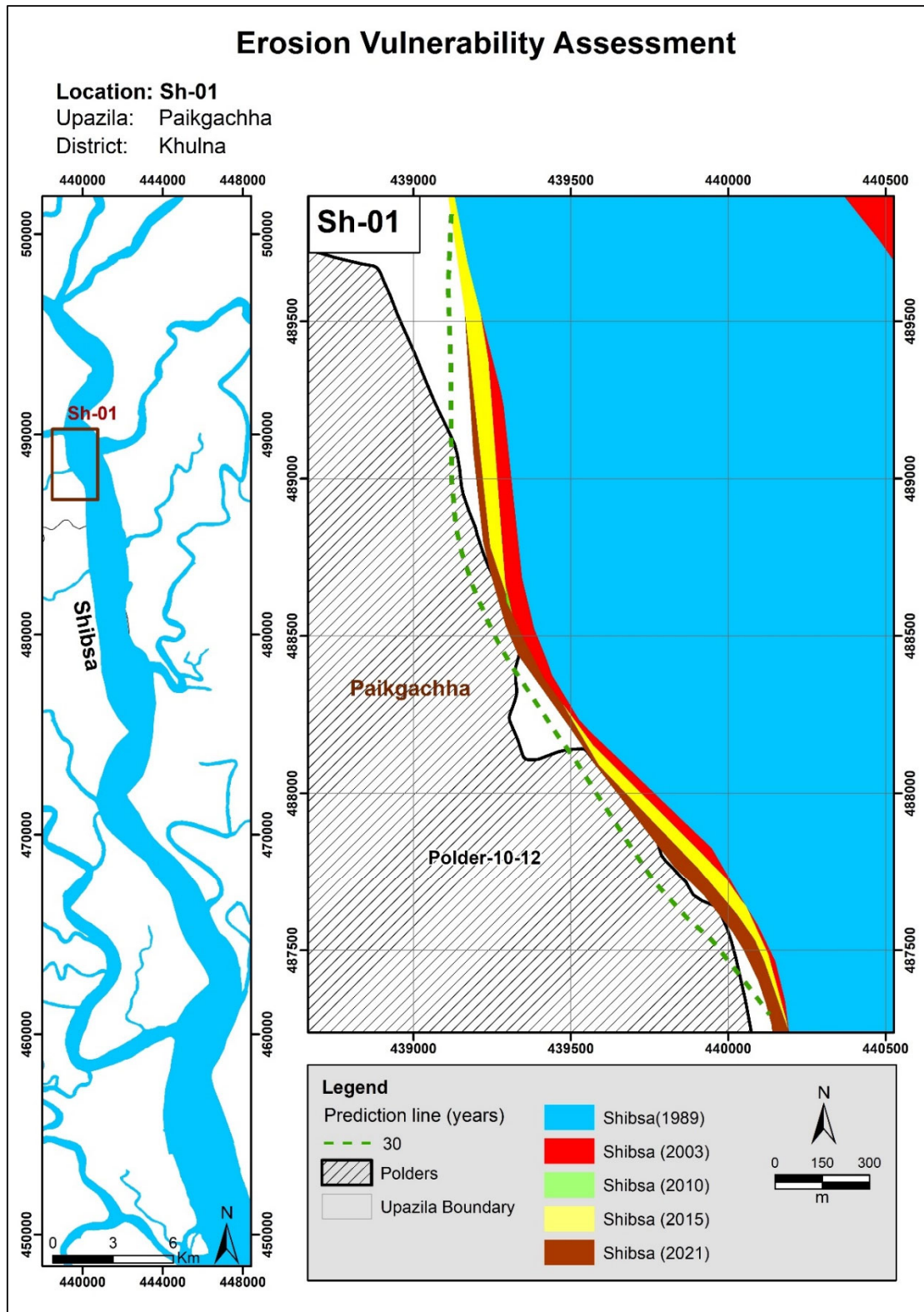


Figure 6.45: Bend migration in the next 10, 20, and 30 years in Shibsaa River

7. Morphological Analysis of the River in the Barishal Area

System Analysis (Chapter 5) indicates that ages of sediment deposition in the tidal plain are less than that in the Khulna area. The presence of Calcium Carbonate in the deposited sediment is less than that in the Khulna area. Rivers in Barishal Area receive fresh water during the dry season through the distributaries like the Gorai, Arial Khan, Shandha, and Tetulia. The CEGIS study found that these distributaries are changing alignments and receiving more freshwater flow both in dry and monsoon. Increasing freshwater flow in this area has long-term effects on the system and should be included in long-term monitoring activities. Rivers adjacent to the polders that can be analyzed through satellite images, i.e., Burishwar-Payra, Baleshwar, and Tentulia Rivers, have been selected for the Barishal Region. These rivers have been considered dynamic throughout the years. The study analyzed the historical development, bank lines shifting, bend migration, change in width and sinuosity, erosion-accretion quantification, and prediction for these rivers. However, in the predictions of the small rivers, it was impossible to delineate the bank lines using coarse resolution (30 m* 30 m) of the satellite image. Expert judgment was applied through knowledge of the system and understanding of the study area for assessing the small rivers. The small rivers did not pose an erosion threat to the Polders. Existing bank protection works have not been included in this study because of the uncertainty of the location and the lack of enough data. **Figure 7.1** shows the rivers focused in this study.

As the freshwater flow is increasing through the Baleshwar, Burshawar, and Bishkhali, the rivers that are taking off from the Tetulia are declining, as their parent river Tetulia is declining.

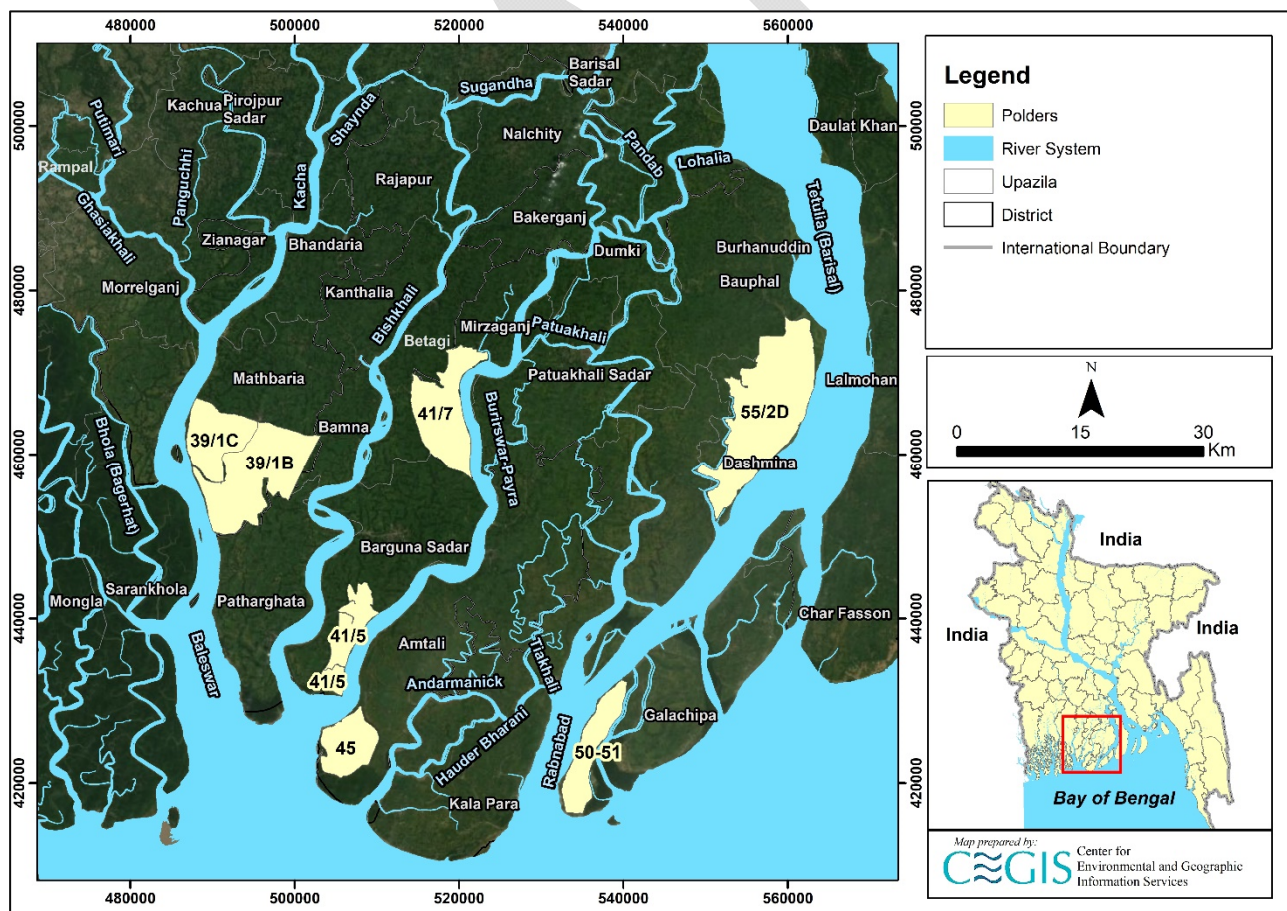


Figure 7.1: Map showing rivers considered in Barishal Region

7.1 Burishwar-Payra River

Burishwar-Payra River originates from Pandab River in Bakerganj Upazila (Barishal). It is a perennial river, and flooding occurs during monsoon by overtopping both banks. It outfalls into the Bay of Bengal by following through Dumki, Mirjaganj, Barguna Sadar, and Amtali. The tidal range of this river is about 2.25 m.

Historical Development of the Burishwar-Payra River

1943 map and satellite images of 1989, 2003, and 2021 were referred to assess the historical development of the Burishwar-Payra River (**Figure 7.2**). Comparing the map and the images, it is evident that the alignment of the river has not changed over the past 78 years. In addition, no cut-off has been observed during this period.

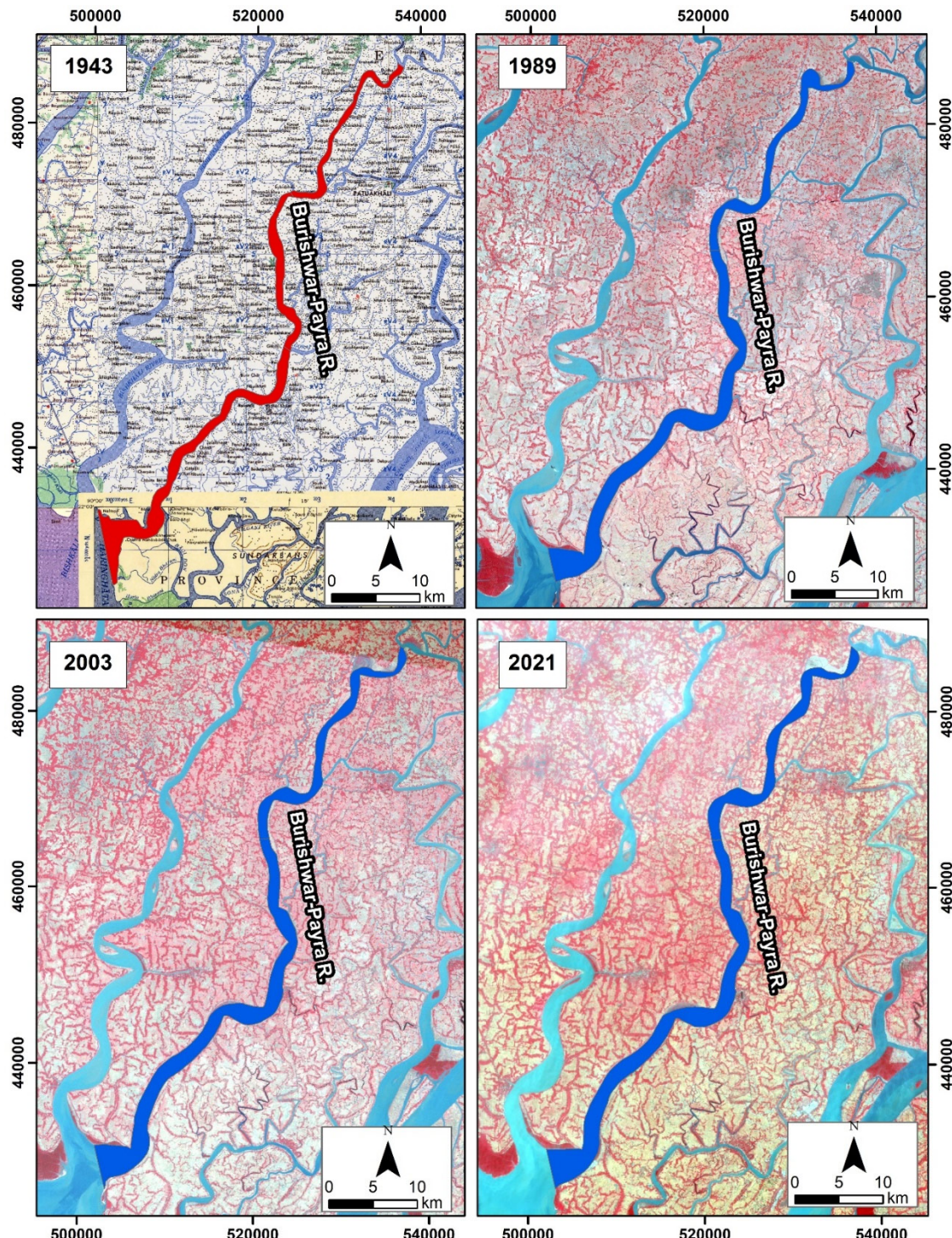


Figure 7.2: Historical Development of Burishwar-Payra River

Erosion-Accretion Analysis of the Burishwar-Payra River

The Burishwar-Payra River bank lines were delineated using the Arc-GIS tool to assess erosion-accretion. Then, bank lines of 1989, 2003, 2015, and 2021 were superimposed to evaluate erosion and accretion of the river within the study route. The erosion-accretion of the

Burishwar-Payra River is presented in Figure 7.4. The erosion and accretion-prone areas along the Burishwar-Payra River are presented in Figure 7.3 and marked red and green, respectively.

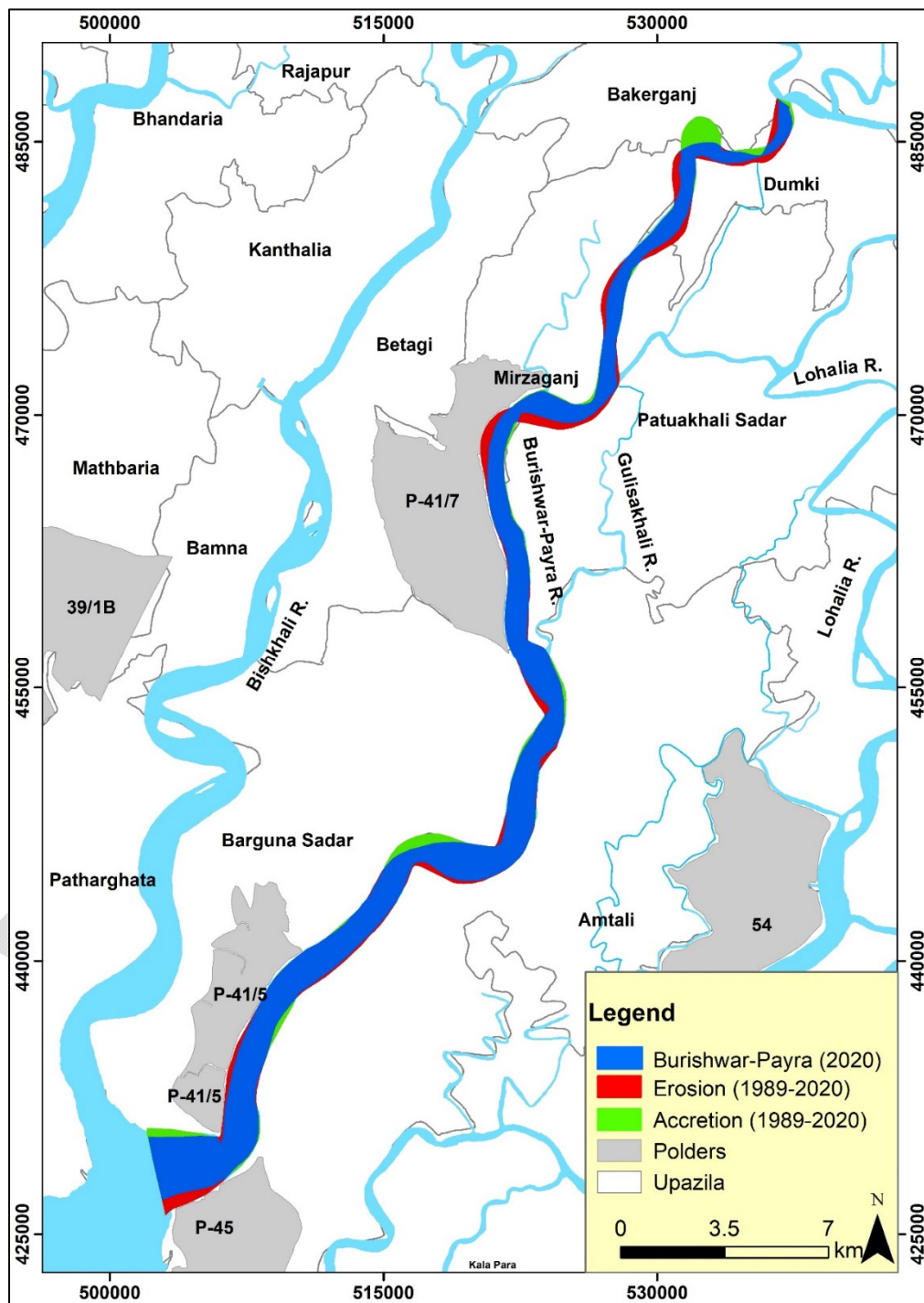


Figure 7.3: Erosion-accretion of the Burishwar-Payra River during (1989-2021)

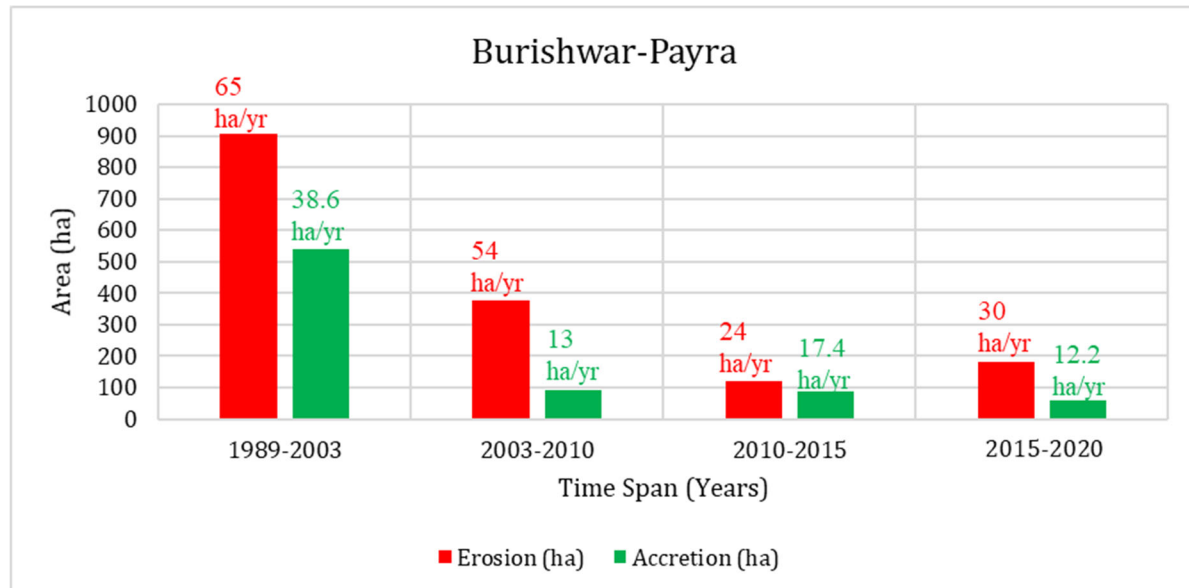


Figure 7.4: Erosion-accretion of Burishwar-Payra River over the years

The study suggests that the rivers have been very erosion prone over the last 30 years. The average width is increasing, which also supports high erosion. This might be due to the tidal effect. But both erosion-accretion of Burishwar-Payra River is following a decreasing trend. The study observed during 1989-2003, erosion and accretion were about 908 ha (65 ha/year) and 540 ha (38.6 ha/year), respectively. However, during 2003-2010 erosion and accretion were about 378 ha (54 ha/year) and 90 ha (13 ha/year), respectively. Again during 2010-2015, erosion and accretion were about 120 ha (24 ha/year) and 87 ha (17.4 ha/year), respectively. During 2015-2020 erosion and accretion were about 180 ha (30 ha/year) and 61 ha (12.2 ha/year), respectively. The higher erosion rate during 2015-2020 compared to 2010-2015 might be due to the dredging performed in the Karkhana River, which increases the flow velocity in the Burishwar-Payra River.

Average Width of the Burishwar-Payra River

The shortest distance between two banks is defined as the river's width. However, at any river, the width varies at a different locations. Thus average width of the rivers changes over time; however, the study has taken the width data using ArcGIS. The average width of any river computation includes the total area enclosed by the riverbanks and divided by the length of the centerline of the river. Changes in the river width from 1989 to 2021 have been assessed and presented in **Figure 7.5**. The study suggests the Burishwar-Payra river has been widening from 1989 to 2020 (about 1350 m to 1462 m), which supports the higher erosion rate in the river.

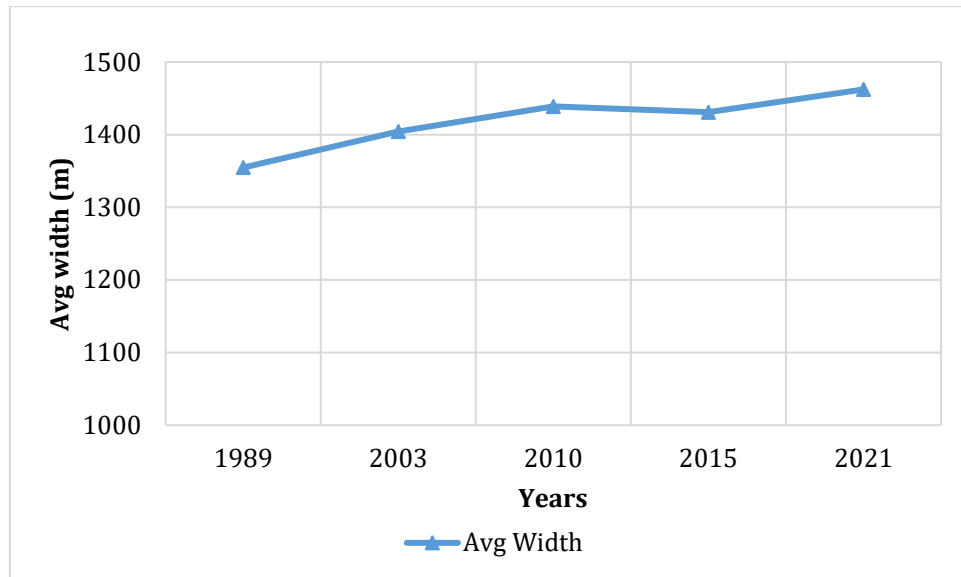


Figure 7.5: Average width of Burishwar-Payra River over the years.

The sinuosity of the Burishwar-Payra River

Channel sinuosity is simple geometric information that signifies the river's deviation from a straight line. It calculates the length along the river divided by the straight-line distance along the river valley. The sinuosity of the Burishwar-Payra River for 1989, 2003, 2015, and 2021 is marked in **Figure 7.6**. The river's sinuosity reaches a slight decreasing trend from 1989 to 2021.

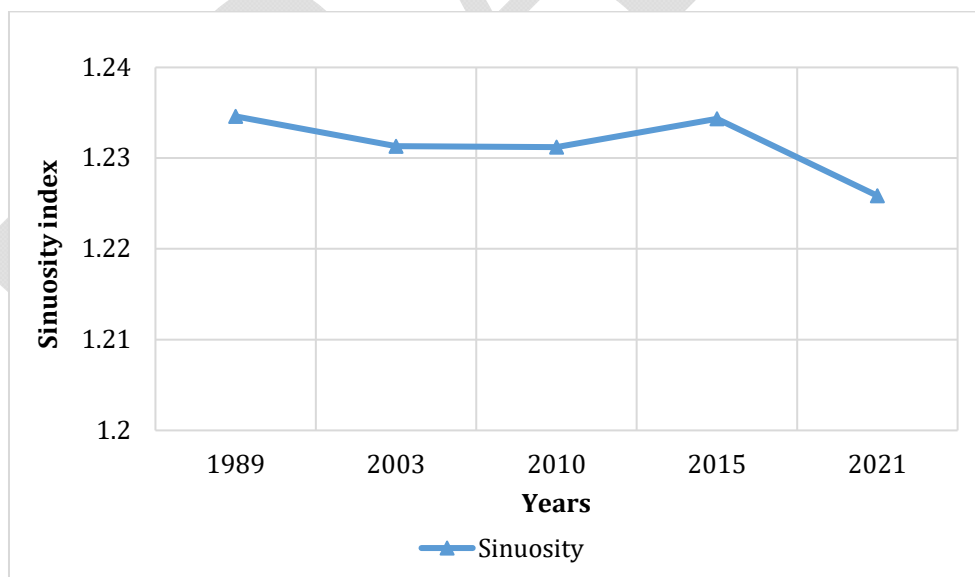


Figure 7.6: Sinuosity of Burishwar-Payra River over the years.

Bend Migration of the Burishwar-Payra River

Bend migration has been analyzed from 1989-2021. In **Figure 7.7**, the Bend migrations are shown at seven (7) major locations where maximum migration occurred. Locations, Extent of

Bend migration, and direction of Bend migration are shown in **Table 7.1**. The average life span of bends of this river has been calculated to be 28 ± 10 years.

Table 7.1: Locations, Extent of Bend migration, and Migration direction for Burishwar-Payra River

| Location | The extent of Bend migration (m) | Migration rate (m/yr.) | Migration direction |
|----------|----------------------------------|------------------------|--------------------------|
| A | 350, 376 | 12, 12.5 | North- West, South- East |
| B | 445, 355 | 15, 12 | West, South- East |
| C | 316 | 10.5 | North- West |
| D | 534, 553 | 18, 18 | North- West, South- East |
| E | 360 | 12 | South- West |
| F | 246 | 8 | West |
| G | 673 | 22 | South- East |

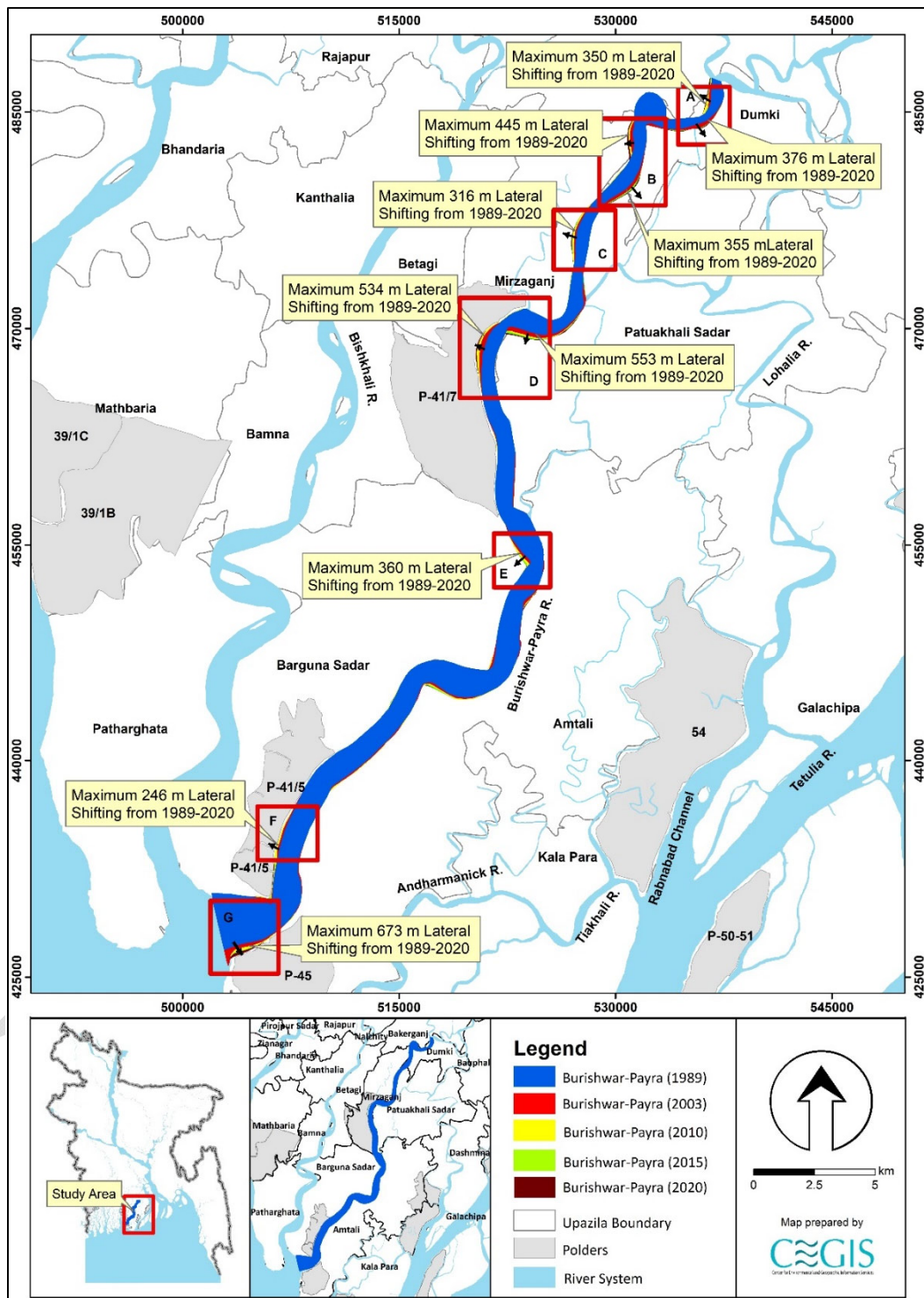


Figure 7.7: Bend migration of the Burishwar-Payra River (1989-2021)

Projection of the Burishwar-Payra River

A statistical analysis has been done for three (3) locations of Burishwar-Payra River to predict future Bend migration for the next 10, 20, and 30 years. Locations adjacent to the polders have been selected and named "Bu-01" to "Bu-03". The existing trend of the bend migration rate

has been considered while predicting this river's future lines. Bend migrations less than 5 times the image resolution have been considered only for 30 years of prediction. Prediction lines of 10 and 20 years have been avoided to reduce uncertainty. As no cut-off has been seen in this river in the last 78 years, no cut-off criteria has been considered. Future migration lines for the next 10, 20, and 30 years at the selected river locations are shown in Figures 7.8 to **7.10**.

Bu-01 location is adjacent to Polder 41/7. This location has migrated 534m of the bank from 1989 to 2021. It is noticeable that maximum erosion occurred from 1989 to 2003. After that, the erosion rate slowed down, and after 2010 the decline became negligible. From **Figure 7.8**, it is also seen that the bend was translating southward. Thus prediction lines for the next 10, 20, and 30 years have been drawn considering the abovementioned criteria. Bu-02 location is adjacent to Polder 41/5. This location has migrated a maximum of 246m of the bank from 1989 to 2021. It is noticeable that maximum erosion occurred from 1989 to 2003 (**Figure 7.9**). After that, the erosion rate slowed; after 2010, the decline became negligible. Thus prediction lines for the next 10, 20, and 30 years have been drawn considering the above mentioned criteria. Additionally, the Bu-03 location is adjacent to Polder 45. This location has migrated a total of 673m of the bank from 1989 to 2021. It is noticeable that maximum erosion occurred from 1989 to 2003 (**Figure 7.10**). Erosion was found minimum from 2010-2015. Thus prediction lines for the next 10, 20, and 30 years have been drawn considering the abovementioned criteria.

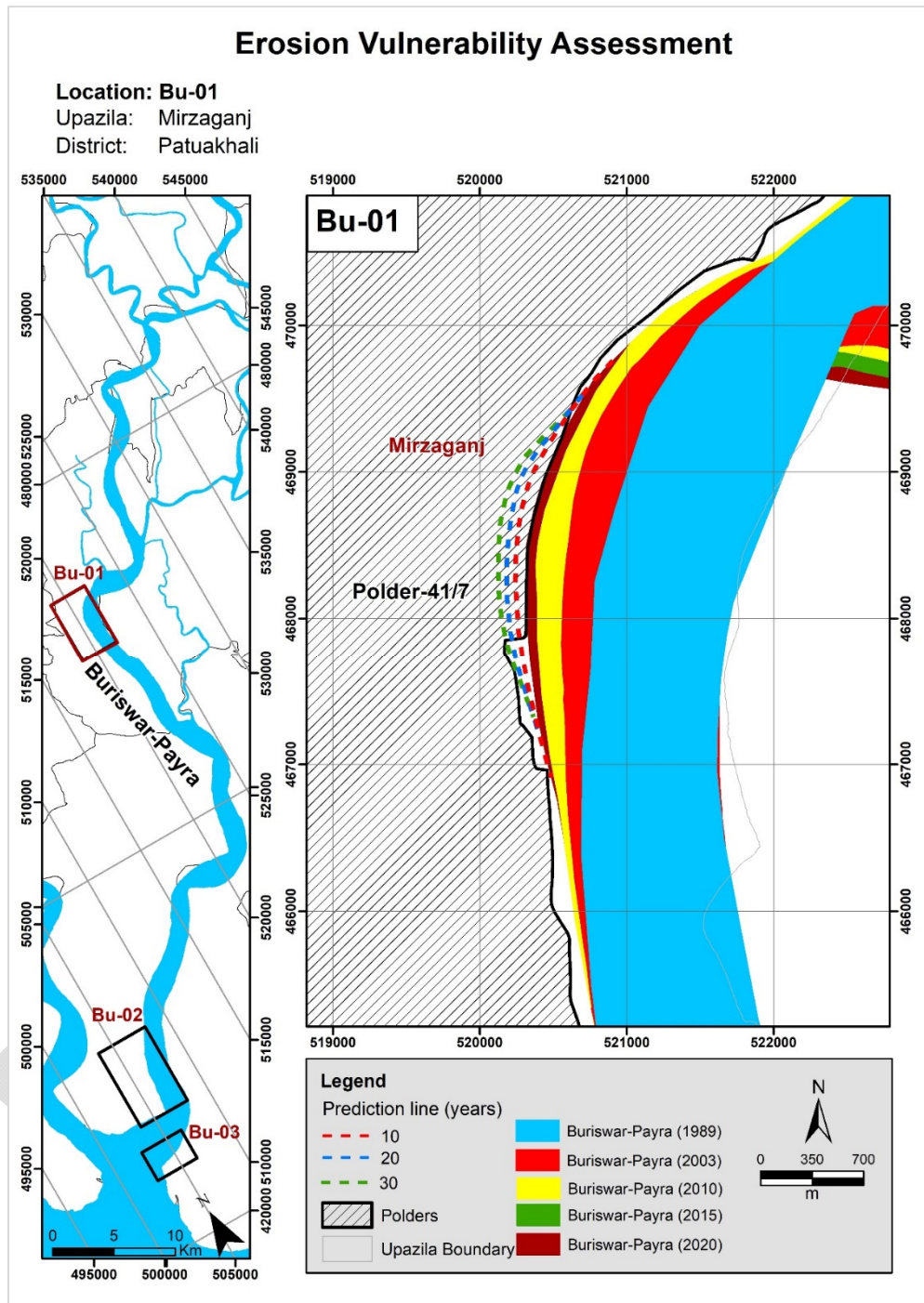


Figure 7.8: Bend migration in the next 10, 20, and 30 years in the Burishwar-Payra River

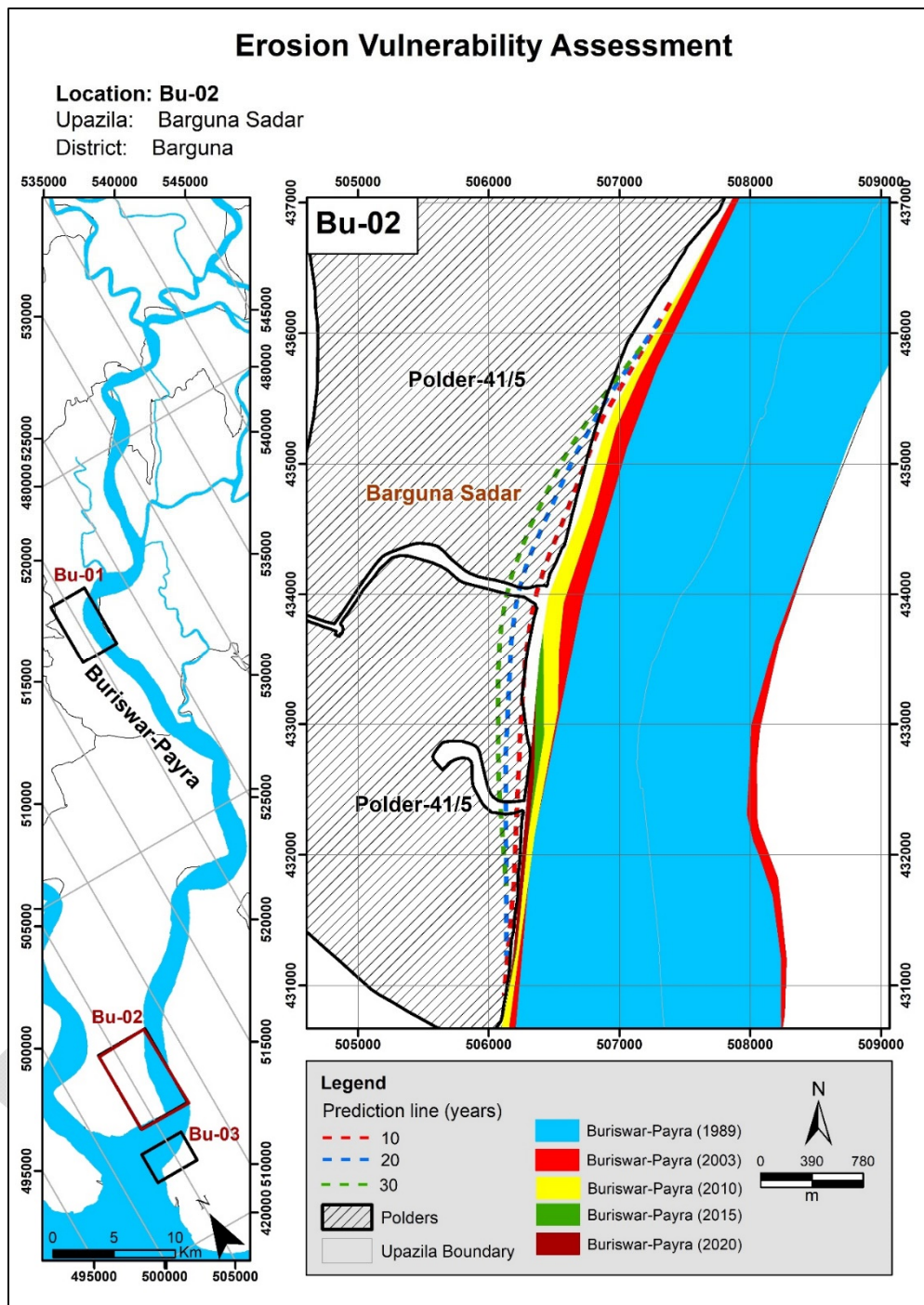


Figure 7.9: Bend migration in the next 10, 20, and 30 years in the Burishwar-Payra River

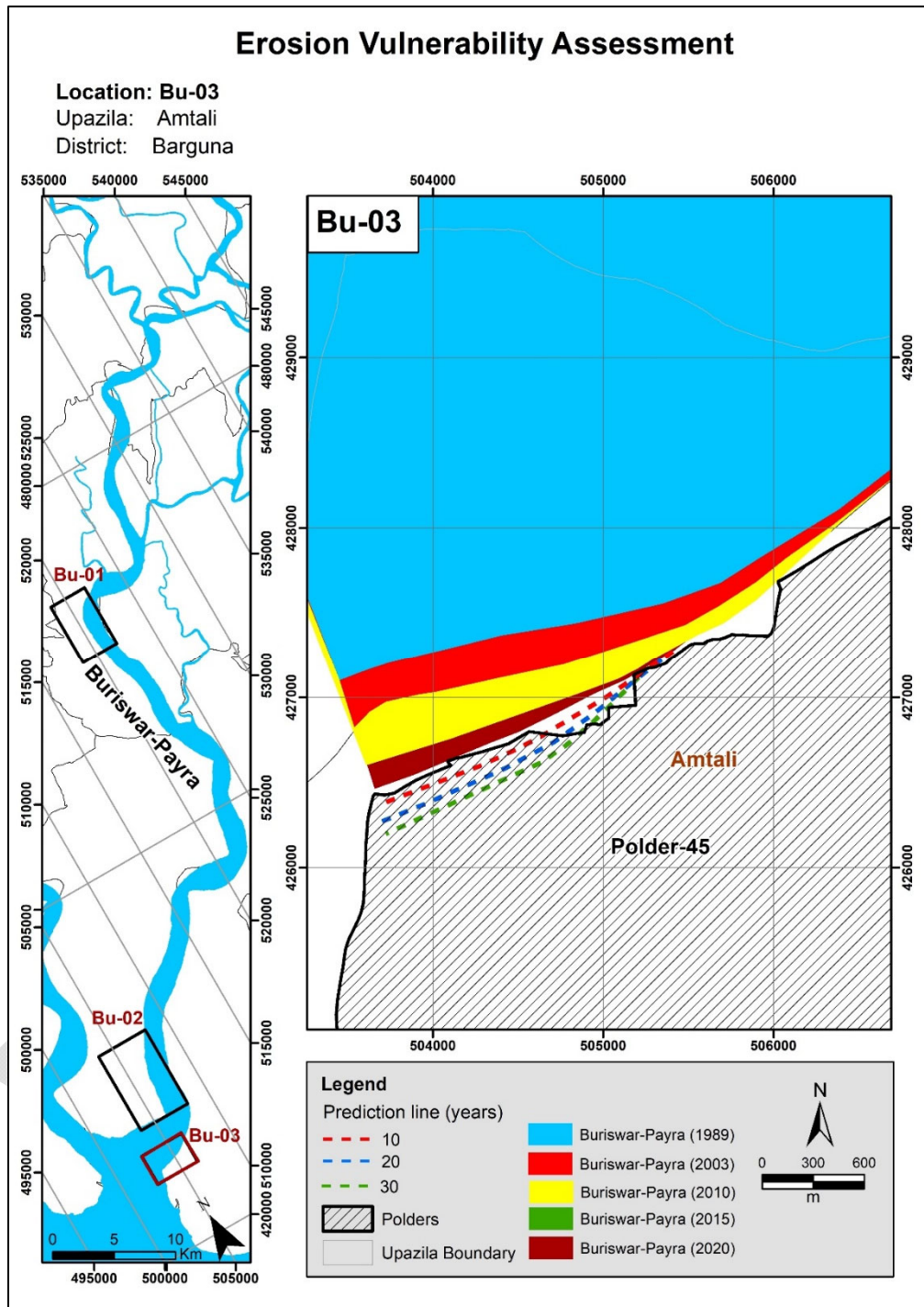


Figure 7.10: Bend migration in the next 10, 20, and 30 years in the Burishwar-Payra River

7.2 Baleshwar River

Baleshwar River originates from Kaliganga (Pirojpur) River at Nazirpur (Pirojpur) and outfalls in the Bay of Bengal. The river is of perennial type and gets over-flooded during monsoon.

Historical Development of the Baleshwar River

A 1943 map and satellite images of 1989, 2003, and 2021 were used to assess the historical development of the Baleshwar River (**Figure 7.11**). Comparing the map and the images, it is evident that the alignment of the river has not changed over the past 78 years.

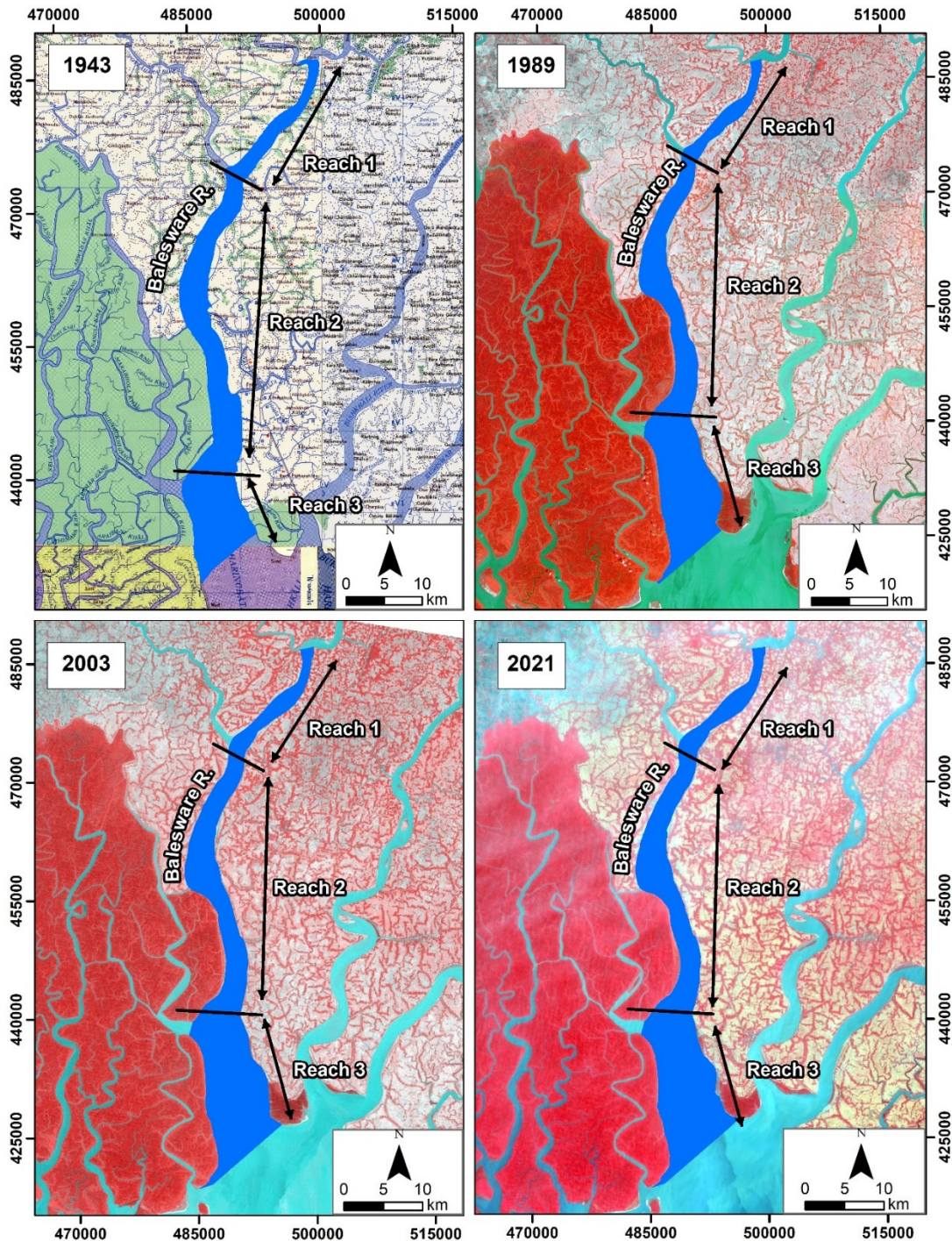


Figure 7.11: Historical Development of the Baleshwar River

Erosion-Accretion Analysis of the Baleshwar River

The Baleshwar River bank lines were delineated using the Arc-GIS tool to assess erosion-accretion. Then, bank lines of 1989, 2003, 2010, 2015, and 2021 were superimposed to assess erosion and accretion of the river within the study route. The study river is divided into two reaches to understand the morphology better. Reach-1 from Pattashi to Balipara, Reach-2 from Balipara to Sharankhola Range union, Reach-3 from Sharankhola Range to outfall the Bay of Bengal.

The erosion and accretion-prone areas along the Baleshwar River are presented in **Figure 7.12** and marked red and green, respectively. It is observed that the Baleshwar River has been erosion prone throughout the past three decades. The erosion-accretion of Reach-1, Reach-2, and Reach-3 of Baleshwar River is presented in **Figures 7.13** and **Figure 7.15**.

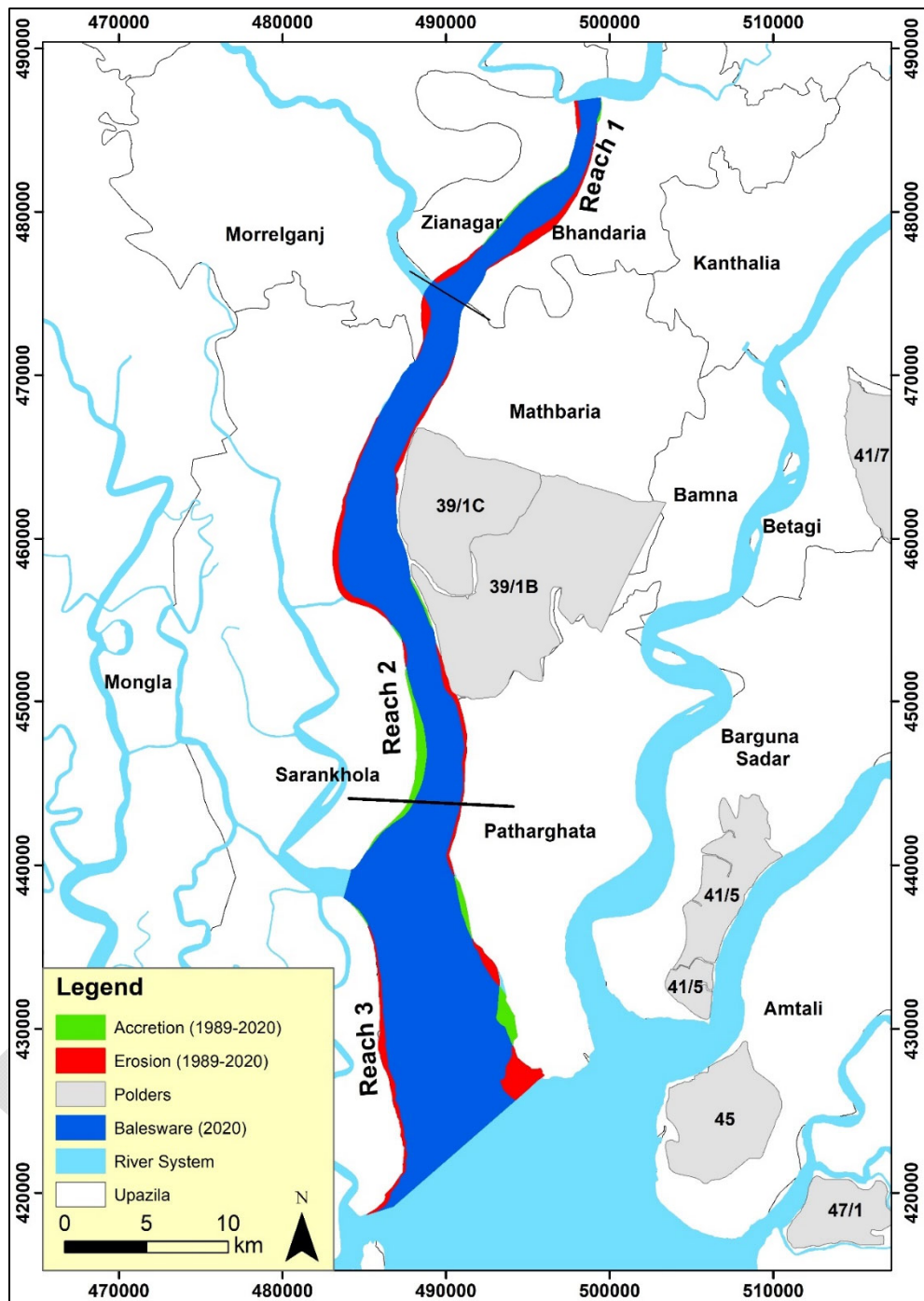


Figure 7.12: Erosion-accretion of the Baleshwar River during (1989-2021)

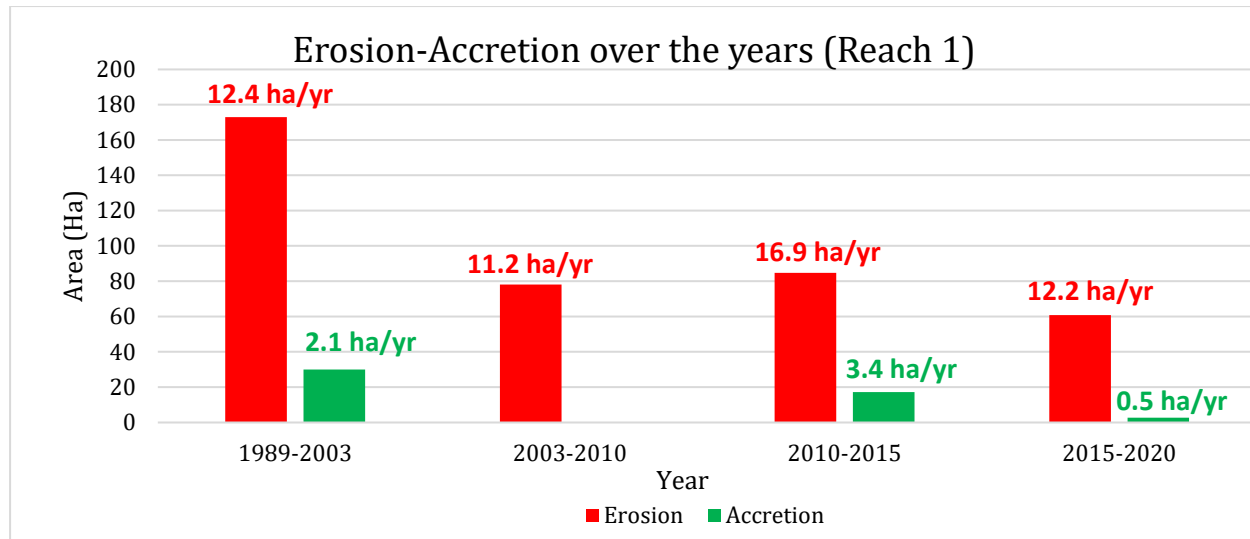


Figure 7.13: Erosion-accretion of Baleshwar River over the years (Reach-1)

Figure 7.13 shows that reach-1 of the Baleshwar River has been erosion-prone in the last three decades. The maximum amount of erosion was observed during the 1989-2003 timespan (172 ha), and the maximum amount of accretion was seen during this time (about 30 ha). From 2003-2010, no accretion occurred while erosion continued at 11.2 ha/yr. In the 2010-2015 timespan, the erosion rate increased to 16.9 ha/yr, and a small accretion rate (3.4 ha/yr) was observed. From 2015 to 2020, the erosion rate declined slightly (12.2 ha/yr), and the accretion rate declined (0.5 ha/yr).

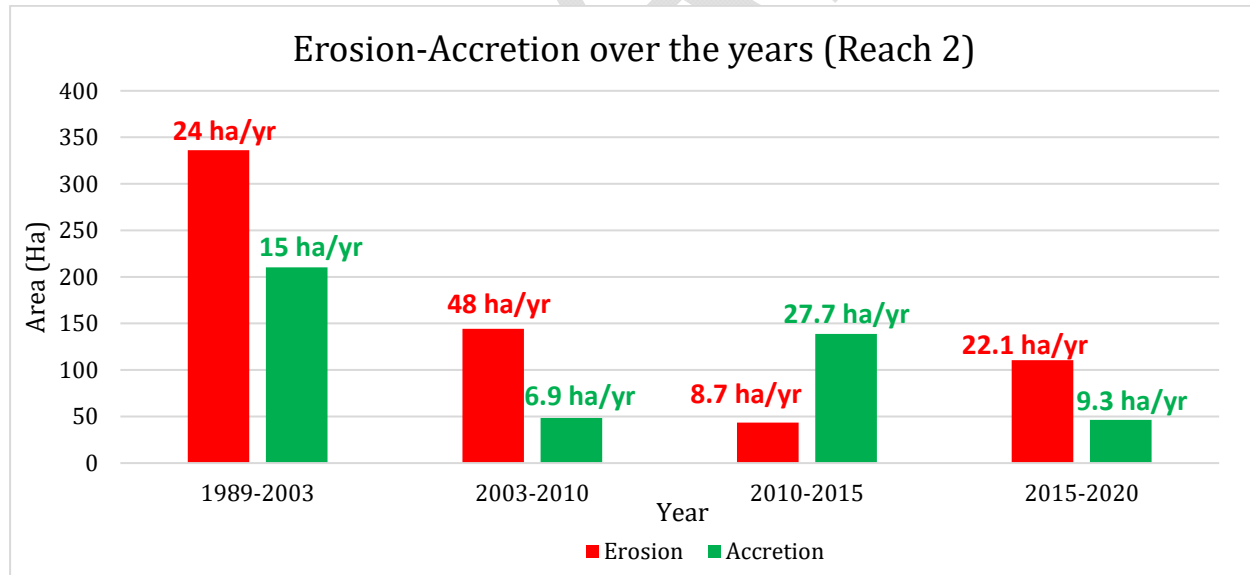


Figure 7.14: Erosion-accretion of Baleshwar River over the years (Reach-2)

From **Figure 7.14**, it is observed that Reach-2 is also erosion prone like Reach-1. In the 1989-2003 timespan, about 336 ha of land eroded and about 210 ha of land accreted. In the 2003-2010 timespan, a maximum erosion rate is observed (48 ha/yr), while the accretion rate was low. In the 2010-2015 timespan, the erosion rate declined (8.7 ha/yr), and the accretion rate increased significantly (27.7 ha/yr). In the 2015-2020 timespan, the erosion rate increased (22.1 ha/yr), and the accretion rate decreased (9.3 ha/yr).

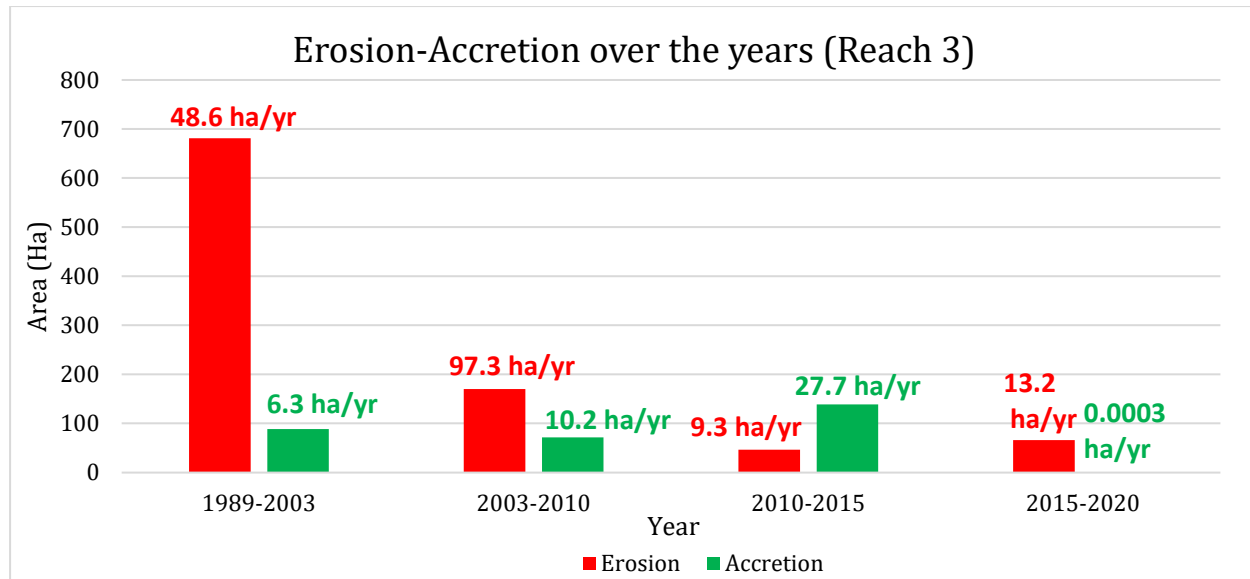


Figure 7.15: Erosion-accretion of Baleshwar River over the years (Reach-2)

Figure 7.15 shows that about 680 ha of land eroded and about 88 ha of land accreted in this reach in 1989-2003 timespan. This massive amount of erosion occurred because of erosion in left bank at the outfall to Bay of Bengal at Patharghata. Moreover, the maximum erosion rate was observed (97.3 ha/yr), and only 10.2 ha/yr of accretion rate was observed. In the 2010-2015 timespan, the erosion rate declined significantly as no noticeable amount of erosion occurred in Patharghata. However, the accretion rate increased to 27.7 ha/yr in this time. In 2015-2020, the erosion rate again increased slightly, and no significant amount of accretion occurred.

Finally, it can be concluded that the flow of the Baleshwar River fully depends on the flow of the Lower-Meghna River. As the Lower Meghna River is morphologically active and dynamic throughout the year, this region's flow pattern is also very dynamic. Thus, the erosion-accretion rate differs year to year in this river.

Average Width of the Baleshwar River

The shortest distance between two banks is defined as the river's width. However, at any river, the width varies at a different locations. Thus, to evaluate the changes in the river over time, the average width of the rivers has been calculated using ArcGIS. To compute the average width of any river, the total area enclosed by the riverbanks is divided by the length of the centerline of the river. For estimating the average width, the river has been divided into two reaches based on the width variation in this river. Changes in the river width from 1989 to 2020 have been assessed and presented in **Figure 7.16**.

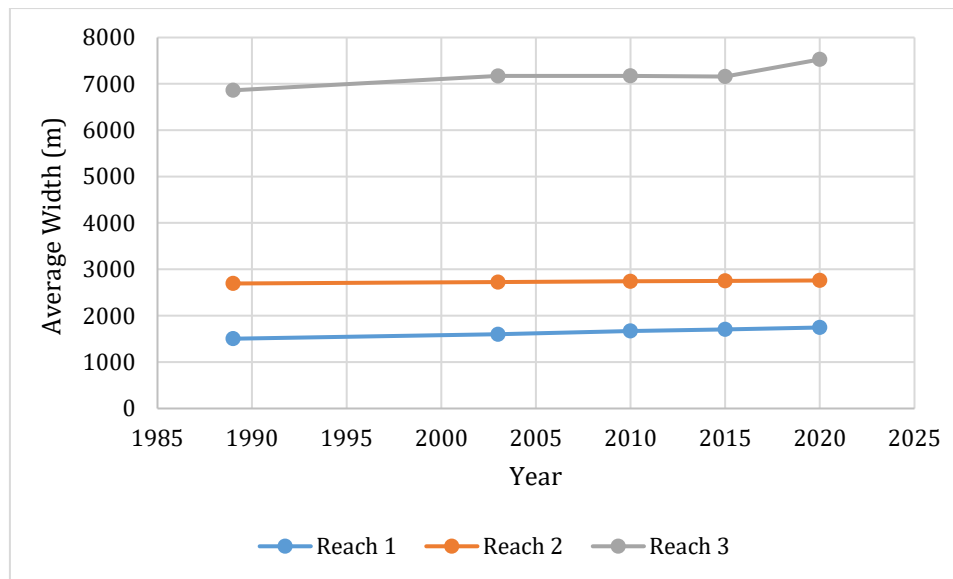


Figure 7.16: Average width of Baleshwar River over the years

Figure 7.40 shows that the average width of Reach-1 has a slightly increasing trend from 1989 to 2020 (about 1500 m to 1745 m). However, in Reach-2, no significant change has been observed. Reach-3 has a slightly increasing trend from 1989 to 2020 (about 6860 m to 7527 m).

The sinuosity of the Baleshwar River

Channel sinuosity is simple geometric information that signifies the river's deviation from a straight line. It is calculated as the length along the river divided by the straight-line distance along the river valley. The sinuosity of the Baleshwar River is represented in **Figure 7.17**.

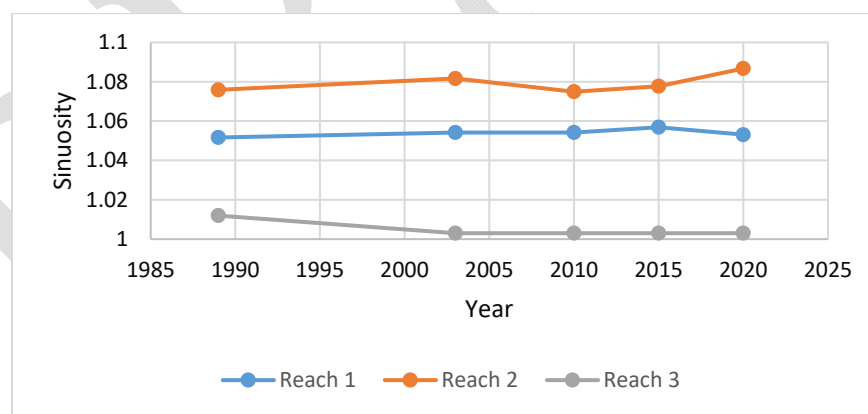


Figure 7.17: Sinuosity of Baleshwar River over the years

The sinuosity of the Baleshwar River has not changed significantly for all of the reaches. The sinuosity of both of the reaches indicates of straight kind of river.

Bend Migration of the Baleshwar River

Bend migration has been analyzed from 1989-2021 for the Baleshwar River. Locations, Extent of Bend migration, migration rate and direction of Bend migration are shown in Table 7.2. In

Figure 7.18, the Bend migrations are shown at seven major locations where maximum migration occurred. The life span of this river is calculated at 31 ± 10 years.

Table 7.2: Locations, Extent of Bend migration, and Migration direction for Baleshwar River

| Location | The extent of Bend migration (m) | Migration Rate (m/yr) | Migration direction |
|-----------------|---|------------------------------|----------------------------|
| A | 335 | 11 | South-West |
| B | 575 | 19 | South- East |
| C | 520 | 17 | North- West |
| D | 400 | 13 | South-West |
| E | 325 | 10 | North-East |
| F | 600 | 19 | North-East |
| G | 2150 | 69 | North-East |

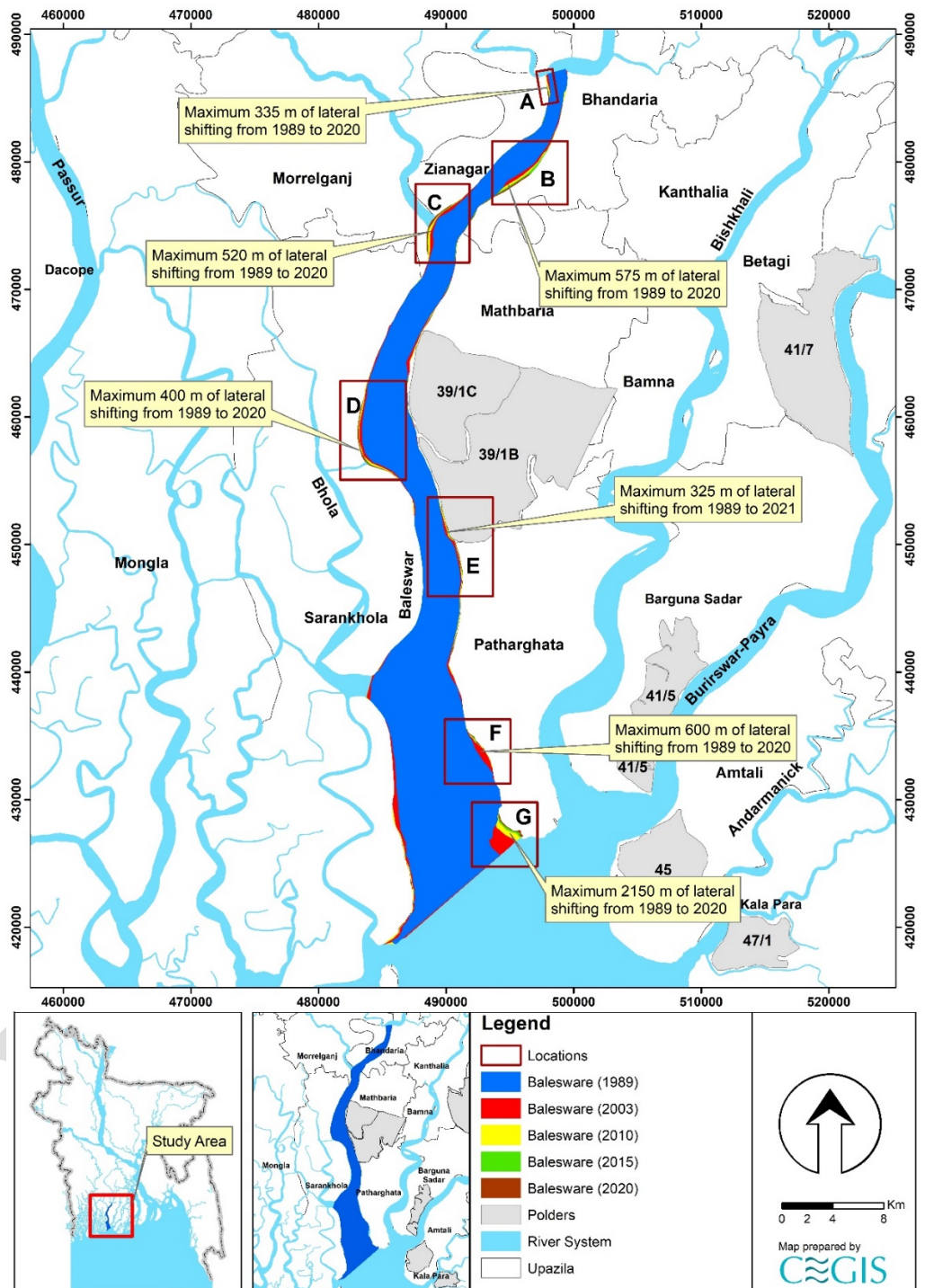


Figure 7.18: Bend migration of the Baleswar River (1989-2021)

Projection of the Baleswar River

It is difficult to predict the morpho-dynamics of a river since the Baleswar River is very active. Thus, the uncertainty of predicting future migration is very high. However, statistical analysis has been done for two (2) Baleswar River locations to predict future Bend migration for the next 10, 20, and 30 years. Locations adjacent to the polders have been selected and named

"Ba-01" to "Ba-02". The existing trend of the Bend migration rate has been considered while predicting this river's future lines. Bend migrations extent less than 5 times the image resolution have been considered only for 30 years of prediction. Prediction lines of 10 and 20 years have been avoided to reduce uncertainty. As no cut-off has been seen in this river in the last 78 years, no cut-off criteria has been considered. Future migration lines for the next 10, 20, and 30 years at the selected river locations are shown in Figures 7.19 to **7.20**. Detailing prediction lines from Ba-01 to Ba-02 in this river is discussed below.

Ba-01 location is adjacent to Polder 39/1C. This location has migrated a maximum of 250 m of the bank from 1989 to 2020. From **Figure 7.19**, maximum erosion occurred in this location from 1989 to 2003 timespan. Since then, a slight amount of erosion occurred in 2015. Thus, the probability of future migration to this location is less. Thus, only a prediction line of 30 years has been drawn for this location.

On the other hand, the Ba-02 location is adjacent to Polder 39/1B. This location has migrated a maximum of 320 m of the bank from 1989 to 2021. Figure 7.20 shows that the river bank in this location has been migrating continuously over the last 32 years. Thus, prediction lines for the next 10, 20, and 30 years have been drawn, calculating the migration rate in this location.

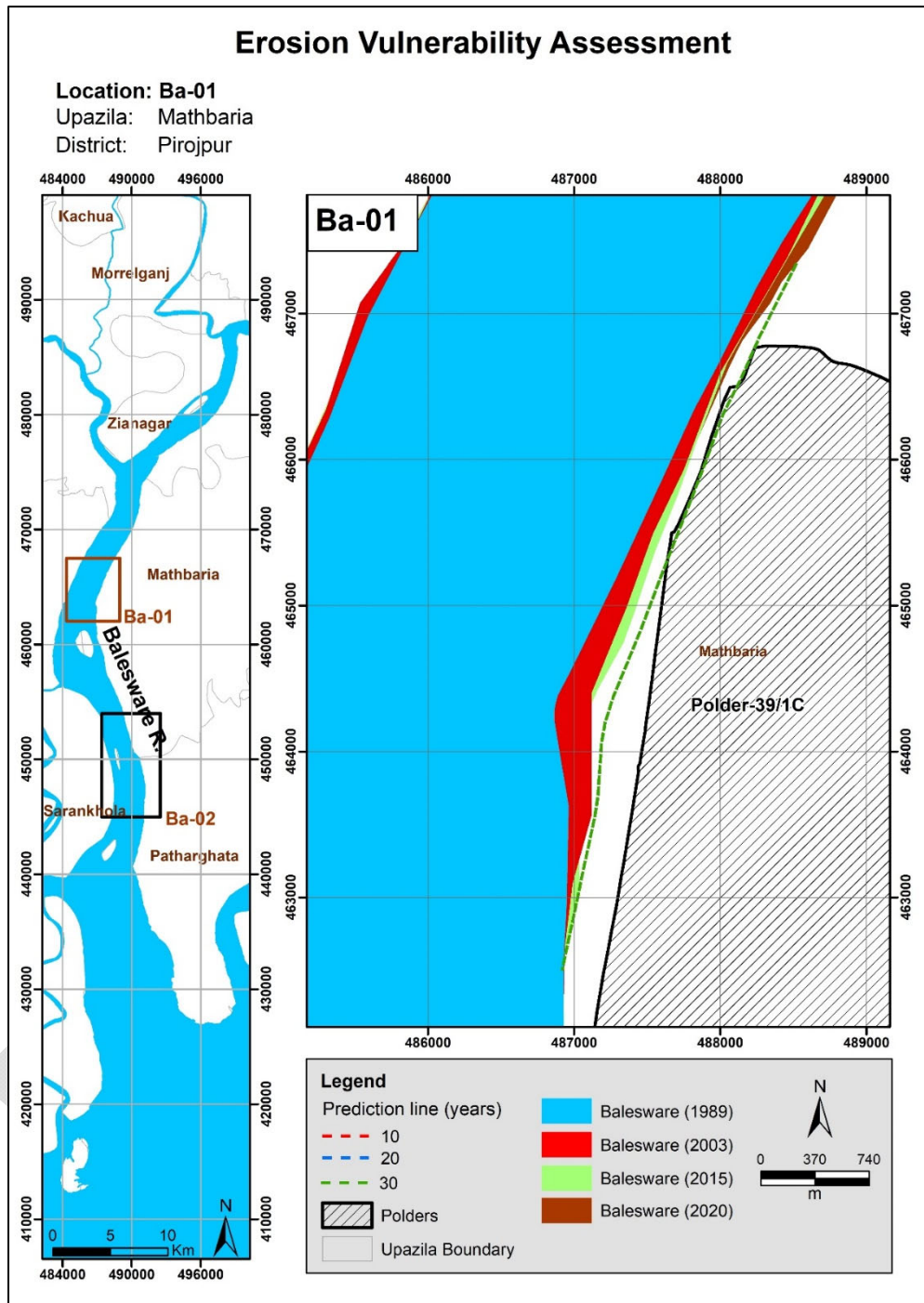


Figure 7.19: Bend migration in the next 10, 20, and 30 years in the Baleshwar River

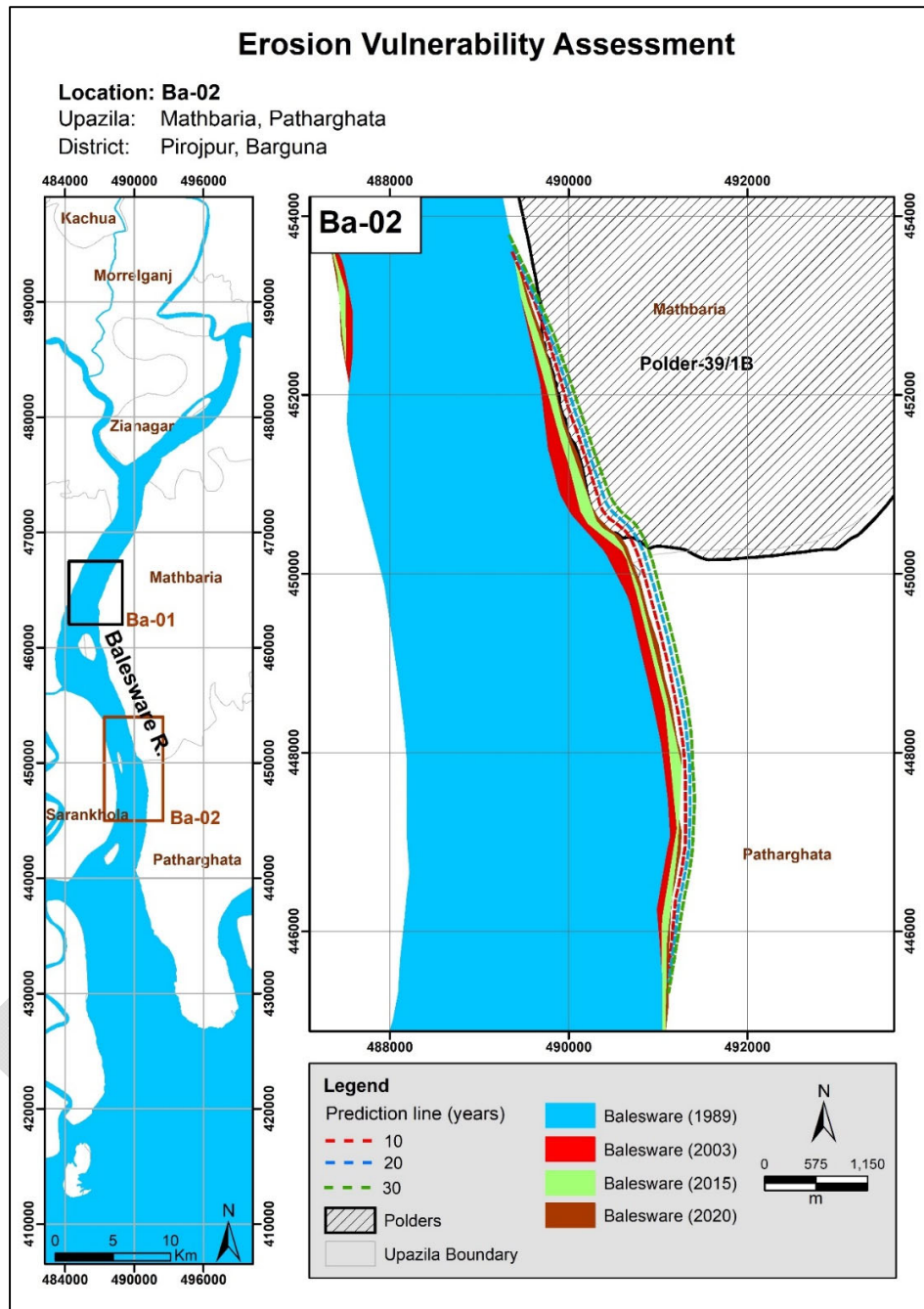


Figure 7.20: Bend migration in the next 10, 20, and 30 years in the Baleswar River

7.3 Tentulia River

Tentulia River originates from the Lower-Meghna River at Illisha union in Bhola Sadar (Bhola). The river flows through Charkajal, Panpatti, Chalitabunia Union, and outfalls in the Bay of Bengal. This river is also perennial.

Historical Development of the Tentulia River

The 1943 map and satellite images of 1980, 2003, and 2019 have been analyzed to understand the historical development of this river (**Figure 7.21**). No significant shift in the banks has been observed here. It can be confirmed that the river is very dynamic with growing chars and sand bars.

DRAFT

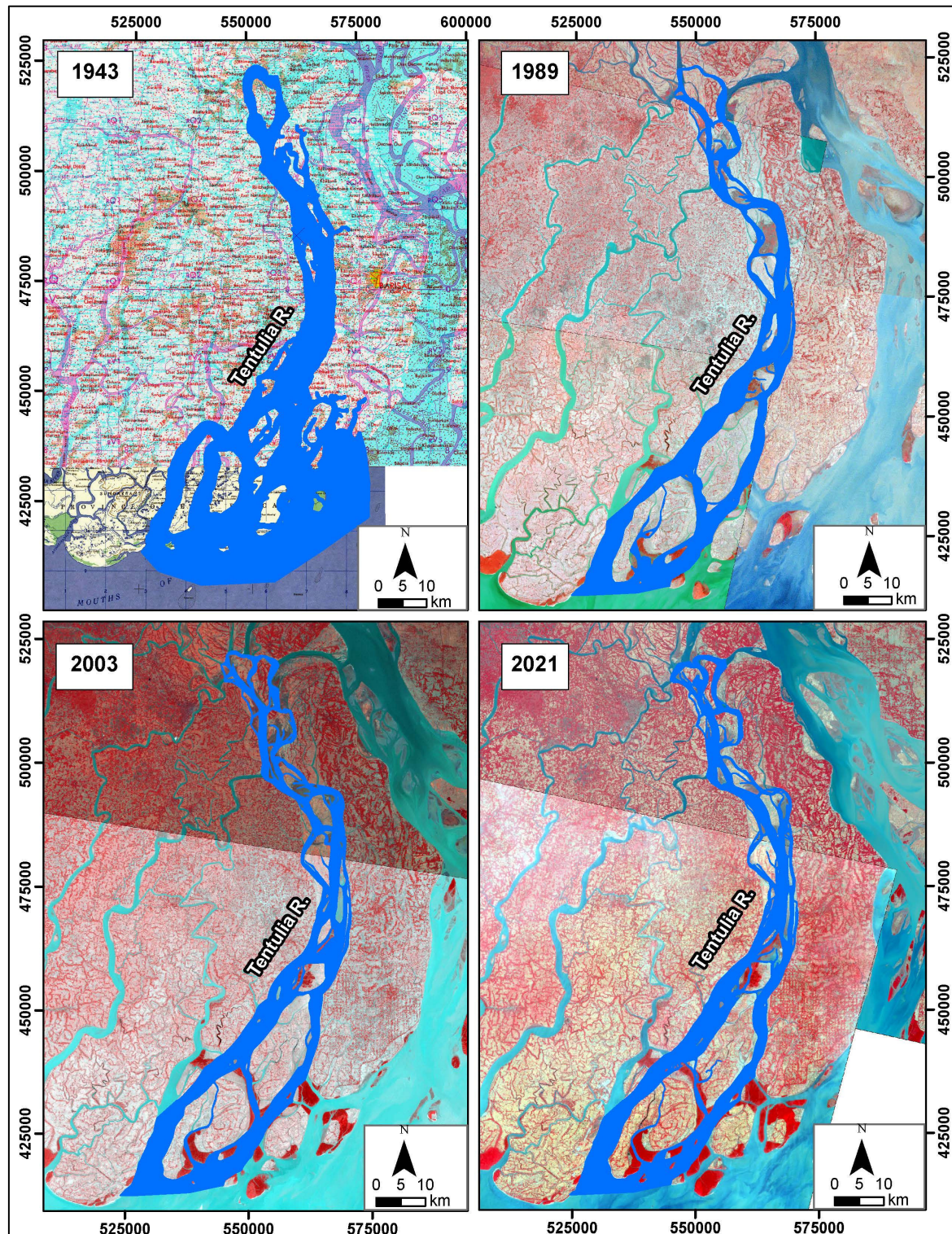


Figure 7.21: Historical development of Tentulia River (1943-2021)

Erosion-Accretion Analysis of the Tentulia River

For the assessment of erosion-accretion, the Tentulia River bank lines were delineated using the Arc-GIS tool. Then, bank lines of 1989, 2003, 2010, 2015, and 2021 were superimposed to assess erosion and accretion of the river within the study route. The erosion and accretion-prone areas along the Tentulia River are presented in **Figure 7.22** and marked red and green, respectively. Erosion-accretion of Tentulia River along the banks and chars are shown in **Figures 7.23** and **7.24**.

DRAFT

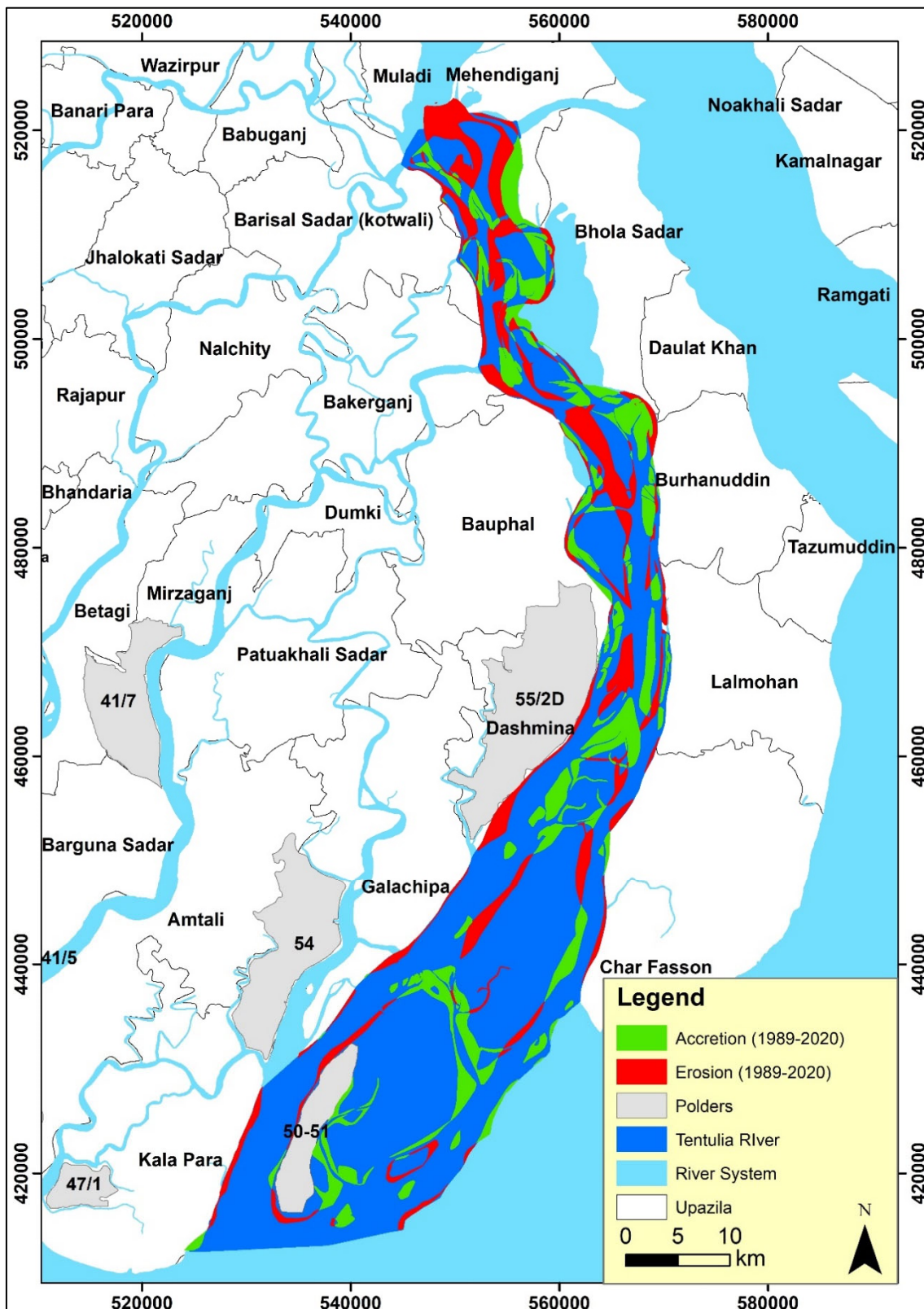


Figure 7.22: Erosion-accretion of Tentulia River (1989-2021)

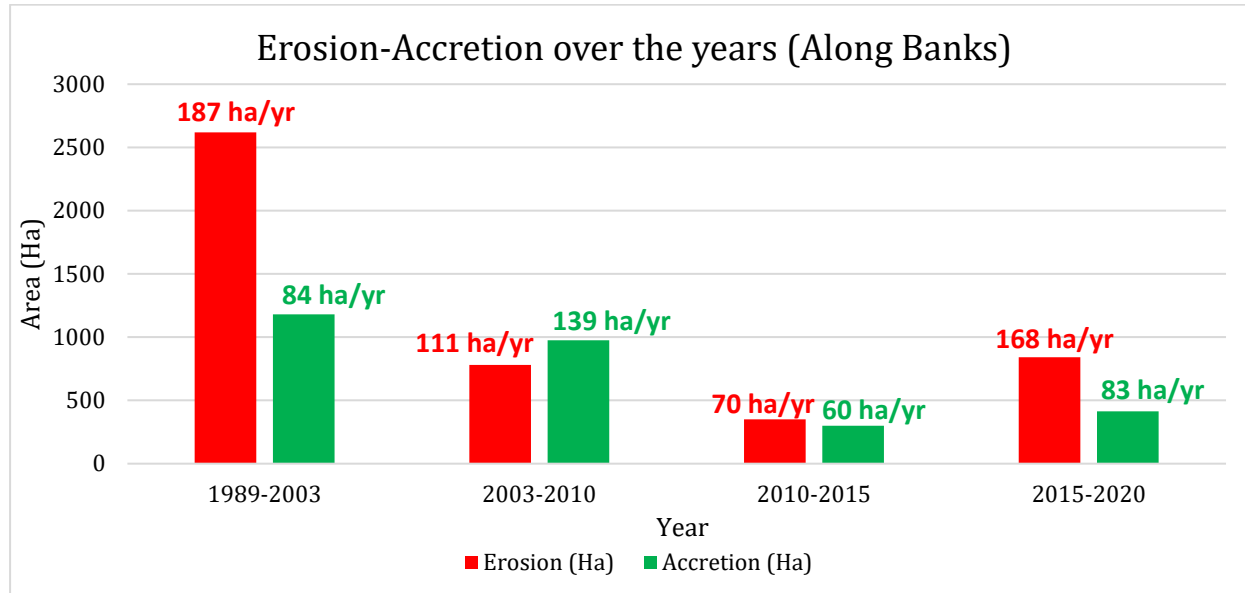


Figure 7.23: Erosion-accretion of Tentulia River along both of the banks (1989-2021)

Figure 7.23 shows that about 2619 ha of land had been eroded, while about 1180 ha of land was accreted along the banks during the 1989-2003 timespan. In the 2003-2010 timespan, the erosion rate decreased (111ha/yr), and the accretion rate increased (139 ha/yr). In the 2010-2015 timespan, both erosion (70 ha/yr) and accretion rate (60 ha/yr) decreased. However, erosion and accretion rates increased in the 2015-2020 timespan. It is noticeable that erosion occurs mainly at Bhola Sadar, Bakerganj, Burhanuddin, and Dashmina Upazila.

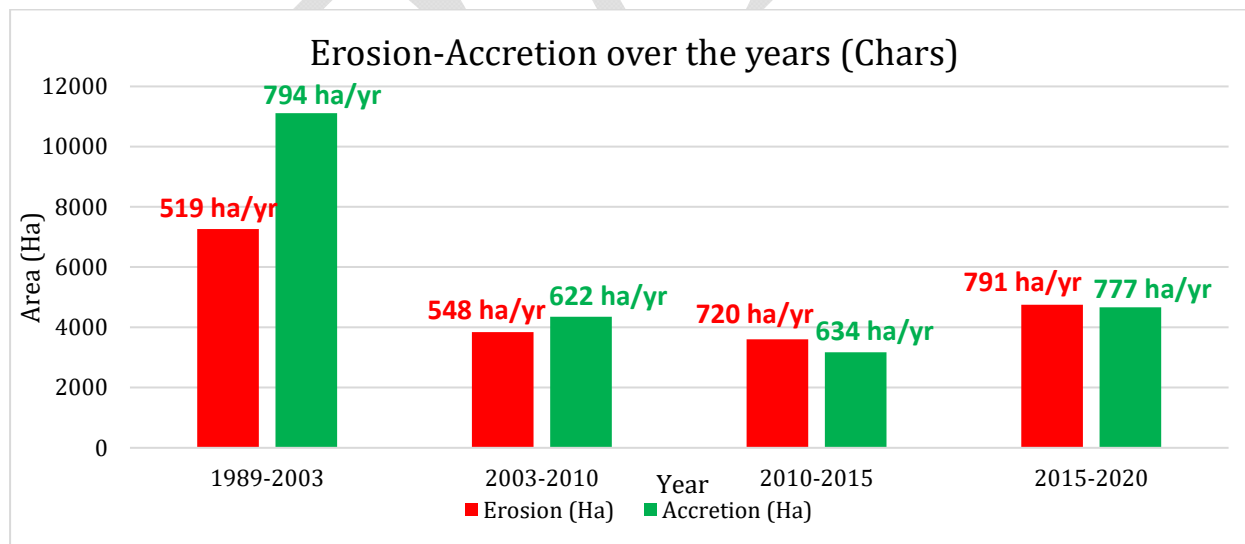


Figure 7.24: Erosion-accretion of chars of Tentulia River (1989-2021)

It is stated that the chars have been very dynamic throughout the last 30 years. From 1989 to 2003, accretion dominated erosion as 11109 ha of land was accreted, and 7262 ha of land eroded. After that, no significant trend has been observed in erosion and accretion rate till 2020. The study observed that though erosion-accretion of Tentulia River along the banks has declined throughout the years, the chars have been very dynamic in the last three decades.

Bend Migration of the Tentulia River

Bend migration has been analyzed from 1989-2021 for the Tentulia River. In **Figure 7.25**, the Bend migrations are shown at seven major locations where maximum migration occurred. Locations, Extent of Bend migration, migration rate, and direction of bend migration are shown in **Table 7.3**. The lifespan of this river along its banks is calculated at 31 ± 10 years.

Table 7.3: Locations, Extent of Bend migration, and Migration direction for Tentulia River

| Location | The extent of Bend migration (m) | Migration rate (m/yr) | Migration direction |
|----------|----------------------------------|-----------------------|---------------------|
| A | 830 | 27 | South-East |
| B | 1400 | 45 | South-West |
| C | 1300 | 42 | North-East |
| D | 500 | 16 | South-West |
| E | 400 | 13 | North-West |
| F | 1640 | 53 | North-West |
| G | 400 | 13 | South-East |

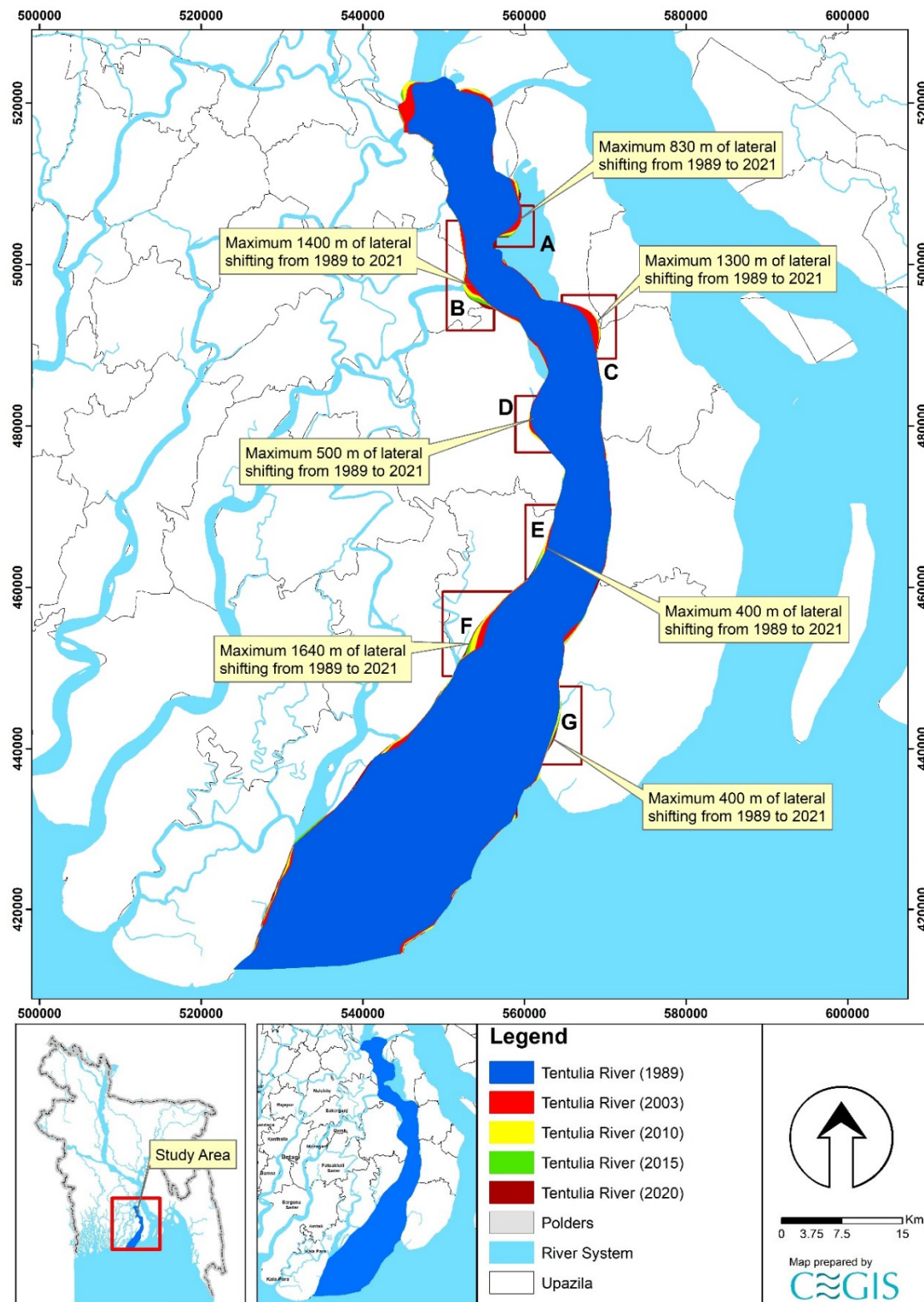


Figure 7.25: Bend migration of Tentulia River (1989-2021)

Projection of the Tentulia River

It is difficult to predict the morpho-dynamics of a river since the Tentulia River is active. Thus, the uncertainty of predicting future migration is very high. However, statistical analysis has been done for two (2) locations of Tentulia River to predict future Bend migration for the next 10, 20, and 30 years. Locations adjacent to the polders have been selected and named "Te-01" to "Te-02". The existing trend of the Bend migration rate has been considered while predicting this river's future lines. Bend migrations, less than 5 times, the image resolution has been considered only for 30 years of prediction. Prediction lines of 10 and 20 years were avoided to reduce uncertainty. As no cut-off has been seen in this river in the last 78 years, no cut-off criteria has been considered. Future migration lines for the next 10, 20 and 30 years at the river's selected locations are shown in Figures 6.57 to Figure 6.58. Detailing prediction lines from Te-01 to Te-02 in this river is discussed below.

Te-01 location is adjacent to Polder 55/2D. From Figure 7.26, it is observed that river bank in this location have been migrating continuously over last 32 years and migration rate has been declining throughout the years. A maximum of 1640 m of the bank have been migrated from 1989 to 2020 in this location. Thus, prediction lines for the next 10, 20, and 30 years have been drawn, calculating the migration rate in this location.

Te-02 location is adjacent to Polder 50-51. This location has migrated a maximum of 700 m of Charland from 1989 to 2020. Figure 7.27 shows that Charland in this location has been migrating continuously over the last 32 years, and the migration rate has been declining. Thus, prediction lines for the next 10, 20, and 30 years have been drawn, calculating the migration rate in this location.

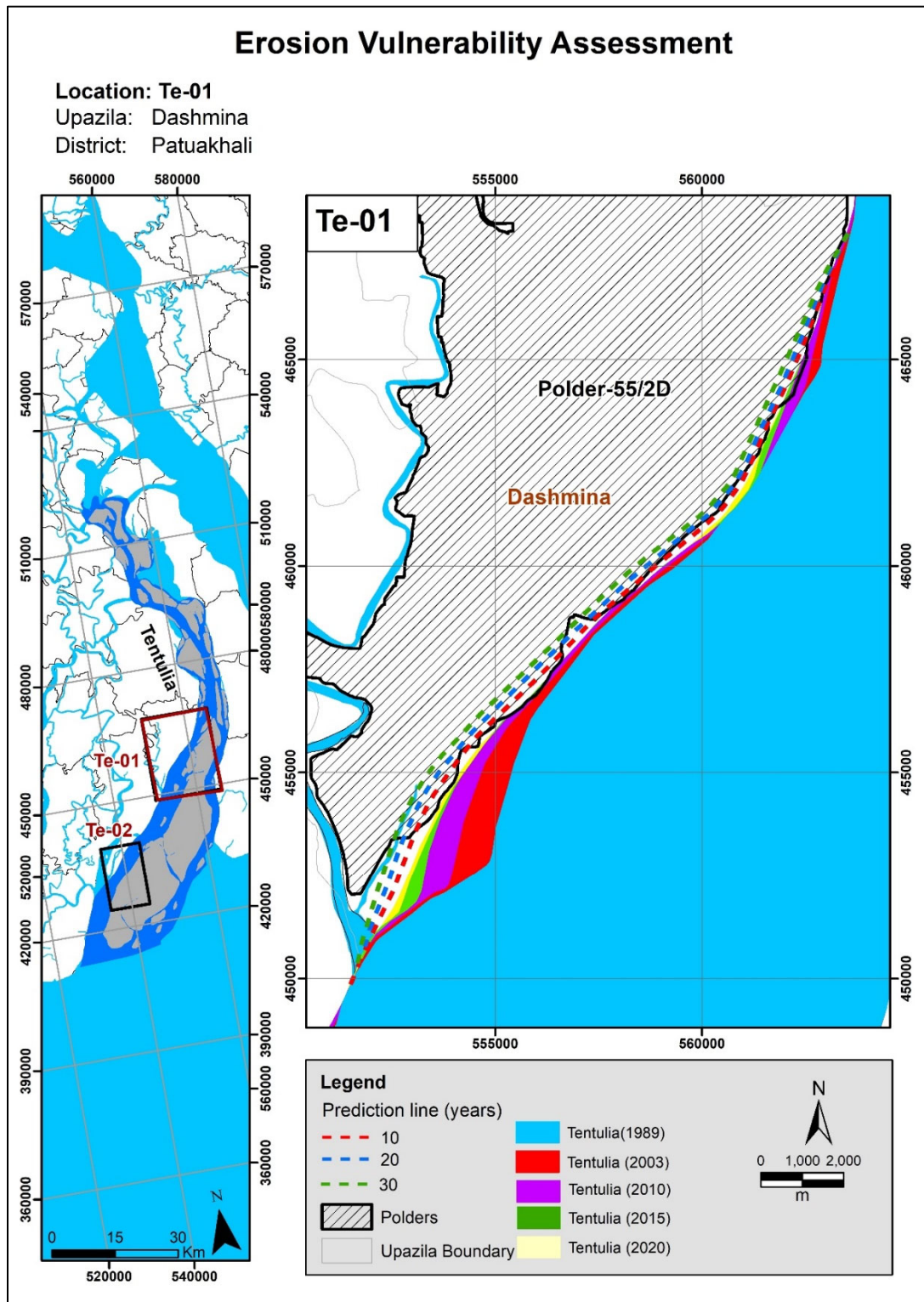


Figure 7.26: Bend migration in the next 10, 20, and 30 years in Tentulia River

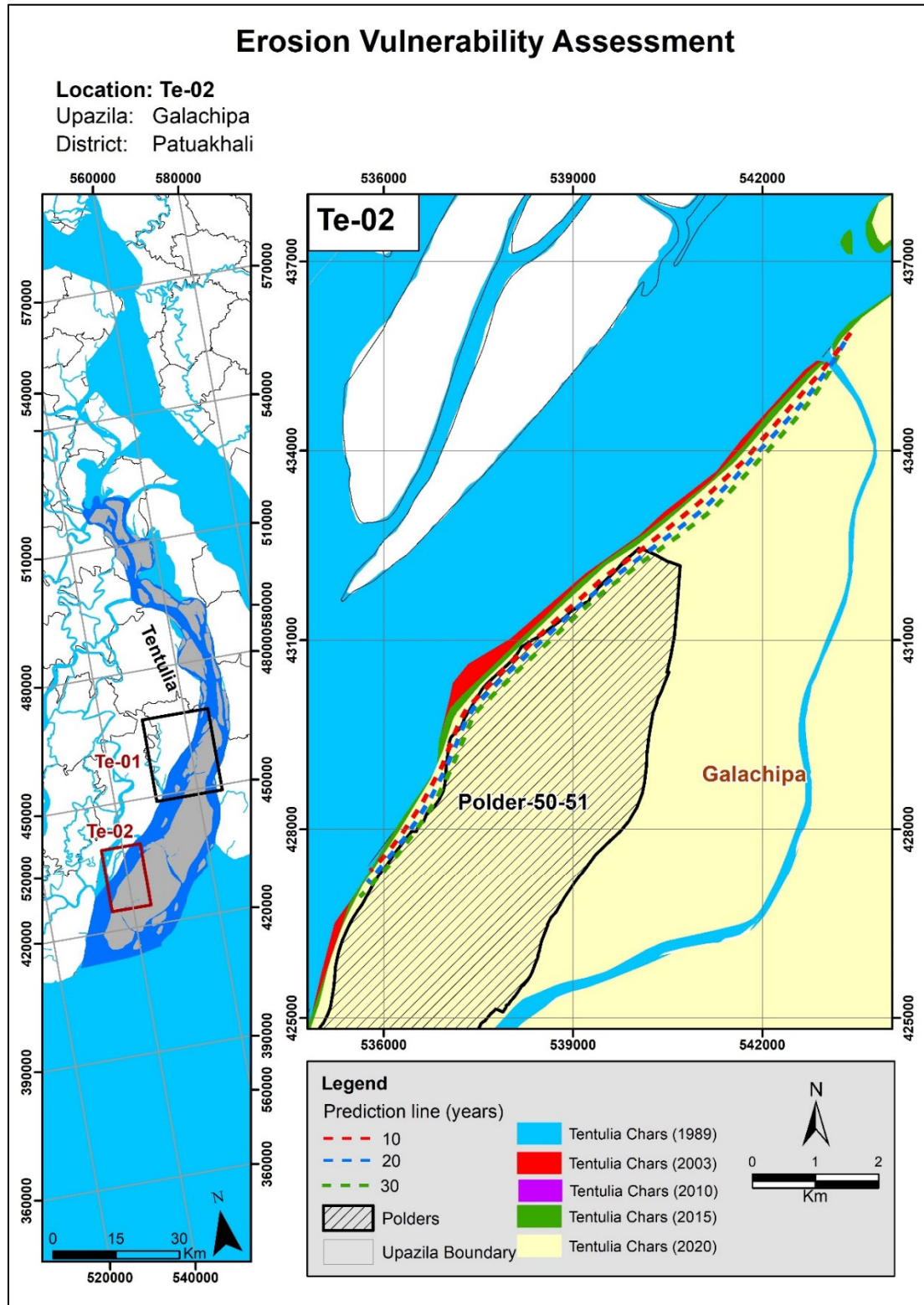


Figure 7.27: Bend migration in the next 10, 20, and 30 years in Tentulia River

8. Length of the Prediction Lines, Maximum Lateral Distance, and Length of Eroded Existing Embankment

8.1 Length of the Prediction Lines and Maximum Lateral Distance

It is important to assess the length of the prediction lines for different periods. At the same time, the maximum lateral distance would help plan purposes. The length of the prediction lines for 10, 20, and 30 years and their related lateral distance from the present bank lines are provided in **Table 8.1** and **Table 8.2** for the Khulna and Barishal areas, respectively. The tables also show the estimated length of existing embankment that would erode. The embankment alignments which have been used for these estimations are based upon the centerlines of the embankments. The embankments are a few meters thick (no more than 6 m). Therefore, there is an uncertainty in the eroded length. For example, the edge of the eroded length may only erode the toe of the embankment, and not the centerline, and would consequently not be included in the estimation. However, this uncertainty is negligible compared to the uncertainty inherent in long-term morphological predictions, as well as taking into consideration the 30 x 30 m resolution of the satellite images.

Table 8.1: Length and lateral distance of the prediction lines for the Khulna area

| River Name | ID | Year | Length of Eroded Bankline | Lateral Distance from the bank line of 2021 | Length of Eroded Existing Embankment (m) |
|------------|-------|------|---------------------------|---|--|
| Kapotakshi | Ka-01 | 10 | 2583 | 70 | 2334.88 |
| | | 20 | 2748 | 130 | 2487.79 |
| | | 30 | 2846 | 180 | 2605.78 |
| | Ka-02 | 10 | 1418 | 65 | 1207.64 |
| | | 20 | 1415 | 120 | 1233.31 |
| | | 30 | 1372 | 165 | 1253.12 |
| | Ka-03 | 10 | 1027 | 60 | 1070.79 |
| | | 20 | 1047 | 150 | 1193.46 |
| | | 30 | 1080 | 240 | 1324.44 |
| | Ka-04 | 10 | 4626 | 85 | 3613.37 |
| | | 20 | 4915 | 160 | 4377.41 |
| | | 30 | 5212 | 240 | 5262.01 |
| | Ka-05 | 10 | 2021 | 70 | 1551.58 |
| | | 20 | 1949 | 130 | 1679.61 |
| | | 30 | 1989 | 190 | 1650.08 |
| Kholpetua | Kh-01 | 10 | 918 | 30 | 208.37 |
| | | 20 | 976 | 60 | 470.9 |
| | | 30 | 1022 | 85 | 784.71 |
| | Kh-02 | 10 | - | - | - |
| | | 20 | - | - | - |
| | | 30 | 995 | 90 | 968.13 |

| River Name | ID | Year | Length of Eroded Bankline | Lateral Distance from the bank line of 2021 | Length of Eroded Existing Embankment (m) |
|------------|-------|------|---------------------------|---|--|
| Kh-03 | Kh-03 | 10 | - | - | - |
| | | 20 | - | - | - |
| | | 30 | 1298 | 55 | 1020 |
| | Kh-04 | 10 | 755 | 25 | 474.74 |
| | | 20 | 730 | 50 | 747.40 |
| | | 30 | 701 | 90 | 776.07 |
| | Kh-05 | 10 | 4768 | 40 | 3966.23 |
| | | 20 | 4968 | 70 | 4207.25 |
| | | 30 | 5095 | 100 | 4594.41 |
| | Kh-06 | 10 | 2242 | 60 | 1444.8 |
| | | 20 | 2277 | 100 | 1747.18 |
| | | 30 | 2348 | 180 | 1680.93 |
| | Kh-07 | 10 | 5129 | 80 | 5003.69 |
| | | 20 | 5088 | 150 | 5131.17 |
| | | 30 | 4868 | 215 | 5066.97 |
| | Kh-08 | 10 | 1382 | 120 | 688.96 |
| | | 20 | 1362 | 250 | 1638.10 |
| | | 30 | 1348 | 380 | 1836.84 |
| | Kh-09 | 10 | - | - | - |
| | | 20 | - | - | - |
| | | 30 | 150 | 6213.030095 | 1420.44 |
| Shibsa | Sh-01 | 10 | - | - | - |
| | | 20 | - | - | - |
| | | 30 | 2856 | 80 | 1757.38 |

Table 8.2: Length and lateral distance of the prediction lines for the Barishal area

| River Name | ID | Year | Length | Lateral Distance from bank line of 2020 | Length of Eroded Existing Embankment (m) |
|------------|-------|------|--------|---|--|
| Baleshwar | Ba-01 | 10 | | - | - |
| | | 20 | | - | - |
| | | 30 | 5142 | 120 | 1317.46 |
| | Ba-02 | 10 | 8527 | 90 | 2793.37 |
| | | 20 | 8661 | 150 | 3019.76 |
| | | 30 | 8933 | 220 | 3225.91 |

| River Name | ID | Year | Length | Lateral Distance from bank line of 2020 | Length of Eroded Existing Embankment (m) |
|-----------------|-------|------|--------|---|--|
| Burishwar-Payra | Bu-01 | 10 | 2892 | 60 | 1632.68 |
| | | 20 | 2392 | 120 | 1715.40 |
| | | 30 | 2115 | 180 | 1754.01 |
| | Bu-02 | 10 | 5556 | 70 | 4190.07 |
| | | 20 | 5151 | 160 | 5094.15 |
| | | 30 | 4422 | 280 | 5469.42 |
| | Bu-03 | 10 | 1965 | 70 | 1335.31 |
| | | 20 | 1911 | 180 | 1574.26 |
| | | 30 | 1764 | 250 | 1828.02 |
| Tentulia | Te-01 | 10 | 22376 | 260 | 11820.24 |
| | | 20 | 21304 | 470 | 17468.96 |
| | | 30 | 21948 | 670 | 18413.72 |
| | Te-02 | 10 | 11559 | 110 | 2125.19 |
| | | 20 | 11573 | 230 | 4542.91 |
| | | 30 | 11612 | 330 | 6251.78 |

8.2 Translation of the Prediction lines to Erosion Risk

Prioritization Report

Based on the historical erosion trends and rate, future embankment erosion risk has been assessed for the polders in the Khulna and Barishal areas (CEIP Prioritization Report, 2021). Further, based on the river erosion rate, erosion risk has been categorized as High, Medium, and Low (**Figure 8.3** and **Figure 8.4**).

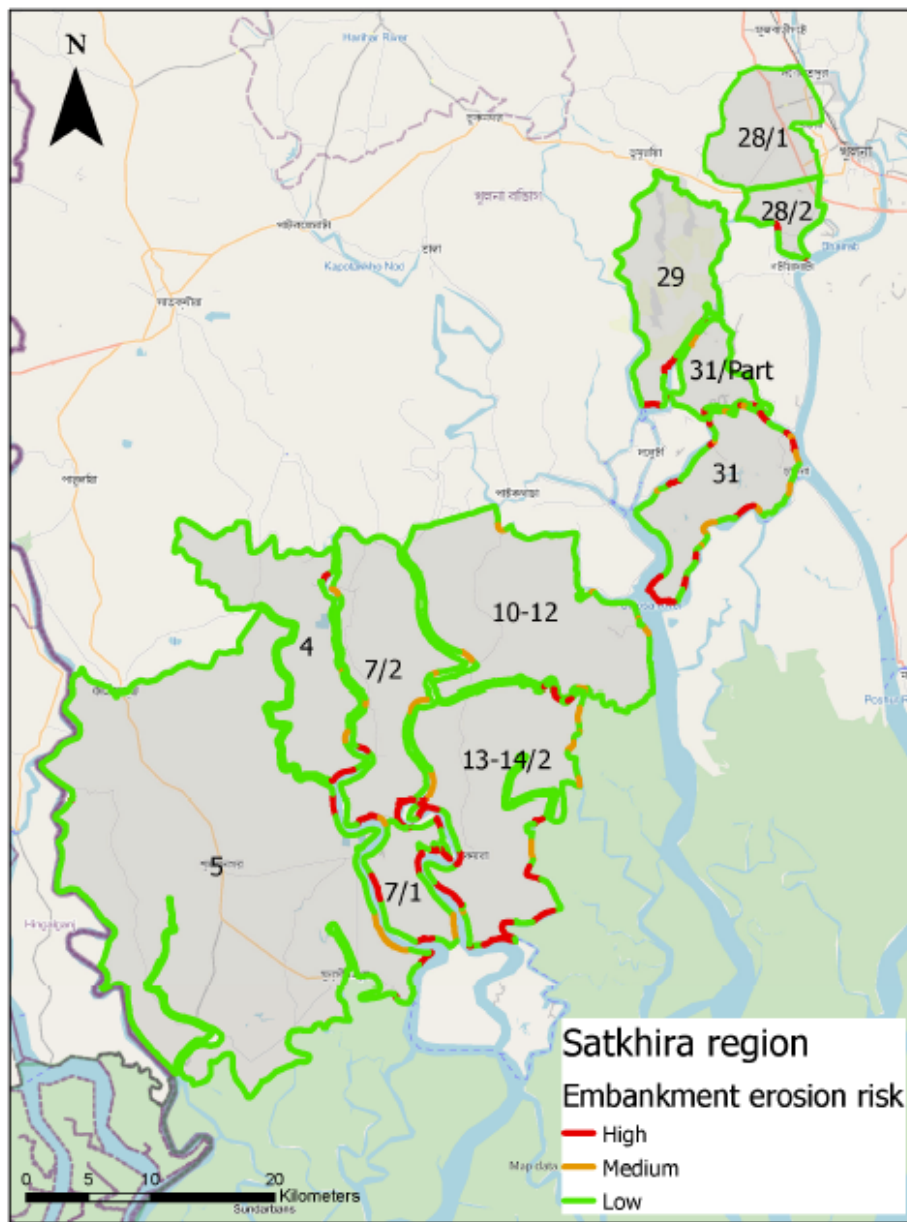


Figure 8.3: Erosion risk to the embankment for the polders in Khulna/Satkhira area
(source: CEIP Prioritization Report, 2021)

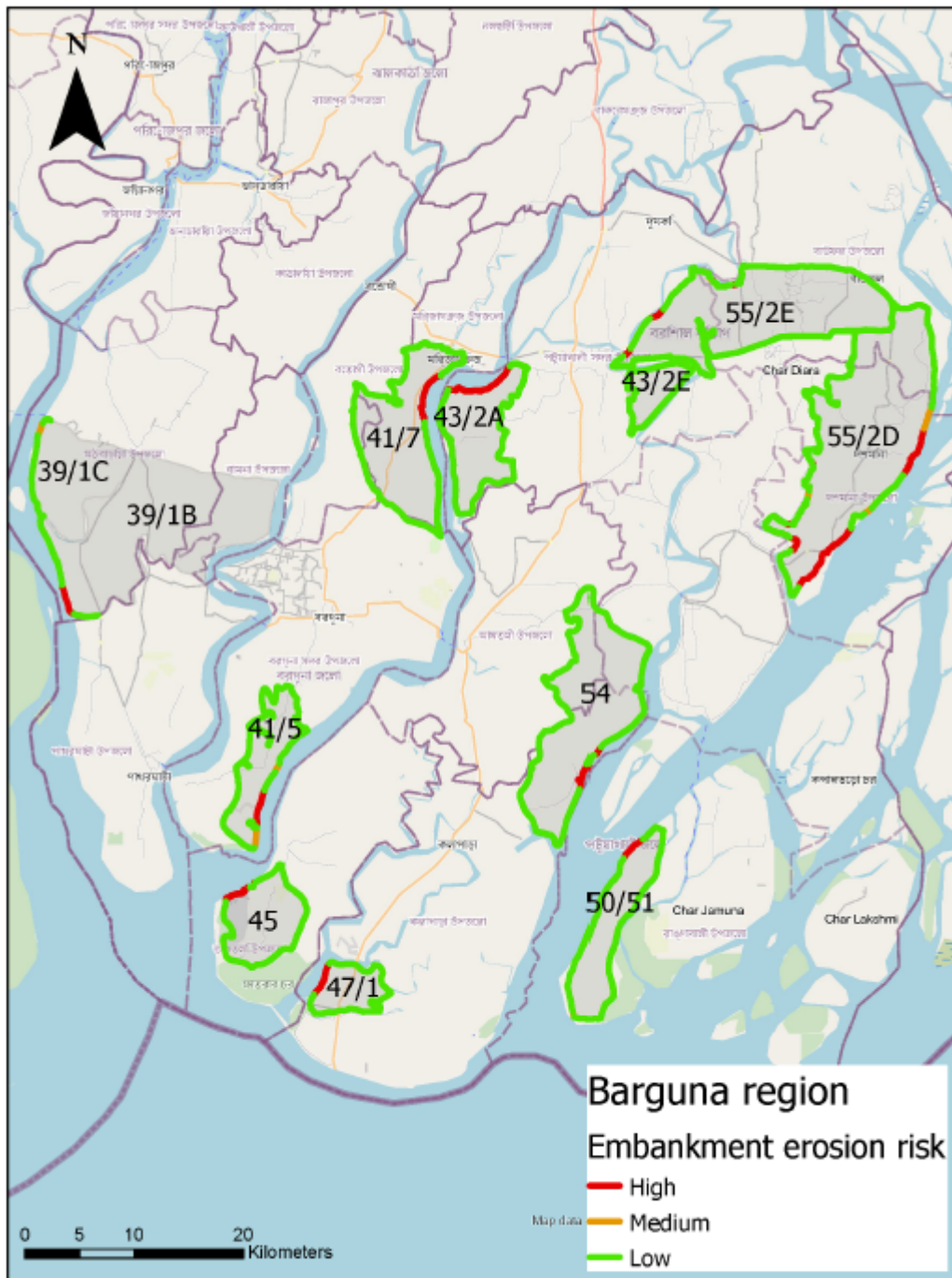


Figure 8.4: Erosion risk to the embankment for the polders in Barishal/Barguna area (source: CEIP Prioritization Report, 2021)

High indicates embankment at risk of medium/high erosion rates now or shortly, while Medium means embankment at risk of low/medium erosion rates now or shortly, and Low denotes the embankment is not at erosion risk. Additionally, the high erosion rate is the average erosion rate is more than 10 m/year. On the other hand, the medium erosion rate is the average erosion rate between 5 – 10 m/year, whereas Low is the average erosion rate is lower than 5 m/year.

This is to mention here that the same erosion rate has been considered to assess the erosion risk both for the polders in the Khulna and Barishal areas. In reality, when it comes to the risk, other factors are associated with the fact area infrastructures along the river bank and the lateral distance. The more the damage, the more chance of a risk. But it isn't easy to assess within this short time by considering the present data. This analysis provides an indication that is very helpful in the planning process.

CEGIS Study

Based on the assessment of historical migration of the bank lines and the erosion trend of rivers, prediction lines have been translated into the erosion risk assessment for the embankment in the different polders in the Khulna and Barishal areas. The erosion risk is different for the different areas that need detailed information about the infrastructures, settlements and other important features. Like the priority report, erosion risk has also been categorized as High, Medium, and Low. This study considers high risk at a particular location when there is continuous erosion from 1989 to 2015/2020. Medium erosion risk termed lateral shifting of the bankline from 1989 to 2003/2010 means these locations have not shifted in recent years. Low erosion risk is considered where there has been no erosion in the last two decades. Erosion risk maps of the embankment for the Khulna and Barishal regions are provided in **Figures 8.5** and **Figure 8.6**.

However, this risk assessment should consider more parameters like bank materials, bed material, whole river system, etc., rather than only lateral bank erosion. Thus, this limitation should be kept in mind while assessing vulnerability.

The polders in Package-3 under CEIP-I have also been included in this analysis and presented in **Figure 8.5**.

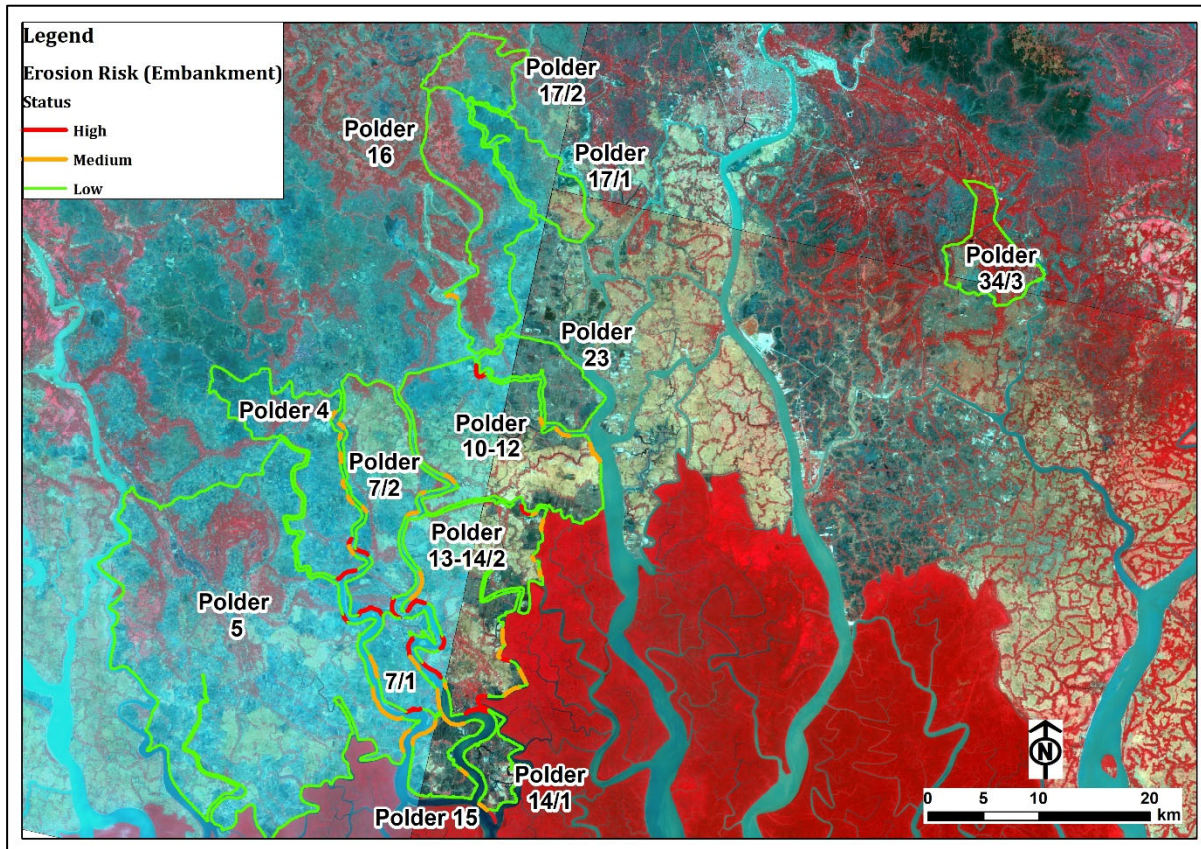


Figure 8.5: Erosion risk of embankment in polders of Khulna area

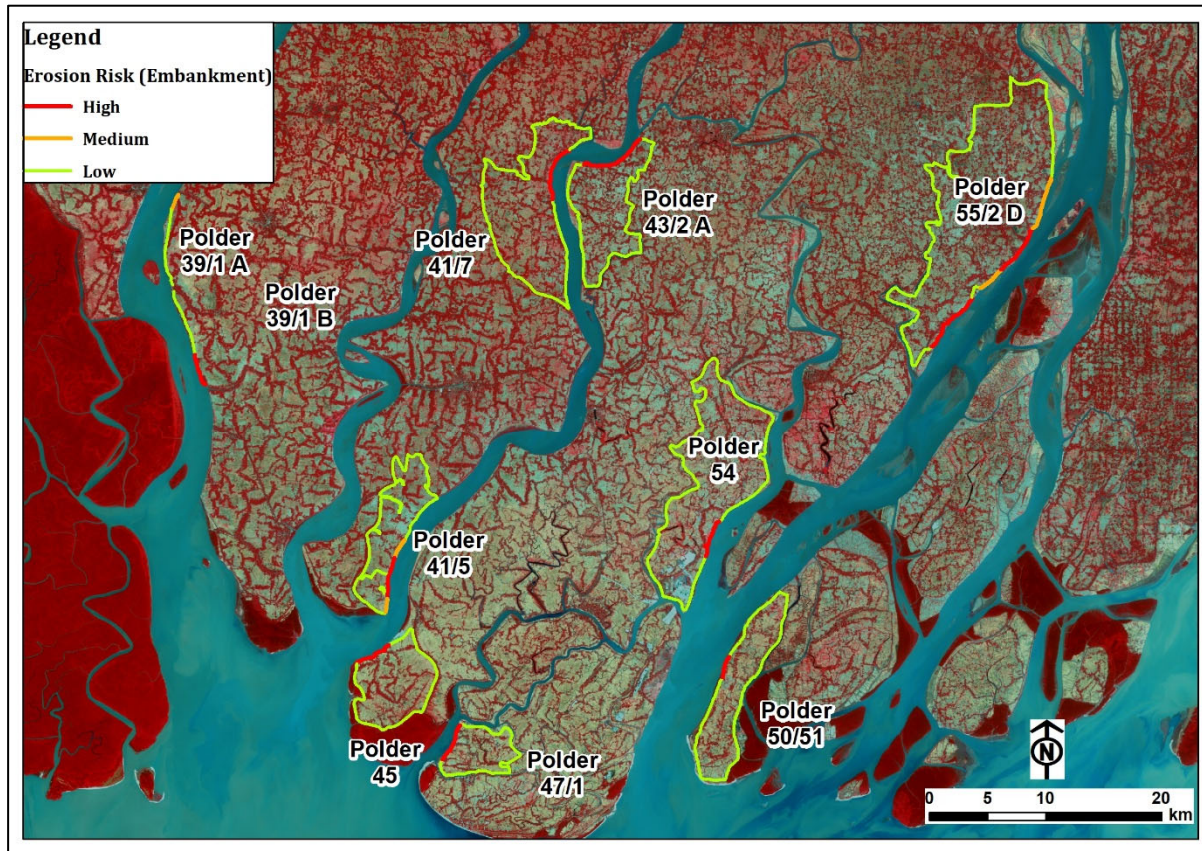


Figure 8.6: Erosion risk of embankment in polders of Khulna area

In the prediction of the small rivers, it was impossible to delineate the bank lines using the image's coarse resolution (30 m * 30 m). However, expert judgment was applied through knowledge of the system and understanding of the study area for assessing the small rivers. It was observed from the prioritization report and CEGIS study that both have similar findings considering the location of the embankment's high, medium, and low erosion risk.

Based on the morphological assessment and the risk assessment, to protect the existing embankment alignments, the estimated length of bank protection that is recommended to mitigate both high-risk and medium-risk bank lines is shown in **Table 8.3** and **Table 8.4**. For design, these lengths will be revised based on the finalized embankment alignment and locations of existing bank protection. The identified bank protection shown in Figure 1.2 has not been considered while determining the values presented in **Table 8.3** and **Table 8.4** because of the uncertainty in the location of the existing bank protection and the condition of the existing bank protection.

Table 8.3: The estimated length of bank protection due to high and medium risk for the Khulna Region

| River Name | ID | Year | The total length of estimated bank protection to protect high-risk bank lines (m) | The total length of estimated bank protection to protect medium-risk bank lines (m) | The total length of estimated bank protection to protect both medium and high-risk bank line (m) |
|------------|-------|------|---|---|--|
| Kapotakshi | Ka-01 | 10 | 2334.88 | 0 | 2334.88 |
| | | 20 | 2487.79 | 0 | 2487.79 |
| | | 30 | 2605.78 | 0 | 2605.78 |
| | Ka-02 | 10 | 1207.64 | 0 | 1207.64 |
| | | 20 | 1233.31 | 0 | 1233.31 |
| | | 30 | 1253.12 | 0 | 1253.12 |
| | Ka-03 | 10 | 1070.79 | 0 | 1070.79 |
| | | 20 | 1193.46 | 0 | 1193.46 |
| | | 30 | 1324.44 | 0 | 1324.44 |
| | Ka-04 | 10 | 3613.37 | 0 | 3613.37 |
| | | 20 | 4377.41 | 0 | 4377.41 |
| | | 30 | 5262.01 | 0 | 5262.01 |
| | Ka-05 | 10 | 1551.58 | 0 | 1551.58 |
| | | 20 | 1679.61 | 0 | 1679.61 |
| | | 30 | 1650.08 | 0 | 1650.08 |
| Kholpetua | Kh-01 | 10 | 0 | 208.37 | 0 |
| | | 20 | 0 | 470.9 | 0 |
| | | 30 | 0 | 784.71 | 0 |
| | Kh-02 | 10 | - | 0 | - |
| | | 20 | - | 0 | - |
| | | 30 | 0 | 605 | 0 |
| | Kh-03 | 10 | - | 0 | - |
| | | 20 | - | 0 | - |
| | | 30 | 735 | 0 | 735 |
| | Kh-04 | 10 | 474.74 | 0 | 474.74 |
| | | 20 | 747.4 | 0 | 747.4 |
| | | 30 | 776.07 | 0 | 776.07 |
| | Kh-05 | 10 | 3966.23 | 0 | 3966.23 |
| | | 20 | 4207.25 | 0 | 4207.25 |
| | | 30 | 4594.41 | 0 | 4594.41 |
| | Kh-06 | 10 | 1444.8 | 0 | 1444.8 |
| | | 20 | 1747.18 | 0 | 1747.18 |

| River Name | ID | Year | The total length of estimated bank protection to protect high-risk bank lines (m) | The total length of estimated bank protection to protect medium-risk bank lines (m) | The total length of estimated bank protection to protect both medium and high-risk bank line (m) |
|------------|-------|------|---|---|--|
| Kh-07 | Kh-07 | 30 | 1680.93 | 0 | 1680.93 |
| | | 10 | 0 | 5003.69 | 5003.69 |
| | | 20 | 0 | 5131.17 | 5131.17 |
| | | 30 | 0 | 5066.97 | 5066.97 |
| | Kh-08 | 10 | 688.96 | 0 | 688.96 |
| | | 20 | 1638.1 | 0 | 1638.1 |
| | | 30 | 1836.84 | 0 | 1836.84 |
| | Kh-09 | 10 | 0 | - | 0 |
| | | 20 | 0 | - | 0 |
| | | 30 | 0 | 1420.44 | 1420.44 |
| Shibsa | Sh-01 | 10 | - | - | - |
| | | 20 | - | - | - |
| | | 30 | 0 | 1757.38 | 1757.38 |

Table 8.4: The estimated length of bank protection due to high and medium risk for the Barishal Region

| River Name | ID | Year | Length | Lateral Distance from the bank line of 2020 | The total length of estimated bank protection to protect high-risk bank lines (m) | The total length of estimated bank protection to protect medium-risk bank lines (m) | The total length of estimated bank protection to protect both medium and high-risk bank line (m) |
|-----------------|-------|------|----------|---|---|---|--|
| Balesware | Ba-01 | 10 | - | - | 0 | 0 | 0 |
| | | 20 | - | - | 0 | 0 | 0 |
| | | 30 | 5142.096 | 120 | 0 | 1460.58 | 1460.58 |
| | Ba-02 | 10 | 8526.605 | 90 | 2852.92 | 0 | 2852.92 |
| | | 20 | 8660.514 | 150 | 2807.92 | 0 | 2807.92 |
| | | 30 | 8932.562 | 220 | 2684.18 | 0 | 2684.18 |
| Burishwar-Payra | Bu-01 | 10 | 2892.457 | 60 | 1632.68 | 0 | 1632.68 |
| | | 20 | 2391.916 | 120 | 1715.4 | 0 | 1715.4 |
| | | 30 | 2114.805 | 180 | 1754.01 | 0 | 1754.01 |
| | Bu-02 | 10 | 5556.011 | 70 | 3021 | 1169 | 4190 |
| | | 20 | 5150.898 | 160 | 3925 | 1169 | 5094 |
| | | 30 | 4422.383 | 280 | 4300.42 | 1169 | 5469.42 |
| | Bu-03 | 10 | 1965.1 | 70 | 1335.31 | 0 | 1335.31 |
| | | 20 | 1910.629 | 180 | 1574.26 | 0 | 1574.26 |
| | | 30 | 1763.984 | 250 | 1828.02 | 0 | 1828.02 |
| Tentulia | Te-01 | 10 | 22375.86 | 260 | 5931.642 | 5888.598 | 11820.24 |
| | | 20 | 21303.64 | 470 | 11580.362 | 5888.598 | 17468.96 |
| | | 30 | 21947.76 | 670 | 12525.122 | 5888.598 | 18413.72 |
| | Te-02 | 10 | 11559.07 | 110 | 0 | 2125.19 | 2125.19 |
| | | 20 | 11573.08 | 230 | 0 | 4542.91 | 4542.91 |
| | | 30 | 11611.69 | 330 | 0 | 6251.78 | 6251.78 |

9. Long Term Monitoring (LTM)

Erosion-accretion for different periods was observed for the rivers in the Khulna and Barishal areas during the CEIP-I study, termed as Long Term Monitoring (LTM) data. CEGIS also observed the historical erosion-accretion in this study using time-series satellite images. Data were extracted for the whole river. But quantity differences in the data between LTM and CEGIS were observed and detailed in the following paragraphs.

9.1 LTM Observations

In Long Term Monitoring (LTM) analysis, riverbank lines were created by finding an optimal threshold of the MNDWI to differentiate between water and land (Hanqiu, 2006). Otsu's method was used to find the optimal threshold in the distribution of the MNDWI values. The threshold can contain errors when not enough water pixels are present in the image. A canny edge filter extended the Otsu method to overcome this problem (Donchyts et al., 2016). The canny edge filter detects sharp changes in the MNDWI values to reduce the number of input pixels to those located near the water and land boundaries. Additionally, the edges were buffered to half the pixel size to include small river channels. Long-term erosion-accretion data for 2010-2015 and 2015-2020 for the rivers in the Khulna and Barishal areas are placed in Tables 9.1 and 9.2.

9.2 Observations by CEGIS

CEGIS developed a method of defining the shoreline using satellite images to mitigate the influence of tidal fluctuation (2009). The aerial and satellite images were geo-referenced then river bank lines were delineated through image interpretation by ArcGIS tools. Although dry season satellite images were used in this study, bank lines were delineated considering the wet season extent of the rivers. Furthermore, bank lines were used to observe the maximum shifting of the river to both banks and for further analysis. The bank lines of several years were superimposed in ArcGIS, and then erosion-accretion was calculated using the 'erase' command.

CEGIS delineated bank lines for the Kholpetua, Kapotakshi, and Shibsaa rivers in the Khulna area using dry season Landsat satellite images. In contrast, rivers in the Barishal area are Burishwar-Payra, Andharmanick, Haider-Bharani, Lohalia-Rabnabad, Baleshwar, Bishkhali, and Tentulia Rivers. CEGIS delineated bank lines using their techniques and expert judgment as they have long-term experiences doing the same for the rivers in Bangladesh (outlined in Section 2.4. Historical changes (2020-2015 and 2015-2020) of the erosion-accretion for the rivers observed by CEGIS are provided in Tables 9.1 and 9.2. Erosion and accretion polygons having < 50 m of lateral distance have been neglected to refine accuracy considering the image resolution.

9.3 Comparison between the results

These two results from LTM and CEGIS observation are compared in tabular form and presented in the following tables.

Table 9.1: Comparison of erosion-accretion between LTM & CEGIS (Khulna area)

| River | | Erosion (Ha) | Accretion (Ha) | Erosion (Ha) | Accretion (Ha) |
|------------------|-----|--------------|----------------|--------------|----------------|
| | | 2010-2015 | 2010-2015 | 2015-2020 | 2015-2020 |
| Ichamati-Kalindi | LTM | 9 | 2 | 54 | 27 |

| River | | Erosion (Ha) | Accretion (Ha) | Erosion (Ha) | Accretion (Ha) |
|------------|-------|--------------|----------------|--------------|----------------|
| | | 2010-2015 | 2010-2015 | 2015-2020 | 2015-2020 |
| | | CEGIS | 17 | - | - |
| Khulpetua | LTM | 40 | 30 | 88 | 72 |
| | CEGIS | 61 | 156 | 10 | - |
| Kapotakshi | LTM | 138 | 130 | 126 | 184 |
| | CEGIS | 45 | 361 | 69 | 139 |
| Shibsa | LTM | 201 | 11 | 116 | 16 |
| | CEGIS | 12 | 3 | 33 | 4 |

Table 9.2: Comparison of erosion-accretion between LTM & CEGIS (Barishal area)

| River | | Erosion (Ha) | Accretion (Ha) | Erosion (Ha) | Accretion (Ha) |
|-----------------|-------|--------------|----------------|--------------|----------------|
| | | 2010-2015 | 2010-2015 | 2015-2020 | 2015-2020 |
| Burishwar-Payra | LTM | 447 | 142 | 418 | 244 |
| | CEGIS | 120 | 87 | 180 | 61 |
| Tentulia | LTM | 1159 | 381 | 994 | 640 |
| | CEGIS | 349 | 299 | 419 | 193 |
| Balesware | LTM | 368 | 200 | 398 | 112 |
| | CEGIS | 174 | 382 | 162 | 173 |

Tables 9.1 and 9.2 show that erosion and accretion areas for the rivers of the Khulna-Satkhira and Barishal region differ from LTM to CEGIS. In most cases, erosion and accretion areas found in LTM are greater than CEGIS observations. The main input for the calculation of erosion-accretion is the bank line. The study observed that the bank lines were delineated in LTM based on the automated software that could not pick the water line correctly. This has resulted in a difference in the total quantity. An example of the difference in bank line delineation for the Ichamati-Kalindi River is referred to in **Figure 9.1**.



Google Earth Image (2016)



Google Earth Image (2021)

Figure 9.1: Reason for the difference in erosion area between LTM and CEGIS (Ichamati-Kalindi River)

Figure 9.1 represents a bend of the Ichamati-Kalindi River. It indicates that there is no significant change in the bend location. But according to LTM analysis, erosion has occurred in the bend of about 9.4 Ha. In CEGIS analysis, this location has not considered erosion or accretion. Similarly, there are several locations where this type of situation was observed in all the rivers. Annex-A and Annex-B provide the detailed erosion-accretion difference between LTM and CEGIS with maps covering the whole rivers.

9.4 CEGIS proposed LTM

In the following para outline of the LTM suggested by CEGIS is presented. During the analysis, CEGIS found some drawbacks due to the shortage and limited available spatial data. There is also a shortage of good quality and fine temporal data resolution. So most cases, the derived results are indicative only. So for effective and sustainable management of the water resources, good predictability and quantitative results will be required. For this, we need to have a long-term monitoring system. Three themes:

System based

CEGIS performed the system-based analysis, which would be adequate for understanding the interaction between the different systems such as SW, SC, and ME. Understanding these systems will help recognize the polders' long-term morphological processes and enhance predictability. Understanding of the system was based on short period data with limited accuracy. Presently human interventions create waterlogging problems in the SW region and which causes severe river bed sedimentation. Downstream, these rivers are degrading, probably due to the tidal amplification. Long-term monitoring data should have good quality and fine resolution, increasing predictability.

CEGIS studies (Sarker et al., 2013, Akter et al., 2016) suggest that the distributaries in the SC region are diverting their courses toward the southwest direction and carrying a higher quantity of fresh water during the dry season. It has a great significance for the long-term planning of the SC. Long-term monitoring data such as time-series satellite images and discharge and salinity will be required to enhance the understanding of the process.

Process-based

Sedimentation processes are very important in the SW region. Polders in the SW region caused sedimentation on the riverbed and the tidal plains, a crucial issue for managing the water resources. There are two types of sedimentation processes. One is sedimentation during monsoon, and the second is sedimentation during the dry season. To date, knowledge is limited on the mention. Researching sedimentation processes is recommended to understand the processes and develop techniques for controlling sedimentation.

Polder based

While carrying out the study to assess the vulnerability of the polders, the study team of CEGIS faced the problem of having good quality (in terms of spatial and temporal data) data. Each polders might have different issues to address and subsequently measures would also be different. Long-term monitoring is required to improve the situation.

10. Conclusions & Recommendations

10.1 Conclusion

Detailed morphological analysis of the Study Rivers in the Khulna-Barisal region shows the geomorphological characteristics of the study area. The rivers in the Khulna and Satkhira regions fall under the SW region, and the rivers in the Barisal region fall under the SC region. The rivers in the Khulna region are susceptible to more sedimentation than those in the Barisal region. The Gorai is the primary flow source for the SW region, and its flow has declined significantly in the past years. The rivers in the SC region are getting the sufficient upstream flow and are in the active delta building process. The rivers in this region are shifting towards the South-West direction from upstream to downstream. Due to sufficient upstream flow, the rivers in the Barisal region are less susceptible to sedimentation, and the length averaged width of these rivers are greater than those in the Khulna-Satkhira region. Both regions' rivers' downstream portion is wider than the upstream reaches due to the tidal effect. The prediction lines (10, 20 & 30 years) have been drawn following the bends movement and its extent. For bend migration, less than 100 meters, prediction lines for 10 & 20 years were excluded for high uncertainty. Thus, while implementing the rehabilitation of the polders in this study area, it has been suggested to consider the morphological aspects of this region for proper utilization of the resources and reducing the possible future hazard.

10.2 Recommendations

Long-term monitoring should be performed to monitor the future projection of the bank lines and better understand the river system of the SW, SC, and Meghna estuary region.

Access to high-resolution satellite images would help delineate the bank lines more accurately, providing better results.

Annex-A

**Comparison between CEGIS and Long Term Monitoring (LTM) Data
(Khulna Region)**

DRAFT

Comparison between CEGIS and Long Term Monitoring (LTM) Data (2010-2015)
(Khulna Region)

DRAFT

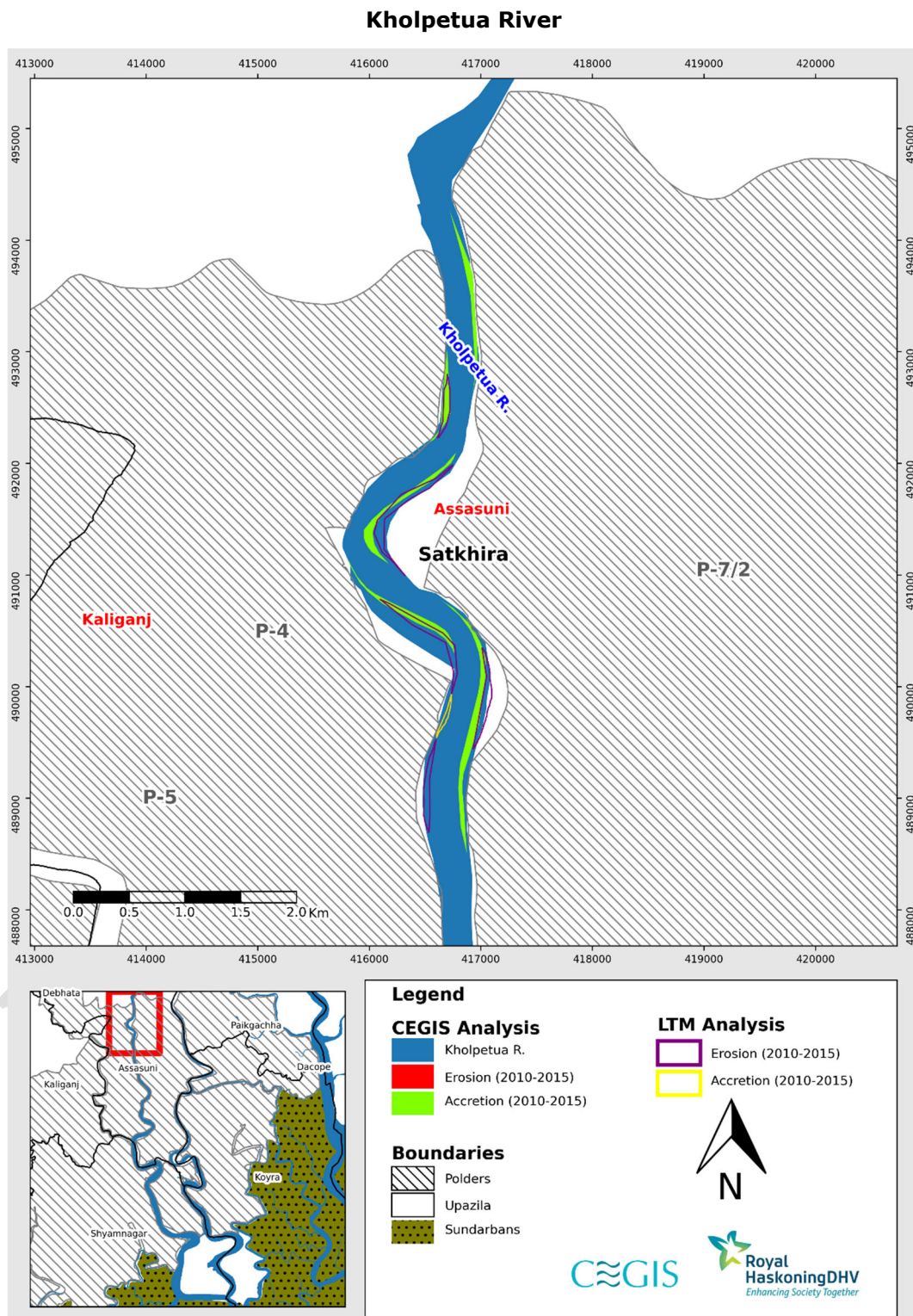


Figure 1.1: Difference between erosion and accretion of LTM and CEGIS in Kholpetua River (Reach-1) (2010-2015)

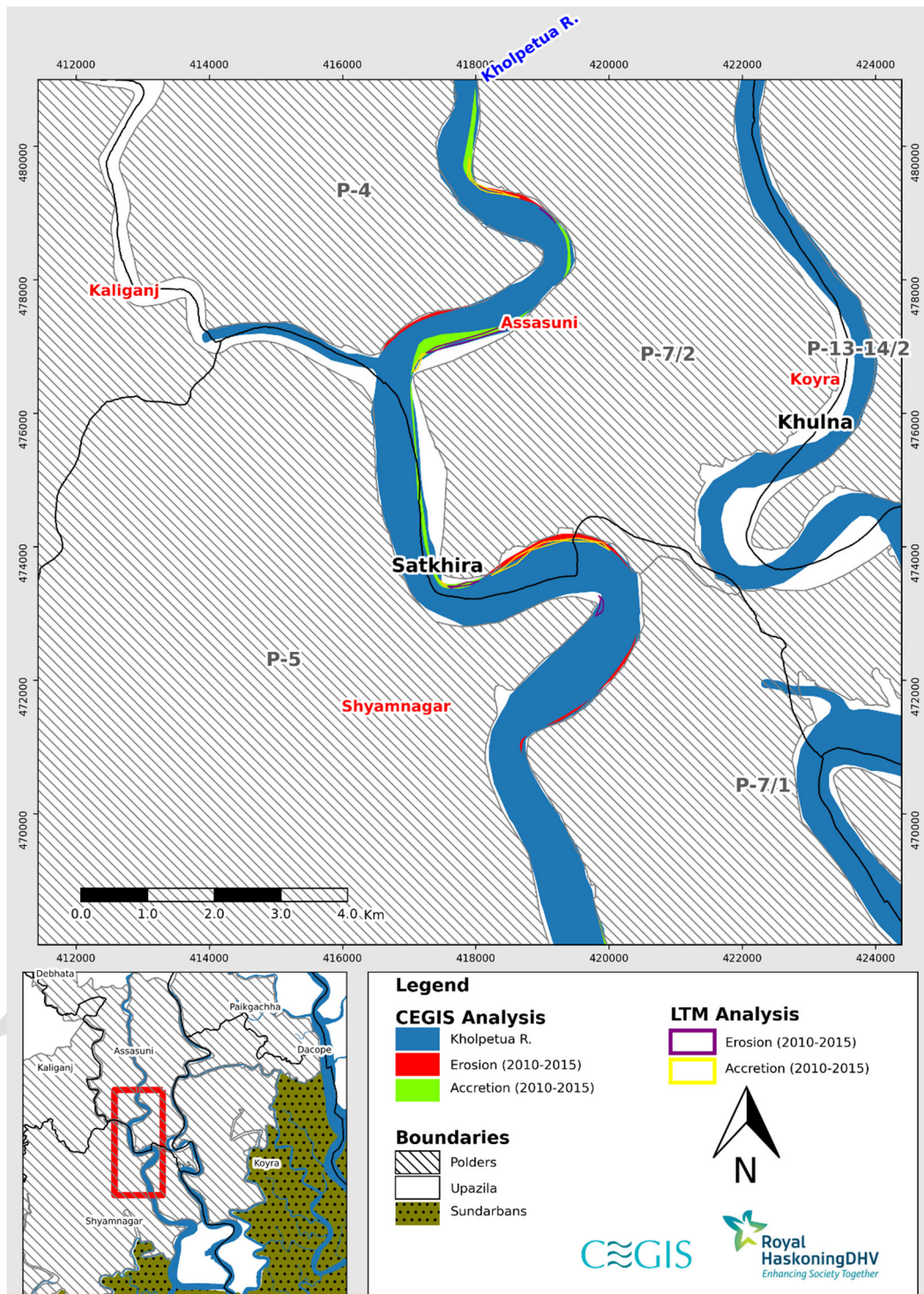


Figure 1.2: Difference between erosion and accretion of LTM and CEGIS in Kholpetua River (Reach-2) (2010-2015)

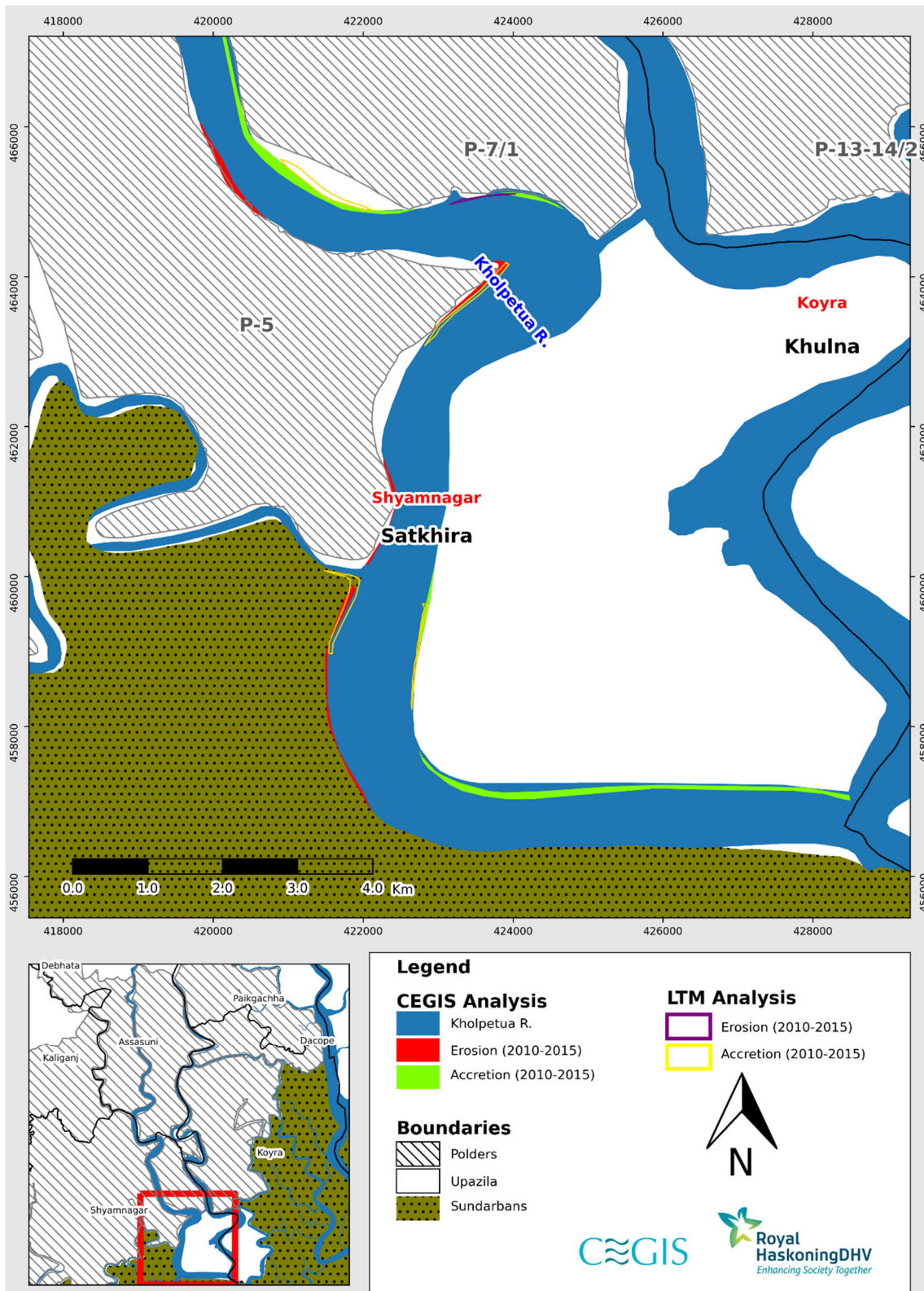


Figure 1.3: Difference between erosion and accretion of LTM and CEGIS in Kholpetua River (Reach-3) (2010-2015)

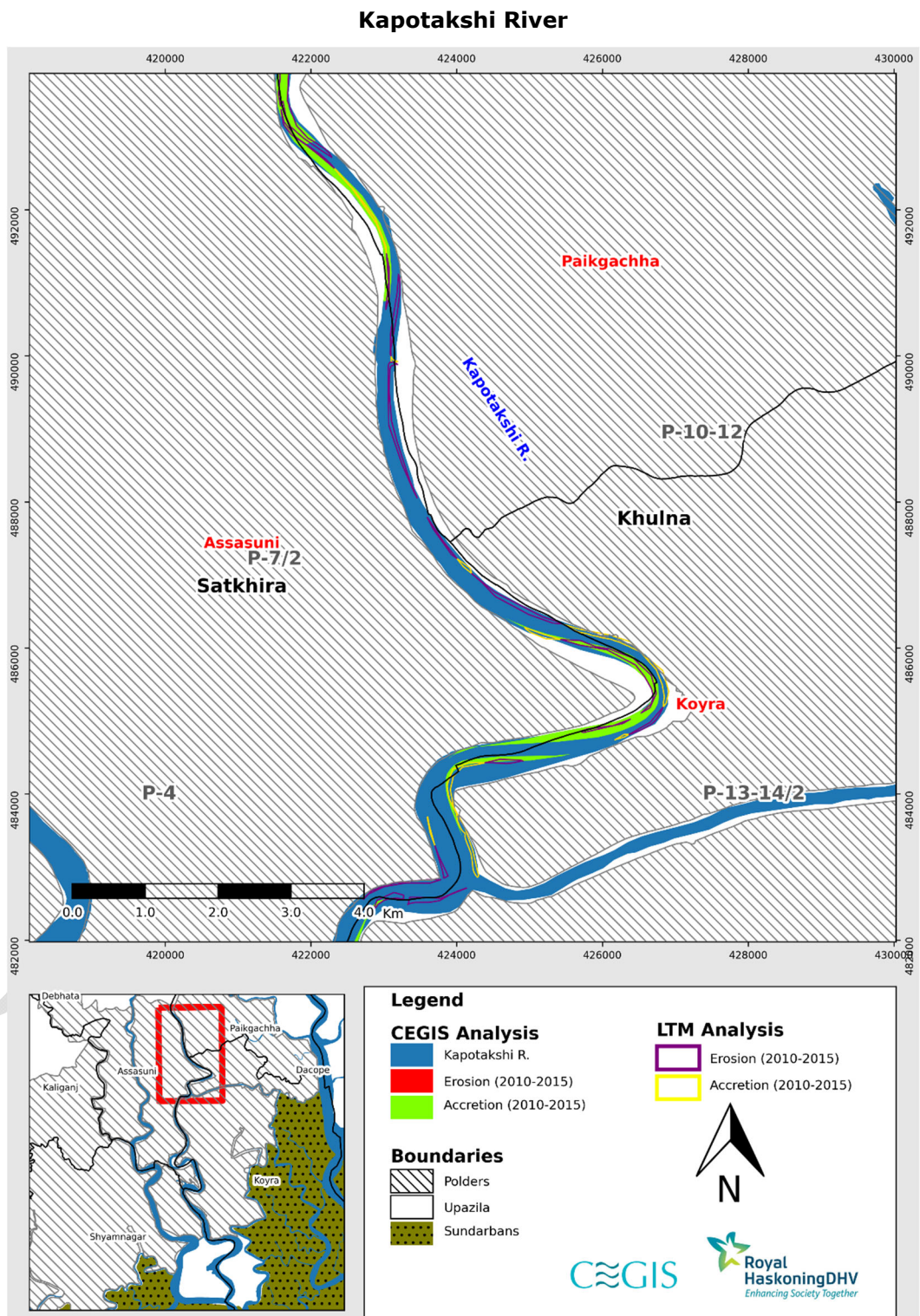


Figure 1.4: Difference between erosion and accretion of LTM and CEGIS in Kapotakshi River (Reach-1) (2010-2015)

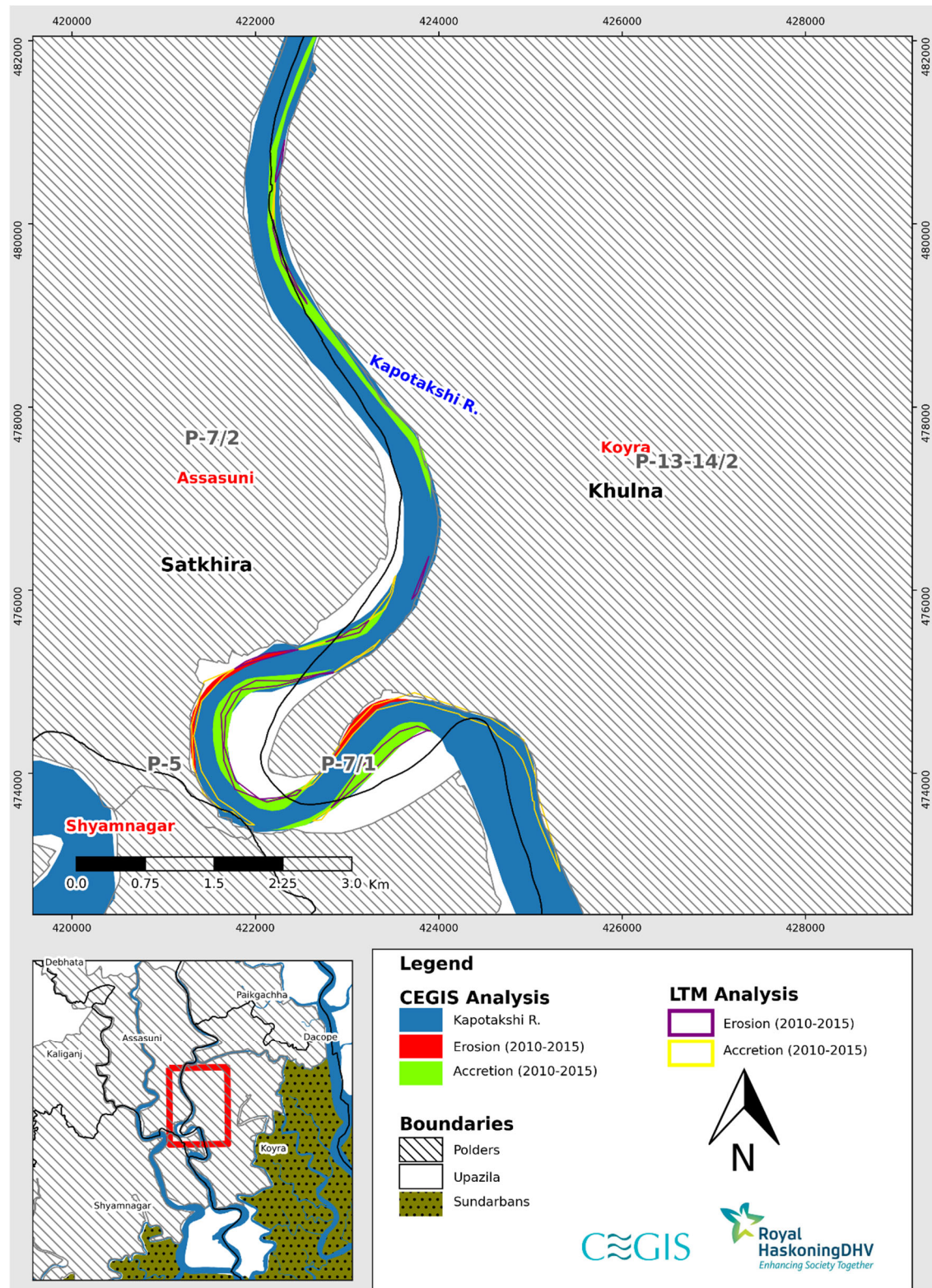


Figure 1.5: Difference between erosion and accretion of LTM and CEGIS in Kapotakshi River (Reach-2) (2010-2015)

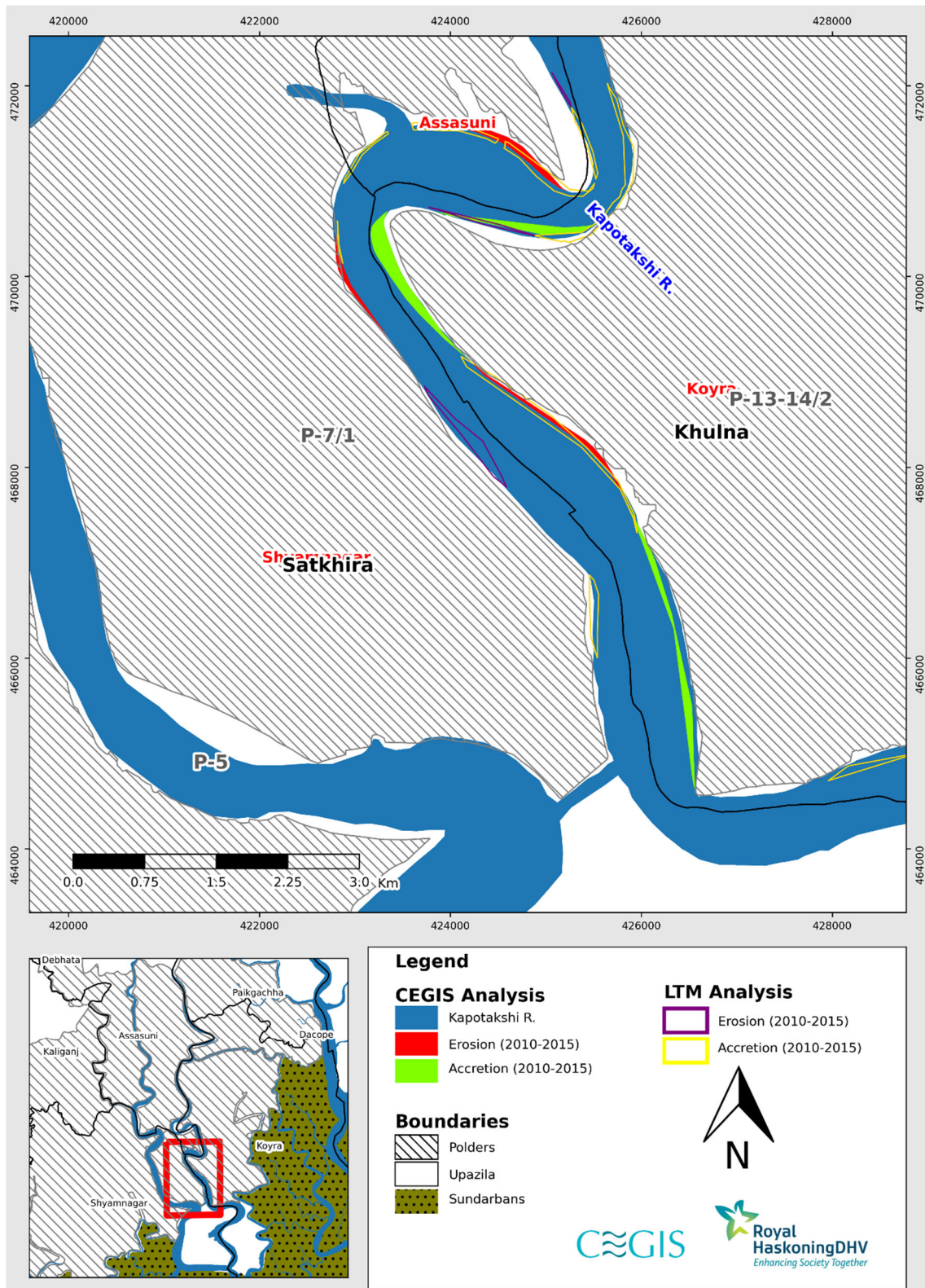


Figure 1.6: Difference between erosion and accretion of LTM and CEGIS in Kapotakshi River (Reach-3) (2010-2015)

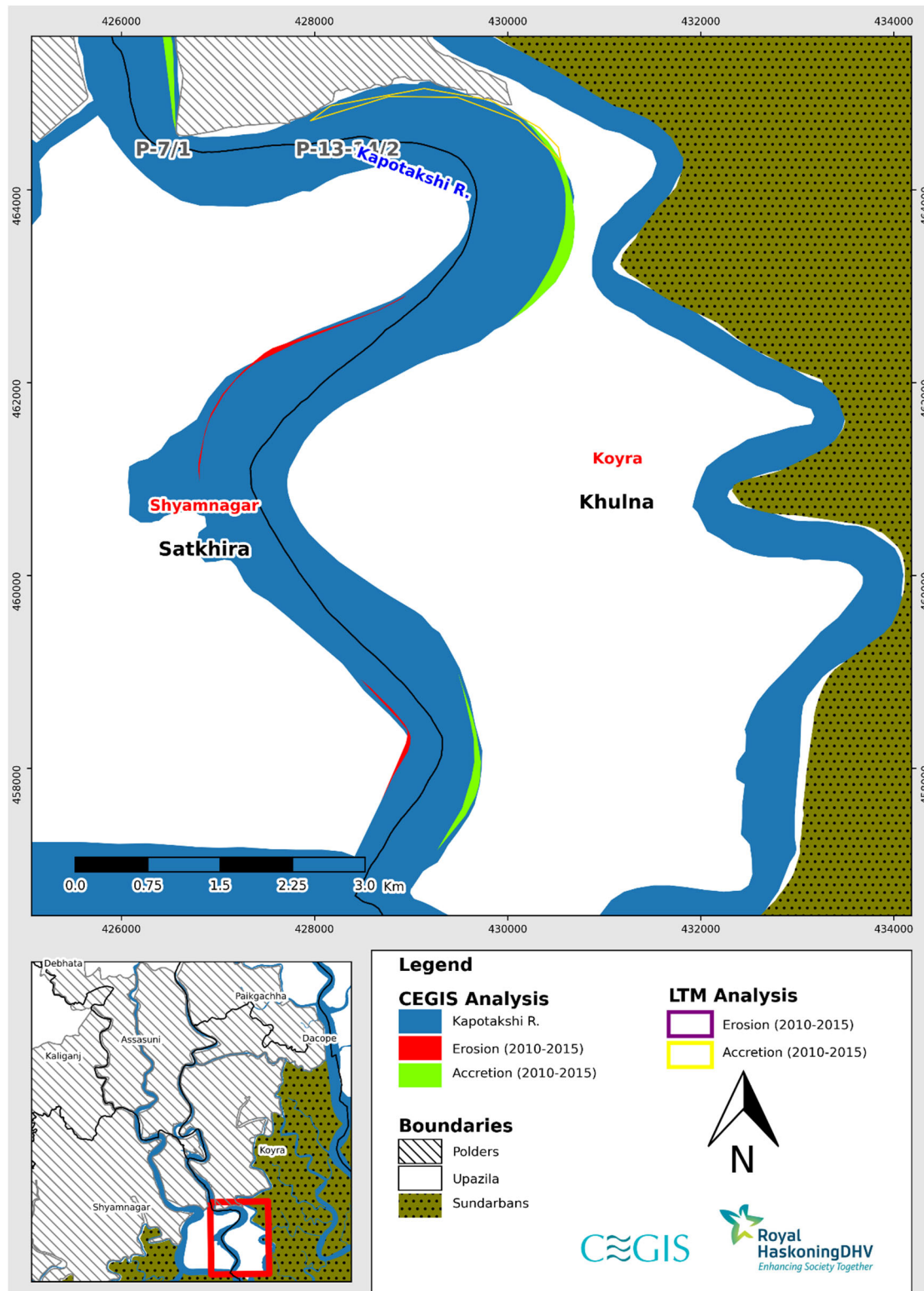


Figure 1.7: Difference between erosion and accretion of LTM and CEGIS in Kapotakshi River (Reach-4) (2010-2015)

Shibsa River

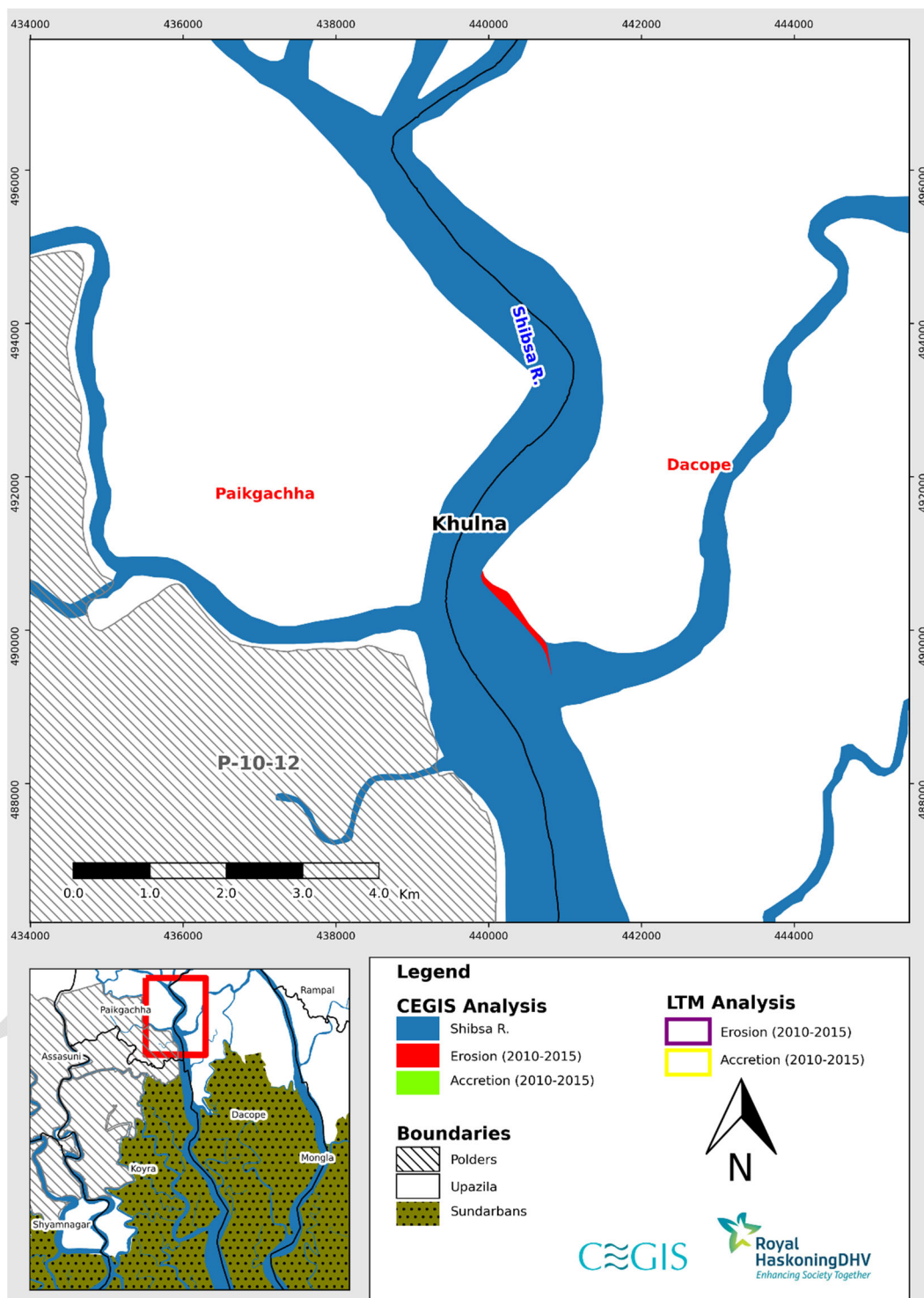


Figure 1.8: Difference between erosion and accretion of LTM and CEGIS in Shabsa River (Reach-1) (2010-2015)

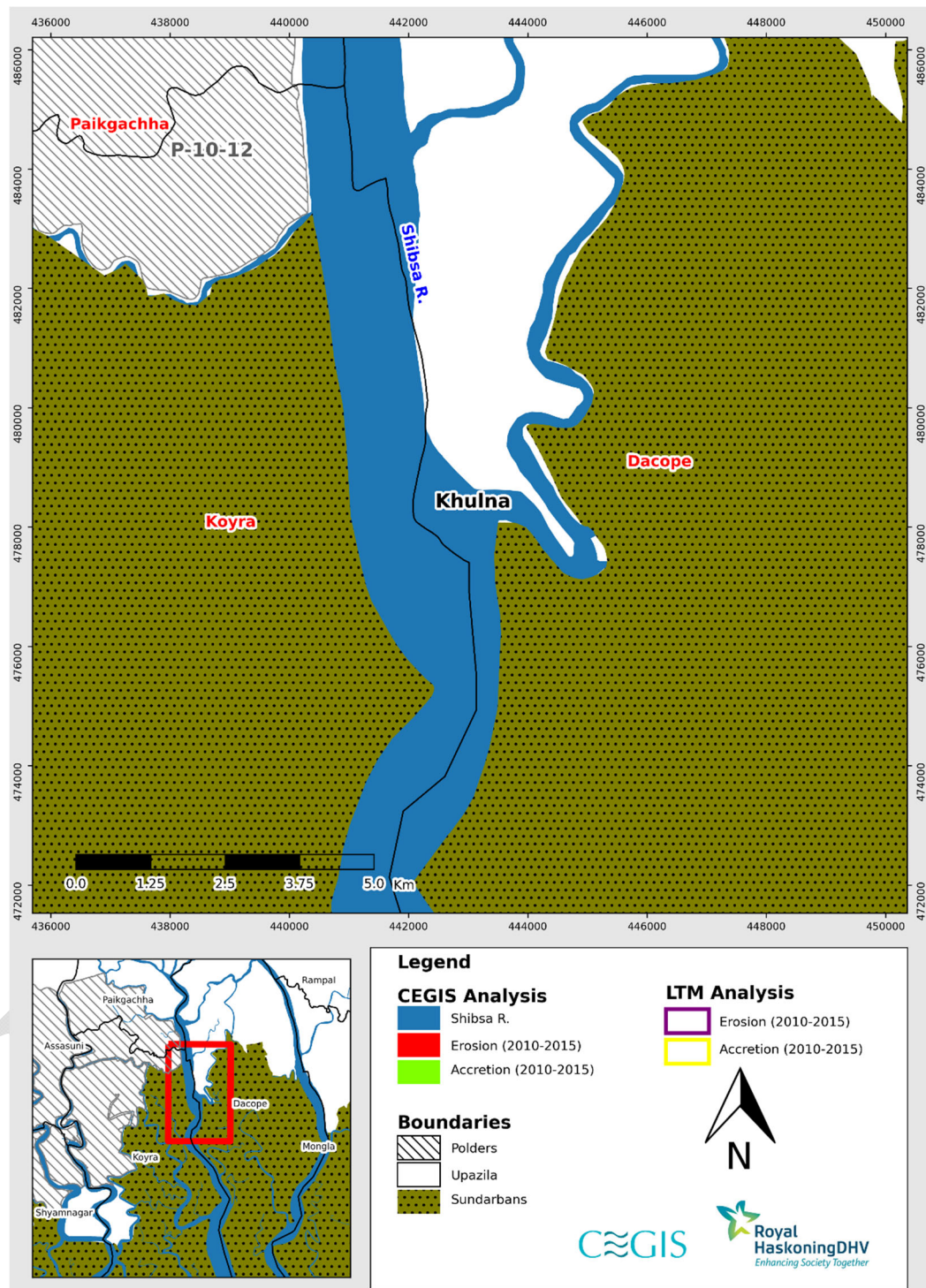


Figure 1.9: Difference between erosion and accretion of LTM and CEGIS in Shibsa River (Reach-2) (2010-2015)

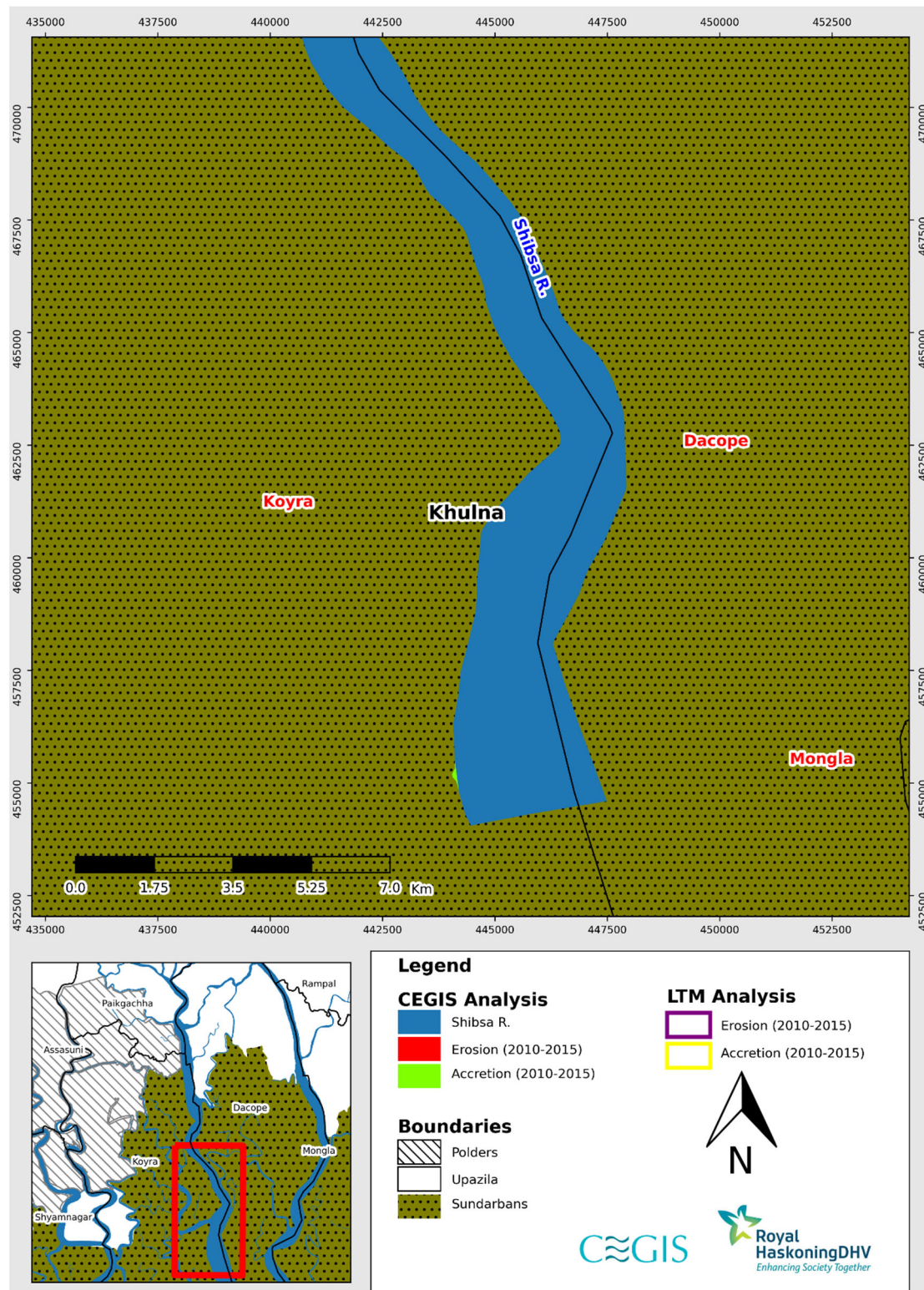


Figure 1.10: Difference between erosion and accretion of LTM and CEGIS in Shibsa River (Reach-3) (2010-2015)

Comparison between CEGIS and Long Term Monitoring (LTM) Data (2015-2020)
(Khulna Region)

DRAFT

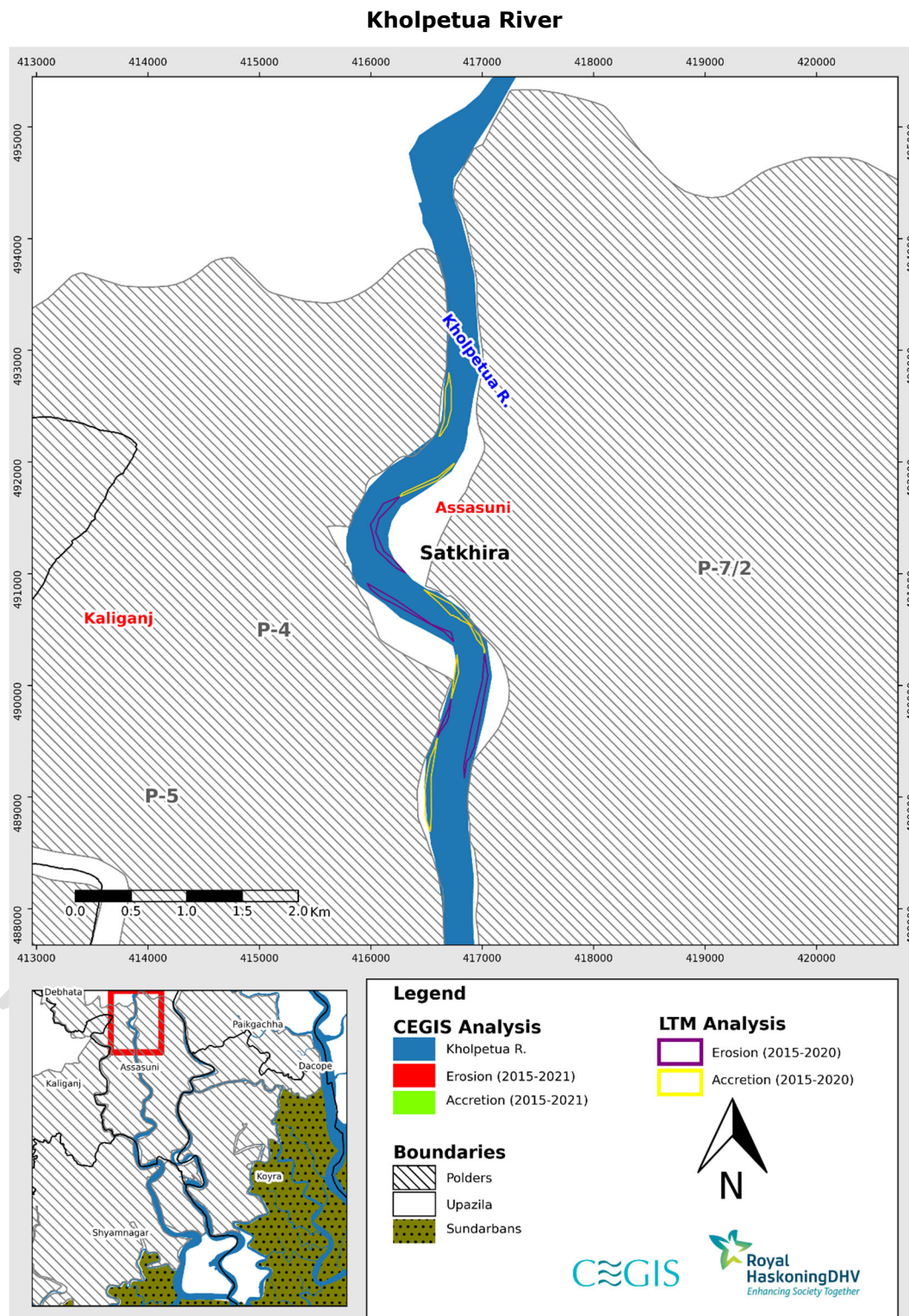


Figure 1.11: Difference between erosion and accretion of LTM and CEGIS in Kholpetua River (Reach-1) (2015-2020)

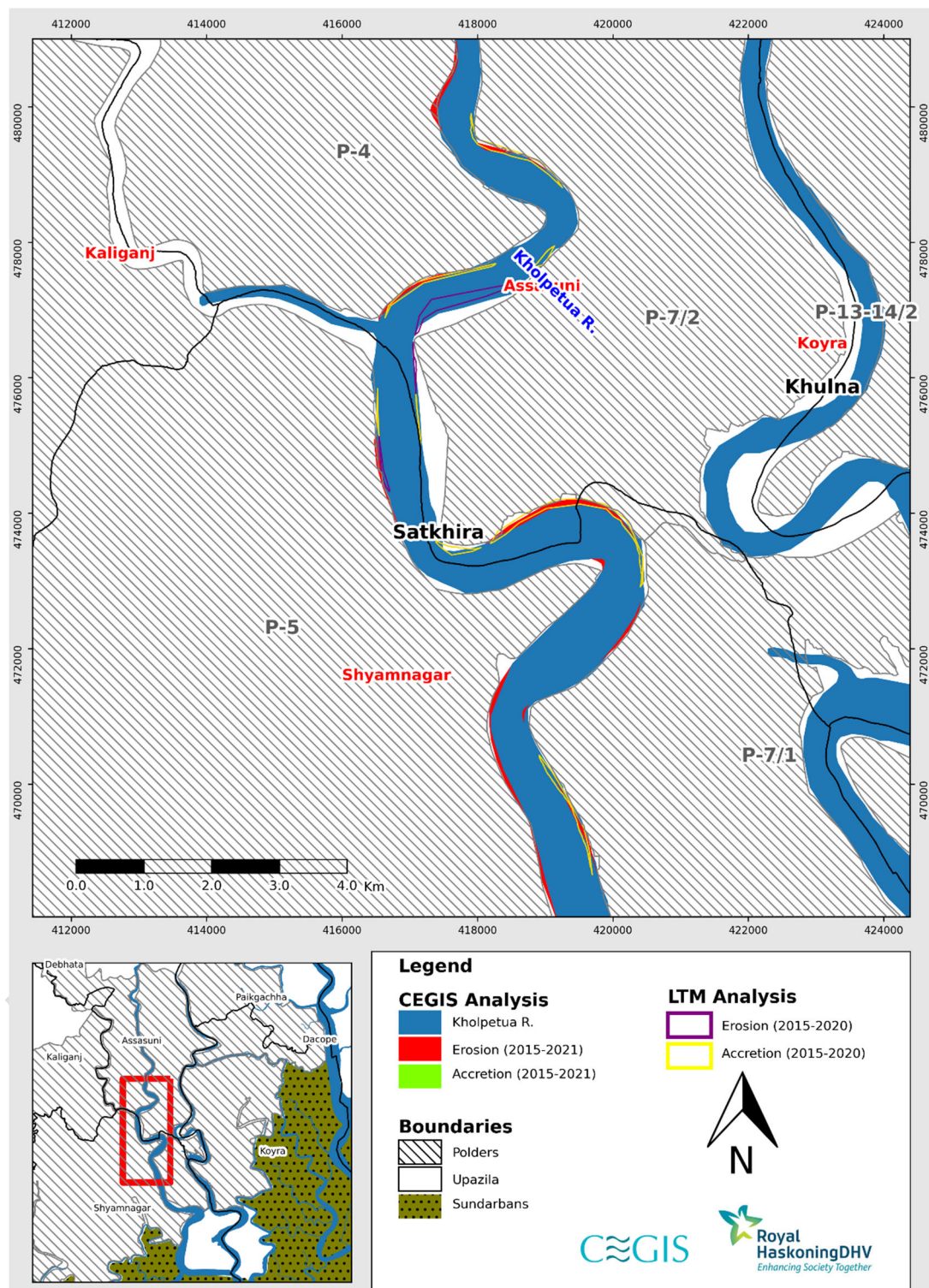


Figure 1.12: Difference between erosion and accretion of LTM and CEGIS in Kholpetua River (Reach-2) (2015-2020)

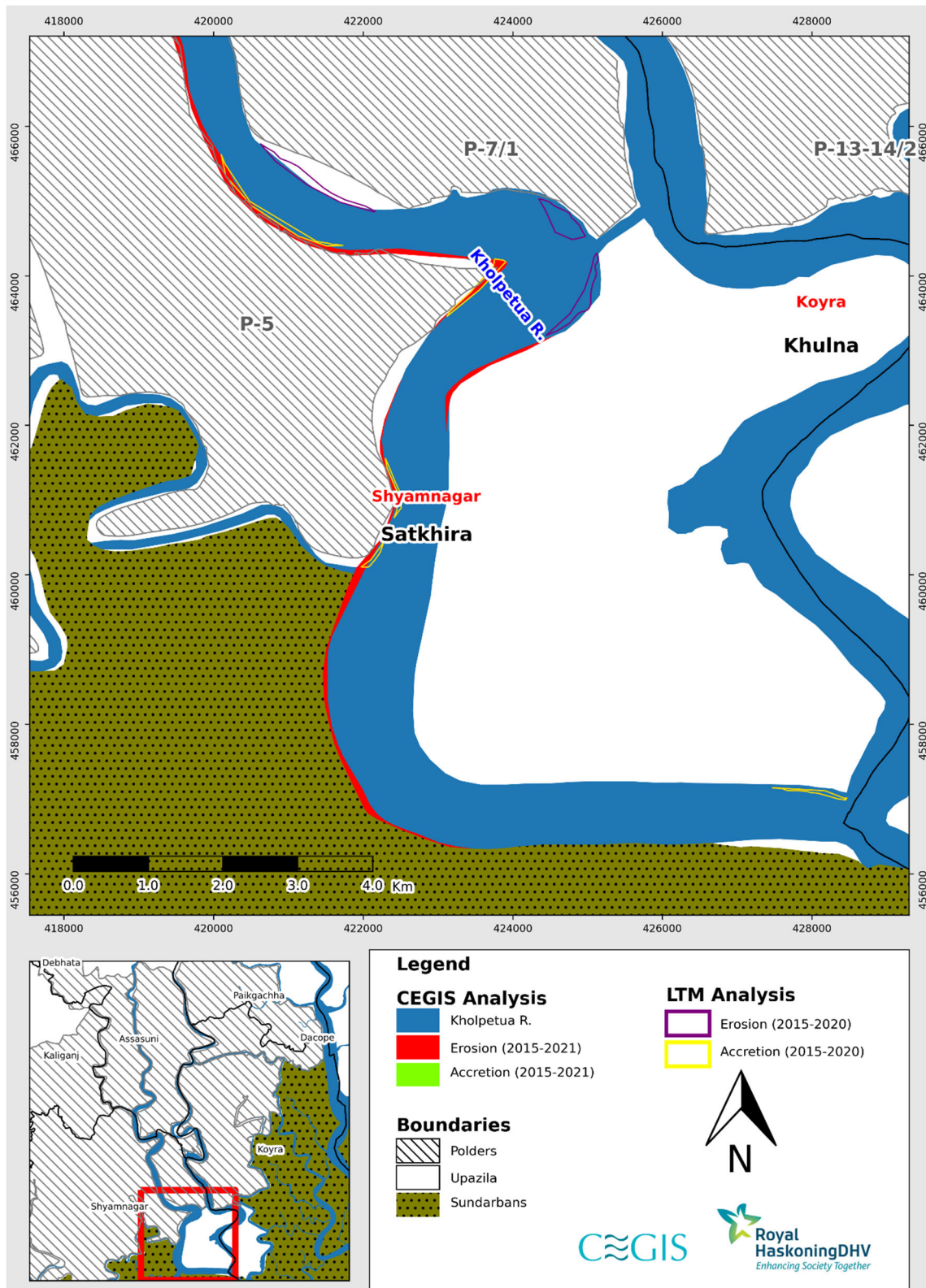


Figure 1.13: Difference between erosion and accretion of LTM and CEGIS in Kholpetua River (Reach-3) (2015-2020)

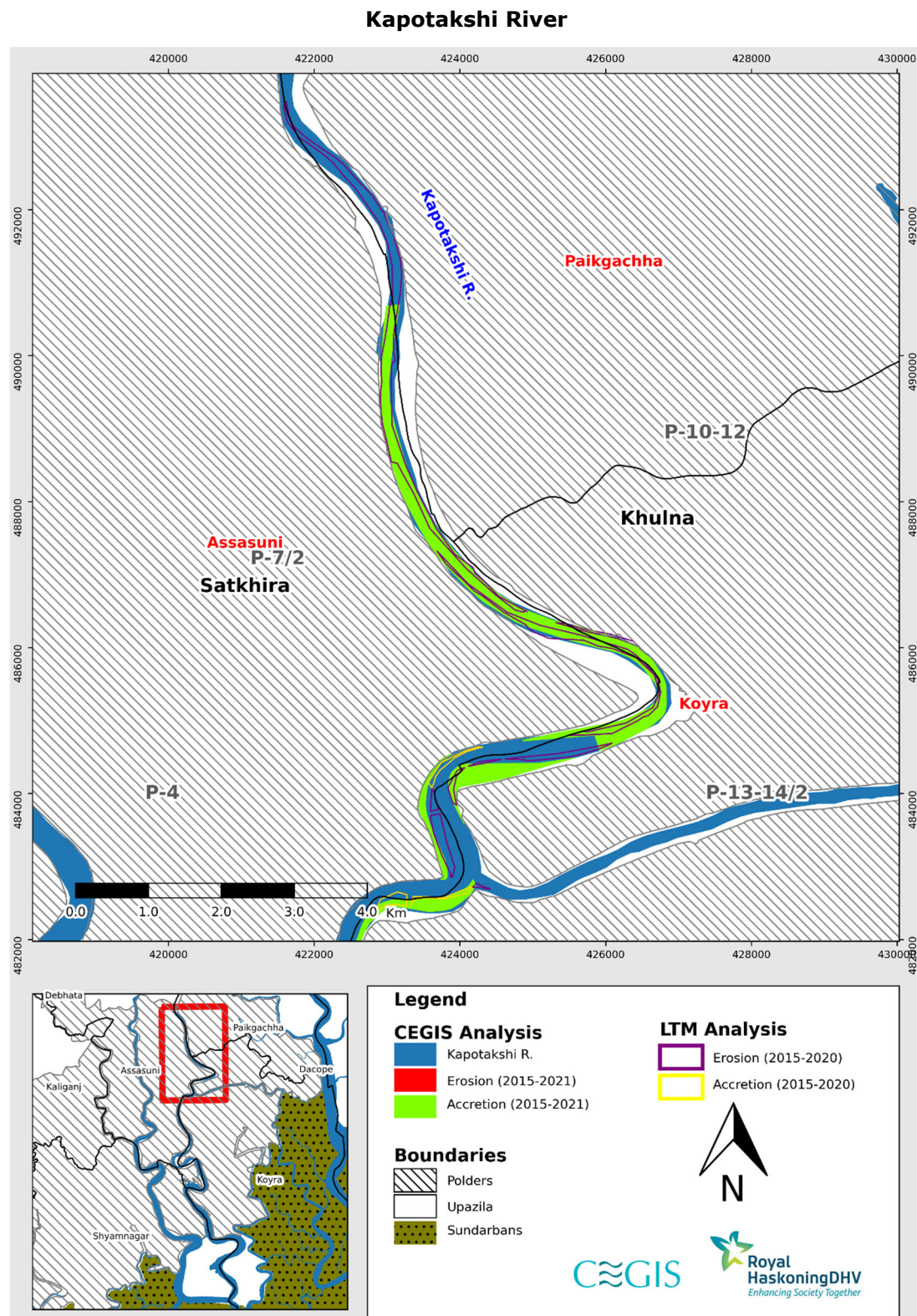


Figure 1.14: Difference between erosion and accretion of LTM and CEGIS in Kapotakshi River (Reach-1) (2015-2020)

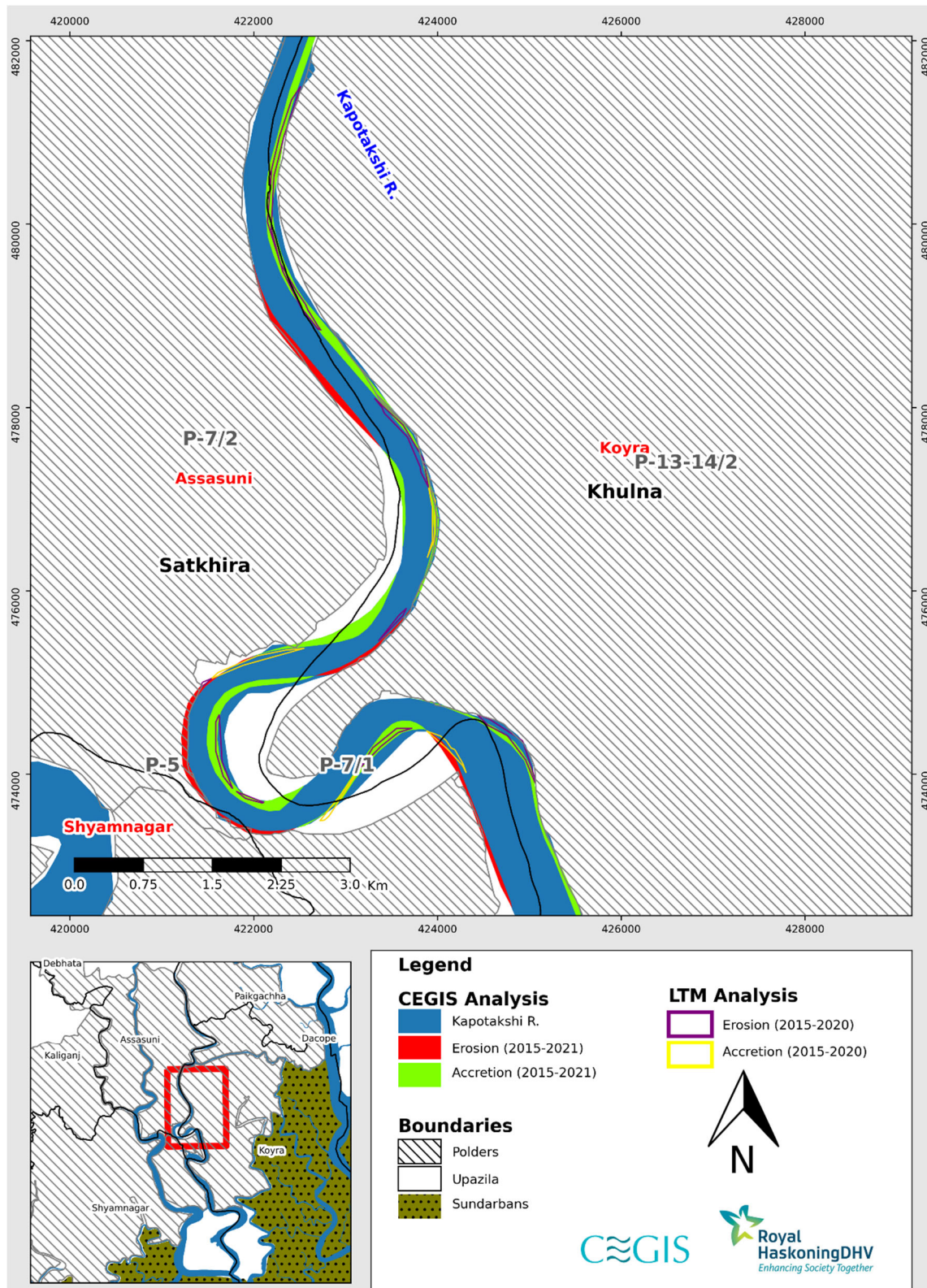


Figure 1.15: Difference between erosion and accretion of LTM and CEGIS in Kapotakshi River (Reach-2) (2015-2020)

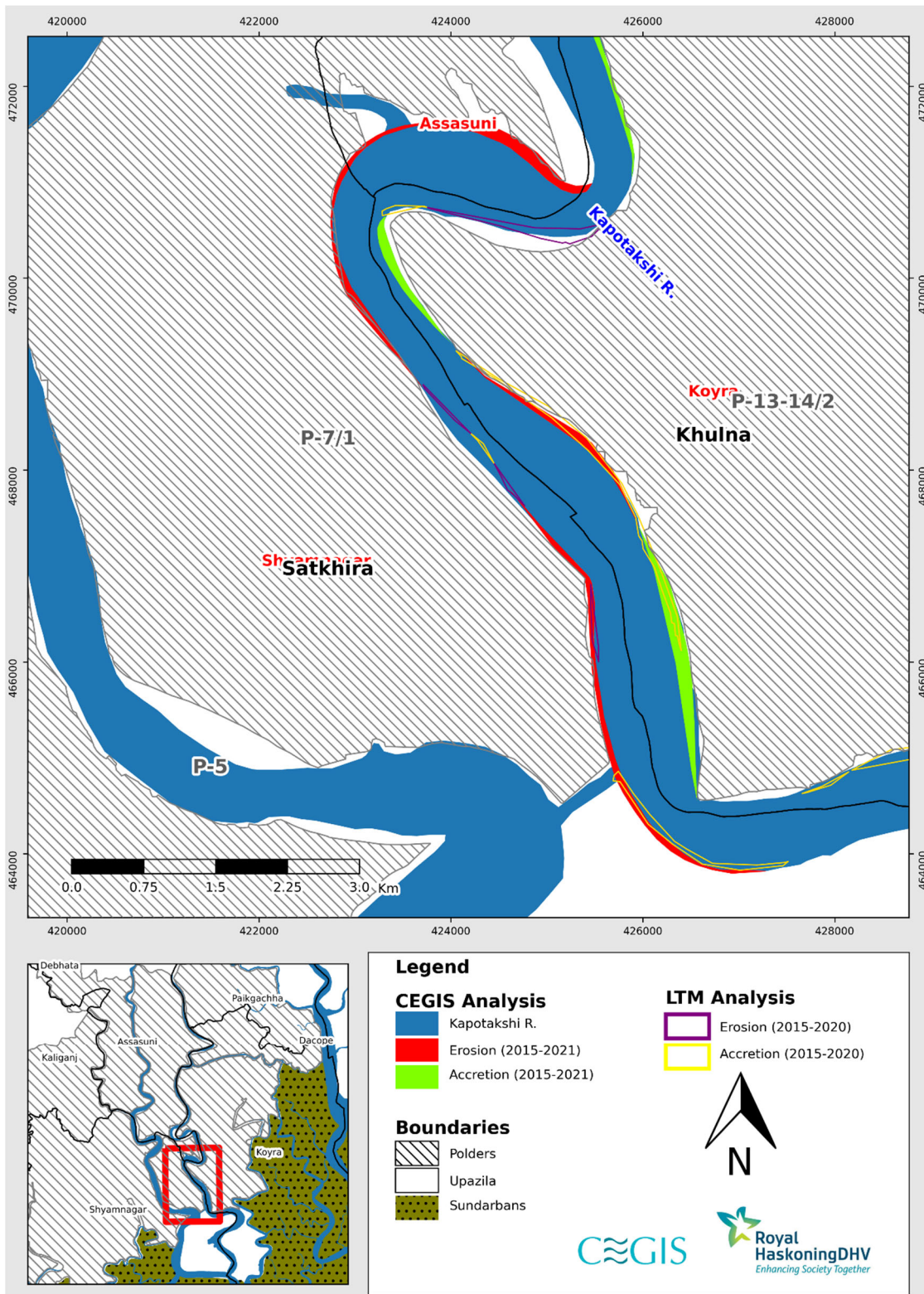


Figure 1.16: Difference between erosion and accretion of LTM and CEGIS in Kapotakshi River (Reach-3) (2015-2020)

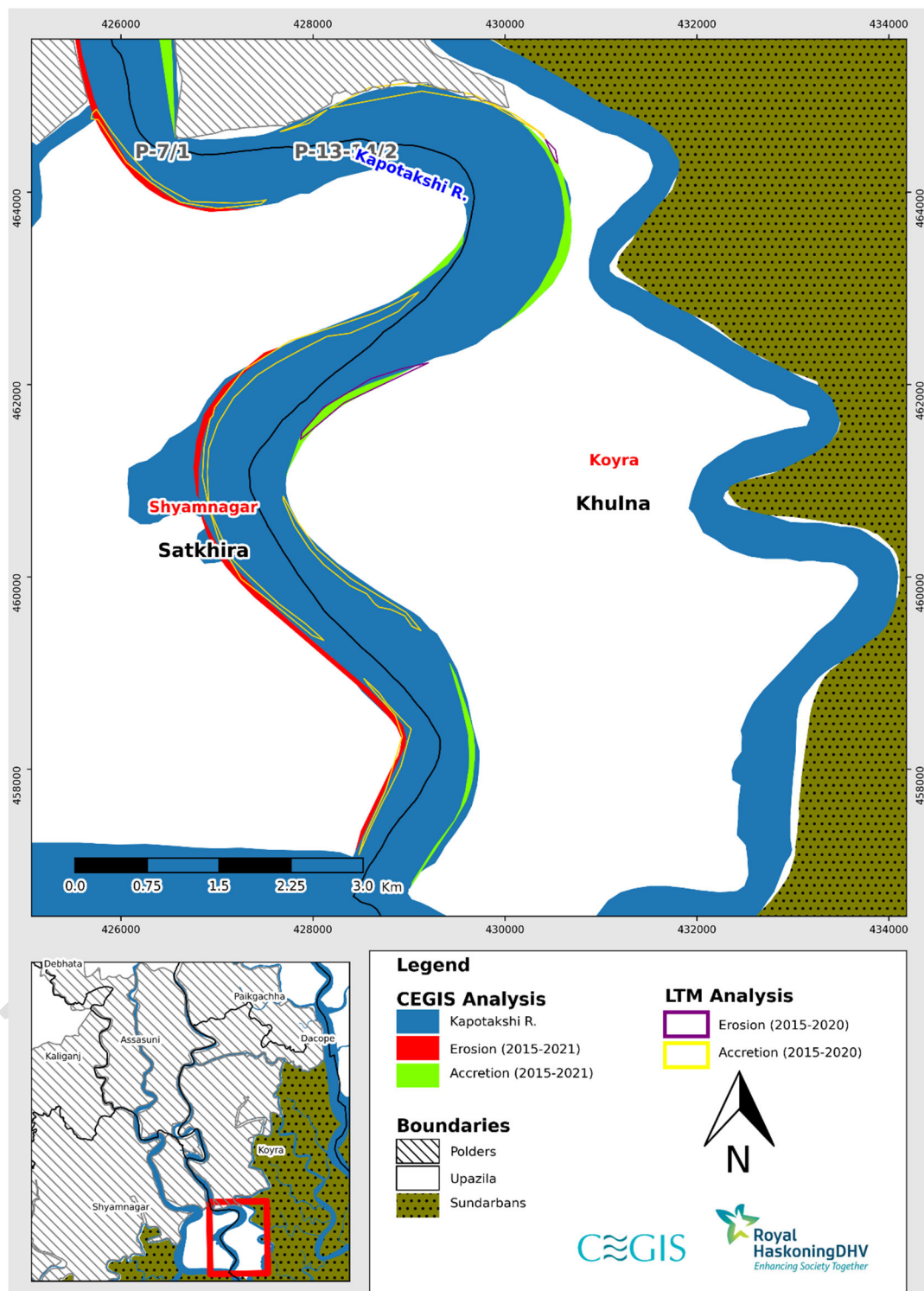


Figure 1.17: Difference between erosion and accretion of LTM and CEGIS in Kapotakshi River (Reach-4) (2015-2020)

Shibsa River

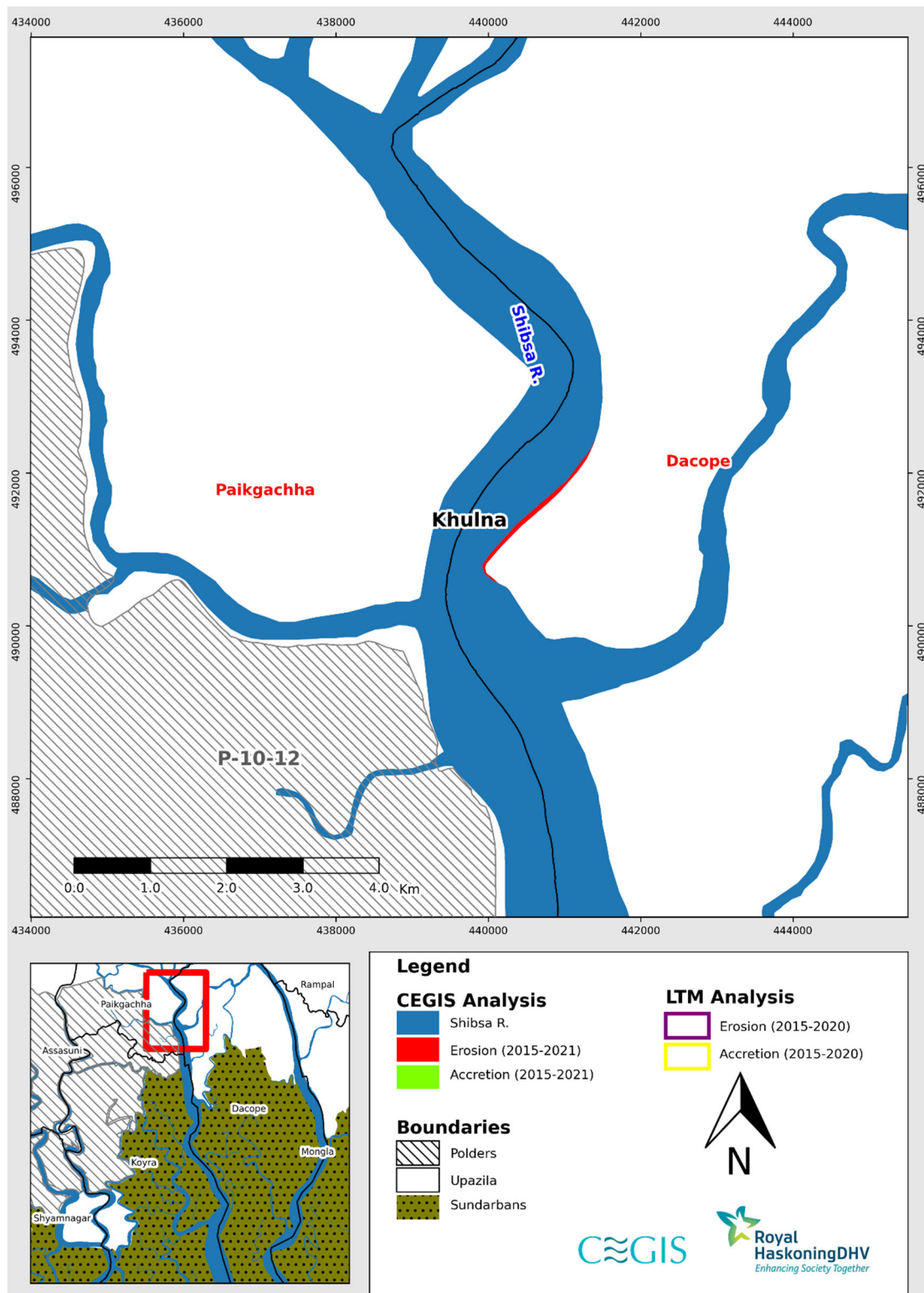


Figure 1.18: Difference between erosion and accretion of LTM and CEGIS in Shibsa River (Reach-1) (2015-2020)

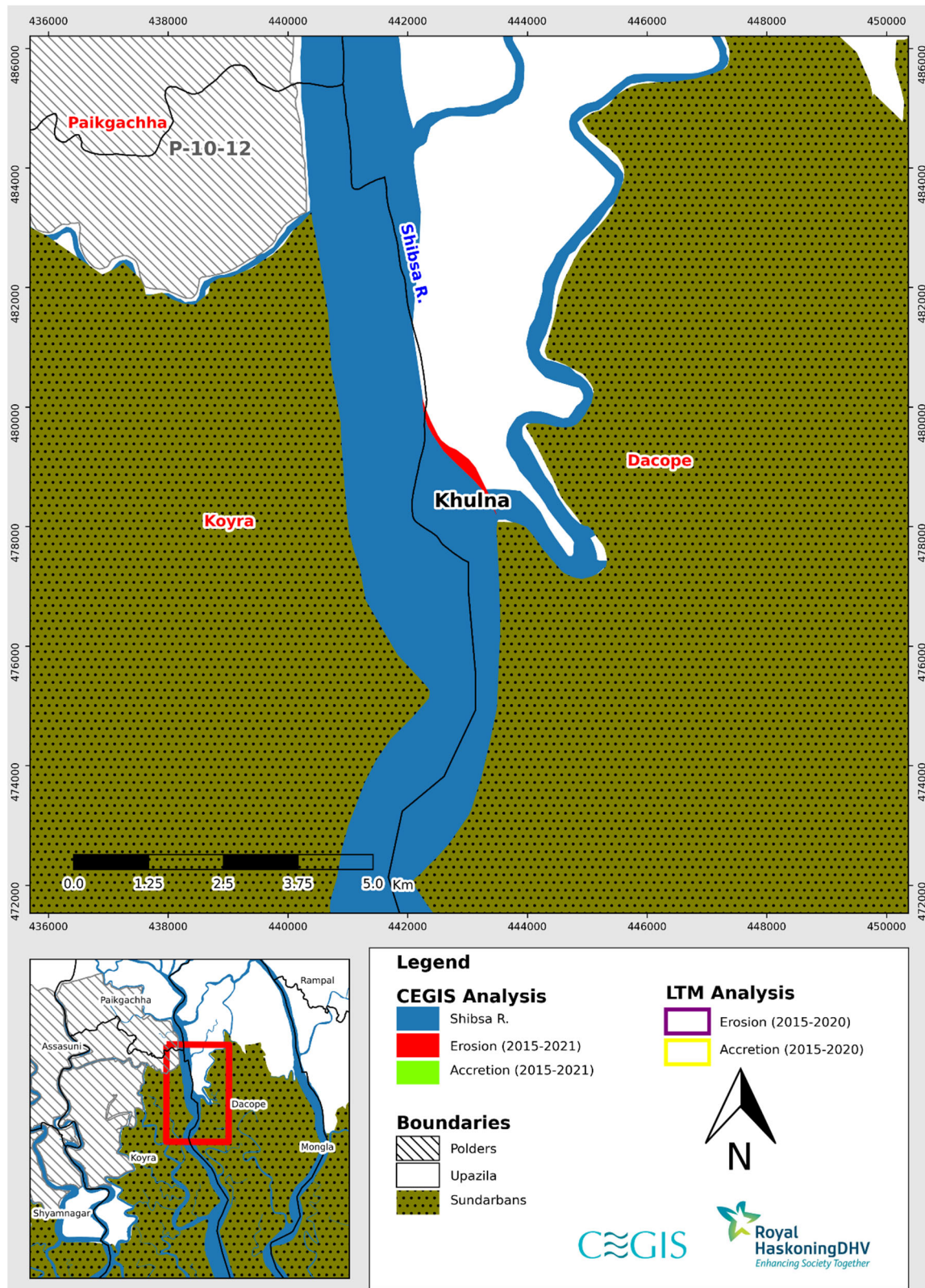


Figure 1.19: Difference between erosion and accretion of LTM and CEGIS in Shubra River (Reach-2) (2015-2020)

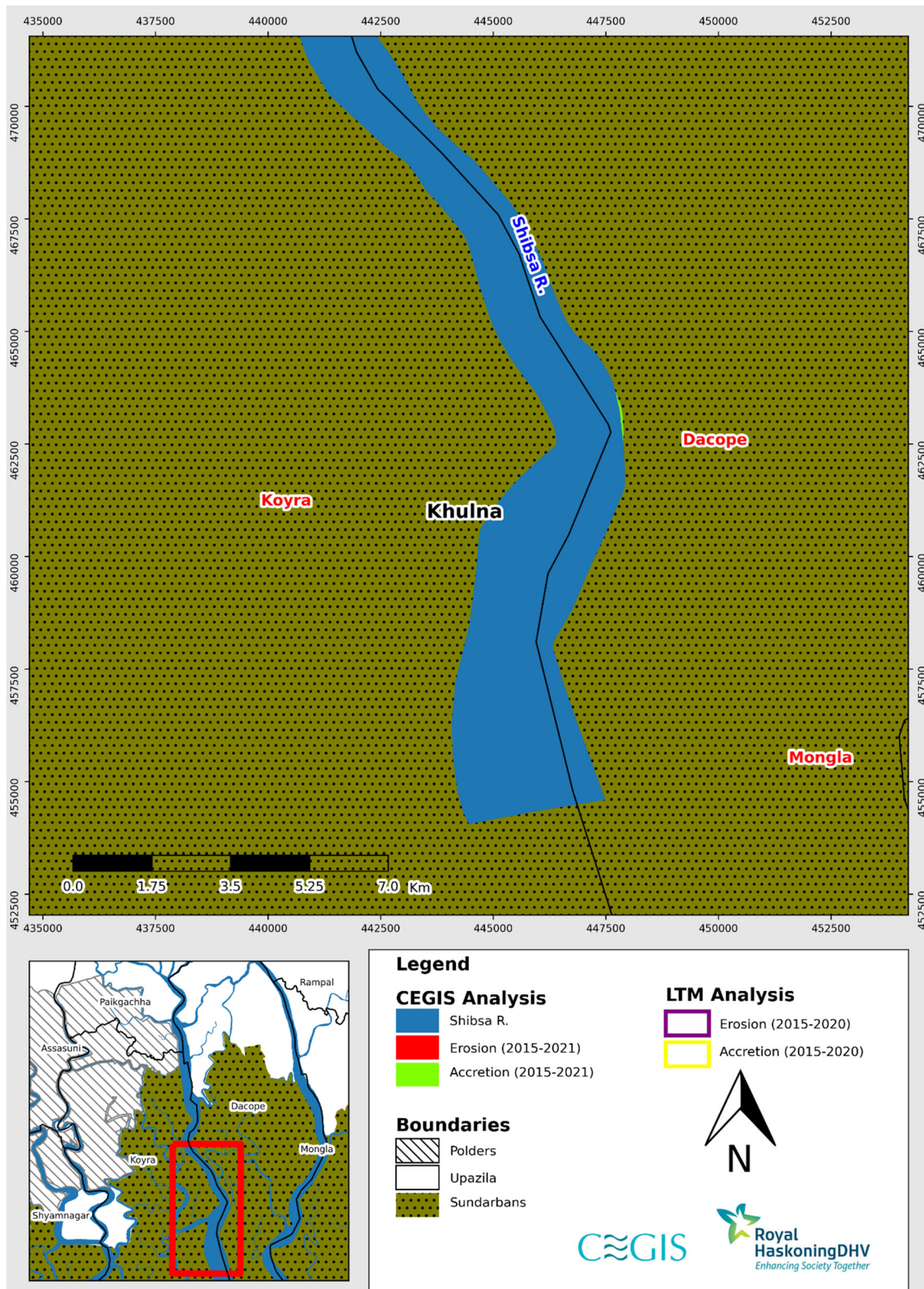


Figure 1.20: Difference between erosion and accretion of LTM and CEGIS in Shibsa River (Reach-2) (2015-2020)

Annex-B

**Comparison between CEGIS and Long-Term Monitoring Data
(Barishal Region)**

DRAFT

Comparison between CEGIS and Long Term Monitoring Data (2010-2015)
(Barishal Region)

DRAFT

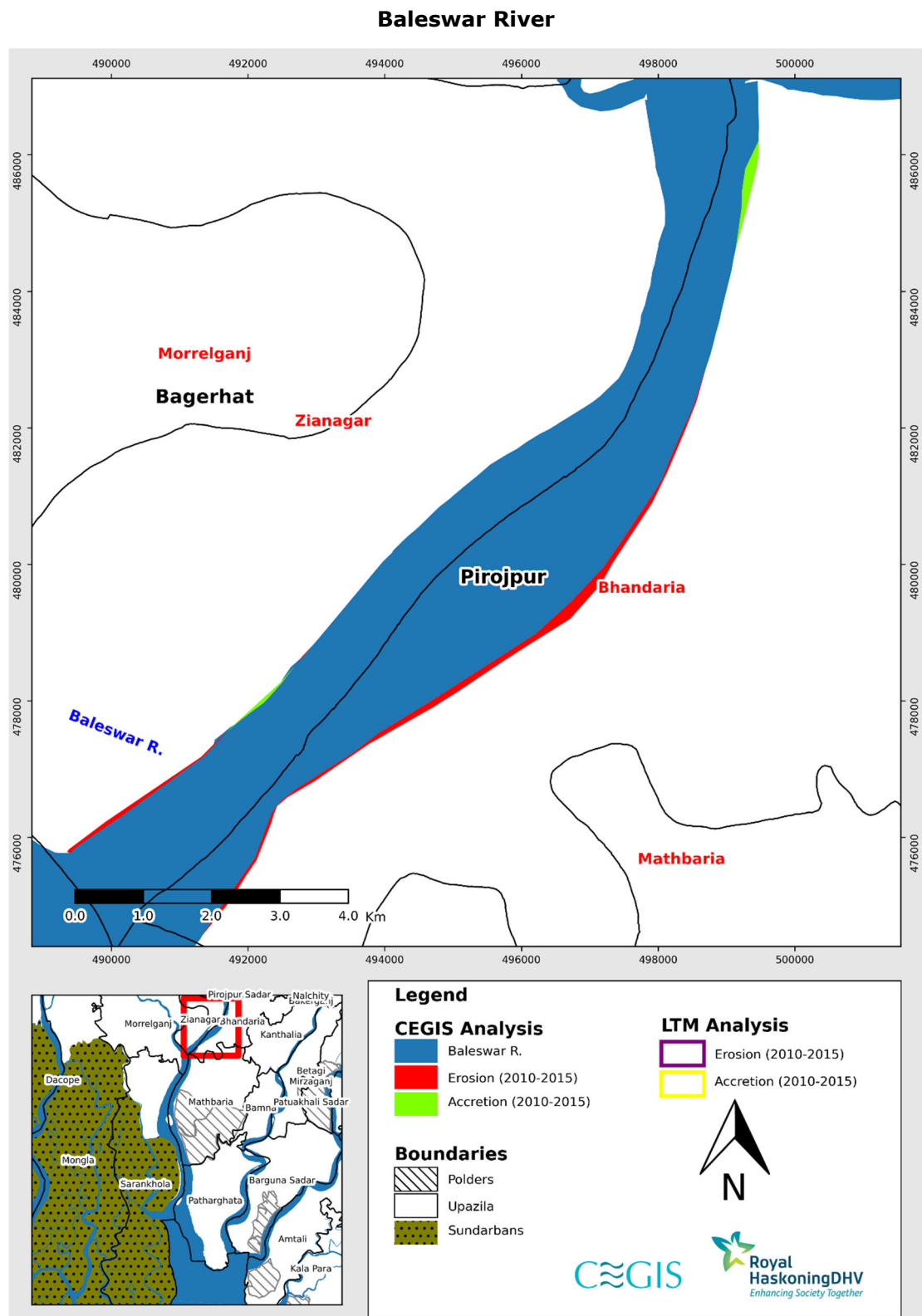


Figure 2.1: Difference between erosion and accretion of LTM and CEGIS in Baleswar River (Reach-1) (2010-2015)

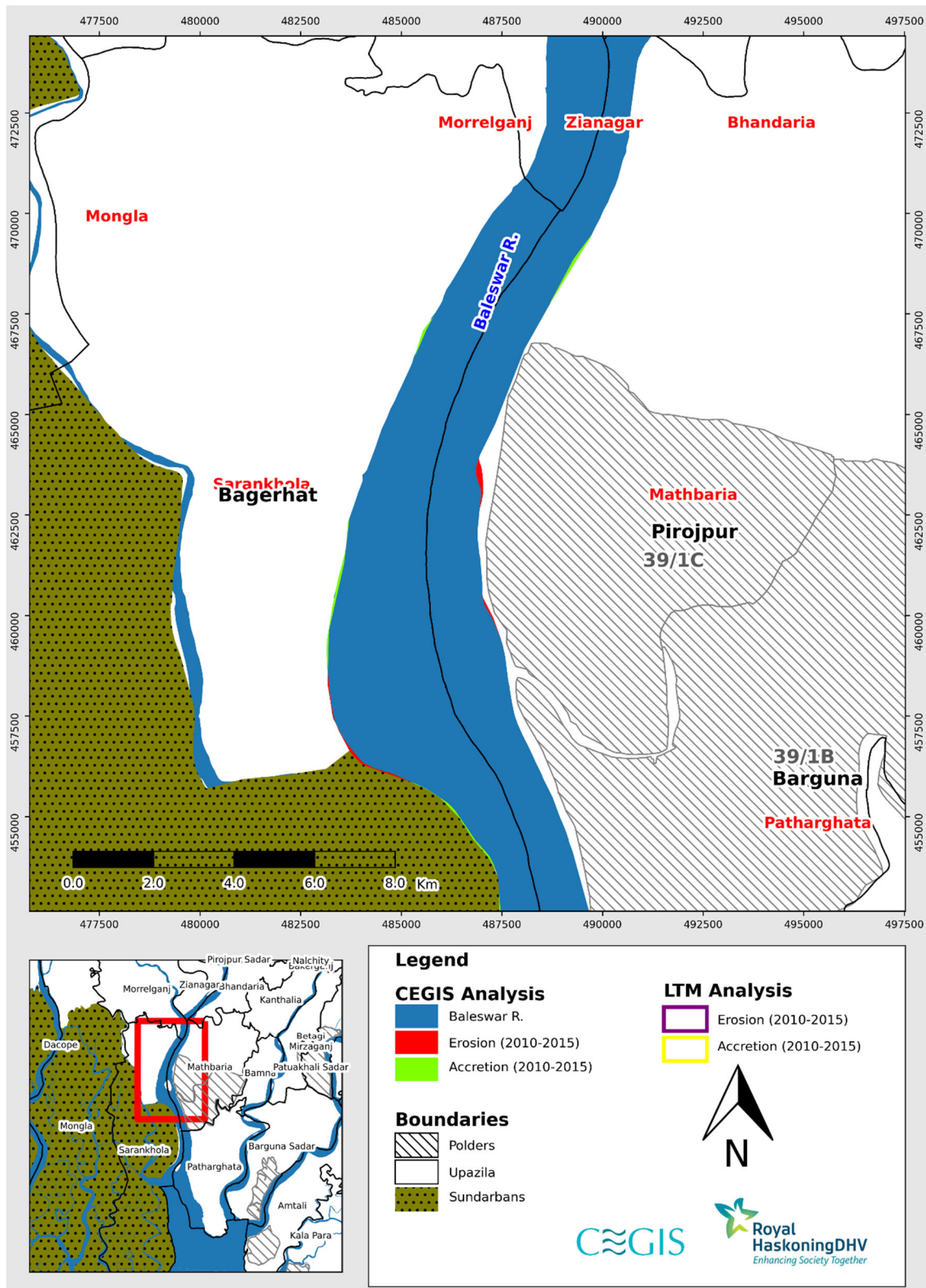


Figure 2.2: Difference between erosion and accretion of LTM and CEGIS in Baleswar River (Reach-2) (2010-2015)

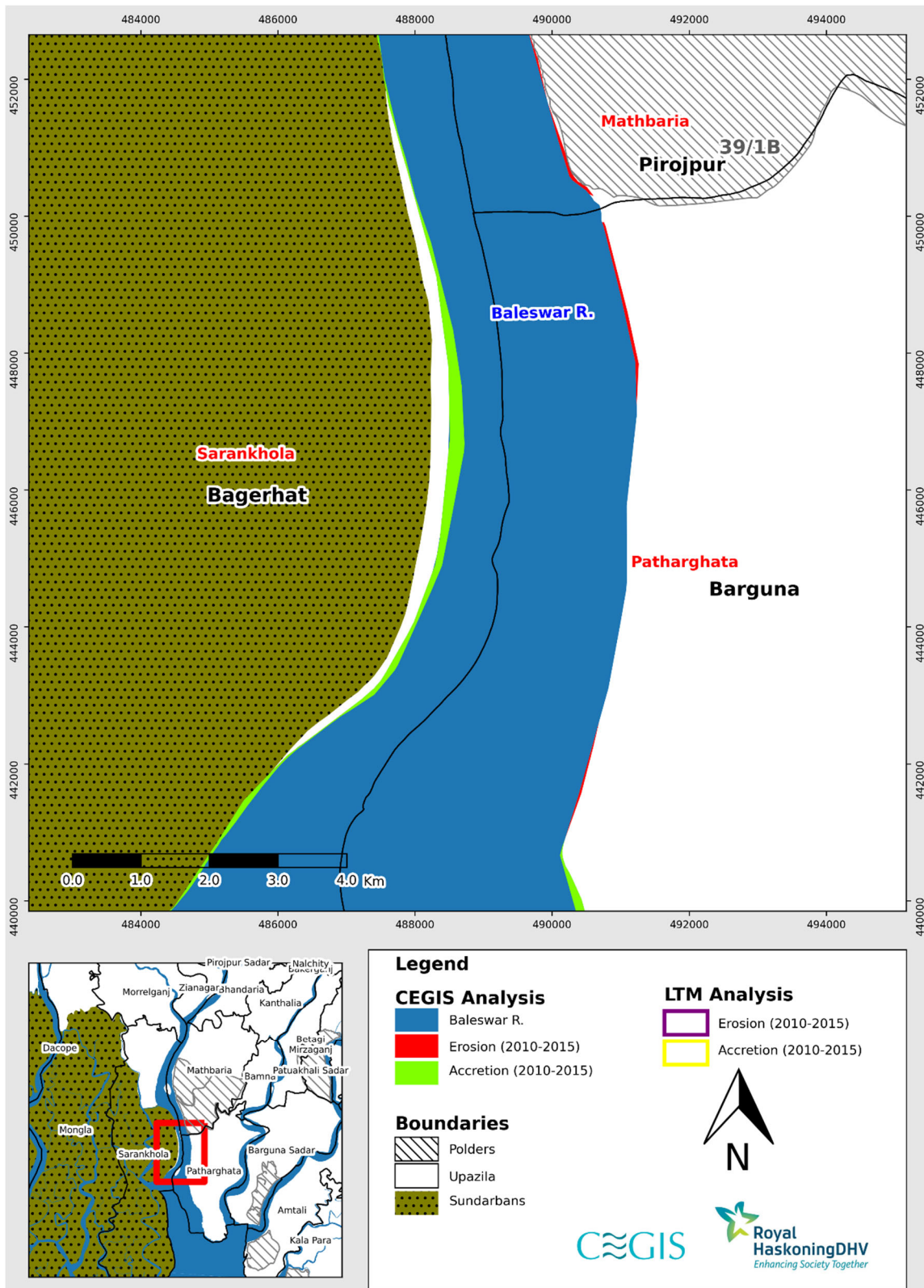


Figure 2.3: Difference between erosion and accretion of LTM and CEGIS in Baleswar River (Reach-3) (2010-2015)

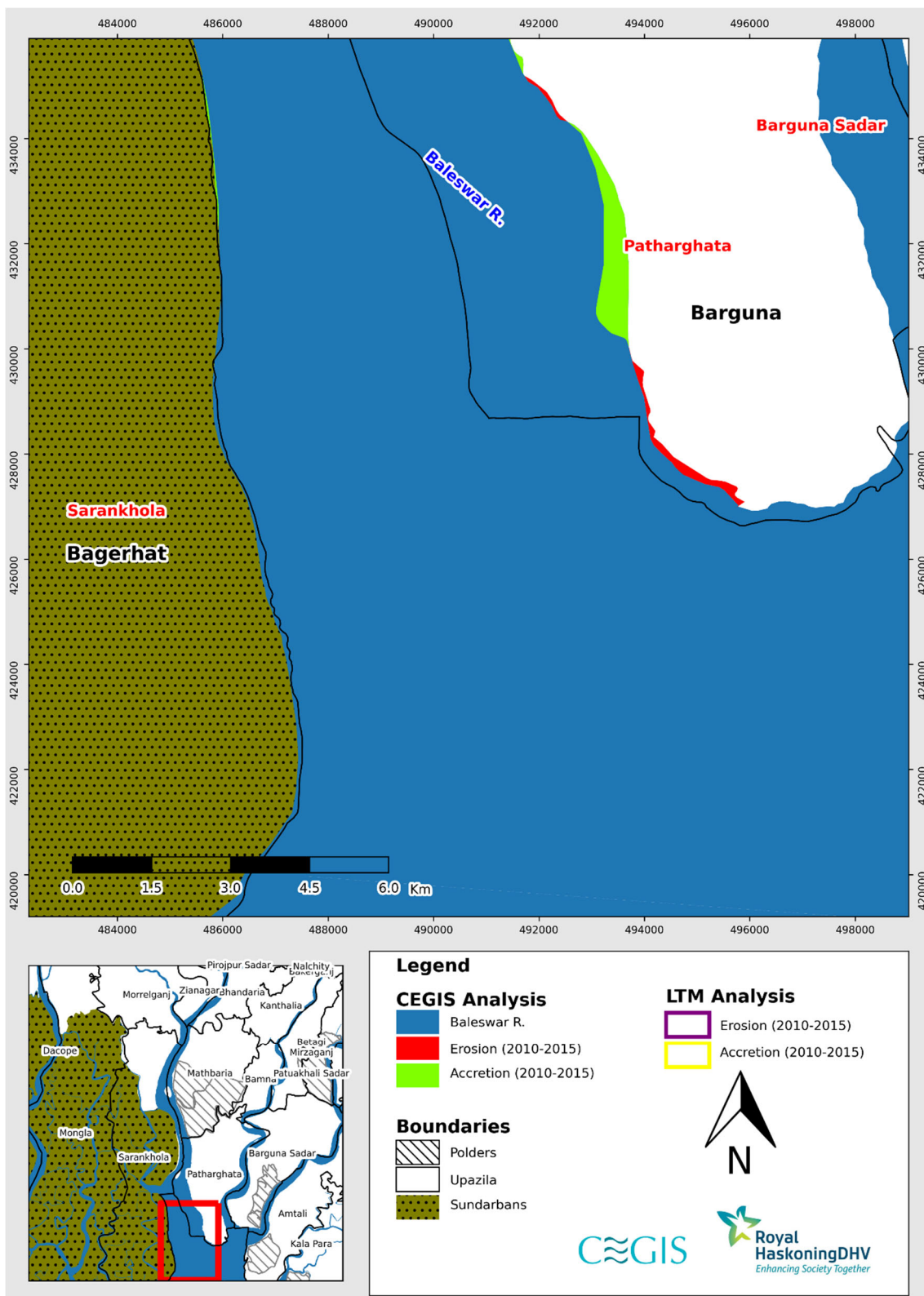


Figure 2.4: Difference between erosion and accretion of LTM and CEGIS in Baleswar River (Reach-4) (2010-2015)

Burishwar-Payra River

Feasibility Studies and Detailed Design for next the Phase of CEIP
Morphology Report - December 2022

Page 182 of 207

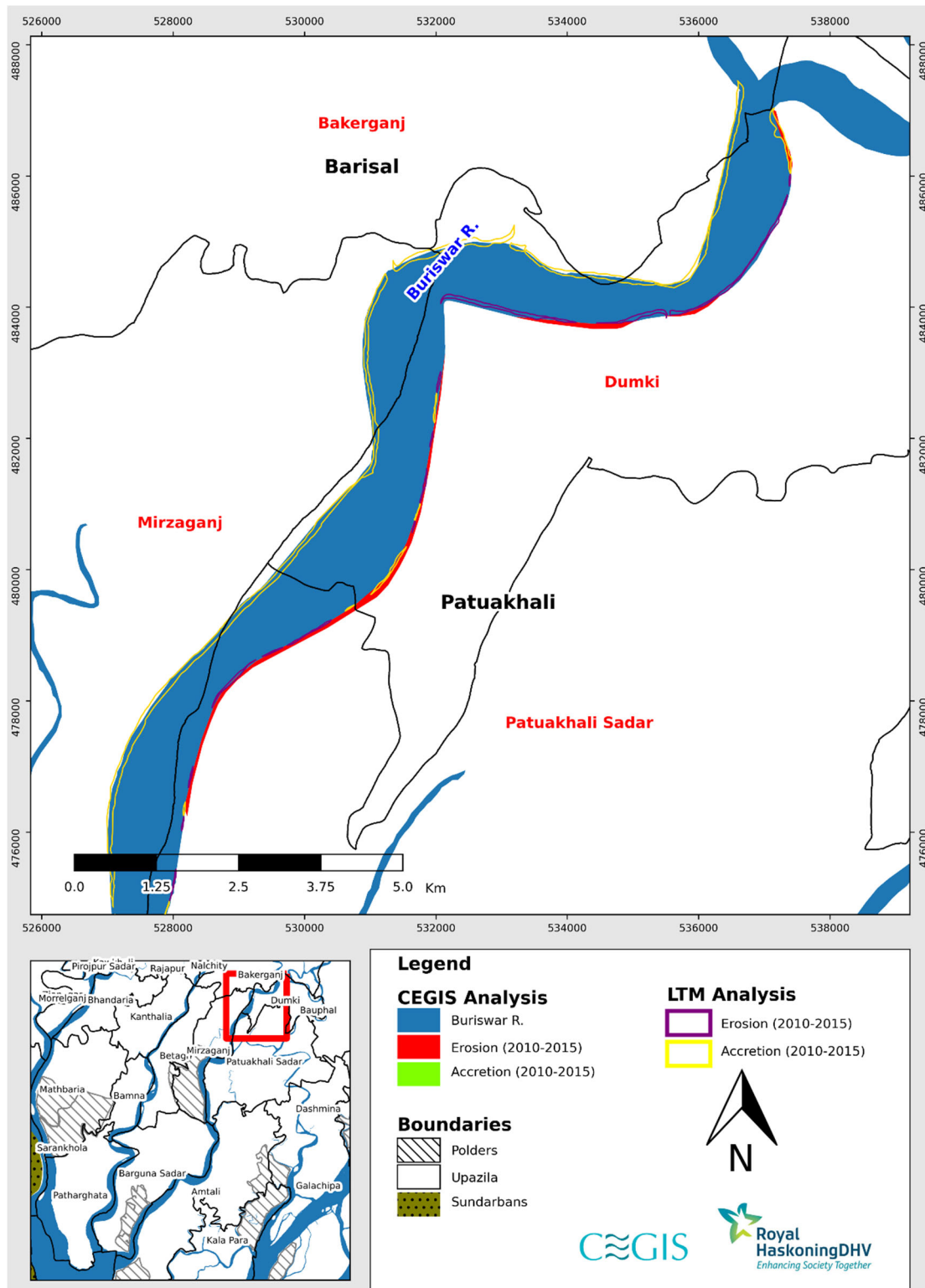


Figure 2.5: Difference between erosion and accretion of LTM and CEGIS in Burishwar-Payra River (Reach-1) (2010-2015)

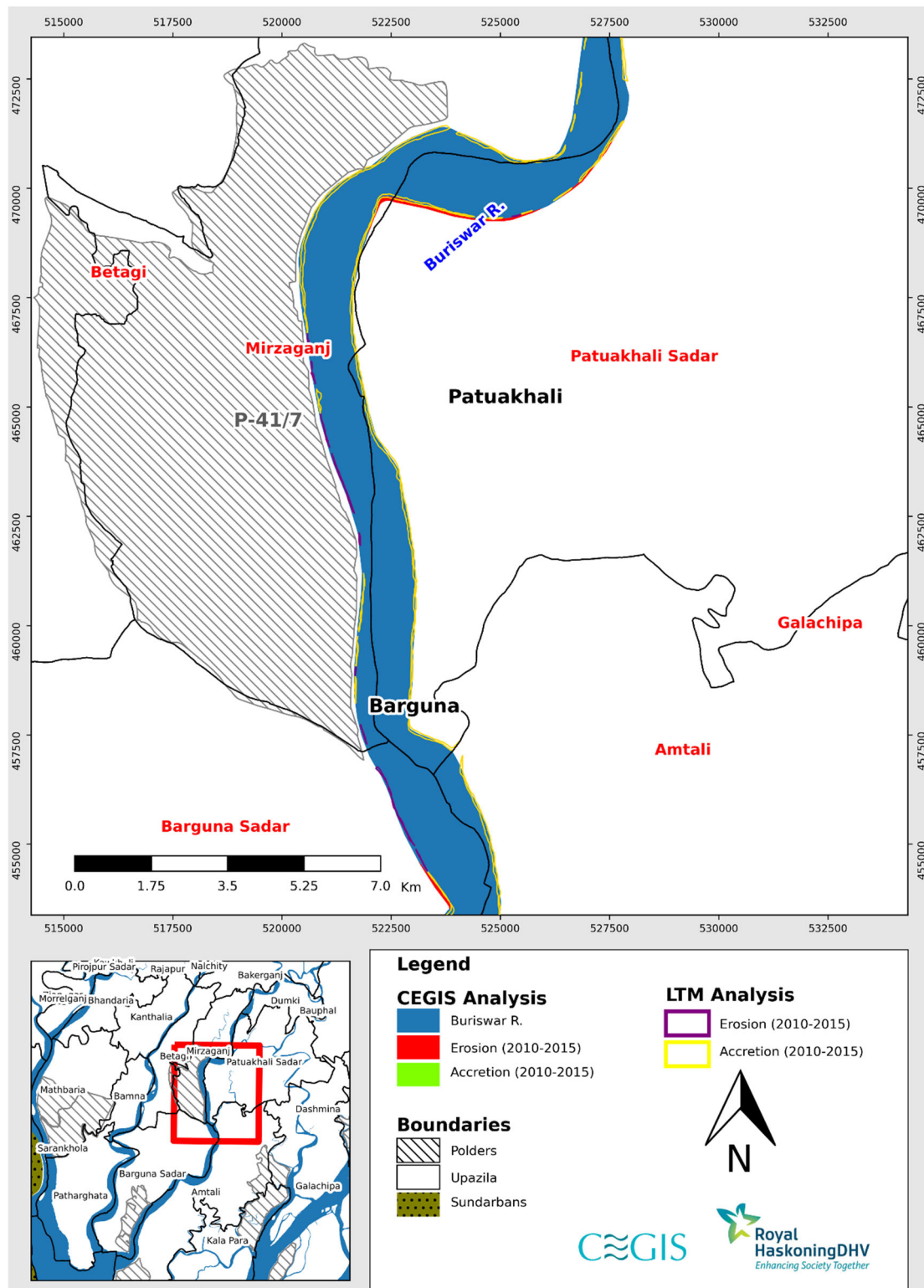


Figure 2.6: Difference between erosion and accretion of LTM and CEGIS in Burishwar-Payra River (Reach-2) (2010-2015)

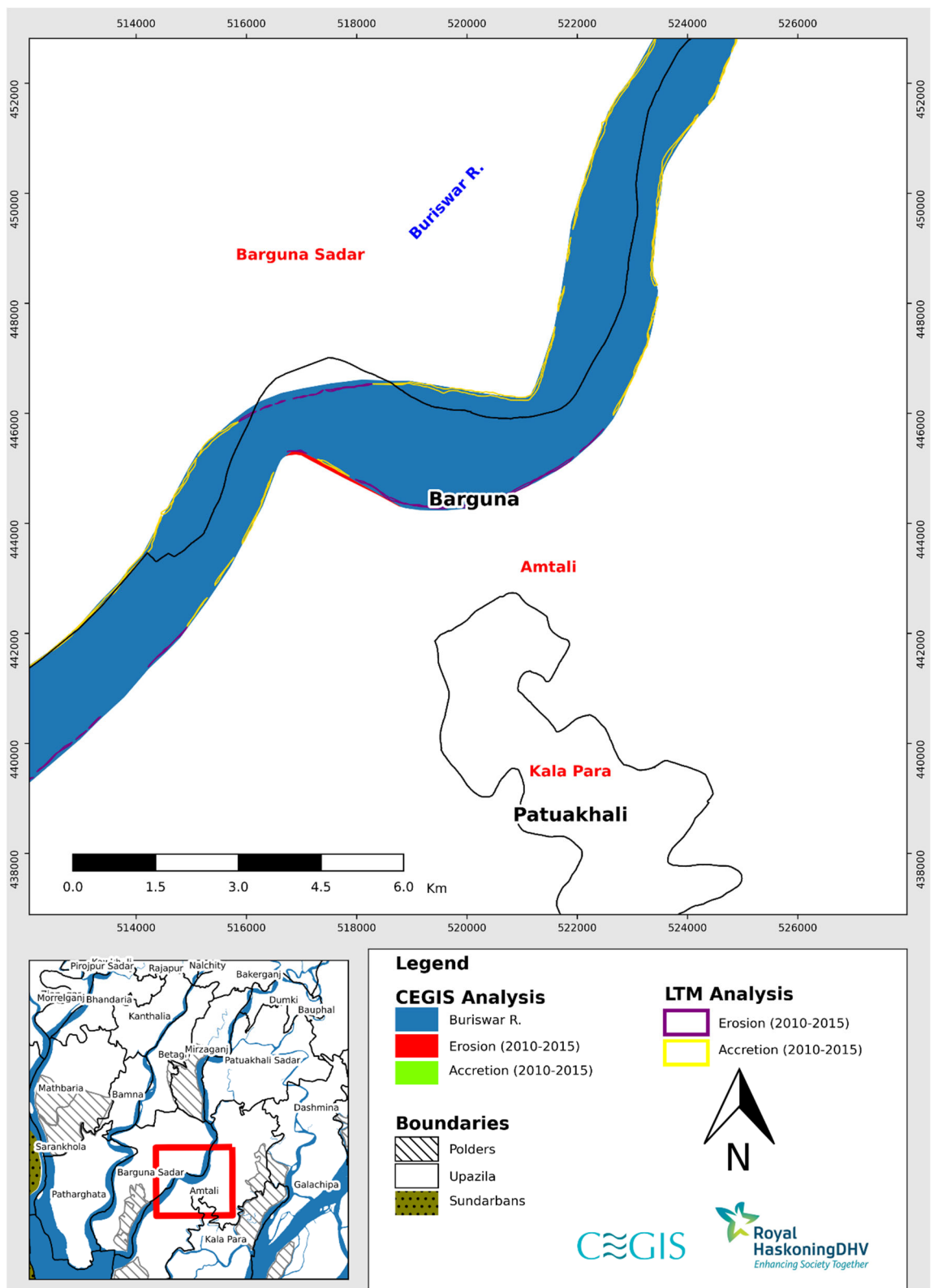


Figure 2.7: Difference between erosion and accretion of LTM and CEGIS in Burishwar-Payra River (Reach-3) (2010-2015)

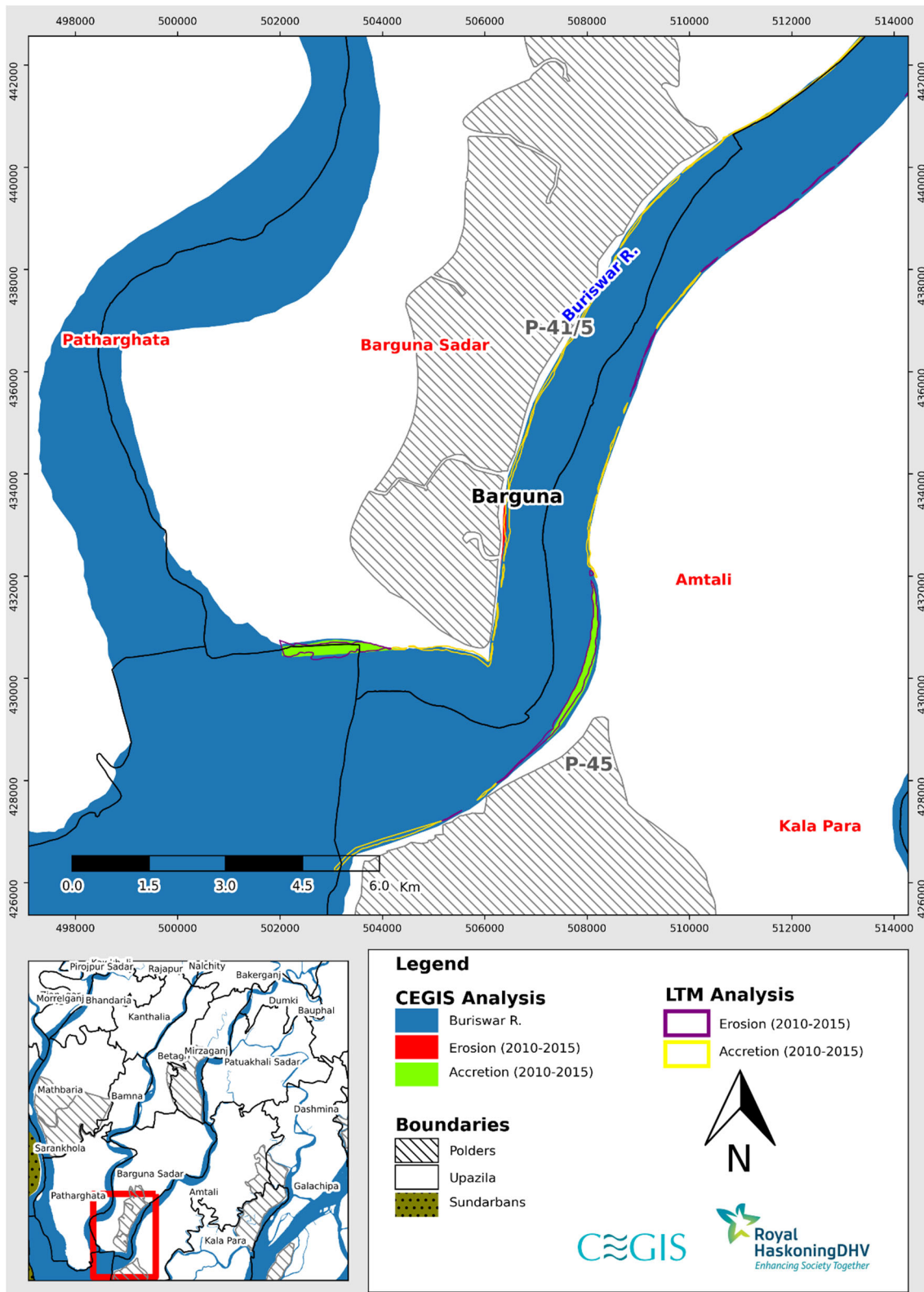


Figure 2.8: Difference between erosion and accretion of LTM and CEGIS in Burishwar-Payra River (Reach-4) (2010-2015)

Tentulia River

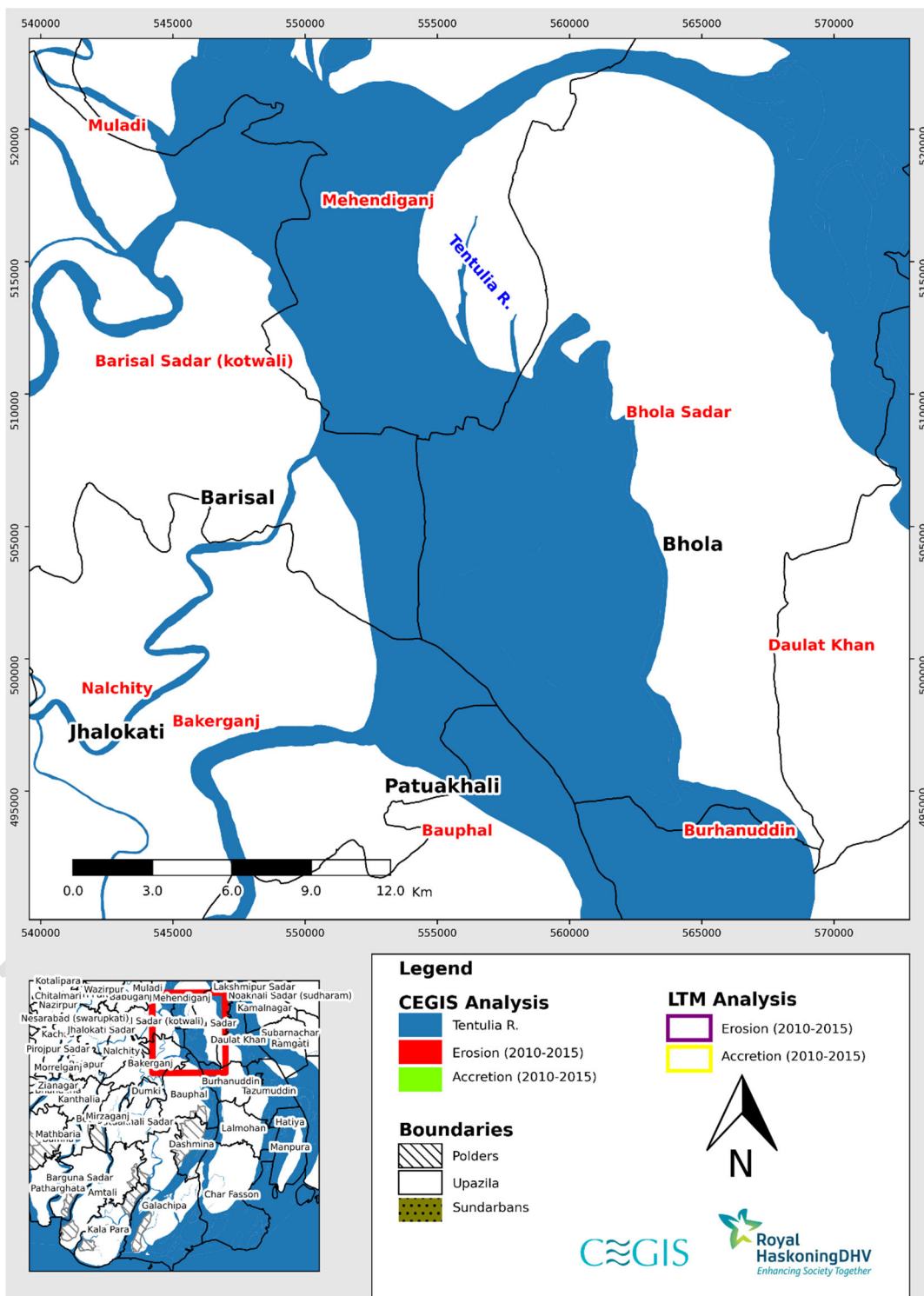


Figure 2.9: Difference between erosion and accretion of LTM and CEGIS in Tentulia River (Reach-1) (2010-2015)

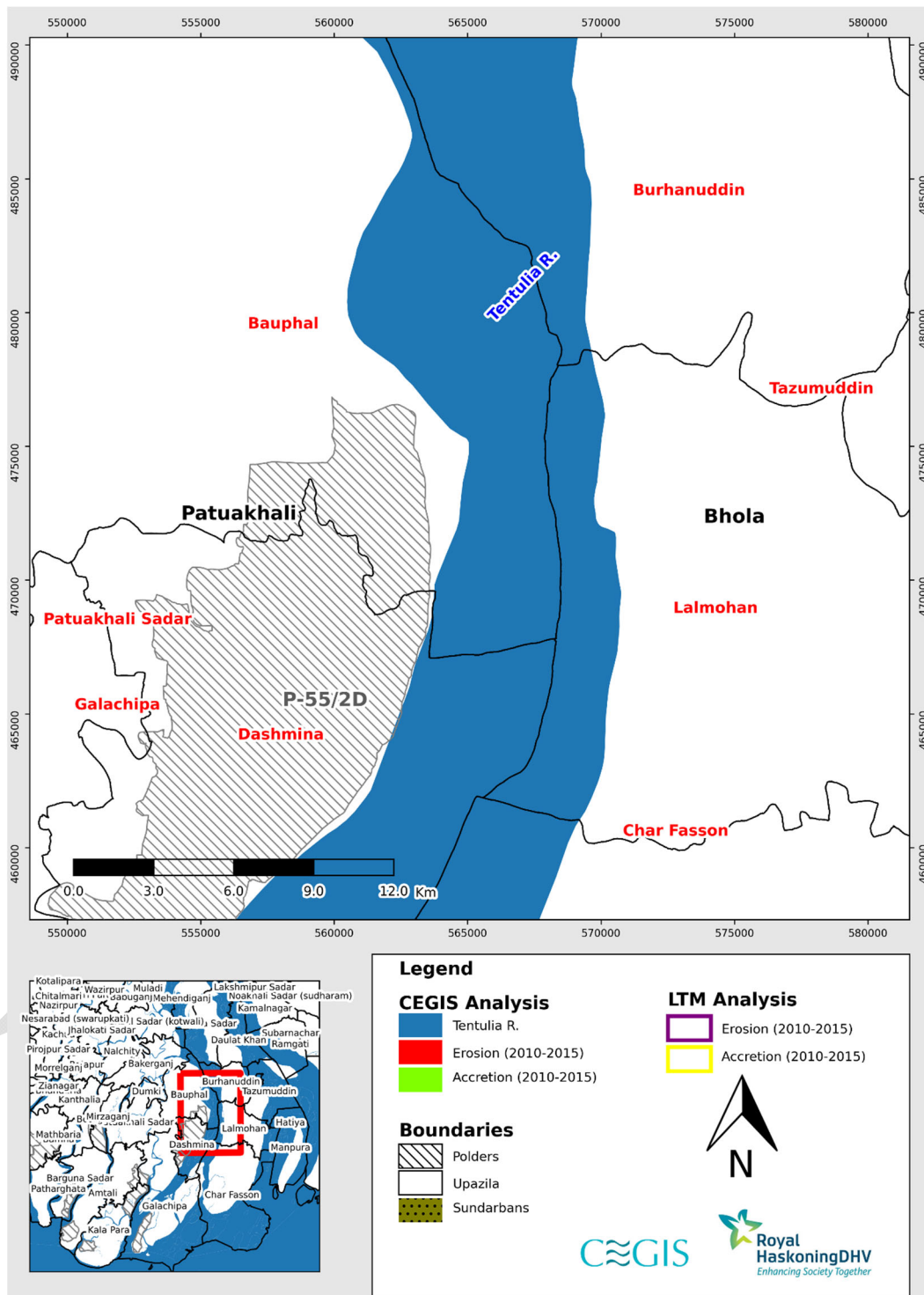


Figure 2.10: Difference between erosion and accretion of LTM and CEGIS in Tentulia River (Reach-2) (2010-2015)

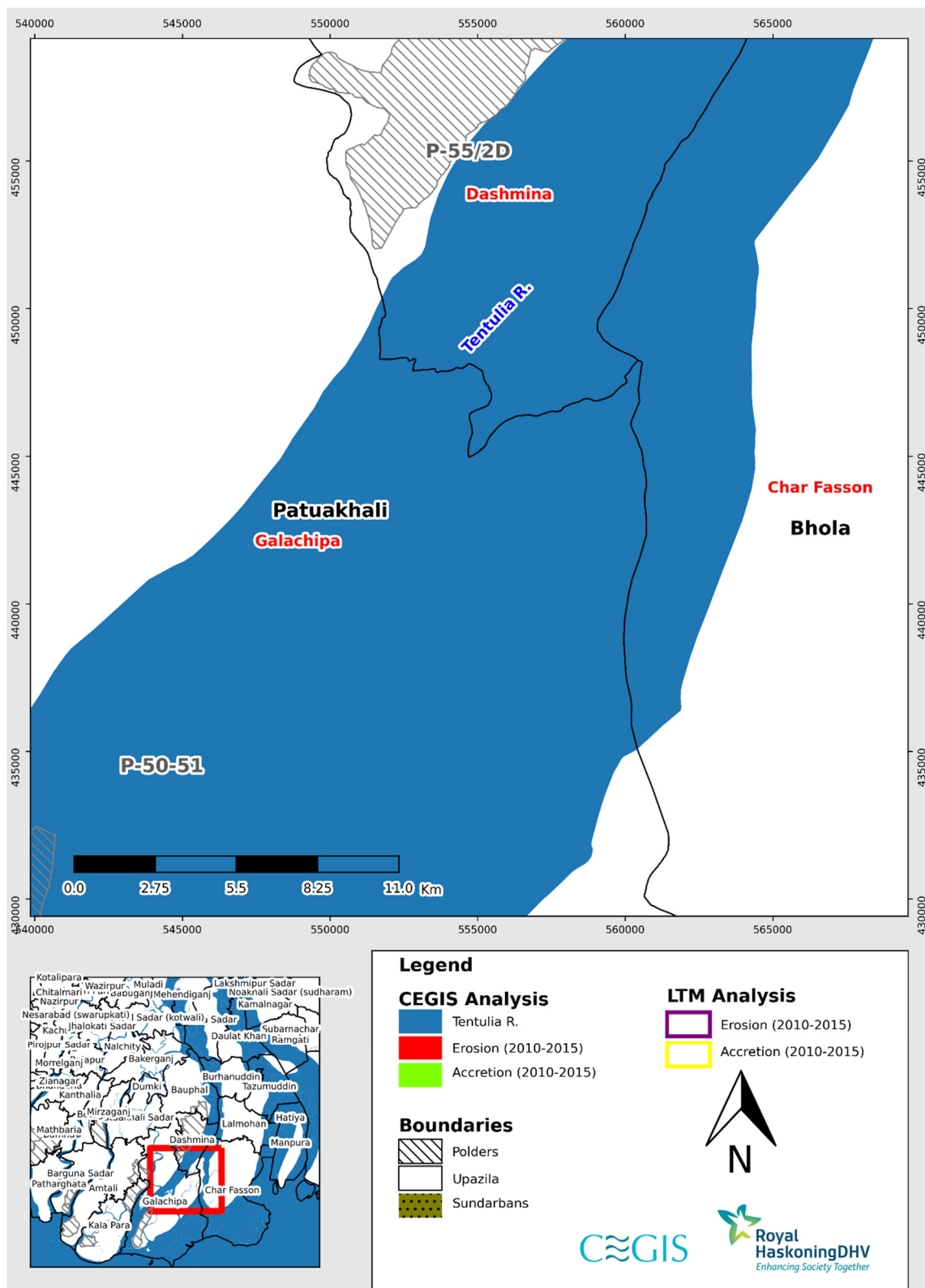


Figure 2.11: Difference between erosion and accretion of LTM and CEGIS in Tentulia River (Reach-3) (2010-2015)

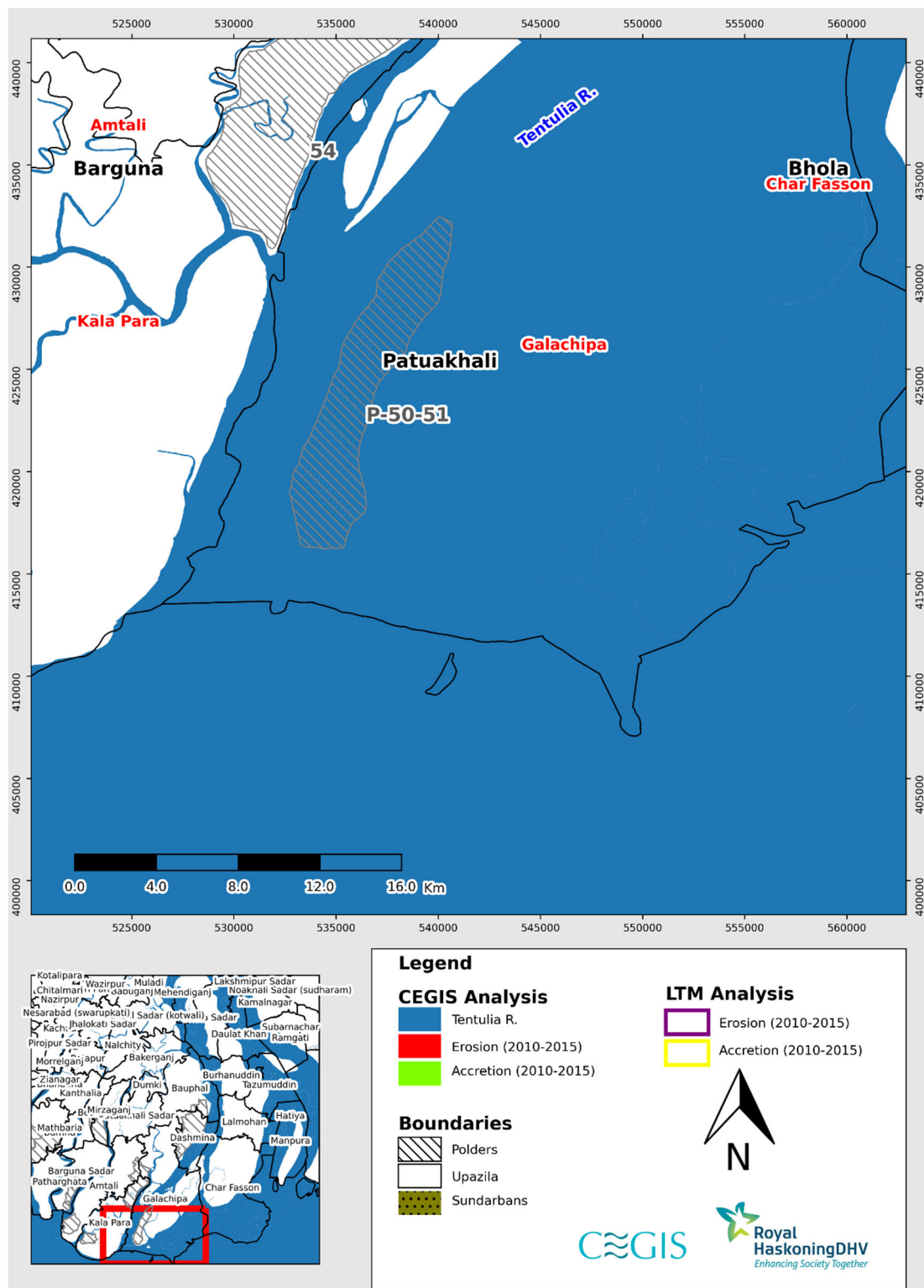


Figure 2.12: Difference between erosion and accretion of LTM and CEGIS in Tentulia River (Reach-4) (2010-2015)

Comparison between CEGIS and Long Term Monitoring Data (2015-2021)
(Barishal Region)

DRAFT

Baleswar River

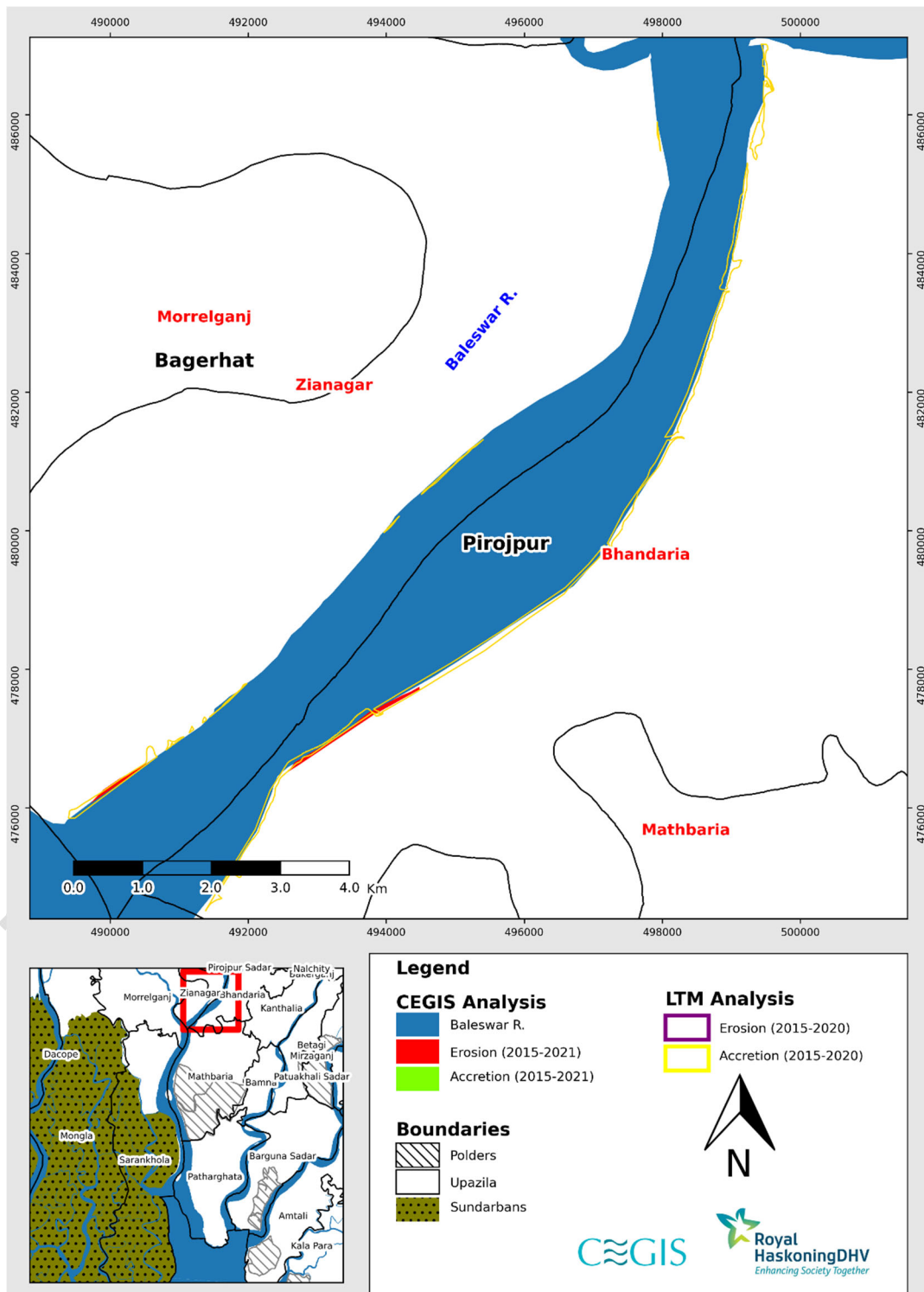


Figure 2.13: Difference between erosion and accretion of LTM and CEGIS in Baleswar River (Reach-1) (2015-2021)

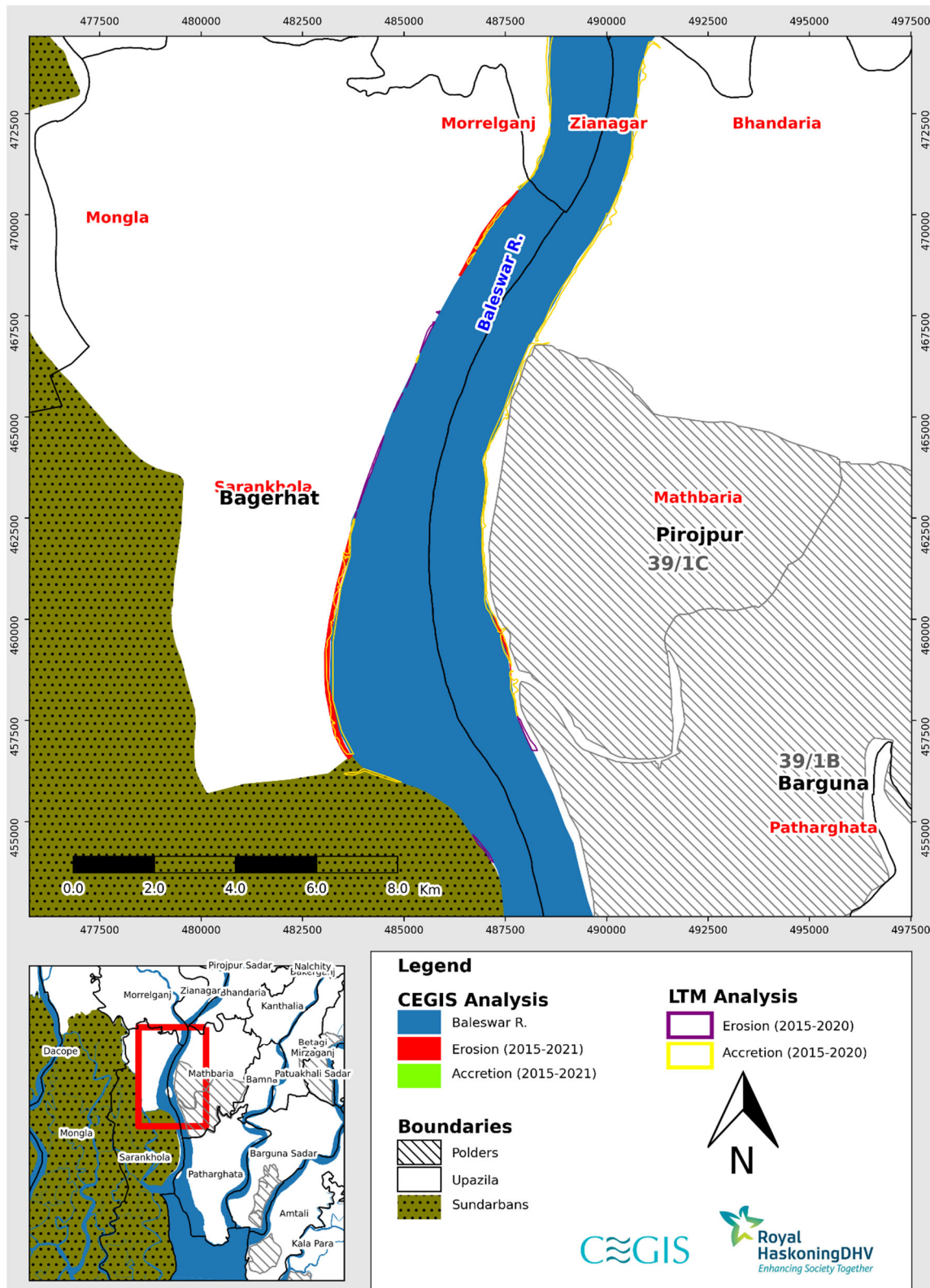


Figure 2.14: Difference between erosion and accretion of LTM and CEGIS in Baleswar River (Reach-2) (2015-2021)

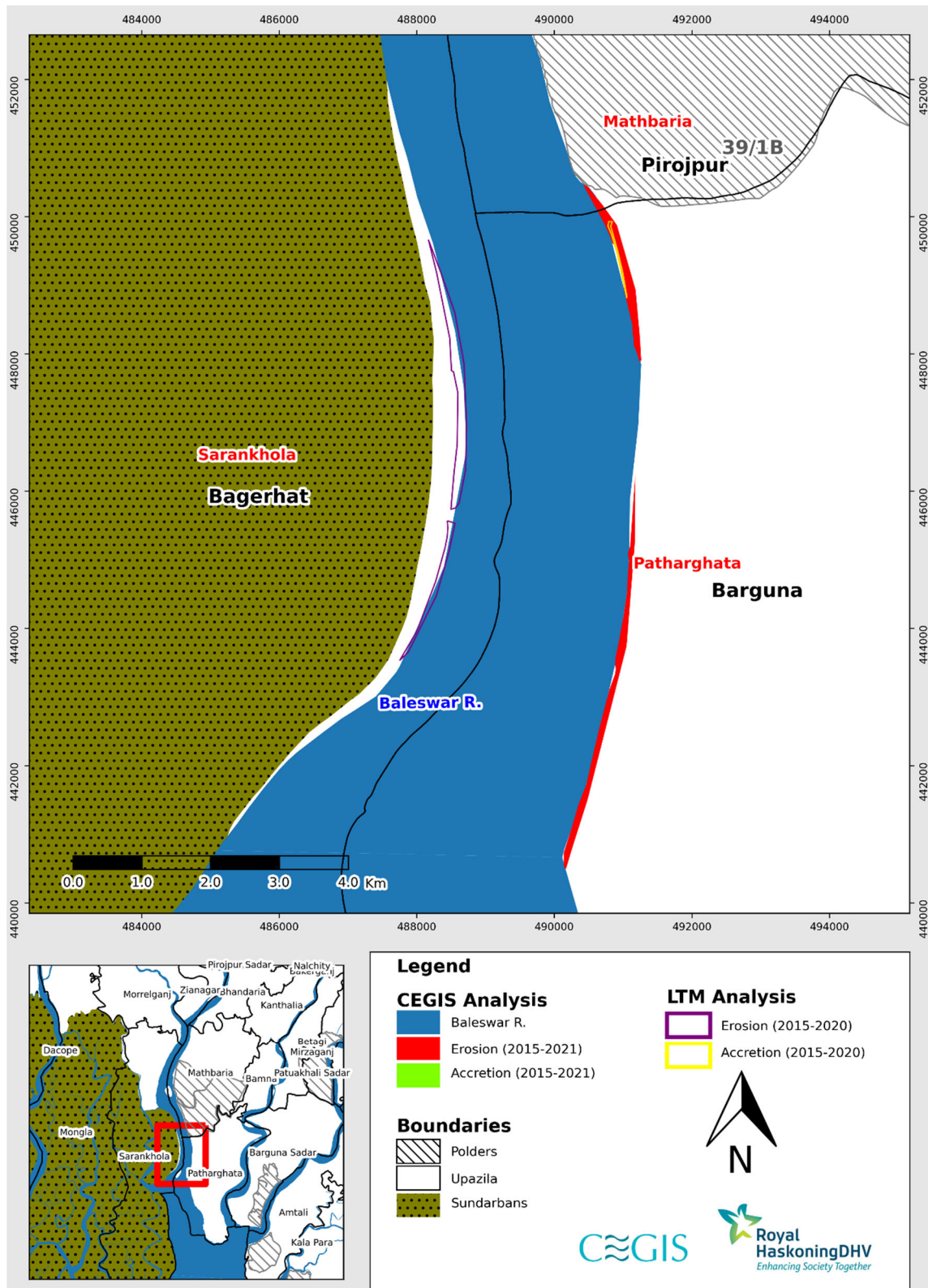


Figure 2.15: Difference between erosion and accretion of LTM and CEGIS in Baleswar River (Reach-3) (2015-2021)

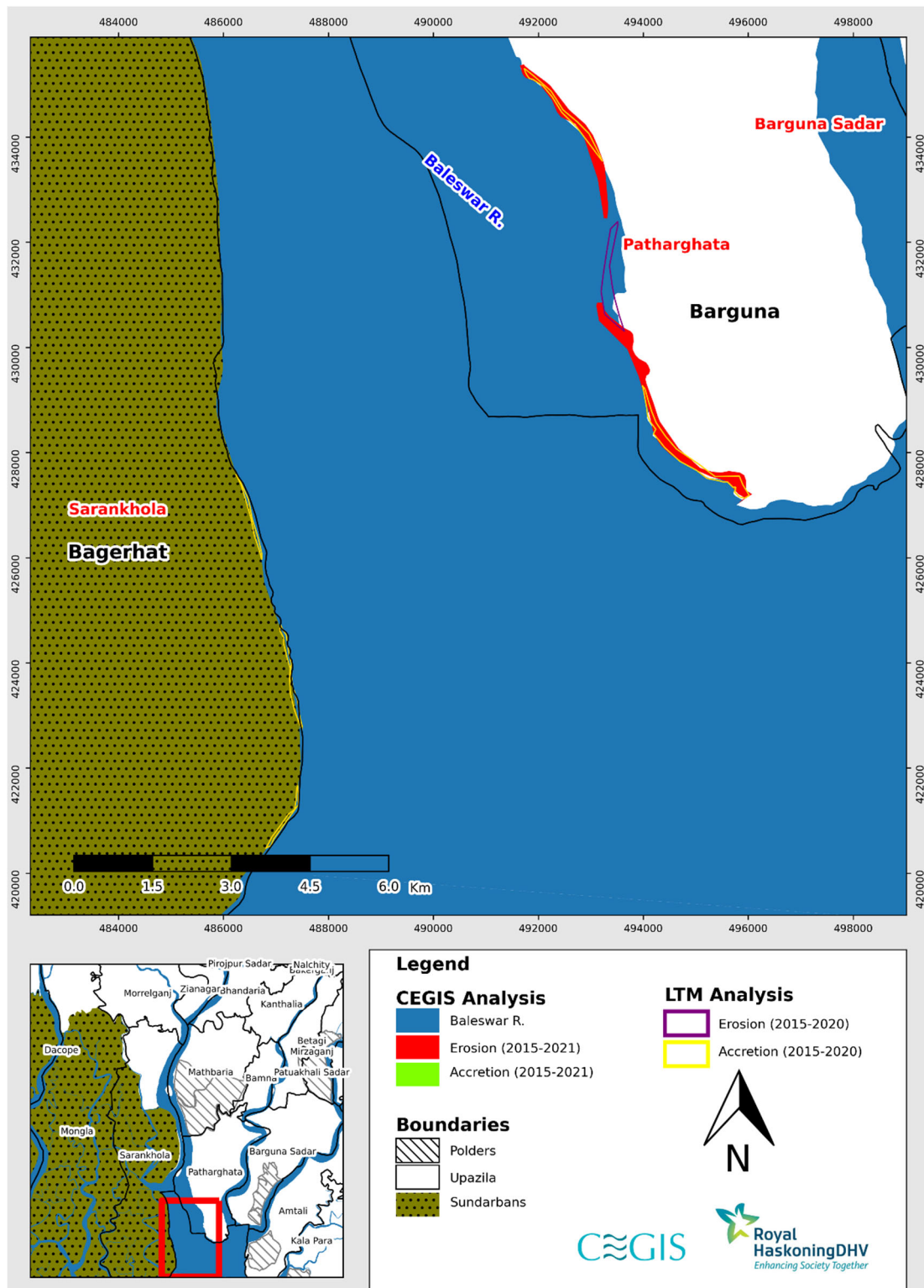


Figure 2.16: Difference between erosion and accretion of LTM and CEGIS in Baleswar River (Reach-4) (2015-2021)

Burishwar-Payra River

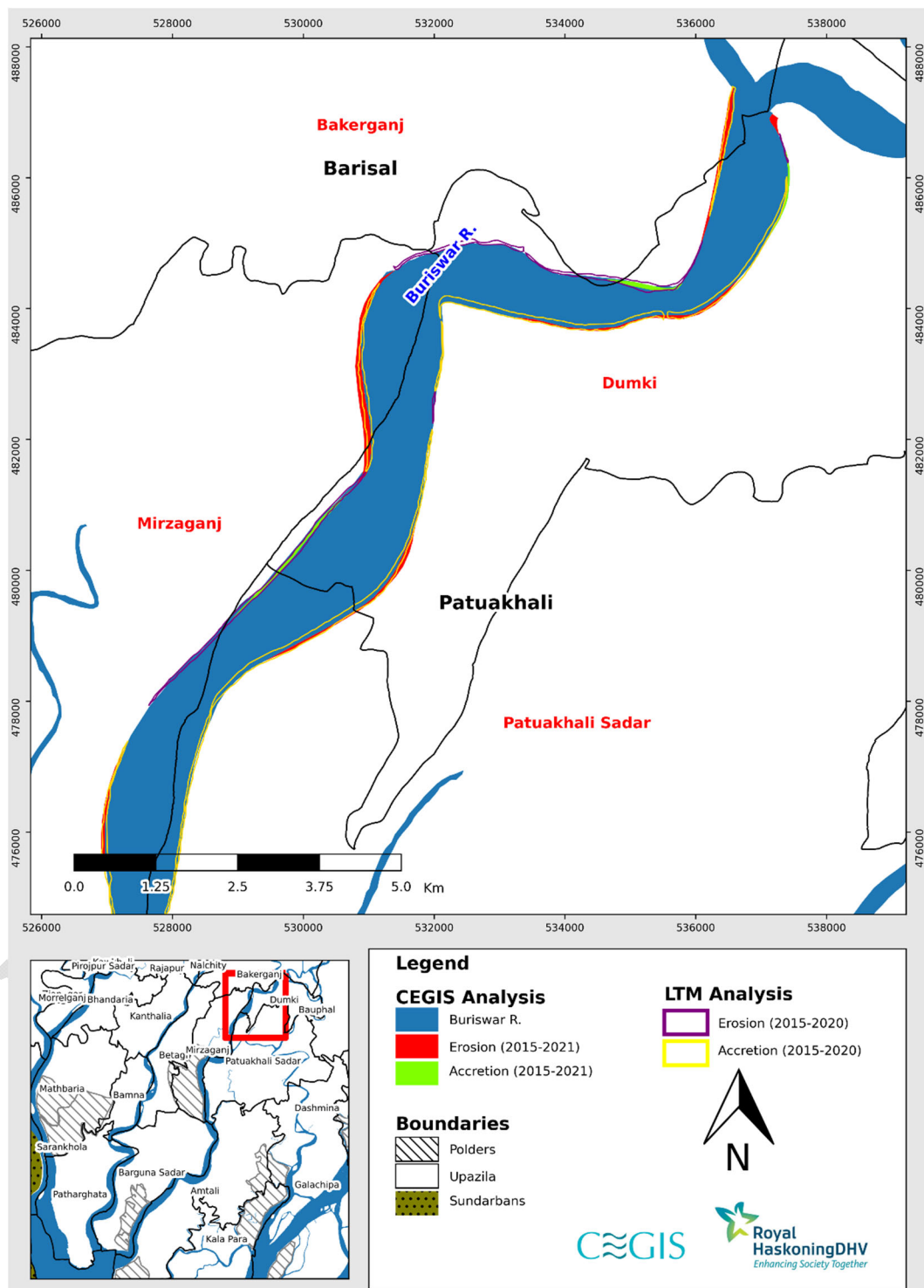


Figure 2.17: Difference between erosion and accretion of LTM and CEGIS in Burishwar-Payra River (Reach-1) (2015-2021)

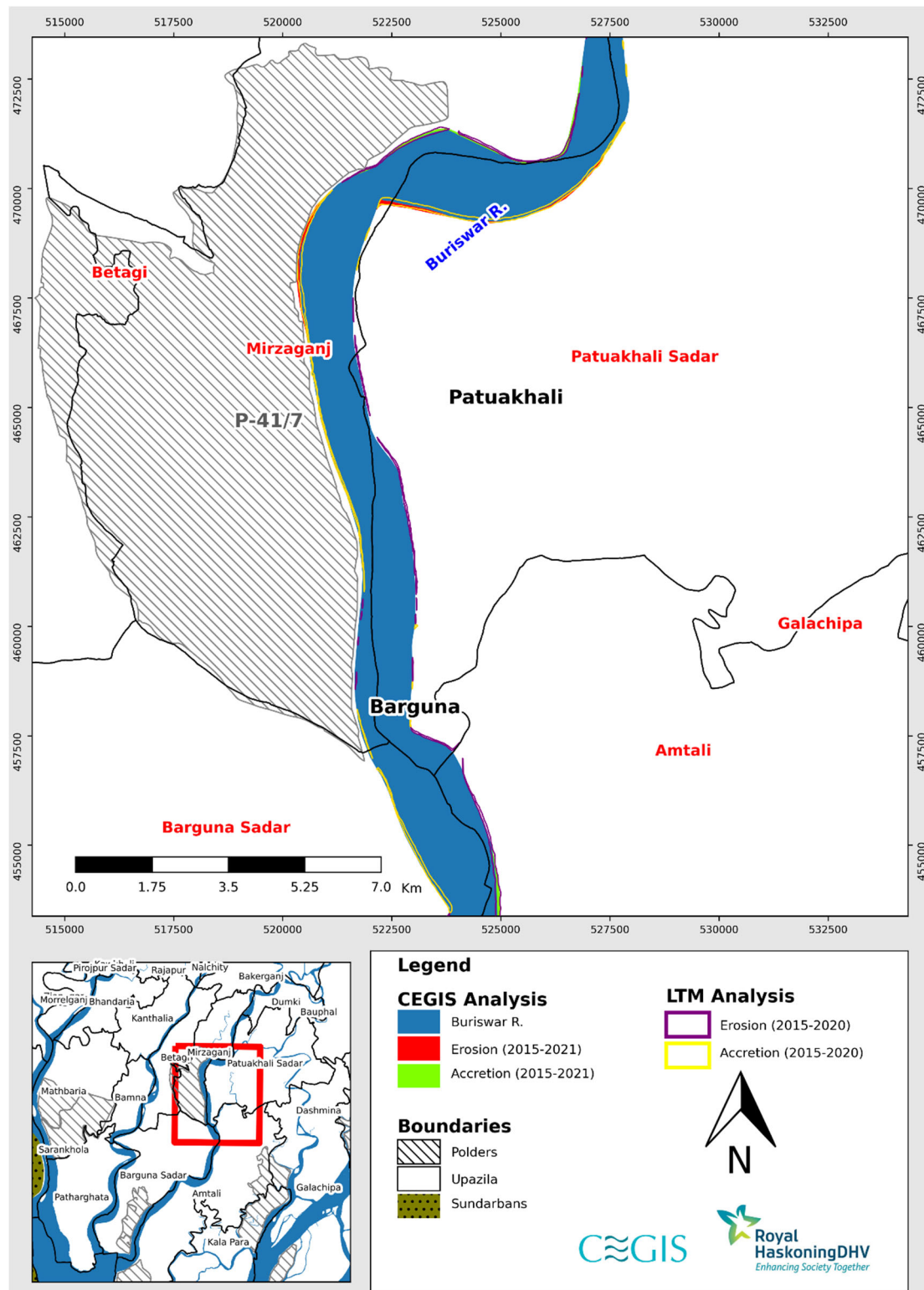


Figure 2.18: Difference between erosion and accretion of LTM and CEGIS in Burishwar-Payra River (Reach-2) (2015-2021)

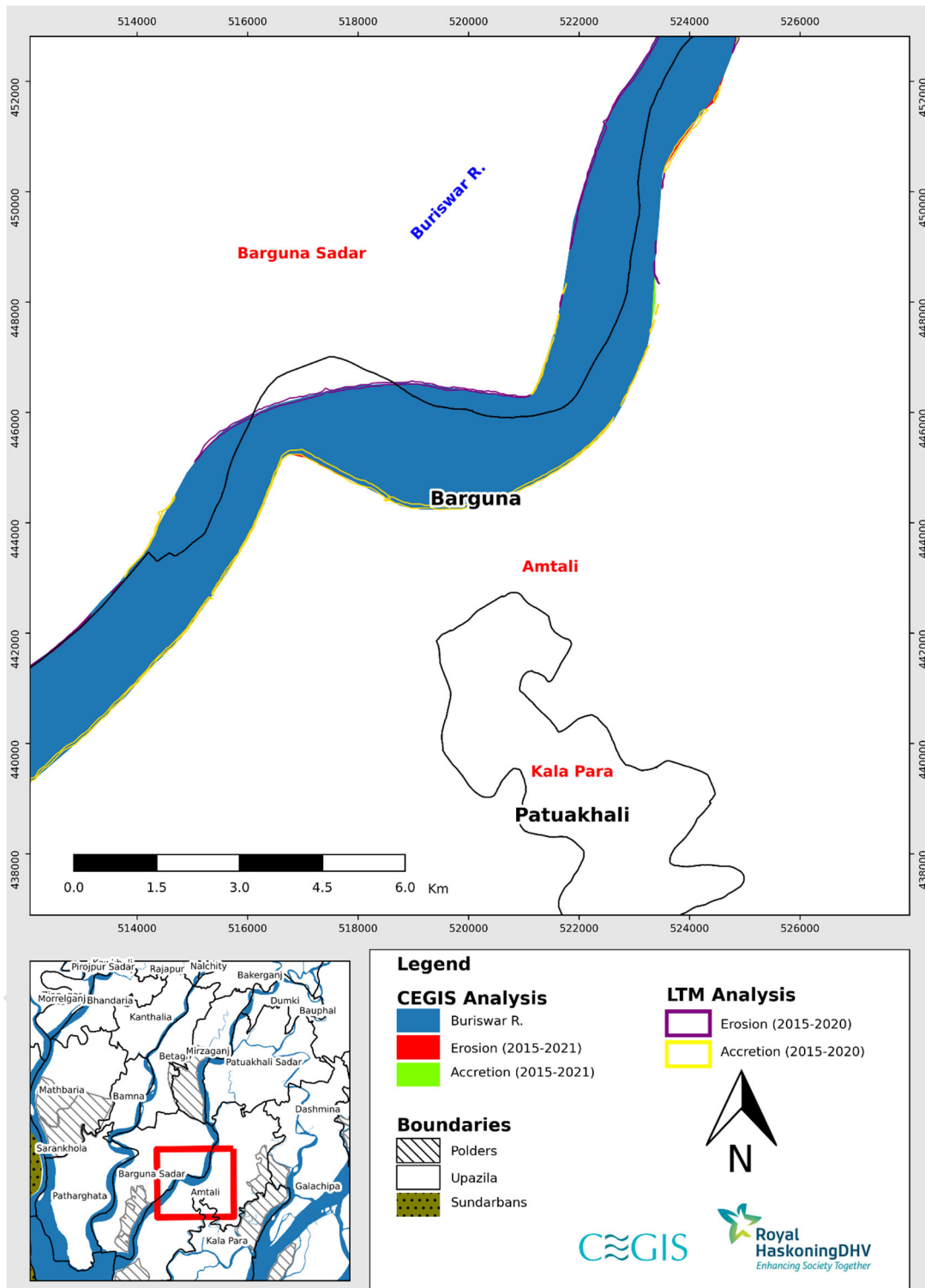


Figure 2.19: Difference between erosion and accretion of LTM and CEGIS in Burishwar-Payra River (Reach-3) (2015-2021)

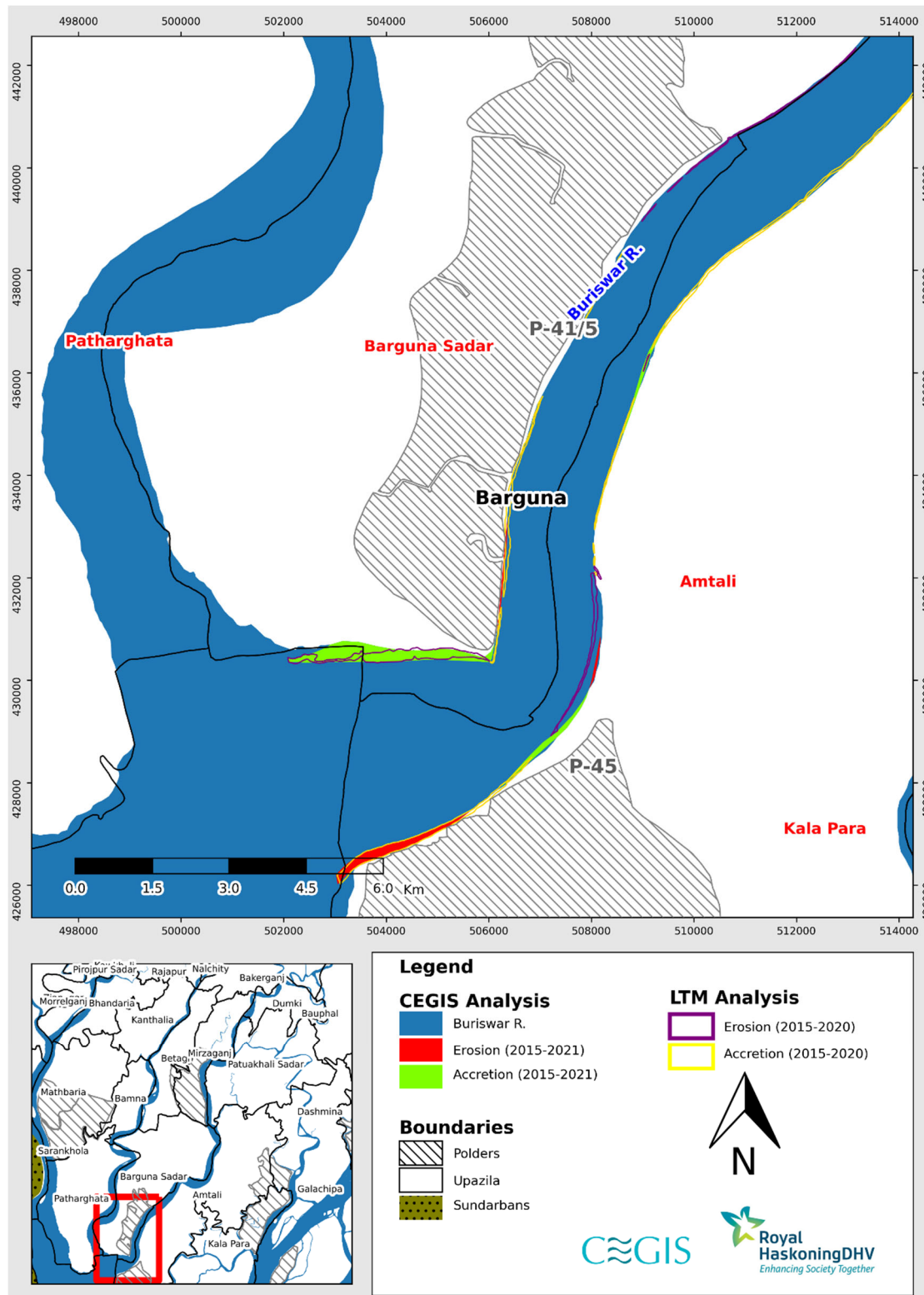


Figure 2.20: Difference between erosion and accretion of LTM and CEGIS in Burishwar-Payra River (Reach-4) (2015-2021)

Tentulia River

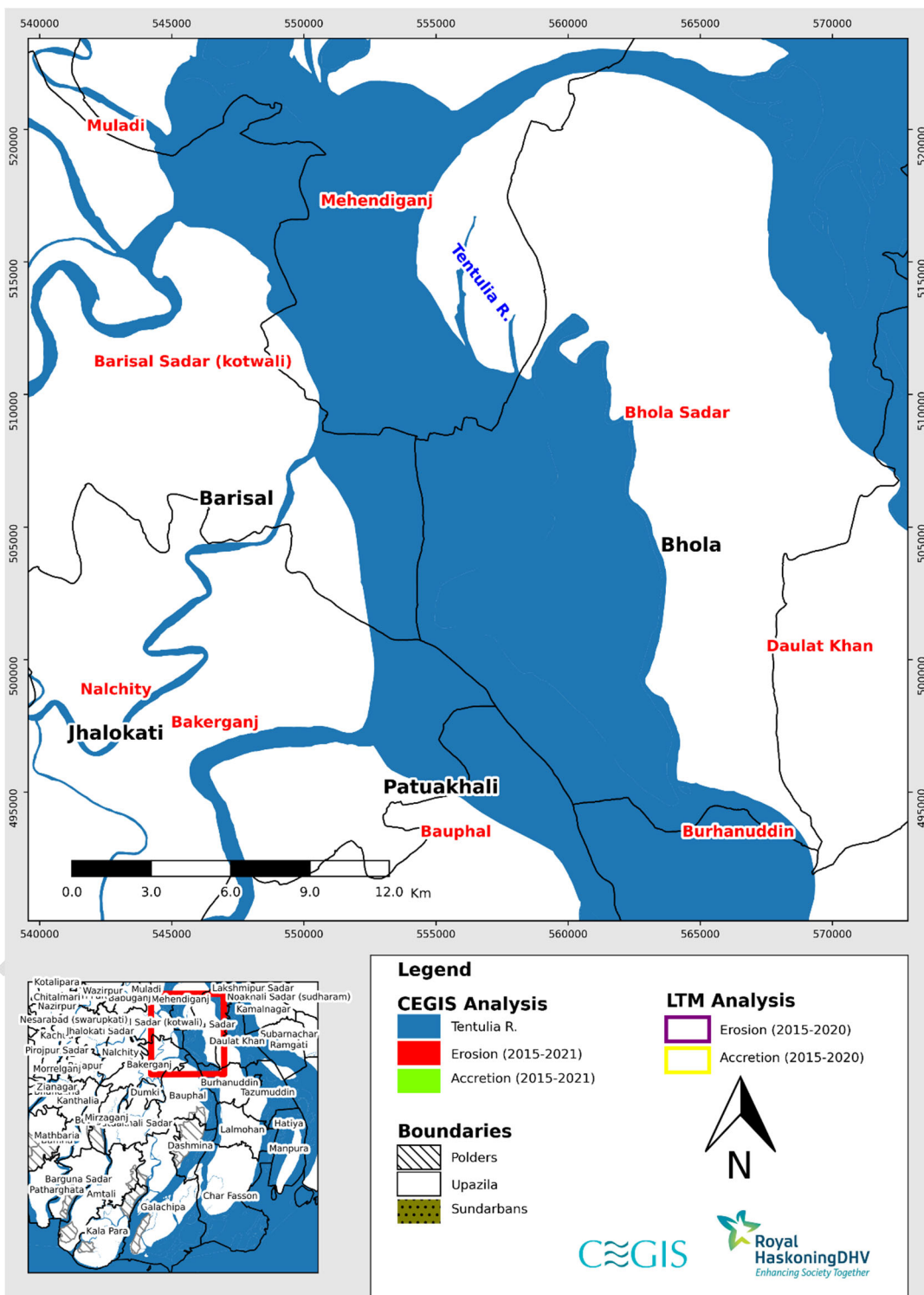


Figure 2.21: Difference between erosion and accretion of LTM and CEGIS in Tentulia River (Reach-1) (2015-2021)

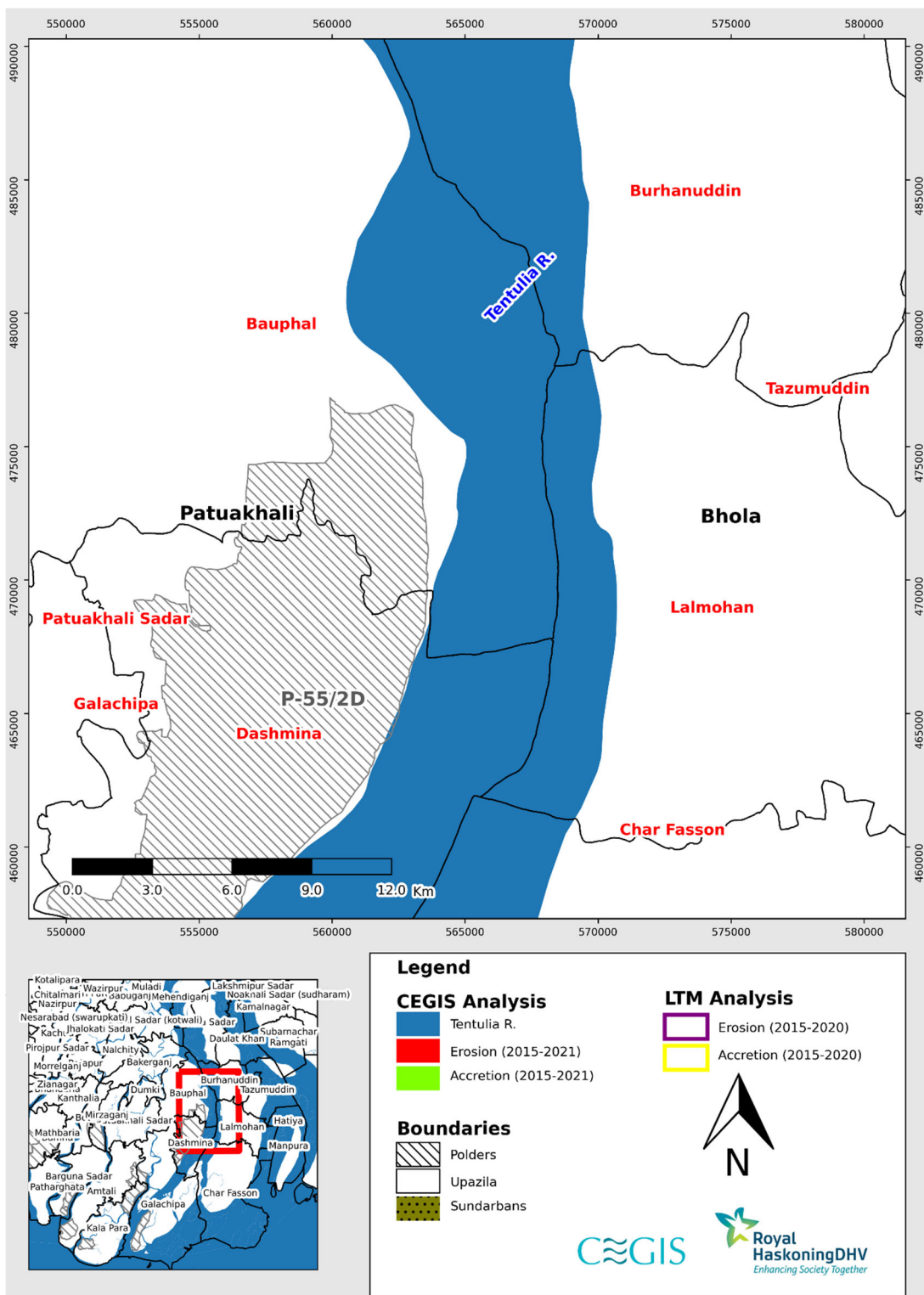


Figure 2.22: Difference between erosion and accretion of LTM and CEGIS in Tentulia River (Reach-2) (2015-2021)

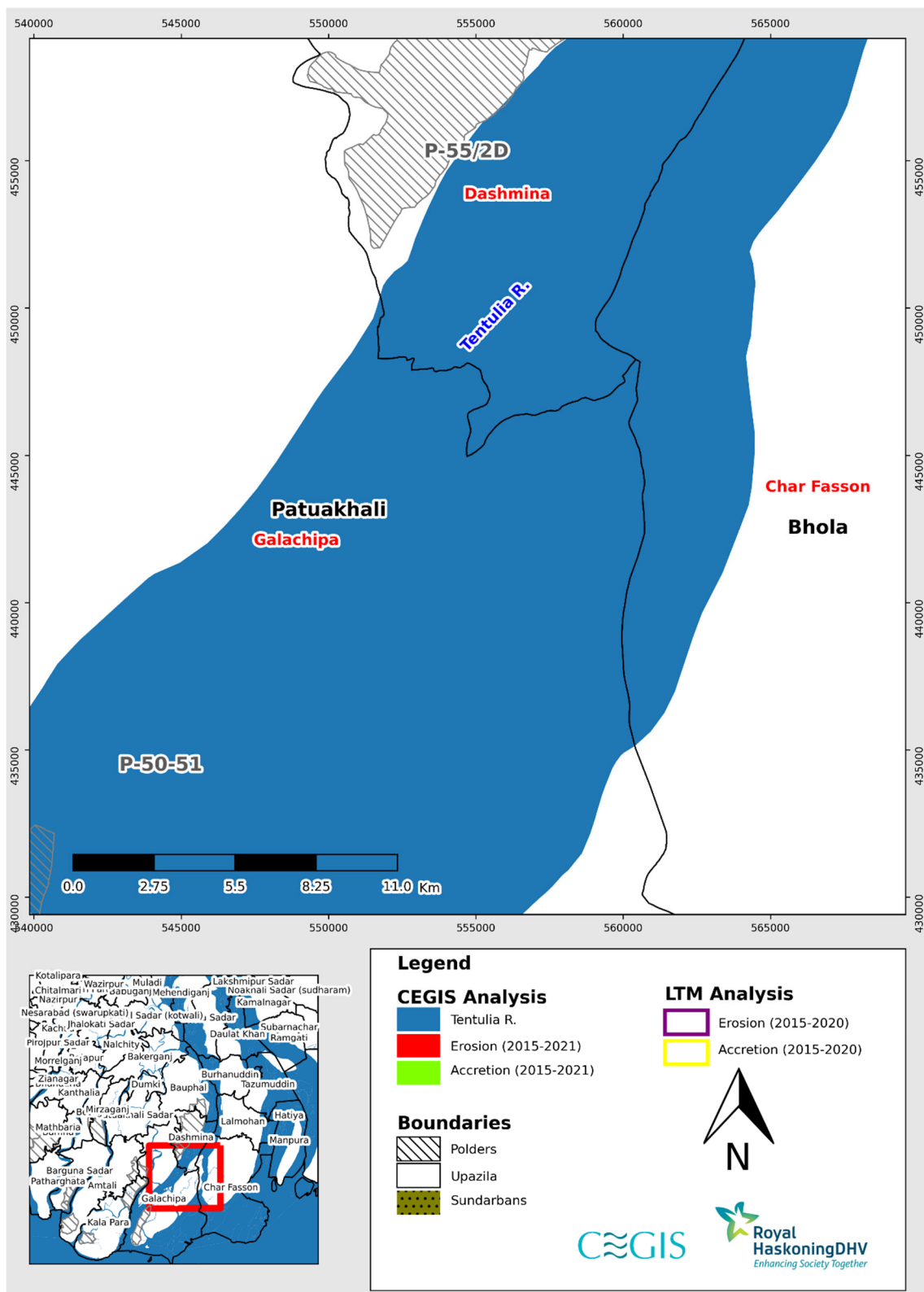


Figure 2.23: Difference between erosion and accretion of LTM and CEGIS in Tentulia River (Reach-3) (2015-2021)

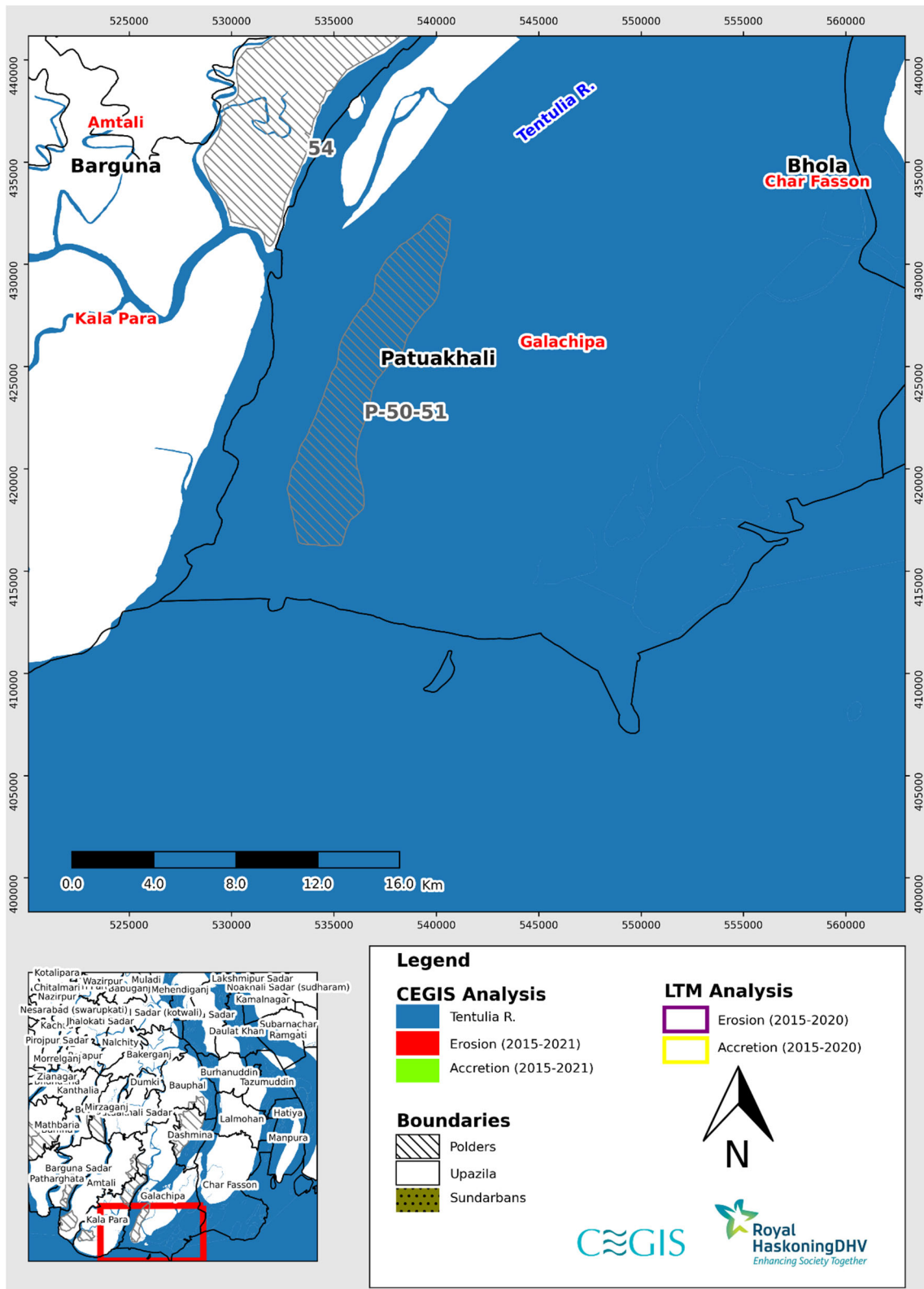


Figure 2.24: Difference between erosion and accretion of LTM and CEGIS in Tentulia River (Reach-4) (2015-2021)

References

- Ahmad, H., 2019. Bangladesh Coastal Zone Management Status and Future Trends, Journal of Coastal Zone Management.
- Allison MA, Khan SR, Goodbred SR, Kuehl SA, 2003. Stratigraphic evolution of the Late Holocene Ganges-Brahmaputra lowers delta plain. *Sed Geol* 155:317–342
- Bangladesh Water Development Board (BWDB), 1983. Design Manual Procedures for Designs of Polders in Tidal Areas in Bangladesh, Md. Abdul Quassem, P.F. Raijmakers, J. Burger, Delta Development Project.
- Bangladesh Water Development Board (BWDB), 2012. Coastal Embankment Improvement Project, Draft Final Report, Sept 2012.
- Bhuiya, A.II., 1993; Fluvial System and Geomorphology Case Point in Bangladesh, Proc. of the International Workshop on Morphological Behavior of the Major Rivers in Bangladesh, Publ. FPCO, Dhaka, Bangladesh, 29-53.
- Brammer, H., 1995; Geography of soils of Bangladesh, The University Press Limited, Dhaka, Bangladesh, pp. 287.
- Curry, Joseph R., 1994. Sediment volume and mass beneath the Bay of Bengal. *Earth and Planetary Science Letters*, 125 (1). 371-383 doi:10.1016/0012-821x(94)90227-5.
- Donchyts, G.; Schellekens, J.; Winsemius, H.; Eisemann, E.; Van de Giesen, N., 2016. A 30 m Resolution Surface Water Mask Including Estimation of Positional and Thematic Differences Using Landsat 8, SRTM and OpenStreetMap: A Case Study in the Murray-Darling Basin, Australia. *Remote Sens.*, 8, 386. <https://doi.org/10.3390/rs8050386>.
- Fergusson J., 1863. On recent changes in the delta of the Ganges. *Q J Geol Soc* 19:321–353.
- Goodbred SL Jr, Kuehl SA, 2000a. Enormous Ganges-Brahmaputra sediment discharge during strengthened early Holocene monsoon. *Geology* 28:1083–1086
- Goodbred Jr. S.L., Kuehl, S.A., 2000b; Enormous Ganges-Brahmaputra sediment discharge during strengthened early Holocene monsoon, *Geology*, Vol. 28, 1083-1086.
- Goodbred Jr., S.L., Kuehl, S.A., Stecler, M.S. and Sarker, M.I1., 2003; Controls on facies distribution and stratigraphic preservation in the Ganges-Brahmaputra delta sequence, *Sedimentary Geology*, Vol. 155, 301·316.
- Haque, U., Hashizume, M., Kolivras, K.N., Overgaard, H.J., Das, B. and Yamamoto, T., 2012. Reduced death rates from cyclones in Bangladesh: what more needs to be done?. *Bulletin of the World Health Organization*, 90, pp.150-156.
- River channel changes. Hooke, J. M., 1977. "The distribution and nature of changes in river channel patterns: The example of Devon" In Gregory, K., J. edition. John Wiley and Sons. Chichester, UK. 265-280.
- (Jensen Localization, 2018), <https://www.jensen-localization.com/blog/polder-thetherlands/>
- Kuehl, S.A., Hariu, T.M. and Moore, W.S., 1989. Shelf sedimentation off the Ganges Brahmaputra River System: evidence for sediment bypassing to the Bengal Fan. *Geology*. 17, 1132-1135.

Kuehl SA, Allison MA, Goodbred SL, Kudrass H, 2005. The Ganges–Brahmaputra Delta. In Gosian L, Bhattacharya J (eds) River Deltas: concepts, models, and examples. Tulsa, Oklahoma. SEPM, Special Publication 83.

Leopold, L.B. and Langbein, W.B., 1966. River meanders. Scientific American, 214(6), pp.60-73.

Ministry of Agriculture (MoA), 2010. SRMAF Project, Soil Resource Development Institute Bangladesh.

Ministry of Water Resources (MoWR), 2003. The administrative delineation of the Coastal Zone comprises 19 districts, 147 Upazilas, and the exclusive economic zone. Delineation of the Coastal Zone, Program Development Office for Integrated Coastal Zone Management Plan (PDO-ICZMP), WP005.

Morgan, J. P., and McIntire, W.G., 1959; Quaternary Geology of the Bengal Basin, East Pakistan, and India, Bulletin of the Geological Society of America, Vol. 70, 319-342.

Sarker, M.H., Akter, J., Huque, I., Oberhagemann, K., Akand, M.K., 2021. Formation and Dynamics of Coastal Chars in Bangladesh. In: Zaman, M., Alam, M. (eds) Living on the Edge. Springer Geography. Springer, Cham. https://doi.org/10.1007/978-3-030-73592-0_9

Schumm, S.A., 1977; The Fluvial System, Hohn Wiley & Sons, NY.

Tessler, Z.D., Vörösmarty, C.J., Grossberg, M., Gladkova, I., Aizenman, H., Syvitski, J.P. and Foufoula-Georgiou, E., 2015. Profiling risk and sustainability in coastal deltas of the world. Science, 349(6248), pp.638-643.

Umitsu M, 1993. Late quaternary sedimentary environments and landforms in the Ganges Delta. Sed Geol 83:177-186.

Williams CA, 1919. History of the rivers in the Ganges Delta 1750-1918. Bengal Secretariat Press, Calcutta.

Xu, Hanqiu., 2006. Modification of Normalized Difference Water Index (NDWI) to Enhance Open Water Features in Remotely Sensed Imagery. International Journal of Remote Sensing. 27. 3025-3033. 10.1080/01431160600589179.

DRAFT

DRAFT